University of Zagreb

Faculty of Science
Department of Geology

Ana Ramljak

RESPONSE OF BENTHIC MICROBIAL COMMUNITIES TO ANTHROPOGENIC PRESSURES IN COASTAL ZONES OF THE EASTERN ADRIATIC

DOCTORAL THESIS

Zagreb, 2025

University of Zagreb

Faculty of Science
Department of Geology

Ana Ramljak

RESPONSE OF BENTHIC MICROBIAL COMMUNITIES TO ANTHROPOGENIC PRESSURES IN COASTAL ZONES OF THE EASTERN ADRIATIC

DOCTORAL THESIS

Mentor:
Ines Sviličić Petrić, PhD, Scientific advisor

Zagreb, 2025

Sveučilište u Zagrebu

Prirodoslovno-matematički fakultet
Geološki odsjek

Ana Ramljak

ODGOVOR BENTOSKIH MIKROBNIH ZAJEDNICA NA ANTROPOGENA OPTEREĆENJA PRIOBALNIH ZONA ISTOČNOG JADRANA

DOKTORSKI RAD

Mentor:
dr. sc. Ines Sviličić Petrić, znanstvena savjetnica

Zagreb, 2025.

This doctoral thesis was carried out as part of the postgraduate program in Oceanology at the University of Zagreb, Faculty of Science, Department of Geology, under the supervision of Ines Sviličić Petrić, PhD, scientific advisor. The research was conducted as part of the project *Structure and Function of Microbial Communities as a Missing Link for Quality Assessment of Anthropogenically Disturbed Coastal Zones* (MicroLink), funded by the Croatian Science Foundation (project number IP-2020-02-6510; principal investigator: Ines Sviličić Petrić, PhD). The experimental part of the research was carried out in the Laboratory for Environmental Microbiology and Biotechnology, Division for Marine and Environmental Research, Ruđer Bošković Institute (Zagreb, Croatia). Part of the bioinformatic analyses were conducted at the University of Thessaly (Larissa, Greece) and the Helmholtz Institute for Environmental Research (Leipzig, Germany).

Zahvale

Najprije želim zahvaliti svojoj mentorici, dr. sc. Ines Sviličić Petrić na pruženoj prilici, svim savjetima, idejama, druženjima i kavama, strpljenju, ohrabrivanju i veselom duhu. Bez Vaše podrške i prijateljstva, put do ovog doktorata bi bio puno teži!

Hvala puno i svim kolegicama iz Laboratorija za okolišnu mikrobiologiju i biotehnologiju, a posebno Heleni i Anastaziji s kojima sam dvije godine dijelila najbolji ured, suze i smijeh.

Hvala svim prijateljicama i prijateljima, starima i novima, a posebno mojoj Sari – na svim zajedničkim pauzama i uzbudljivoj doktorskoj avanturi koju smo zajedno prolazile od početka.

Hvala mom M. – nije ti bilo lako i zato sam ti beskrajno zahvalna.

Hvala mojoj obitelji na vječnoj podršci.
Ovaj doktorat posvećujem svojim roditeljima – mami Zvjezdani i tati Zdenku!

Thank you note

Another thank you, this time in English, goes out to all the wonderful people in Greece who made my three months in Larissa special. My heartfelt thanks to Maria, Mark and Dimitra, as well as Sotirios and Dimitrios for hosting me!

Many thanks to everyone in Leipzig for the great collaboration and shared knowledge, especially Stephanie and Antonis.

"It is a curious situation that the sea, from which life first arose, should now be threatened by the activities of one form of that life. But the sea, though changed in a sinister way, will continue to exist; the threat is rather to life itself."
- Rachel Carson

University of Zagreb
Faculty of Science
Department of Geology

Doctoral thesis

RESPONSE OF BENTHIC MICROBIAL COMMUNITIES TO ANTHROPOGENIC PRESSURES IN COASTAL ZONES OF THE EASTERN ADRIATIC

Faculty of Science, Department of Geology

Marine coastal ecosystems are consistently exposed to multiple human-induced pressures, which inevitably impact the environmental status of marine sediments. Sediments are highly diverse habitats inhabited by responsive and adaptable marine microorganisms. Microbial indicators are considered potentially valuable tools for monitoring pollution and for guiding the development of marine protection strategies and policy frameworks. This doctoral thesis aimed to investigate the responses of benthic prokaryotes, fungi and protists to chronic anthropogenic pressures in coastal zones of the eastern Adriatic. Total DNA was extracted from sediment samples collected across seven polluted ports and bays. A multilevel approach was employed to investigate microbial structure, functions and interactions. High-throughput sequencing (amplicon and metagenomic sequencing) and advanced statistical methods were used to assess changes and define microbial indicators of anthropogenic pressures. The results demonstrated shifts in microbial diversity and community structure between contaminated and non-contaminated locations, highlighting the presence of both tolerant and sensitive taxa. Furthermore, biogeographic patterns emerged as critical factors in shaping microbial communities in marine sediments. Through differential abundance analyses, prokaryotes were identified as the most promising indicators, while protistan and fungal communities showed limited reliability. Notably, members of *Rhodobacteraceae*, *Thermoanaerobaculaceae* and *Ectothiorodospiraceae* exhibited contamination tolerance, while sensitive taxa such as *Lactobacillaceae* and *Pseudomonadaceae* were more abundant in non-contaminated sediments. Heavy metal stress was shown to significantly weaken microbial interactions, particularly between prokaryotes and protists, potentially disrupting essential ecosystem services. Additionally, the Boruta algorithm identified 47 microbial taxa and 44 genes that differentiate between contaminated and non-contaminated locations. Several taxa from the family *Bacillaceae* demonstrated resistance to heavy metals and tributyltin, confirming their potential role in developing bioremediation strategies for polluted sediments. The findings of this doctoral thesis suggest that microbial communities have the potential to serve as indicators of anthropogenic pollution and support their integration into environmental assessments and policy frameworks, such as the Marine Strategy Framework Directive (MSFD) of the European Union. In summary, this study provides valuable insights into microbial community dynamics in vulnerable coastal ecosystems facing continuous anthropogenic pressures.

(173 pages, 23 figures, 5 tables, 261 references, 35 supplements, original in English)

Keywords: microbial communities, marine sediment, anthropogenic pressures, coastal ecosystems, Adriatic Sea, environmental monitoring, ecosystem services, microbial indicators

Supervisor: Ines Sviličić Petrić, PhD, Scientific advisor

Reviewers:
1. Tomislav Ivanković, PhD, Associate Professor
2. Marino Korlević, PhD, Senior research associate
3. Jelena Godrijan, PhD, Senior research associate

Sveučilište u Zagrebu
Prirodoslovno-matematički fakultet
Geološki odsjek

Doktorski rad

ODGOVOR BENTOSKIH MIKROBNIH ZAJEDNICA NA ANTROPOGENA OPTEREĆENJA PRIOBALNIH ZONA ISTOČNOG JADRANA

Prirodoslovno-matematički fakultet, Geološki odsjek

Morski obalni ekosustavi kontinuirano su izloženi brojnim pritiscima uzrokovanima ljudskim djelovanjem, što neupitno utječe na ekološko stanje morskih sedimenata. Sedimenti su staništa visoke raznolikosti naseljena morskim mikroorganizmima osjetljivim i prilagodljivim na promjene okoliša. Mikrobni indikatori smatraju se potencijalno vrijednim alatima za praćenje onečišćenja te usmjeravanje razvoja strategija zaštite mora i odgovarajućih politika. Cilj doktorskog rada bio je istražiti odgovore bentoskih prokariota, gljiva i protista na kronična antropogena opterećenja u priobalnim područjima istočnog Jadrana. Ukupna DNA izolirana je iz uzoraka sedimenata prikupljenih u sedam onečišćenih luka i zaljeva. Primijenjen je višerazinski pristup koji je obuhvatio analizu strukture, funkcija i međusobnih interakcija mikrobnih zajednica. Za praćenje promjena i identifikaciju mikrobnih indikatora antropogenog opterećenja korištene su metode sekvenciranja nove generacije (na razini amplikona i metagenoma) u kombinaciji s naprednim statističkim analizama. Dobiveni rezultati ukazali su na razlike u mikrobnoj raznolikosti i strukturi zajednice između onečišćenih i neonečišćenih lokacija, pri čemu su identificirane i tolerantne i osjetljive skupine bentoskih mikroorganizama. Biogeografski obrasci prepoznati su kao ključni čimbenici u oblikovanju mikrobnih zajednica u morskim sedimentima. Analiza diferencijalne zastupljenosti istaknula je prokariote kao najučinkovitije indikatore, dok su protisti i gljive pokazali manju pouzdanost. Članovi porodica *Rhodobacteraceae*, *Thermoanaerobaculaceae* i *Ectothiorodospiraceae* pokazali su toleranciju na onečišćenje, dok su osjetljive skupine, poput porodica *Lactobacillaceae* i *Pseudomonadaceae*, bile češće zastupljene u neonečišćenim sedimentima. Utvrđeno je kako stres uzrokovan prisutnošću teških metala značajno narušava mikrobne interakcije, osobito između prokariota i protista, što može imati negativni utjecaj na ključne usluge ekosustava. Nadalje, Boruta algoritam identificirao je 47 mikrobnih taksona i 44 gena koji jasno razlikuju onečišćene od neonečišćenih lokacija. Nekoliko taksona iz porodice *Bacillaceae* pokazalo je otpornost na teške metale i tributilkositar, potvrđujući njihov potencijal u razvoju strategija bioremedijacije onečišćenih sedimenata. Spoznaje proizašle iz ovog doktorskog rada ukazuju na potencijal mikrobnih zajednica kao indikatora antropogenog onečišćenja te podupiru njihovu integraciju u procjene stanja okoliša i okolišne politike, poput Okvirne direktive o morskoj strategiji Europske unije. Ovo istraživanje pruža značajne uvide u dinamiku mikrobnih zajednica u osjetljivim obalnim ekosustavima pod stalnim antropogenim opterećenjima.

(173 stranice, 23 slike, 5 tablica, 261 literaturni navod, 35 priloga, jezik izvornika: engleski)

Ključne riječi: mikrobne zajednice, morski sediment, antropogena opterećenja, obalni ekosustavi, Jadransko more, praćenje stanja okoliša, usluge ekosustava, mikrobni indikatori

Mentor: dr. sc. Ines Sviličić Petrić, znanstvena savjetnica

Povjerenstvo za obranu:
1. izv. prof. dr. sc. Tomislav Ivanković
2. dr. sc. Marino Korlević, viši znanstveni suradnik
3. dr. sc. Jelena Godrijan, viša znanstvena suradnica

Information about the supervisor

Ines Sviličić Petrić, PhD, Scientific advisor

Ines Sviličić Petrić, PhD, was born in Zagreb where she graduated in Biology from the Faculty of Science, University of Zagreb, in 2003. She obtained her PhD in Biology from the same institution in 2009. From 2009 to 2010, she worked as a postdoctoral researcher at the French National Institute for Agricultural Research in Dijon, France.

Since 2012, Dr. Sviličić Petrić has been employed at the Laboratory for Environmental Microbiology and Biotechnology, where she is currently a scientific advisor and the leader of the project *MicroLink* (full name: *Structure and function of microbial communities as a missing link for quality assessment of anthropogenically disturbed coastal zones*), funded by the Croatian Science Foundation.

To date, she has been the principal investigator and coordinator of five international scientific projects and has been involved in 11 additional research projects as a consultant. Dr. Sviličić Petrić has published 37 scientific papers, as indexed by WoS and 40 according to Scopus. She has actively participated in more than 40 international conferences and co-organized seven international conferences in Croatia. She is also one of the initiators of the *InspireAdriatic Scientific Symposium: Interdisciplinary Approach to the Scientific Research of the Adriatic Sea*, held in Zagreb in 2023 and 2025. Additionally, she has supervised three doctoral theses and two master's theses.

Her scientific interests include investigating the response of microbial communities to climate change and anthropogenic pressures, such as pesticides and heavy metals, in both soil and marine sediments. She also investigates the biodegradation of these pollutants, with potential applications in bioremediation. Beyond her scientific research, she is actively involved in science popularization, highlighting the crucial role of microorganisms in maintaining ecosystem stability.

Table of contents

1. Introduction

1.1. Benthic microorganisms: historical perspectives, ecosystem services and community dynamics

1.1.1. Historical background of marine microbiology

The discovery of solid media for bacterial cultivation in the 19th century marked the beginning of the golden age of bacteriology, with major contributions from Robert Koch, Fannie Hesse and Julius Petri. However, it is estimated that more than 99% of marine microorganisms remain uncultured under laboratory conditions (Jannasch and Jones, 1959; Ferguson et al., 1984; Wang et al., 2021; Rodrigues and Carvalho, 2022). Microbiological methods today are classified into two categories: culture-dependent, relying on nutrient-rich media, and culture-independent, which gained importance in the 1970s with the development of DNA extraction and high-throughput sequencing (Pepper and Gerba, 2009; Bouchez et al., 2016). These advancements launched the omics era, including genomics, transcriptomics, proteomics and metabolomics, although traditional culturing remains important for studying microbial morphology and physiology (Bouchez et al., 2016; Wang et al., 2021).

Early marine microbiology research by Waksman and ZoBell, in the mid-20th century, highlighted the ecological importance of marine bacteria in biogeochemical cycles, organic matter decomposition and confirmed the presence of microorganisms in marine sediments (Waksman, 1934; Zobell, 1946; Sherr and Sherr, 2008). Their work laid the foundations for the Pomeroy's concept of the "microbial loop", emphasizing the critical role of microorganisms in sustaining marine food webs (Pomeroy, 1974; Stal, 2022). Landmark expeditions such as the *Challenger* expedition (1872–1876), the Danish *Deep-Sea Expedition* and the *Ocean Drilling Program Leg 201* expanded knowledge of microbial life in extreme environments and deep-sea marine sediments (Manten, 1972; D'Hondt et al., 2003; Jørgensen and Boetius, 2007). Following the 2010 *Deepwater Horizon* oil spill in the Gulf of Mexico, studies employing advanced omics technologies highlighted the pivotal role of microorganisms in hydrocarbon degradation, although much of the research focused on the water column rather than deep-sea sediments (Acosta-González and Marqués, 2016). More recently, the *Tara Oceans* expedition (2009–2012) collected 35,000 seawater samples in 210 locations worldwide, building a vast genetic database and uncovering 40 million previously unknown microbial genes (Munn, 2020).

1.1.2. Functional roles of benthic microorganisms

In the dynamic and intricately interconnected marine ecosystems that cover 70% of the Earth's surface, the seafloor is predominantly covered by sediment, which is one of the most diverse habitats (Hoshino et al., 2020). Sediments are estimated to harbor between 10^3 and 10^{10} cells/cm^3 in contrast to seawater, which contains approximately 10^4 to 10^7 cells/ml (Wang et al., 2021). The current estimate is that sediment microorganisms account for 0.18 – 3.6% of the total living biomass on Earth or 2.9×10^{29} cells (Kallmeyer et al., 2012). Benthic microorganisms are linked to the seafloor as their habitat, living on or in the sediment. The benthic microbial communities include prokaryotes (bacteria and archaea), fungi, protists and viruses (Munn, 2020). Microbial communities within sediments are sorted along a vertical gradient, exhibiting an overall decrease in abundance with depth and sediment age (Hoshino et al., 2020). The availability of organic matter, which is influenced by sedimentation rates and primary production in the overlying water columns, also affects differences between microbial communities (D'Hondt et al., 2019; Lai et al., 2020). Deep-sea microorganisms experience nutrient limitation due to low sedimentation and reduced input of organic material, in contrast to nutrient-rich coastal sediments (Lai et al., 2020).

In addition to their abundance, the diverse roles and ecosystem services provided by microorganisms are essential to the overall ecosystem functioning (Caruso et al., 2015). They play crucial roles in maintaining ecosystem health by participating in biogeochemical cycles of nitrogen, phosphorus, carbon and sulfur, as well as in the degradation and regeneration of organic matter (Falkowski et al., 2008; Gadd, 2010). Furthermore, they contribute to oceanic carbon sequestration, microbial food web dynamics and the detoxification and transformation of pollutants (Danovaro et al., 2017; Gao et al., 2022). Marine sediments serve as critical carbon reservoirs, however, anthropogenic disturbances raise concerns that these sediments could become sources of carbon dioxide (CO_2), thereby contributing to global climate change (Atwood et al., 2020). Within the microbial food web, heterotrophic prokaryotes utilize dissolved organic carbon, transferring it to higher trophic levels through predation (grazing) by protists, such as flagellates and ciliates, as well as larger organisms (Caruso et al., 2015).

Prokaryotes, i.e. bacteria and archaea, dominate the biomass of marine sediments (Trouche et al., 2021). Although morphologically similar, bacteria and archaea differ in cell structure and molecular mechanisms. In 1990, Woese et al. proposed *Archaea* as a new domain of life, initially believed to consist exclusively of extremophiles (Woese et al., 1990). While many archaeal lineages remain unculturable, recent research has identified mesophilic archaeal groups thriving in non-extreme habitats (Zou et al., 2025). Among the most widely distributed and frequently studied archaeal groups are ammonia-oxidizing archaea (AOA), which, along with ammonia-oxidizing bacteria (AOB), mediate the transformation of nitrogen compounds in aerobic sediments, contributing to the global nitrogen cycle (Zou et al., 2025, Lai

et al., 2020). Both groups contain the *amoA* gene, commonly used as a molecular marker for their identification (Pajares and Ramos, 2019). Another essential part of the nitrogen cycle is denitrification, through which nitrogen compounds are converted back to atmospheric nitrogen (N_2) (Zou et al., 2025). Prokaryotes are also crucial for carbon metabolism, including both carbon remineralization and carbon fixation. In sediments, chemolithoautotrophic microorganisms drive carbon fixation, though the research on their role remains limited. Notably, *Gammaproteobacteria* have been identified as the major contributor, accounting for approximately 70% of total carbon fixation (Dyksma et al., 2016). In anaerobic sediments, methanogenesis occurs, with the *mcrA* gene, encoding methyl-coenzyme M reductase, found in many archaeal groups (Zou et al., 2025). Furthermore, methanotrophic bacteria utilize methane (CH_4) as their sole carbon source, highlighting the roles of both bacteria and archaea in regulating methane cycling and greenhouse gas emissions (Euler et al., 2020). In phosphorus metabolism, phosphate-solubilizing bacteria (PSB) enhance phosphorus exchange at the sediment-water interface, influencing its transport, transformation and indirectly, environmental conditions. PSBs are associated with genera such as *Bacillus*, *Pseudomonas*, *Acinetobacter* and *Burkholderia* (Tu et al., 2024). In anoxic marine sediments, prokaryotes also participate in sulfate reduction, which coexists with methanogenesis but may be subject to competition between sulfate-reducing bacteria (SRB) and methanogens (Sela-Adler et al., 2017). Nevertheless, microbial dissimilatory sulfate reduction remains the primary pathway for organic matter mineralization in anoxic coastal marine sediments (Jørgensen et al., 2019).

Marine fungi were first described in the 19th century and their definition has evolved as research technologies have advanced. Early studies found fungal taxa similar or even identical to non-marine fungi (Sarma, 2019). Currently, marine fungi are defined as organisms that grow and/or sporulate in the marine environment, as well as those that adapt, evolve, remain metabolically active or form symbiotic relationships with other marine organisms (Cunliffe, 2022). Due to their specific nutrient requirements, laboratory cultivation techniques have had limited success. The most significant achievements in marine fungal research have been made through culture-independent techniques. To date, approximately 2,100 species have been identified, with an estimated total diversity of around 10,000 species (https:// www.marinefungi.org, Jones et al., 2019; Amend et al., 2019). Their ecological roles are still not completely understood, however, they are known to contribute to organic matter recycling, sulfate reduction, methanogenesis and the degradation of recalcitrant compounds, including anthropogenic pollutants (Rubin-Blum et al., 2022; Burgaud et al., 2022; Rojas-Jimenez et al., 2020). Additionally, marine fungi have been found in symbiotic associations with corals, sponges and other macroorganisms, and are considered crucial for marine food webs, regulating phytoplankton populations by top-down control (Tisthammer et al., 2016). Although benthic marine fungi are typically less abundant than prokaryotes in

marine sediments, both groups actively participate in microbial interactions, including the production of antifungal compounds by bacteria and the release of antibacterial compounds by fungi (Yurchenko et al., 2021).

Protists are a highly diverse group of unicellular eukaryotic organisms, ranging in size from less than 1 μm to over 100 μm, with distinct morphological and functional characteristics (Munn, 2020). Additionally, protists are a paraphyletic, yet practical, category that includes eukaryotes other than animals, plants and fungi (Adl et al., 2019; Burki et al., 2020). While research on benthic protists remains limited, existing evidence suggests a higher diversity of benthic protistan species compared to planktonic species (Forster et al., 2016). In marine ecosystems, protists have essential ecological functions in nutrient cycling and food web dynamics, acting as primary producers, predators, decomposers and parasites (Massana et al., 2015). Dominant protistan communities found in coastal sediments include diatoms and dinoflagellates, as well as predators such as ciliates and cercozoans and obligate parasites such as apicomplexans (Kalu et al., 2023). One of the most significant roles in marine food webs is the bacterial grazing by protistan predators, which regulates bacterial abundance and diversity in aquatic ecosystems (Bock et al., 2020).

Viruses, though non-cellular biological entities, are often considered microbes under a broader definition (Munn, 2020). Despite being the most abundant when compared to other microorganisms, their study faces challenges due to their unculturability and the absence of a conserved marker gene (He et al., 2024). Marine virology research has mostly focused on bacteriophages, with significant advancements achieved through electron microscopy and metagenomic analyses (Weynberg, 2018). By infecting bacterial cells, marine viruses cause the loss of up to 20% of microbial biomass daily, which can lead to the destabilization of microbial food webs (Caruso et al., 2015; He et al., 2024).

These ecosystem services underscore the need for further in-depth research into the functional roles of each benthic microbial community (prokaryotes, protists and fungi). While most studies to date have relied on amplicon sequencing, the metagenomic approach to studying benthic microorganisms has gained increasing attention in recent years. Given that most benthic microorganisms remain unculturable, metagenomic analysis presents a powerful approach for exploring their genetic diversity and functional roles (Siallagan et al., 2024).

1.1.3. Microbial community assembly and ecological drivers

For our understanding of benthic microbial ecology and biogeography, it is crucial to identify the mechanisms responsible for the assembly and distribution of microorganisms. Four key processes that drive microbial community assembly are: diversification, dispersal, selection and drift, as described in Vellend's conceptual synthesis of community ecology (Vellend, 2010; Nemergut et al., 2013). Although these processes are well-documented, there is an ongoing scientific debate regarding the specific processes that drive shifts in microbial communities. These processes of microbial community assembly have been shown to depend also on the scale considered (regional or local), despite the well-known scientific standpoint by Baas Becking that “everything is everywhere, but the environment selects” (Baas Becking, 1934; Fillinger et al., 2019).

Diversification refers to the generation of new genetic variations, while drift describes random changes in relative abundances of microbial taxa within a community through time (Vellend, 2010). Dispersal, shaped by factors such as geographic location, region, depth and sediment grain size, refers to the movement of microorganisms across space via wind, water or by attaching to mobile macroorganisms. In contrast, selection is determined by environmental factors, including physicochemical parameters such as pH, salinity and temperature, as well as biotic factors, such as microbial interactions, which remain underexplored (Nemergut et al., 2013). Additionally, selection pressures may result from exposure to pollutants, such as heavy metals (Zhao et al., 2021).

The distance-decay relationship (DDR) is one of the most studied biogeographical patterns in microbial ecology. It describes how the dissimilarity between two communities decreases with increasing spatial distance through drift, selection, dispersal and diversification (Nekola and White, 2004; Clark et al., 2021; Milke et al., 2022). It has been suggested that prokaryotes, due to their small size and high dispersal potential, are less affected by dispersal limitations than eukaryotes such as protists and fungi (Zhao et al., 2022). As a result, prokaryotic communities could be more strongly shaped by environmental factors (Z.-B. Wang et al., 2020). Additionally, DDR tends to be weaker in aquatic environments compared to more structured and heterogenous habitats such as soils and sediments, likely due to the greater dispersal ability of aquatic microbes and higher habitat connectivity (Clark et al., 2021). Microorganisms also enhance their dispersal capabilities through dormant forms, such as cysts and spores, which they form under unfavorable conditions (Nemergut et al., 2013; Clark et al., 2021).

Sediment processes, including suspension, deposition, erosion and dispersal by currents, along with substantial small-scale heterogeneity, also shape benthic microbial communities (Chen et al., 2019a; Trouche et al., 2021; Clark et al., 2021). However, previous studies have reported conflicting findings regarding the nature of microbial assembly processes. Some studies on coastal sediments suggest that

prokaryotic community assembly occurs randomly (Liu et al., 2019; Trouche et al., 2021). Similarly, although benthic fungal communities have been considered randomly assembled, local environmental conditions appear to exert a stronger influence than geographical distance (Tisthammer et al., 2016; Zhao et al., 2022). At a regional scale, protistan communities in the surface waters exhibited a strong distance-decay relationship, suggesting spatial structuring by dispersal limitation. However, the variation in temperature also contributed to community composition, indicating that both dispersal and environmental factors shape surface communities. In contrast, in mid- and bottom waters, where temperature showed minimal variability, the distance-decay relationship was weaker, and community composition was more strongly influenced by other local environmental conditions (Mars Brisbin et al., 2020).

The responses of individual microbial communities, especially bacteria, have been extensively studied. However, microbial interactions as biotic drivers of community assembly remain largely underexplored, particularly under the influence of multiple pressures in coastal ecosystems (Liu et al., 2019). Microbial interactions are known to occur through competition for resources or cooperation, following ecological principles such as mutualism, parasitism, predation and commensalism (Nawaz et al., 2022).

Given the crucial role of microbial interactions in maintaining ecosystem function and health, advancing research in microbial ecology remains imperative. As highlighted by the Intergovernmental Panel on Climate Change (IPCC) Synthesis report (2023), “Widespread and rapid changes in the atmosphere, ocean, cryosphere and biosphere have occurred”. These changes raise critical questions regarding microbial responses to climate change, which will, in turn, influence the ecosystem services they provide and the overall ecosystem stability. Understanding these dynamics is essential for predicting and mitigating the broader ecological consequences of climate change.

1.2. Response of benthic microorganisms to pollutants and their bioremediation potential

Microbial communities in coastal areas are, among other parameters, shaped by natural gradients of salinity, sedimentation, bottom topography, turbidity and nutrient availability (Misson et al., 2016). Specifically, benthic microbial communities are closely associated with sediment particles and elevated pollution levels in coastal areas can alter sediment conditions, causing a microbial response. These environmental changes may lead to shifts in microbial community structure, diversity or functionality (Nogales et al. 2011). Pollutants can also be resuspended into the water column and bioaccumulated in marine organisms, ultimately influencing all trophic levels within the food web, as well as human health (Roberts, 2012). Microbial responses may vary depending on the specific microbial community, but also due to the differences in cell size, metabolic activity and dispersal potential (Zhao et al., 2022).

Microbial response to disturbance can be either resistance or resilience (Nogales et al., 2011). According to Nogales et al. (2011), resistance indicates no change after a disturbance, while resilience indicates a change in composition, but eventually, the community reverts to its original composition. On the other hand, disturbances can also impact the functionality of microbial communities, potentially leading to negative effects on ecosystem functioning. However, disturbances may also affect microbial community composition without altering the functional processes carried out by microorganisms. This phenomenon, known as functional redundancy, suggests that different microbial species can perform similar ecological roles, thus maintaining ecosystem functions despite compositional changes (Nogales et al., 2011).

Some microorganisms have been found to tolerate and transform pollutants. In this way microorganisms accumulate the pollutants through their metabolic activity and transform them into less toxic forms or reduce their concentration. This process is called bioremediation (Dell'Anno et al., 2021a; Alvarado-Campo et al., 2023; Maglione et al., 2024). There are two frequently used bioremediation strategies: biostimulation, which indicates the addition of specific compounds to stimulate the growth of microbial communities and bioaugmentation, which involves the addition of specific microbial taxa able to detoxify or biodegrade the pollutants (Dell'Anno et al., 2021a). To date, bacteria, fungi and microalgae have been considered promising bioremediators due to their ability to thrive in a range of environmental conditions, as well as the fast replication rate (Maglione et al., 2024).

Due to the long-term accumulation of pollutants, coastal sediments host diverse microbial strains capable of tolerating pollution. These microorganisms can reduce pollutant concentration in a sustainable and ecologically acceptable manner, which is increasingly important under ongoing environmental changes (Dell'Anno et al., 2021a). The usual method for removing contaminated sediments involves dredging technologies through which the contaminated sediments are transported and stored.

This method degrades the marine environment and negatively impacts surrounding biodiversity (Cecchi et al., 2021). Additionally, chemical treatments, electrochemical techniques and physical adsorption are also frequently used methods for polycyclic aromatic hydrocarbons (PAHs) and heavy metal removal. These methods are usually expensive, not effective enough and produce toxic sludges and by-products (Dell'Anno et al., 2023).

To date, most studies have focused on investigating the tolerance and biodegradation of benthic microorganisms, mostly bacteria and fungi, to heavy metals and PAHs (Bargiela et al., 2015; Catania et al., 2015; Dell'Anno, 2020; Dell'Anno et al., 2021b; Pereira-García et al., 2024). In the study by Dell'Anno et al. (2020) benthic bacteria which proved to most effectively reduce lead (Pb) from polluted sediments from Gulf of Naples, included a consortium of *Halomonas* sp. and *Alcanivorax* sp. with a degradation rate of 73%. Additionally, a consortium of *Epibacterium* sp. and *Halomonas* sp. reduced the concentrations of arsenic (As) and cadmium (Cd) by 44% and 36%, respectively. However, no effect of tested isolates was observed for copper (Cu) and zinc (Zn). Furthermore, the study proved the higher effectiveness when using consortia instead of individual bacterial isolates (Dell'Anno et al., 2020). In a more recent study by the same authors, *Halomonas alkaliantarctica* strain SRM2 and *Alcanivorax xenomutans* strain SRM1, isolated from the mouth of Sarno river, were indicated as successful biodegraders of Pb, Cd and chromium (Cr) (Dell'Anno et al., 2023). Some other bacterial genera isolated from marine sediments which showed heavy metal tolerance and/or biodegradation capacity include *Vibrio*, *Pseudoalteromonas*, *Agarivorans, Pseudomonas* and *Bacillus* (Jroundi et al., 2020; Dell'Anno et al., 2021b, Pereira-García et al., 2024).

Benthic fungi which have been found to effectively detoxify sediments polluted with heavy metals include genera such as *Aspergillus, Trichoderma, Penicillium, Fusarium, Cunninhamella* and *Paradendryphiella* (Cecchi et al., 2021). The fungal species *Paradendryphiella salina* was found to absorb 80-92% of mercury(II) ions (Hg^{2+}) from the liquid media (Panseriya et al., 2019). A greater capacity for biodegradation of complex chemicals was shown for benthic fungi, in comparison with bacteria which degrade simpler chemicals. However, it has been suggested that the future application of microbial consortia of both bacteria and fungi can be used for an even more effective bioremediation (Cecchi et al., 2021).

Among protists, microalgae have been tested for heavy metal bioremediation, reducing bioavailability and toxicity of pollutants by producing exopolysaccharides that adsorb pollutants onto the cell surface (Dell'Anno et al., 2021b). Although relatively few studies have focused on microalgae for heavy metal removal from sediments, the genera *Selenastrum*, *Scenedesmus* and *Chlorella* have been identified as effective biodegraders of PAHs in marine sediments. Furthermore, species such as *Amphora*

coffaeiformis, *Navicula salinicola* and *Dunaliella salina*, isolated from coastal seawater, have shown promising results in the removal of Cd, Pb and Cr (Dell'Anno et al., 2021b; Elleuch et al., 2021).

Despite being widely recognized as nature-based solutions for pollutant removal from marine sediments, boremediation techniques still face several challenges. These include unsuccessful biostimulation of target microorganisms and limited effectiveness of bioaugmentation using laboratory-grown strains (Dell'Anno et al., 2021a). In addition to microbial incompatibility with contaminated environments, bioremediation strategies also face legal restrictions regarding the addition of microorganisms to the natural ecosystems (Tedesco et al., 2024).

1.3. Benthic microorganisms as indicators of anthropogenic pressures

Marine sediments serve as the ultimate reservoir for pollutants entering the marine ecosystems, mainly from coastal anthropogenic activities such as industrial and agriculture runoff, aquaculture, tourism, urban discharge, maritime transport and shipyards (Nogales et al., 2011; Misson et al., 2016). Coastal areas are particularly vulnerable due to multiple sources of pollution and their high population density, with over one-third of the world's population inhabiting regions within 100 km of the coast (Reimann et al., 2023). Sediments have been shown to be polluted by various persistent organic pollutants, such as herbicides, polychlorinated biphenyls (PCBs), petroleum hydrocarbons and heavy metals, among others. (Nogales et al., 2011).

Due to the increasing anthropogenic pressures along the coasts, numerous directives have been introduced with the aim of marine ecosystem protection. The most important directives for preserving the aquatic ecosystems are the Water Framework Directive (WFD, 2000/60/EC) and Marine Strategy Framework Directive (MSFD, 2008/56/EC), adopted by the European Union (EU) (Aylagas et al., 2017). While the WFD considers only coastal waters, the MSFD considers the offshore areas as well as the marine sediment. The main goal of the MSFD is to achieve and maintain Good Environmental Status (GES) of the seas to keep them clean, healthy and productive, preserving them for future generations. This is achieved through continuous monitoring of 11 Descriptors such as biodiversity, eutrophication, contaminants, seabed integrity for a cycle of 6 years after which every member state reviews and updates their strategy (Runko Luttenberger and Slišković, 2020). The foundation for the MSFD application was established by designating, to date, 12% EU marine areas as protected under national law, in accordance with the Habitats Directive (92/43/EEC), the Birds Directive (79/409/EEC) and regional sea conventions (Barcelona, OSPAR and HELCOM conventions) (Aminian-Biquet et al., 2025). Another instrument relying on the MSFD is the Marine Spatial Planning (MSP 2014/89/EU) established in 2014 by the EU, which is an ecosystem-based approach of managing the increased industrialization of the seas by using the boundaries established by the MSFD (Runko Luttenberger and Slišković, 2020).

The MSFD monitoring has been continuously performed in Croatia since 2012. Chemical pollution is assessed through the MSFD Descriptors, especially Descriptor 6 Contaminants, in both seawater and sediment. The contaminants that are continuously monitored are heavy metals, such as aluminum (Al), Cd, mercury (Hg) and Pb, tributyltin (TBT), polycyclic aromatic hydrocarbons (PAHs), specifically fluoranthene, anthracene and benzo(a)pyrene, polybrominated biphenyls (PBDE), di(2-ethylhexyl)phthalate (DEHP), halogenated organic pollutants [e.g. dioxins, hexachlorobenzene, perfluorooctane sulfonate (PFOS)] and pesticides [e.g., cypermethrin and dicofol] (MSFD, 2008/56/EC; Ministry of Environmental Protection and Energetics, 2019). Notably, threshold values for pollutants in

sediments have not been established at the EU level, but adapted from the Norwegian criteria (Bakke et al., 2010). Based on the MSFD report for Croatia from 2019, the measurements from 2017 showed that the GES has not been achieved in 9 water bodies. Specifically, in 7 water bodies due to the high values of fluoranthene, 6 due to anthracene and 1 due to benzo(a)pyrene. Additionally, high concentrations of TBT have been recorded in six water bodies and high Hg concentrations have been identified in two water bodies, resulting in the failure to achieve GES (Ministry of Environmental Protection and Energetics, 2019).

According to Descriptor 4 Food webs of the MSFD, as outlined in Commission Decision (2017/848/EU), the assessment of microorganisms in seawater includes the abundance of heterotrophic bacteria (HB) and heterotrophic nanoflagellates (HNF), the biomass of autotrophic picoplankton (APP; *Synechococcus, Prochlorococcus* and picoeukaryotes), the HB:HNF ratio and the bacterial production. Additionally, ecotoxicological impacts of seawater and sediment on bioluminescent bacteria *Aliivibrio fischeri* is tested using the standardized Microtox test (Fafanđel et al., 2015). Apart from these parameters, microorganisms, especially those inhabiting marine sediments, have been largely overlooked, despite their potential as bioindicators, due to their sensitivity to environmental changes and ability to adapt to new conditions (Aylagas et al., 2017; Caruso et al., 2015). Monitoring campaigns have primarily focused on pathogens, particularly in relation to the sanitary control of bathing waters and the water quality required for shellfish cultivation. This includes assessing fecal pollution indicators such as *Escherichia coli*, coliforms and intestinal enterococci (Caruso et al., 2015). Considering the small size, high turnover rates and responsiveness of microorganisms, they could be used as a tool for early warning signals, helping the management of marine ecosystems and avoiding high costs of consequences of environmental changes (Caruso et al., 2015). Using the high-throughput sequencing, they could be easily detected at a low cost despite their high diversity and the lack of standardized protocols in comparison to macroorganisms (Aylagas et al., 2017; Borja, 2018).

The microgAMBI index was developed based on correlations between marine bacterial communities and sediment pollutants (Borja, 2018). This index has already been applied at numerous locations, showing promising results as a bioindicator for integrative assessments of marine ecosystems through the cost-effective use of environmental DNA (eDNA) and high-throughput sequencing (Borja, 2018; Aylagas et al. 2017; Aylagas et al., 2021). In recent years, machine learning has also been increasingly used for prediction of environmental indicators (Zhao et al., 2022). Caruso et al. (2015) conducted a literature review and recommended incorporating parameters such as total prokaryotic abundance, fecal indicator bacteria and hydrocarbon-degrading bacteria in the MSFD. However, they

highlighted that targeted field studies are needed to identify consistent microbial response patterns between anthropogenically disturbed and pristine sites.

1.4. Research of microbial communities in the eastern Adriatic

The Adriatic Sea is the northernmost part of the Mediterranean Sea, separated from the Ionian Sea and the Mediterranean basin by the Strait of Otranto (Šolić et al., 2016). Long-term measurements in the Adriatic Sea indicate rising temperatures in both surface and deep waters, increasing salinity, a weakening of thermohaline circulation and declining deep-water dissolved oxygen levels, confirming the region as a climate change hotspot (Beg Paklar et al., 2020). According to Beg Paklar et al. (2020), key oceanographic processes in the Adriatic Sea include: i) inflow of warm, oligotrophic Eastern Mediterranean waters with higher salinity via cyclonic circulation, ii) freshwater input from the Po River in the northwest, iii) the formation of dense water masses in the northern Adriatic and the South Adriatic Pit facilitating oxygen transport to greater depths and iv) outflow of dense waters towards the Mediterranean basin. Given its semi-enclosed nature, the Mediterranean basin is recognized as a climate change hotspot, with the Adriatic Sea already exhibiting significant alterations, including a recorded sea surface temperature increase of 1.03°C between 1979 and 2015 (Šolić et al., 2018).

As a shallow coastal basin, the Adriatic Sea exhibits high biogeochemical activity, with sediments accumulating substantial organic material from freshwater inputs, industrial activities and primary production by phytoplankton and benthic microalgae (Šolić et al., 2016). Research on benthic microorganisms in the eastern Adriatic has primarily focused on benthic prokaryotes in polluted locations (Korlević et al., 2015; Di Cesare et al., 2020; Jokanović et al., 2021), seagrass sediments (Markovski et al., 2022) and aquaculture sites (Kolda et al., 2020). However, most studies have examined seawater prokaryotes (Šolić et al., 2018; Beg Paklar et al., 2020; Šantić et al., 2021)

Korlević et al. (2015) analyzed the diversity of benthic microbial community at two sites, Pula and Rijeka, identifying high and very high concentrations of PAHs at two out of seven locations studied. *Proteobacteria* emerged as the dominant phylum, followed by *Firmicutes* and *Bacteroidetes*. At the class level, *Gammaproteobacteria*, *Clostridia* and *Alphaproteobacteria* were the most abundant (Korlević et al., 2015). Investigations in the polluted Port of Pula indicated that heavy metal concentrations influence the benthic microbial composition, with metal resistance genes detected. However, nutrient availability, particularly total carbon and nitrogen, exerted a stronger influence on community structure (Di Cesare et al., 2020).

Regarding benthic protists, previous studies have focused on benthic diatoms and epiphytic diatom communities associated with the seagrass *Posidonia oceanica* and green macroalgae of the

genus *Caulerpa* (Kaleli and Car, 2024). A study of epiphytic diatoms of the invasive *Caulerpa taxifolia* and *Caulerpa cylindracea* revealed 65 genera, with *Mastogloia*, *Amphora*, *Diploneis*, *Nitzschia*, *Navicula* and *Cocconeis* being the most abundant (Car et al., 2019). In the planktonic community, diatoms dominate in the eastern Adriatic, followed by dinoflagellates. Notably, a positive correlation has been observed between phytoplankton abundance, particularly diatoms and coastal areas subject to anthropogenic pressures, such as Šibenik Bay (Viličić et al., 2002).

Fungal communities in the Adriatic Sea remain largely unexplored, particularly in sediments. Early research by Muntañola-Cvetković and Ristanović (1980) identified 498 fungal isolates from seawater samples in the southern Adriatic, with *Penicillium* and *Aspergillus* being the most prevalent. More recently, a substantial fungal presence was found in seawater samples from the anchialine caves in the Kornati islands. The highest relative abundance of fungi (69.9% of the total microbial reads) was detected in hypoxic zones, where genera *Malassezia*, *Cladosporium* and *Pseudobensingtonia* dominated the fungal community (Kajan et al., 2022). Similarly, a study of seawater samples from the Gulf of Trieste found Dikarya (*Ascomycota* and *Basidiomycota*) as dominant, with *Parengyodontium album* being the most abundant species. However, the authors highlighted the challenges in detecting marine fungi due to the use of broad eukaryotic primers targeting the 18S rRNA gene, which may lead to an underestimation of marine fungal diversity. Additionally, the detection of terrestrial fungal spores from nearby coastal areas using the 18S rRNA gene may bias the interpretation of marine fungal communities (Banchi et al., 2024).

Studies on the structure and function of benthic microbial communities in the eastern Adriatic remain limited, particularly regarding fungi and protists. A comprehensive study across multiple coastal sites was needed to identify the drivers of microbial community assembly and interactions, particularly in areas under multiple anthropogenic pressures, such as ports and bays.

2. Aims and objectives

This study aimed to provide novel insights into the dynamics of benthic microbial communities in long-term polluted ports and bays along the Croatian part of the Adriatic coast.

The main objectives of this study were as follows:

1. To determine the structure, diversity and interactions of benthic microbial communities (prokaryotes, fungi and protists) at polluted locations in comparison to control locations along the eastern Adriatic coast.

2. To identify the indicator potential of benthic microbial communities as markers of marine environmental conditions.

3. To identify and characterize bacterial isolates resistant to selected pollutants present in the sediment.

Based on these objectives, the following three hypotheses were tested:

1. Under chronic anthropogenic pressures, the structure, diversity and/or interactions of benthic microbial communities are altered compared to those at control locations.

2. Specific benthic microorganisms and/or their properties exhibit indicator potential for assessing anthropogenic pressures.

3. Members of the benthic bacterial community under chronic anthropogenic pressure develop resistance to pollutants present in the sediment.

3. Materials and methods

To provide a clear overview of the experimental and analytical workflow used in this study, a schematic diagram is presented below (Figure 1).

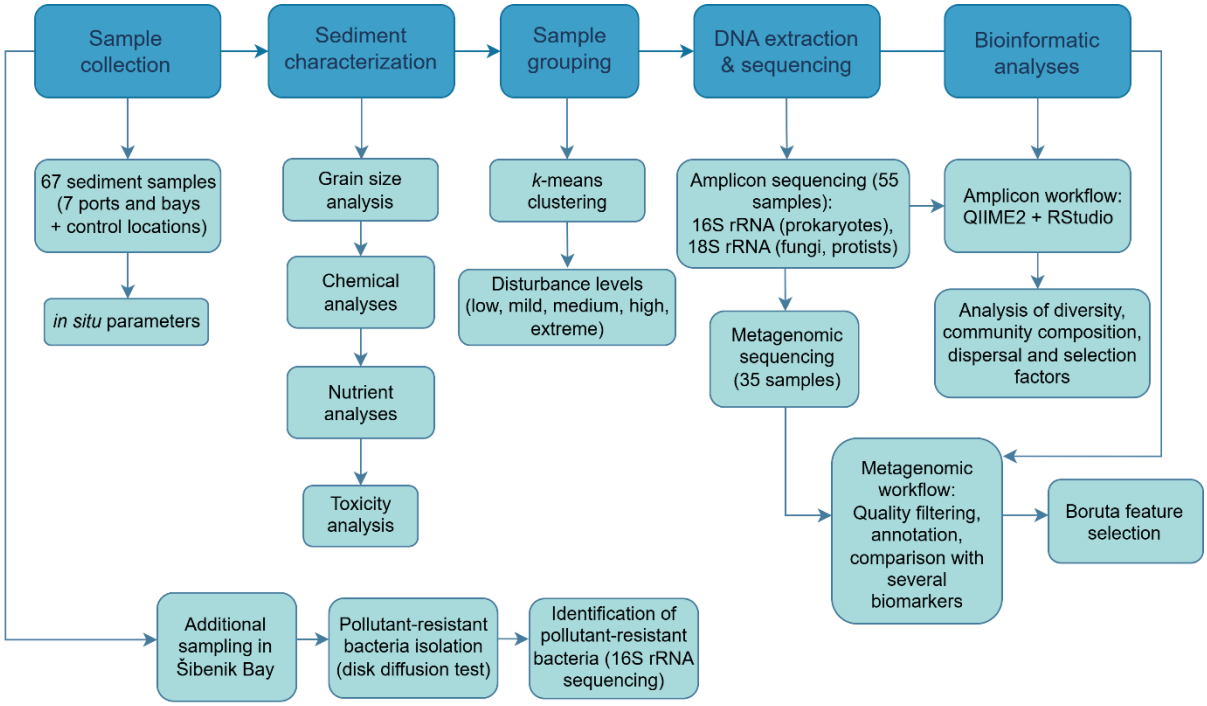

Figure 1. Overview of the methodological workflow used in the study.

3.1. Sampling campaigns and sample preparation

In total, 67 sediment samples were collected in seven ports and bays along the Croatian part of the Adriatic coast during a two-week period in the spring of 2021. The surface sediment (upper 5 cm) was taken from a boat using the Van Veen grab sampler. Detailed information on the sediment samples, including sample names and coordinates, is provided in Table S1. Four sampling locations in the northern Adriatic included: Port of Pula, Raša Bay, Port of Rijeka and Bakar Bay. Three sampling locations in the southern Adriatic included: Šibenik Bay, Vranjic Basin (eastern part of Kaštela Bay) and Port of Split (Figure 2). These locations are known to be continuously exposed to various pressures, caused mainly by anthropogenic activities, as shown in Table 1. They are currently primarily affected by tourism and maritime traffic. Furthermore, the environmental status of these locations is continuously monitored through the national monitoring programme, established under the *Strategy for the Management of the Marine Environment and Coastal Area* of the Republic of Croatia, as part of the implementation of the MSFD (Ministry of Environmental Protection and Energetics, 2019). According to the official monitoring

results provided by Croatian Waters upon request, the ecological status of the selected locations has been classified as “bad” or “very bad”, while the chemical status was “unsatisfactory”.

Additionally, sediment samples were collected from three control locations, one in the north – Cape Kamenjak and two in the south – Zlarin Island and Vis Island (Figure 1). These locations are under minimal influence from anthropogenic activities. Cape Kamenjak and Vis Island also belong to the protected Natura 2000 areas, designated under the EU Habitats Directive (HD, 92/43/EEC).

During the sampling campaigns, physicochemical parameters were measured in the undisturbed sediment immediately after sampling, as well as in the bottom water layer, using the ion-selective electrodes (InLab Redox and InLab Solids, Mettler Toledo). The parameters measured *in situ* included sediment and bottom water temperature, salinity, depth (sediment sampling depth, measured with a handheld digital depth sonar, Vexilar), sediment pH and oxidation-reduction potential (ORP). The ORP values were converted to E_h values (vs. the standard hydrogen electrode) at 25 °C (Nordstrom and Wilde, 1998). Sediment samples were transferred to the laboratory on ice, thoroughly mixed and stored at either −20 °C or 4 °C, depending on the subsequent analysis.

For microbial analysis, grain size analysis, multi-element and toxicity analyses and total nitrogen, phosphorus and TBT content analyses, the samples were frozen at −20 °C. For Hg content analysis, the samples were air-dried. Samples for grain size, multi-element and TBT analyses were further prepared by freeze-drying (Freezone 2.5, Labconco). The latter two were also homogenized into a fine powder using a ball mill (Pulverisette 7, Fritsch). For phosphorus analysis, freeze-dried sediment samples were ground and sieved ($\varphi < 250$ µm).

Additional sampling was conducted in the summer 2023 in Šibenik Bay (corresponding to the previously analyzed SI5 sample) using the same methods described above. In addition, for the isolation of bacteria resistant to specific pollutants, sediment samples were stored at 4 °C and used within 24 h.

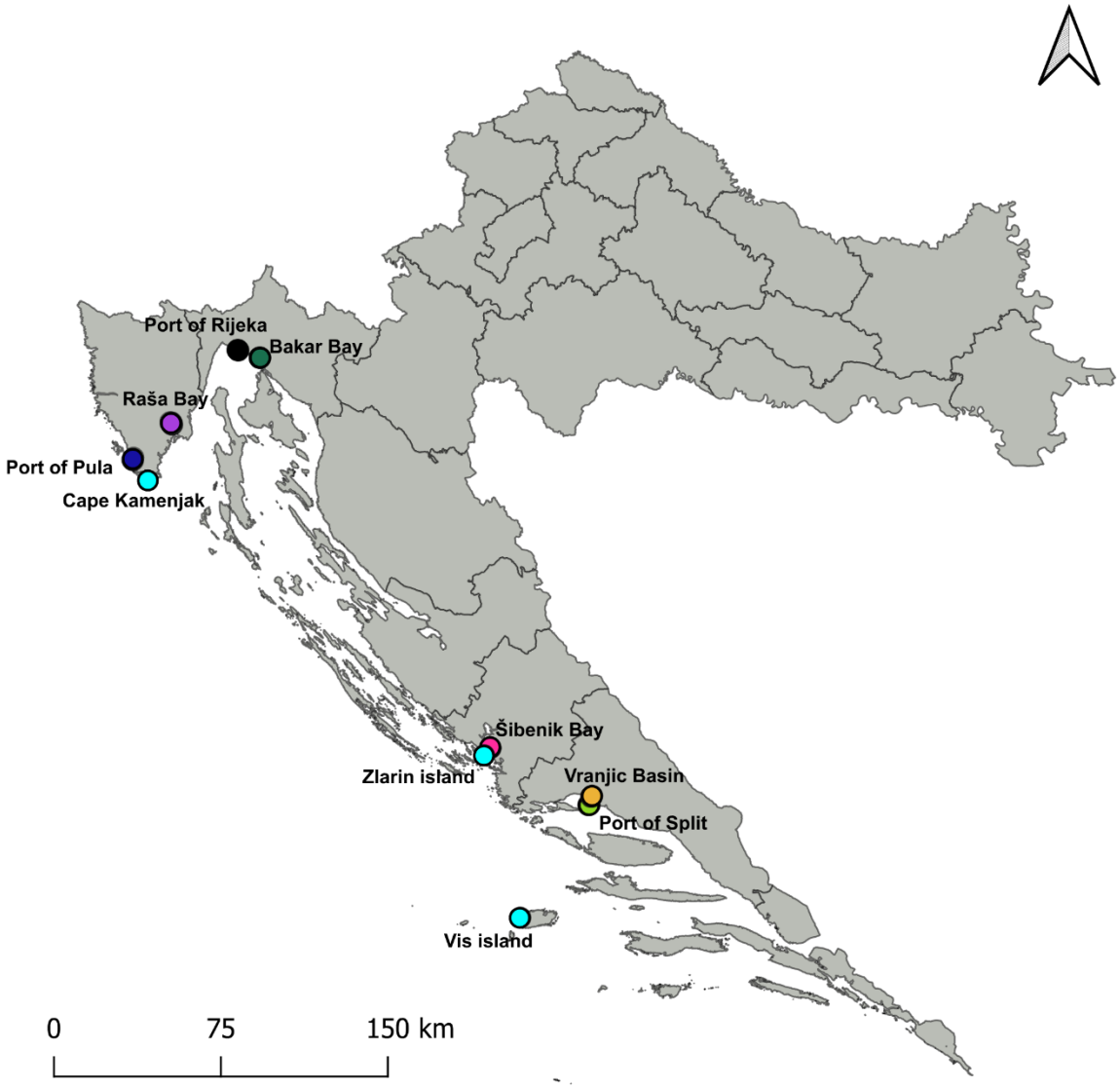

Figure 2. Sampling locations along the eastern Adriatic coast, with control locations marked in cyan blue.

Table 1. Anthropogenic activities in selected polluted sampling locations along the eastern Adriatic coast and the main groups of pressures defined according to ANNEX III of MSFD (2008/56/EC).

Sampling location	Anthropogenic activities	Pressures defined according to MSFD (2008/56/EC) ANNEX III*
Port of Pula (PU1-PU7)	Passenger port terminal (ferries and small boats) Shipyard (est. 1856) Marina Discharge from smaller recreational vessels and former municipal wastewater discharge (until 2015)	Systematic and/or intentional release of substances Nutrient and organic matter enrichment Contamination by hazardous substances Biological disturbance
Raša Bay (RA1-RA10)	Port terminal (general cargo, timber and livestock) Small urban discharge and discharge from smaller recreational vessels Small marina and port Aquaculture Runoff from agricultural areas (estuary)	Systematic and/or intentional release of substances Nutrient and organic matter enrichment Biological disturbance
Port of Rijeka (RI1-RI5)	The third biggest city in Croatia Passenger port terminal (cruise ships, ferries and small boats) Biggest national cargo port Ballast water discharges and small urban discharges Former phosphorous transshipment operations and industry discharges	Nutrient and organic matter enrichment Contamination by hazardous substances Biological disturbance
Bakar Bay (BA1-BA11)	Former coke plant Petroleum refinery Tanker berth Terminal for bulk cargo (iron ore, coal and other bulk cargoes) Urban discharges from wider area	Systematic and/or intentional release of substances Contamination by hazardous substances Biological disturbance Other physical disturbance (underwater noise, marine litter)
Šibenik Bay (SI1-SI7)	Passenger port terminal and marina Discharge from smaller recreational vessels Shipyard (est. 1992) Terminal for bulk cargo Former phosphorous transshipment operations and former industry ferrous alloy production factory (until 1994) Former municipal wastewater discharge (until 2007)	Nutrient and organic matter enrichment Contamination by hazardous substances Biological disturbance Other physical disturbance (underwater noise, marine litter)
Vranjic Basin (VR1-VR9)	Former industrial and municipal wastewater discharge (until 2005) Former chemical industry (until 1991) Shipyard and multipurpose container cargo terminal Grain terminal Dry cement manufacturing Small marina, discharge from smaller recreational vessels Freshwater inflow contamination by several sewage outfalls Septic tanks and small urban discharges Runoff from agricultural areas	Nutrient and organic matter enrichment Contamination by hazardous substances Systematic and/or intentional release of substances Biological disturbance Other physical disturbances (underwater noise, marine litter)
Port of Split (ST1-ST10)	The second largest city in Croatia Passenger port terminals (cruise ships, ferries, small boats, yachts) and multipurpose cargo ports Marina and discharge from smaller recreational vessels Municipal wastewater discharge (city overflow) Third largest passenger port in the Mediterranean and largest in Croatia Shipyard (est. 1932) Natural sulfur spring	Nutrient and organic matter enrichment Contamination by hazardous substances Biological disturbance Other physical disturbances (underwater noise, marine litter)

*Indicative lists of characteristics, pressures and impacts (referred to in Articles 8(1), 9(1), 9(3), 10(1), 11(1) and 24) art.

3.2. Chemical, nutrient and toxicity analyses of collected sediments

Various analyses were performed to determine the level of anthropogenic disturbance in the sampled sediments. These analyses included the following:

1. Grain size analysis
2. Chemical analyses
    1. Multielement analysis and determination of metal(oid)s local enrichment factors (LEFs)
    2. Determination of bioavailable fraction of metal(oid)s
    3. Tributyltin (TBT) analysis
    4. Mercury (Hg) content analysis
3. Nutrient analyses
    1. Total nitrogen (TN) and total carbon (TC) content analysis
    2. Total phosphorus (TP) content analysis
4. Toxicity analysis
    1. Sediment toxicity level (Microtox test)

3.2.1. Grain size analysis

The grain size of sediments was determined using a laser-based particle size analyzer (LS 13 320, Beckman Coulter). Grain size was calculated using Mie theory of light scattering (optical parameters: refractive index = 1.53, absorption index = 0.1). Considering the ratio of different grain-size fractions (clay, silt and sand), sediments were classified according to Shepard classification (Shepard, 1954; Figure S1).

3.2.2. Chemical analyses

3.2.2.1. Multielement analysis and determination of metal(oid)s local enrichment factors (LEFs)

Multielement analyses were performed using high-resolution inductively coupled plasma mass spectrometry (HR ICP-MS; Element 2, Thermo Fisher Scientific), as described in Fiket et al. (2017). Prior to analysis, sediments were digested in a microwave oven (Multiwave 3000, Anton Paar) following a two-step total digestion procedure: Step I – 5 ml HNO_3 (65% p.a.) + 1 ml HCl (36% s.p.) + 1 ml HF (48% s.p.) and Step II – 6 ml H_3BO_3 (40 g/l). For quantification, the external calibration method was employed with diluted multielement standard solutions (in the range of 0.1–10 µg/l), prepared from multielement or combined single reference standard solutions (Analytika). Analytical quality control was performed

through simultaneous analysis of procedural blanks and certified reference materials of marine sediments (MESS-3, NRC). Recovery rates ranged from 90 to 102% (Fiket et al., 2017). The limit of detection (LOD) was calculated as three times the standard deviation of ten consecutive measurements of the procedural blank, with values ranging between 0.01 and 0.03 mg/kg. The limit of quantification (LOQ), calculated as ten times the standard deviation, was approximately three times higher than the LOD.

To assess the pollution level in terms of metal(oid)s in the sediments, the concept of the local enrichment factor (LEF) was applied (Álvarez-Vázquez et al., 2023; Lučić et al., 2023). This approach helps differentiate between natural and anthropogenic origin of elements and is particularly effective in reducing the natural (background) factors, such as grain-size effects, effects of dilution by a predominant matrix phase and the different provenances, that can significantly influence element concentrations in sediments (Matys Grygar and Popelka, 2016; Birch, 2017; Lučić et al., 2023). The background data used for the calculation of LEF derived from a comprehensive dataset collected in the Adriatic Sea since 2012, as part of Croatia's national monitoring program under the WFD and the MSFD. These datasets have been published in several studies (Cukrov et al., 2011; Cukrov et al., 2014; Cukrov et al., 2024; Felja et al., 2016; Fiket et al., 2021; Surricchio et al., 2019; Ujević et al., 2000). The minimum, median and maximum concentrations of the measured elements at control locations, used as background, are provided in Table S2. The LEF was calculated using the formula: $LEF = E / E_{BN}$; $E_{BN} = f(E_{REF})$, where E_{BN} stands for background normalization and E_{REF} for the reference element. In this case, the LEF was determined by the empirical background function $f(E_{REF})$, which best describes the relationship between the target elements (As, barium [Ba], bismuth [Bi], Cd, cobalt [Co], Cu, Cr, manganese [Mn], nickel [Ni], Pb, antimony [Sb], tin [Sn], uranium [U] and Zn) and the predictive element (Al). Al was selected due to its role as a key constituent of the main carriers of potentially toxic elements (PTEs) and its strong correlation with these elements (Figure S2).

3.2.2.2. Determination of bioavailable fraction of metal(oid)s

The bioavailable fraction of metal(oid)s in sediment samples was determined using the modified BCR (Community Bureau of Reference, European Commission) sequential extraction procedure (Kartal et al., 2006). In this procedure, 2.0 g of lyophilized sediment was treated with 20 mL of 0.11 M acetic acid, followed by overnight shaking (300 rpm). The samples were then centrifuged for 20 min at 4000 × *g* and filtered using the Millipore PES (polyethersulfone) membrane filters with 0.45 µm pore size. Finally, the filtrates were diluted 100 times and analyzed by high-resolution inductively coupled plasma mass spectrometry (HR ICP-MS; Element 2, Thermo Fisher Scientific).

3.2.2.3. Tributyltin (TBT) analysis

TBT analysis was conducted following the procedure outlined in Furdek Turk et al. (2020). TBT was extracted using acetic acid and ultrasonic stirring, while derivatization was performed with $NaBEt_4$ in a sodium acetate-acetic acid buffer (pH 4.8) by mechanical shaking. The analysis was performed using a gas chromatograph (GC; Varian CP-3800) with a pulsed flame photometric detector (PFPD; Varian). Quality control was performed by analyzing the standard reference materials certified for TBT in coastal sediments (BCR-462, European Commission, JRC) and freshwater sediments (BCR-646, European Commission, JRC), with recovery values falling within the certified range. Tripropyltin (TPrT) was used as an internal standard. The detection limit was 1.0 ng/g.

3.2.2.4. Mercury (Hg) content analysis

Concentration of Hg in air-dried sediment samples (expressed in mg/kg dry matter) was analyzed at the Institute of Public Health of Primorje-Gorski Kotar County using the AMA254 Mercury Analyzer. The analysis was conducted according to the accredited in-house method M 146–200 (Edition 1, 15 November 2019; Adapted method according to the producer manual: AMA 254 Advanced Mercury analyzer Operation manual, 2002). Accuracy control was performed for each set of samples by using certified reference materials IAEA-405 and IAEA-MEL-2017-01-TE of the International Atomic Energy Agency (IAEA). The recovery ranged from 85 to 105%.

The grain size analysis and the chemical analyses were conducted in collaboration with the Laboratory for Inorganic Environmental Geochemistry and Chemodynamics of Nanoparticles (Ruđer Bošković Institute, Zagreb, Croatia).

3.2.3. Nutrient analyses

3.2.3.1. Total nitrogen and total carbon content

The contents of total nitrogen (TN, %) and total carbon (TC, %) were analyzed at the University of Zagreb, Faculty of Agriculture using a CHNS analyzer (Elementar). The analyses followed standardized ISO methods: *HRN ISO 10694:2004* (Soil quality – Determination of organic and total carbon after dry combustion (elementary analysis)) for TC and *ISO 13878:1998* (Soil quality – Determination of total nitrogen content by dry combustion (elemental analysis)) for TN. Total inorganic carbon (TIC) was determined using the *HRN ISO 10693:2004* (Soil quality – Determination of carbonate content – Volumetric method). Based on TC and TIC the amount of organic carbon (TOC) was calculated. Results are presented in percentages of dry matter (dried at 105 °C to constant mass).

3.2.3.2. Total phosphorus content

The total (TP) and inorganic (IP) phosphorus contents in sediment samples were determined following the method described by Aspila et al. (1976) in the Laboratory for Chemical Oceanography and Sedimentology of the Sea at the Institute of Oceanography and Fisheries (Split, Croatia). Phosphorus concentrations in extracted solutions were measured using a Shimadzu UV-VIS Spectrophotometer. To evaluate the method's accuracy, certified reference sediment PACS-2 (Canadian Institute for National Measurement Standards NRC-CNRC) and estuarine sediment NIST 1646a (National Institute of Standards and Technology) were used.

3.2.4. Toxicity analysis

3.2.4.1. Sediment toxicity level (Microtox test)

The potential toxicity of sediment organic extracts was measured by Microtox bioassay, a sensitive screening tool for determining sediment toxicity in areas under different anthropogenic pressures (Bihari et al, 2007; Fafanđel et al., 2015) in the Laboratory of Marine Ecotoxicology and Bioremediation, in the Center for Marine Research (Rovinj, Croatia). Organic extracts were prepared according to Bihari et al. (2007). Briefly, 50 g of sediment sample (wet weight) was mixed with 100 ml of methanol for 1 h and the methanol extract was then filtered (1 µm pore size filters). Dichloromethane:methanol (2:1; v/v) was added to the sediment (6:1; v/w) and left to mix overnight. The extract was filtered (1 µm pore size filters) and combined with the methanol extract. To remove residual methanol, the combined extract was washed with water several times. Dichloromethane extracts were then evaporated to dryness and dissolved in 50 µl dimethylsulfoxide (DMSO).

The toxicity was measured by observing the decrease in luminescence of the bacterium *Aliivibrio fischeri* after exposure to a series of 1:2 dilutions of the organic extract, according to the BioFix Lumi procedure prescribed by the manufacturer (Macherey-Nagel). The luminescence was measured using the Microtox Model 500 luminometer (AZUR, Environmental). Estimates of EC_{50} values were obtained using MicrotoxOmni Software package. Toxicity level was calculated using the formula: 1 / EC_{50} (µg) × 1000.

3.3. Grouping sediments based on anthropogenic disturbance levels

An unsupervised *k*-means clustering method (Xu et al., 2021; Ikotun et al., 2023) was applied to the dataset, which included all relevant data indicating anthropogenic pressures at the sampling locations. This approach was used to identify potential groupings of sediment samples based on the presence and levels of measured pollution within the samples. The parameters included in the analysis were: LEFs of As, Ba, Bi, Cd, Co, Cu, Cr, Mn, Ni, Pb, Sb, Sn, U, Zn, TBT, TN, TP, Hg and toxicity level. The *k*-means clustering aims to divide the dataset into k non-overlapping clusters, assigning each observation to the nearest center to maximize the between-cluster variance and minimize the within-cluster variance. To address the limitations of *k*-means clustering (poor performance when the variables differ in absolute frequency by several orders of magnitude and the data are highly skewed), the data were log-transformed before *k*-means clustering was applied. The optimal number of clusters was determined using the Silhouette method. The resulting groups were classified according to different levels of anthropogenic disturbance in the sediment samples (hereafter referred to as DL).

3.4. DNA extraction and sequencing

Total DNA was extracted from 0.3 to 0.5 g of wet sediment samples using the DNeasy PowerSoil Pro kit (QIAGEN), following the manufacturer's protocol. The quantity of the extracted DNA was determined using the QUBIT fluorometer (Thermo Fisher Scientific) and the quality was checked using both Biospec Nano (Shimadzu) and agarose gel electrophoresis. Three marker genes were selected for amplicon sequencing using the extracted total DNA as a template: (i) the V4 region of the 16S rRNA gene, (ii) the V7-V8 region of the 18S rRNA gene for fungi (Banos et al., 2018) and (iii) the V9 region of the 18S rRNA gene for protists (Stoeck et al., 2010). The primers used are listed in Table S3. The obtained amplicons were sequenced by Novogene Bioinformatics Technology Co., Ltd. (UK) using the Illumina NovaSeq PE250 platform. Raw sequence reads were deposited into European Nucleotide Archive (ENA) under project accession code PRJEB72621.

3.5. Bioinformatic analyses of amplicon sequence data

The amplicon sequence data were analyzed using the *Quantitative Insights Into Microbial Ecology 2* (QIIME2) software (release 2022.2; Bolyen et al., 2019). The raw, demultiplexed paired-end fastq files were imported into QIIME2 using the manifest file. The imported sequences were denoised, dereplicated and filtered for chimeras using the DADA2 plugin (Callahan et al., 2016). The resulting amplicon sequence variants (ASVs) were aligned with mafft and used to construct a phylogenetic tree using fasttree2 via the q2-phylogeny plugin. Taxonomy was assigned to ASVs using a pre-trained Naïve Bayes classifier and a reference database generated with RESCRIPt (Robeson et al., 2021), based on the Silva SSU Ref NR 99, release 138.1 database (https://www.arb-silva.de; Quast et al., 2013).

3.5.1. Analysis of diversity and composition of microbial communities

Amplicon sequence data processing and visualization was carried out in R (version 4.2.2). Alpha and beta diversity were analyzed using the *phyloseq* package (version 1.46.0; McMurdie and Holmes, 2013) and the results were visualized using the *ggplot2* package (version 3.4.4; Wickham, 2016). For data manipulation packages *tidyr* (version 1.3.0; Wickham et al., 2023), *dplyr* (version 1.1.4; Wickham et al., 2023) and *vegan* (version 2.6.4; Oksanen et al., 2022) were used. For alpha diversity analysis, the Shapiro-Wilk test was used to test the normality of the data distribution. Based on the results, for testing the statistical differences, Kruskal-Wallis and Dunn's post hoc test (with Benjamini-Hochberg adjustment of *p*-values) were used or the one-way ANOVA (Analysis of variance) with Tukey's HSD post hoc test. For testing the significant differences of beta diversity between disturbance levels, PERMANOVA (Permutational analysis of variance) of the Bray-Curtis dissimilarities was performed with the adonis2

function. Afterwards, a pairwise PERMANOVA was used to compare each DL with Benjamini-Hochberg adjustment of *p*-values. The median relative abundance for each disturbance level (DL) was calculated and used for further analysis and visualization of community composition. To examine the changes of relative abundances across the defined disturbance levels, log2 fold changes were calculated based on the relative abundances of families across all samples. To test the significant differences between the DLs, Wilcoxon rank sum test was used with Benjamini-Hochberg adjustment of *p*-values.

3.5.2. Identification of factors structuring microbial communities

The collected data were separated into dispersal and selection factors that shape microbial communities.

Dispersal factors included:

(i) sampling location (Port of Pula, Raša Bay, Port of Rijeka, Bakar Bay, Šibenik Bay, Vranjic Basin, Port of Split, control locations),

(ii) sampling region (northern vs. southern Adriatic),

(iii) grain type (silt, silty sand, sandy silt, clayey silt),

(iv) depth.

Selection factors included:

(i) sediment temperature,

(ii) bottom water layer temperature,

(iii) sediment pH,

(iv) sediment redox potential,

(v) sediment toxicity,

(vi) contamination status (contaminated vs. non-contaminated sites),

(vi) disturbance level (low, mild, medium, high and extreme),

(vii) pollutants: TBT, metals (total and bioavailable fractions),

(viii) nutrients: total nitrogen, total phosphorus, total organic carbon.

Data manipulation and visualization were done using RStudio (version 4.3.2; R Core Team, 2023) and various R packages, including *phyloseq* (version 1.46.0; McMurdie and Holmes, 2013), *vegan* (version 2.6.4; Oksanen et al., 2022), *ggplot2* (version 3.4.4; Wickham, 2016), *data.table* (version 1.14.10; Barrett et. al., 2023), *reshape2* (version 1.4.4; Wickham, 2007), *dplyr* (version 1.1.4; Wickham et al., 2023), *stringr* (version 1.5.1; Wickham, 2023), *cowplot* (version 1.1.3; Wilke, 2024) and *patchwork* (version 1.2.0; Pedersen, 2024). A Principal Coordinate Analysis (PCoA) was used to visualize the

similarity between microbial communities. The distance-decay relationship (DDR) was assessed using a nonlinear regression of Bray-Curtis dissimilarities relative to geographical distance (in kilometers) between communities. The distHaversine function from the *geosphere* package (version 1.5.19; Hijmans, 2023) was used to calculate the shortest distance between two points while assuming a spherical Earth. The function decay.model from *betapart* package (version 1.6; Baselga et al., 2023) was used to fit a nonlinear model describing the increase in microbial dissimilarity with distance. To identify significant factors influencing each microbial community, PERMANOVA analyses (using the adonis2 function) were performed on both abundance-based (Bray-Curtis) and incidence-based (Sørensen) similarity matrices. Factors were categorized as dispersal and selection factors, as described above, with p-values < 0.01 considered significant. To assess the impact of pollution on interactions between microbial communities, specific heavy metal pollutants (selection factors) were selected for the analysis. For each selected pollutant, samples were divided into high- and low- pollution groups based on the median concentration. More specifically, samples with low and mild disturbance levels were assigned to the low-pollution group, while those with medium, high or extreme disturbance levels were classified as high-pollution. Mantel tests (using Pearson correlations) were performed between pairs of microbial communities—prokaryotes–fungi, prokaryotes–protists and protists–fungi—within each pollutant group.

3.5.3. Identification of potential microbial indicators

To identify potential microbial indicators, the *DESeq2* package (version 1.14.1) in RStudio (Love et al., 2014) and Classification and Regression Tree (CRT) methodology (Alkhasawneh et al., 2014) were applied. DESeq2 offers a nuanced view of abundance changes at a finer taxonomic resolution, while CRT offers a broader, model-driven perspective on the environmental impacts on microbial communities. DESeq2 uses a model based on negative binomial distribution, ideal for sequencing data, to analyze differential ASV abundance related to different environmental conditions. It was used to identify specific microbial families or ASVs with differing abundance (i) within distinct DLs and (ii) between polluted samples (integrating mild, medium, high and extreme DLs) and unpolluted samples (low DL). The CRT method, which uses decision tree analysis, creates predictive models for classifying data as “key indicator variables”. By partitioning the dataset based on informative environmental variables, CRT constructs a hierarchical structure of decision rules (Alkhasawneh et al., 2014) and was used to identify specific taxonomic groups as “key indicator variables” that can act as indicators of different DLs. It is important to note that these two analyses were performed using the sequences for all 55 samples after the processing of amplicon sequencing data in QIIME. CRT analyses were done in collaboration with experts at Algebra Bernays University (Zagreb, Croatia).

3.6. Bioinformatic and biostatistical analyses of metagenomic sequence data

Library preparation and metagenomic sequencing were carried out by Novogene Bioinformatics Technology Co., Ltd. (UK) using an Illumina NovaSeq sequencer, which generated 2 x 150 bp reads following standard protocols. Due to financial constraints, a smaller subset of samples (35 samples, as shown in Table S4) was selected for metagenomic sequencing. The retrieved metagenomic sequences were analyzed in collaboration with Biochemistry and Biotechnology Department, University of Thessaly, Greece. Sequence reads underwent quality assessment and trimming, applying a minimum Phred quality score (measurement of the quality of identified bases) of 20 within a sliding window of four bases, while retaining reads of 70 million bp. Where possible, read pairs were assembled into their inserts of origin using the fastp software (version 0.21.0; Chen et al., 2018). These DNA fragments correspond to the inserts where adapters were added via tagmentation during Illumina library preparation. Three types of sequences were used for annotation by comparison against a range of databases: (i) assembled reads, where both paired reads passed quality control and were merged (joined into a single contig), (ii) forward reads from pairs where only the forward read passed quality control and (iii) reverse reads from pairs where only the reverse read passed quality control. In cases where both reads of a pair passed quality control but could not be merged due to a lack of sufficient overlapping, the two reads were kept separate. For mapping against databases, one read per pair was used to avoid double-counting, typically the forward read. The comparison was performed using DIAMOND (version 2.0.15.153; Buchfink et al., 2015), with an e-value threshold of 1×10^{-10}, identities of 70% and a minimum translated sequence length of 30 amino acids. The following databases (hereafter referred to as biomarkers) were used for annotation:

I. *ResFinder* (version 4.0.0; Bortolaia et al., 2020) for clinically relevant antibiotic resistance genes (ARGs; hereafter referred to as *ARG (resfinder)*)
II. *BacMet* (version 2.0; Pal et al., 2014) for resistance to metals and disinfectants (hereafter referred to as *Biocides*)
III. *AromaDeg* (Duarte et al., 2014) for aromatic hydrocarbon degradation genes (hereafter referred to as *AHC degradation*)
IV. *NanoARG* for mobile genetic element marker genes (hereafter referred to as *MGE*; Arango-Argoty et al., 2019)
V. *VFDB* for virulence factor coding genes (hereafter referred to as *Virulence*; Liu et al., 2022)
VI. *SEED* for generic functional gene annotation (hereafter referred to as *SEED;* Overbeek et al., 2014)

VII. *DeepARG* (version 2.0; Arango-Argoty et al., 2018) and diamond-based machine learning algorithm were used for annotating ARGs with increased sensitivity (hereafter referred to as *ARG (deepARG)*)

VIII. *Kaiju* (version 1.7.3; Menzel et al., 2016) was used for the taxonomic annotation of prokaryotes, eukaryotes and viruses (hereafter referred to as *Taxonomy*). Parallel BLAT (version 36x2; Wang and Kong, 2019) was used to search against the SILVA database (version 138; Prüsse et al., 2011) and to quantify 16S rRNA genes. These counts served as a basis for normalizing gene hit counts to approximate per-cell counts and reduce compositional bias in the metagenomic data (Gloor et al., 2017; Jian et al., 2021).

3.6.1. Coverage of genetic content, biomarkers and alpha diversity analysis

The Nonpareil algorithm (version 3.304; Rodriguez-R and Konstantinidis, 2014a; Rodriguez-R and Konstantinidis, 2014b) was applied alongside the Nonpareil data analysis package (version 3.3.1; Rodriguez-R, 2018) in RStudio (version 4.2.2; R Core Team, 2022) on the quality-controlled sequences to assess the achieved sequencing coverage. The Good's coverage estimate (Good, 1953) was employed to assess the achieved coverage of all biomarkers. The post-annotation gene matrices were subjected to alpha diversity analysis. Alpha diversity was assessed using several indices: observed richness, estimated richness via the ACE index (Abundance-based Coverage Estimator; Chao, 1987), the Shannon index (Shannon, 1948), the Simpson's reciprocal index (Simpson, 1949) and the Fisher's α index (Fisher et al., 1943). The calculations of indices were performed using the *entropart* (version 1.6-11; Marcon and Hérault, 2015) and the *vegan* (version 2.6-4; Oksanen et al., 2022) R packages. All data were combined to a phyloseq object for downstream manipulation with the *phyloseq* (version 3.16; McMurdie and Holmes, 2013) R package. Furthermore, read counts were normalized by dividing them by 16S rRNA gene counts as annotated by the SILVA 138 database. This approach addresses the compositionality issue of the sequencing data by using the 16S rRNA gene counts as an internal sample control (Gloor et al., 2017). Additionally, for visualization purposes, range scaling of values (minimum–maximum) was performed using the decostand function from the *vegan* package.

3.6.2. Identification of most important features using Boruta algorithm

The most important features of the dataset were selected based on location (i.e. sampling location) for *Taxonomy*, *SEED*, *AHC degradation*, *Biocides* and *ARG (deepARG)* biomarkers. These features were identified using the *Boruta algorithm*, a random forest algorithm derivative and the corresponding package (*Boruta* version 8.0.0; Kursa and Rudnicki, 2010) in RStudio, exploiting the regression random forest model and the normalized counts (feature read counts divided by the 16S rRNA gene counts) of the sequencing features. Additionally, for visualization purposes, range scaling of values (0–1) was performed using the decostand function from the *vegan* package.

3.7. Isolation and characterization of pollutant-resistant bacteria

To isolate and identify pollutant-resistant bacteria, additional sediment samples were collected from Šibenik Bay in 2023, as described in section 3.1. Bacterial isolates were obtained by inoculating 1 ml of sediment suspension (prepared by mixing one gram of sediment in 100 ml of artificial seawater) onto Difco Marine agar plates. These plates were then incubated at 26 °C until visual growth of colonies. Separate bacterial colonies were picked from the plates using a sterile loop and subcultured several times onto fresh Marine agar plates until pure isolates were obtained. Based on their presence in the sampled sediments and environmental relevance, ten pollutants were selected to test the resistance of the obtained bacterial isolates. These included the heavy metals tin (Sn), lead (Pb), zinc (Zn), chromium (Cr), cadmium (Cd), mercury (Hg), copper (Cu), cobalt (Co), nickel (Ni), as well as the organic compound tributyltin (TBT). A list of compounds used in the experiment is provided in Table S5. The ranges of concentrations were different for each metal, ranging from the environmentally relevant concentration to the hundred-fold concentration. Bacterial resistance to selected pollutants was determined using the disk diffusion method on Difco Marine agar nutrient plates (Figure 3). Cultures of the individual pure bacterial isolates, grown for 24 h in Difco Marine broth, were diluted with 0.85% NaCl to the required concentration of 0.5 McFarland. After dipping a sterile swab into the bacterial suspension, the entire surface of solid marine agar plates was swabbed. To determine the minimum inhibitory concentration (MIC) for each tested metal and TBT, six cellulose disks (6 mm) were placed in a Petri dish inoculated with bacteria. Different concentrations of the listed pollutants (20 µl/disk) were applied to each of the six disks. The radii of the inhibition zones were measured after 24 h of plate incubation at 26 °C, with the MIC determined for each isolate based on the clear zone surrounding the disk.

The Quick-DNA Miniprep Plus Kit (Zymo Research) was used for DNA extraction from bacterial isolates tested for pollutant resistance, following the manufacturer's protocol. DNA concentration was measured using the QUBIT 3.0 fluorometer (Thermo Fisher Scientific). To identify the isolates, the 16S

rRNA marker gene was amplified using standard primers (27F and 1492R) by polymerase chain reaction (PCR; Senko et al., 2024). Amplification success was verified by agarose gel electrophoresis. PCR products (approximately 1400 bp) were sent for Sanger sequencing to a commercial service (Macrogen, Netherlands). The raw sequences obtained were manually edited using Chromas Lite (version 2.6.6; Technelysium) and compared with sequences in the National Center for Biotechnology Information (NCBI) database via the BLASTn program (version 2.16.1+). A neighbor-joining phylogenetic tree, based on 16S rRNA gene sequences, was constructed using ClustalX and Mega X and visualized using the Interactive Tree of Life online tool (Letunic and Bork, 2021), with bootstrap values based on 1000 replicates and a substitution rate of 0.01 per nucleotide position to determine the phylogenetic placement of the isolates and related species. The 16S rRNA sequences of pure bacterial isolates have been deposited in the NCBI GenBank database under accession numbers PV643243-PV643316.

Figure 3. Example of the disk diffusion method used to assess metal and TBT resistance profiles of bacterial isolates. The method was performed on Difco Marine agar plates inoculated with bacterial colonies. Each disk was inoculated with a specific concentration of a selected pollutant.

4. Results

4.1. Chemical, nutrient and toxicity status of the collected sediments

Results from physicochemical measurements, chemical, nutrient and toxicity analyses, as well as sediment grain size analysis, conducted on the 67 sediment samples, are available in Tables S6–S10. The measured bioavailable fraction of metals is shown in Table S11.

The results indicated that sampling was conducted at locations with varying depths, ranging from 2.2 (sample ST1) to 40 m (sample RI6), with a mean sampling depth of 14.6 ± 9.1 m. The temperature of the bottom seawater layer averaged 15.2 ± 2.7 °C. The average salinity of the bottom seawater layer was 36.44 ± 0.93‰, with the highest values observed (> 37‰) in the Ports of Pula and Split, along with the three control locations. The lowest salinity values were recorded in samples from Šibenik Bay (6.52‰–7.65‰), an estuary of the Krka River and in sample RA10 from the Raša Bay (Raša River estuary). The average sediment temperature recorded was 15.1 ± 3.0 °C, with higher temperatures observed in the samples from southern Adriatic (Table S6).

Based on the Shepard's classification, the sediments were categorized into four types: clayey silt, silt, sandy silt and silty sand. Silt was the most prevalent sediment grain type, averaging 64.4 ± 14.1%, followed by sand (21.5 ± 18.6%) and clay (14.1 ± 7.3%) (Table S6).

Tributyltin (TBT) concentrations ranged from 0.5 to 5,940 ng/g d.m., with the highest concentration recorded in sample SI5 from Šibenik Bay. High TBT concentrations were observed in 57% to 78% of sediment samples from the Port of Rijeka, Vranjic Basin and Šibenik Bay, while 16 sediment samples from control locations and Raša Bay showed low TBT concentrations (Table S7).

Concentrations of Hg were low in control locations and Raša Bay, but extremely high in 70% of Šibenik Bay samples and 90% of samples from Port of Pula. The highest concentrations were recorded in sample SI5 (62 mg/kg d.m.) and SI4 (44 mg/kg d.m.) (Table S7).

TOC ranged from 1.38% (ST9) to 50.17% (BA4), with the lowest values in samples from Raša Bay. TN and TP were lowest in control locations, while the highest TP concentration was recorded in SI5 (353.94 µmol/g) and VR5 (127.69 µmol/g) and the highest TN content in BA4 (1.116%) and VR5 (1.073%) (Table S7).

Toxicity levels ranged from below 8 to above 250, with the highest value of 1,000 in sample BA6, followed by 500 in sample SI1, 417 in sample RI4 and 333 in samples PU1 and SI4. Very high toxicity was observed in 27% of sediment samples (Table S7).

Local enrichment factors (LEFs) of metal(oid)s varied considerably between sediment samples (Table S8), with the most frequently enriched elements being Mo, Cd, Sn, Pb, Bi, Cu, Zn and Sb. Very high enrichments of several metal(oid)s were observed in samples PU3, SI4 and SI5 and VR5.

Bioavailable concentrations of Cu, Zn, As, Cd, Sb and Pb varied widely among samples (Table S11). The highest concentrations were found for Pb (31,531.71 mg/kg d.m.) and Zn (219,043 mg/kg d.m.), both in sample PU3. Concentrations of As reached 2,057.67 mg/kg d.m. in sample SI1, while Sb reached 169.57 mg/kg d.m. in sample SI4. Cu showed a maximum of 348 mg/kg d.m. in sample SI1 and Cd had the highest value of 26.29 mg/kg d.m. in sample ST7.

4.2. Identification of anthropogenic disturbance levels in sediments

The *k*-means clustering method was further used to group the 67 sediment samples into different levels of anthropogenic disturbance. Prior to clustering, local enrichment factors (LEFs) for potentially toxic elements (As, Ba, Bi, Cd, Co, Cu, Cr, Mn, Ni, Pb, Sb, Sn, U and Zn) were calculated (Table S8). The data included in the *k*-means clustering analysis were those parameters considered as best for representing anthropogenic disturbance in the samples, which included: grain size, local enrichment factors (LEFs) of metal(oid)s, TBT, TN, TP, Hg and toxicity level. These input parameters revealed that the sediments could be classified into five categories based on *k*-means clustering. These categories represent five different anthropogenic disturbance levels (DLs) (Figure 4, Table 2): low disturbance level (16 samples), mild disturbance level (19 samples), medium disturbance level (18 samples), high disturbance level (10 samples) and extreme disturbance level (4 samples). Samples from control locations and Raša Bay were categorized under the low DL, while most samples from Bakar and Split clustered under the mild and medium DLs, respectively. Samples from the Vranjic Basin showed no clear geographical grouping, while samples from the Port of Pula and Šibenik Bay were assigned to the high or extreme DLs.

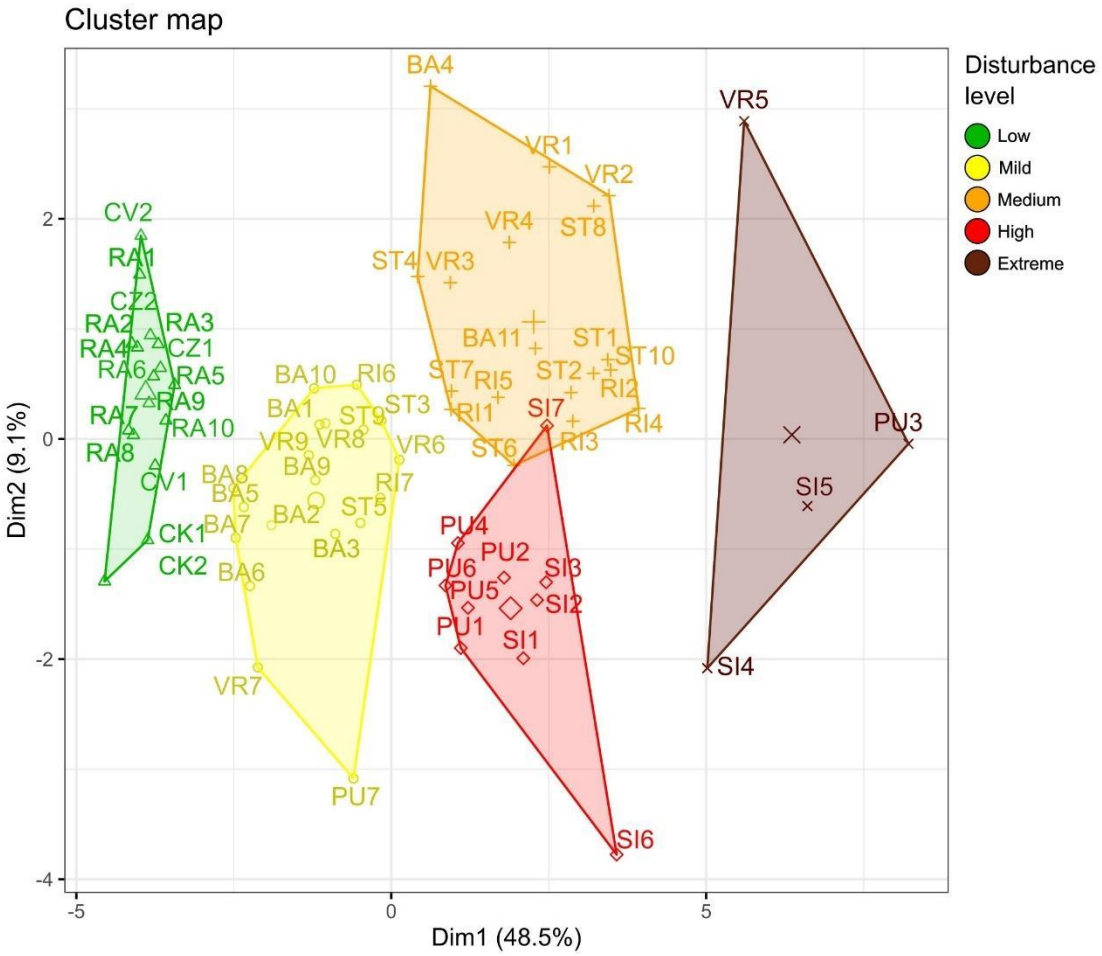

Figure 4. Five levels of anthropogenic disturbance (low, mild, medium, high and extreme) determined for 67 collected sediment samples, based on the *k*-means clustering method. CK, CZ, CV = control locations, PU = Port of Pula, RA = Raša Bay, RI = Port of Rijeka, BA = Bakar Bay, SI = Šibenik Bay, VR = Vranjic Basin, ST = Port of Split.

Table 2. Sediment samples grouped into five levels of anthropogenic disturbance (low, mild, medium, high and extreme), based on the *k*-means clustering method. CK, CZ, CV = control locations, PU = Port of Pula, RA = Raša Bay, RI = Port of Rijeka, BA = Bakar Bay, SI = Šibenik Bay, VR = Vranjic Basin, ST = Port of Split.

Disturbance level				
LOW	**MILD**	**MEDIUM**	**HIGH**	**EXTREME**
CK1	RI6	RI1	PU1	PU3
CK2	RI7	RI2	PU2	SI4
CV1	BA1	RI3	PU4	SI5
CV2	BA2	RI4	PU5	VR5
CZ1	BA3	RI5	PU6	
CZ2	BA5	BA4	SI1	
RA1	BA6	BA11	SI2	
RA2	BA7	VR1	SI3	
RA3	BA8	VR2	SI6	
RA4	BA9	VR3	SI7	
RA5	BA10	VR4		
RA6	PU7	ST1		
RA7	VR6	ST2		
RA8	VR7	ST4		
RA9	VR8	ST6		
RA10	VR9	ST7		
	ST3	ST8		
	ST5	ST10		
	ST9			

4.3. Results of amplicon sequence data analysis

4.3.1. Diversity and community composition of benthic microbial communities

Of the 67 sediment samples collected, DNA was successfully extracted from 55, whereas DNA concentrations in 12 samples (BA4, RA2, RA4, RA6, RA9, RA10, ST, ST6, ST9, VR6, VR8, CV2) were too low. Consequently, these 12 samples were excluded from the study. High-throughput sequencing yielded a total of 10,464,885 high-quality reads which were assigned to 93,914 ASVs. Summary statistics for all three microbial communities across 55 samples are provided in Table S12.

Amplicon sequences were analyzed separately for each of the three microbial communities studied (prokaryotes, fungi and protists) and rarefied in R (version 4.3.2.; R Core Team, 2023). Prokaryotic sequences were rarefied to 37,149 reads per sample, protistan sequences to 4,228 reads per sample and fungal sequences to 2,481 reads per sample. Three samples (CV1 from the control location near Vis Island, ST5 from Port of Split, BA3 from Bakar Bay) were removed due to a low number of reads, resulting in a total of 52 samples used for further bioinformatic analyses.

4.3.1.1. Alpha and beta diversity of benthic microbial communities

Alpha diversity of microbial communities was analyzed individually for each community according to the specified disturbance levels. All alpha diversity indices for each community are provided in Tables S13–S15, while observed richness and Shannon diversity index (Shannon, 1948) are presented in Figure 5. Statistical analyses of both observed richness and Shannon diversity index are presented in Tables S16–S18.

The average observed richness was highest for the prokaryotes (1981 ± 207 ASV), followed by protists (250 ± 47 ASV) and fungi (173 ± 69 ASV) (Figure 4). Prokaryotic observed richness ranged from 1553 ASV (sample RA3) to 2784 ASV (sample CZ2), protistan richness from 120 ASV (sample ST8) to 318 ASV (sample BA11) and fungal richness from 35 ASV (sample RA3) to 423 ASV (sample RA1). The Shapiro-Wilk normality test indicated that observed richness values were not normally distributed ($p < 0.05$). Differences were further analyzed using the Kruskal-Wallis rank sum test, which showed significance ($p < 0.05$) only for fungal community observed richness. Dunn's post hoc test identified significant differences between Mild and Medium DL ($p = 0.025$) and between Medium and High DL ($p = 0.048$) (Figure 5B).

The average Shannon diversity index was highest for the prokaryotes (6.66 ± 0.22), followed by protists (4.52 ± 0.38) and fungi (3.92 ± 0.59) (Figure 5). Prokaryotic diversity ranged from 6.02 (sample RA3) to 7.29 (sample CZ2), protistan from 3.38 (sample RI2) to 5.05 (sample BA1) and fungal from 2.40 (sample BA7) to 5.18 (sample RA1). The Shapiro-Wilk normality test showed that Shannon diversity

values were not normally distributed ($p < 0.05$), except for the fungal community ($p > 0.05$). Differences were further analyzed using the Kruskal-Wallis rank sum test and Dunn's post hoc test for prokaryotes and protists, while one-way ANOVA with Tukey's HSD post hoc test were used for fungi. No significant differences were observed for prokaryotes ($p > 0.05$), whereas significant differences were observed for protists ($p < 0.05$) and fungi ($p < 0.05$). Post hoc tests showed the significant differences between Mild and Medium DL for fungi (Tukey HSD, $p < 0.05$; Figure 5B), while for protists, significant differences were observed between Mild and Medium DL, Mild and High DL and Mild and Extreme DL (Dunn, $p < 0.05$; Figure 5C).

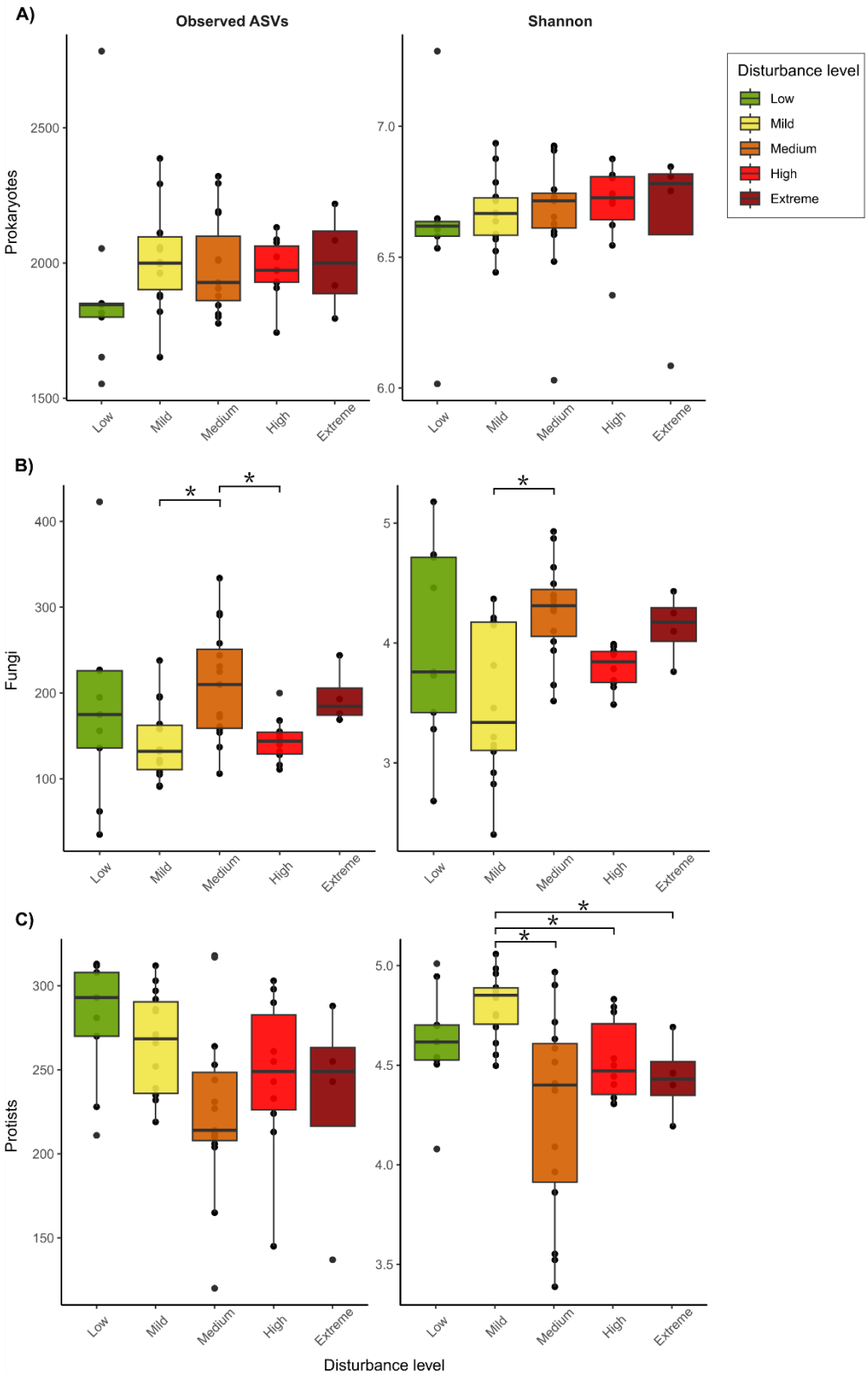

Figure 5. Observed richness (ASVs) and Shannon diversity index box plots for prokaryotic (A), fungal (B) and protistan (C) community, according to the five disturbance levels. Asterisks (*) indicate significant differences ($p < 0.05$).

Beta diversity was also analyzed for all three communities between the five defined disturbance levels (Figure 6). Based on PERMANOVAs of the Bray-Curtis dissimilarities, significant differences between DLs were observed for all three communities (p = 0.001), with R^2 values of 22.574% for prokaryotes, 22.639% for fungi and 22.623% for protists. Pairwise PERMANOVAs revealed the differences between specific DLs, with details provided in Table S19. For prokaryotes, significant differences were observed between all DLs ($p_{adj} < 0.05$), with R^2 values ranging from 9.574% to 19.808% (Table S19). The significant differences ($p_{adj} < 0.05$) were detected between all DLs for fungi and protists, except for Medium-Extreme and High-Extreme ($p_{adj} > 0.05$; Table S19).

Additionally, PERMANOVA analysis revealed that location explained a higher proportion of variation in prokaryotic (p = 0.001, R^2 = 46.919%), fungal (p = 0.001, R^2 = 49.092%) and protistan communities (p = 0.001, R^2 = 51.253%). Pairwise PERMANOVAs confirmed significant differences between all locations ($p_{adj} < 0.01$), except for prokaryotes between the Control locations–Vranjic Basin ($p_{adj} = 0.021$), Control locations–Raša Bay ($p_{adj} = 0.011$) and Port of Split–Vranjic Basin ($p_{adj} = 0.032$). For fungi no significant differences were observed between the Control locations–Raša Bay ($p_{adj} = 0.013$) and Port of Split–Vranjic Basin ($p_{adj} = 0.019$).

Notably, visible separation of the estuarine sediments from Raša Bay was observed in the PCoA, especially for prokaryotes and protists. This was also confirmed by PERMANOVA for prokaryotic (p = 0.001, R^2 = 15.693%), fungal (p = 0.001, R^2 = 8.391%) and protistan (p = 0.001, R^2 = 16.895%) communities (Figure 6).

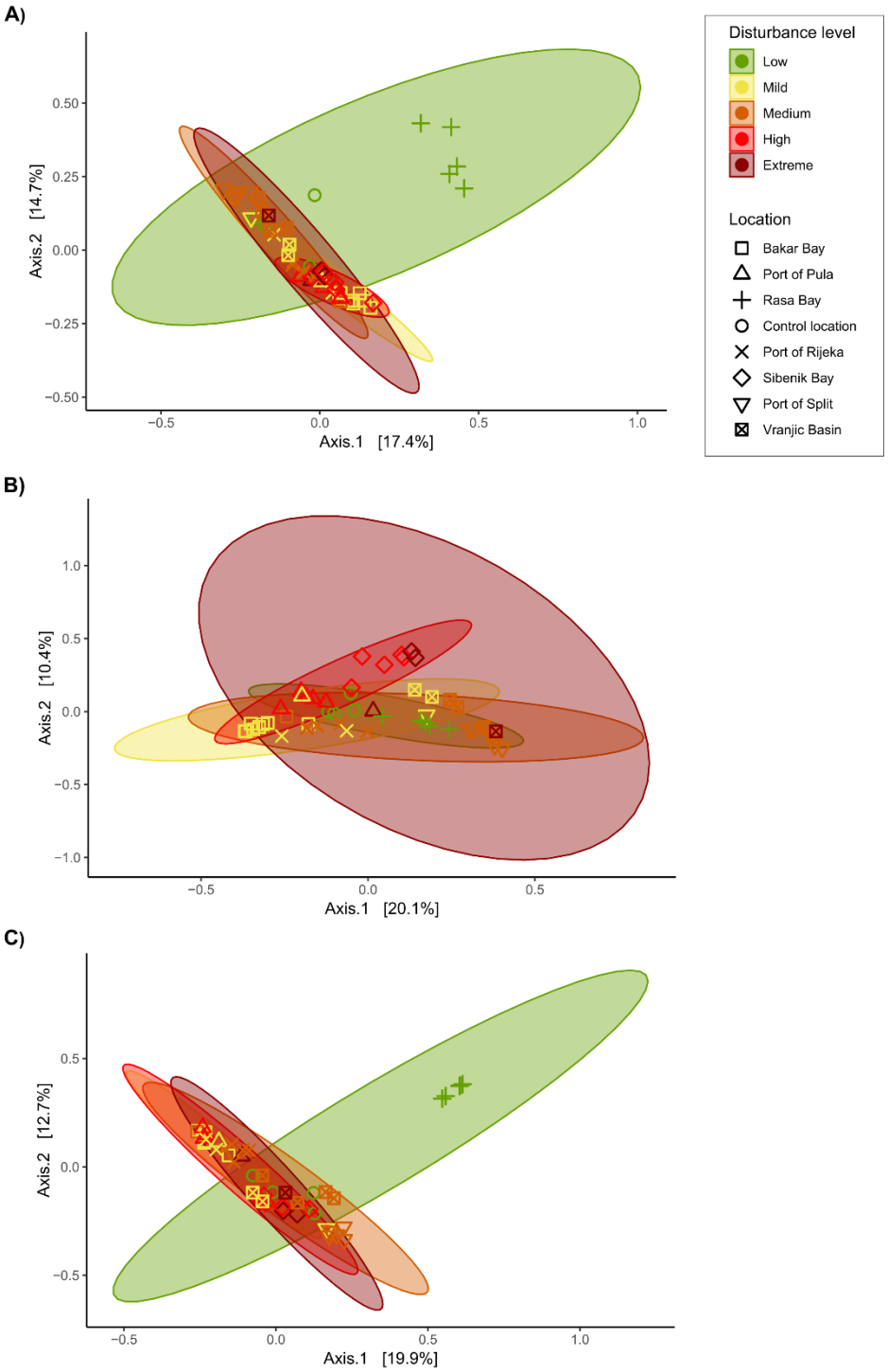

Figure 6. Principal coordinate analysis (PCoA) of each of the three microbial communities (Bray-Curtis dissimilarities) A) prokaryotes, B) fungi and C) protists, according to the five defined disturbance levels (DLs; indicated by color) and sampling location (indicated by symbols).

4.3.1.2. Prokaryotic community composition

The compositions of prokaryotic, protistan and fungal communities were analyzed at the family (Figures 7–9), phylum (Figures S3–S5) and genus levels (data not shown).

Based on the rarefied sequences from 52 samples, 19 prokaryotic genera and 28 families were identified, belonging to 14 different phyla with median relative abundance >1% across the DLs (Figure S3). When considering the whole community, no unclassified sequences were observed at the phylum level, while at the family level, on average 27.73% of sequences were unclassified, along with on average 40.48% at the genus level.

The most abundant phylum was *Proteobacteria* (relative abundance of avg. 34.69 ± 5.48%), followed by *Desulfobacterota* (14.92 ± 3.22%), *Actinobacteriota* (9.18 ± 2.45%), *Acidobacteria* (5.70 ± 1.87%) and *Chloroflexi* (5.83 ± 1.65%). The highest average relative abundances at the family level were observed for *Desulfosarcinaceae* (4.76 ± 1.54%), B2M28 (3.60 ± 1.52%), *Desulfocapsaceae* (3.35 ± 2.11%) and *Pirellulaceae* (3.30 ± 1.6%) (Figure 7). The taxa with <1% relative abundances accounted for avg. 5.68 ± 1.72% at the phylum level, avg. 48.59 ± 5.51% at the family level and avg. 74.61 ± 3.86% at the genus level. The most dominant genera were B2M28 (3.60 ± 1.52%), *Woeseia* (2.44 ± 0.87%), *Sulfurovum* (2.24 ± 3.57%) and Sva0081 sediment group (2.15 ± 0.64%).

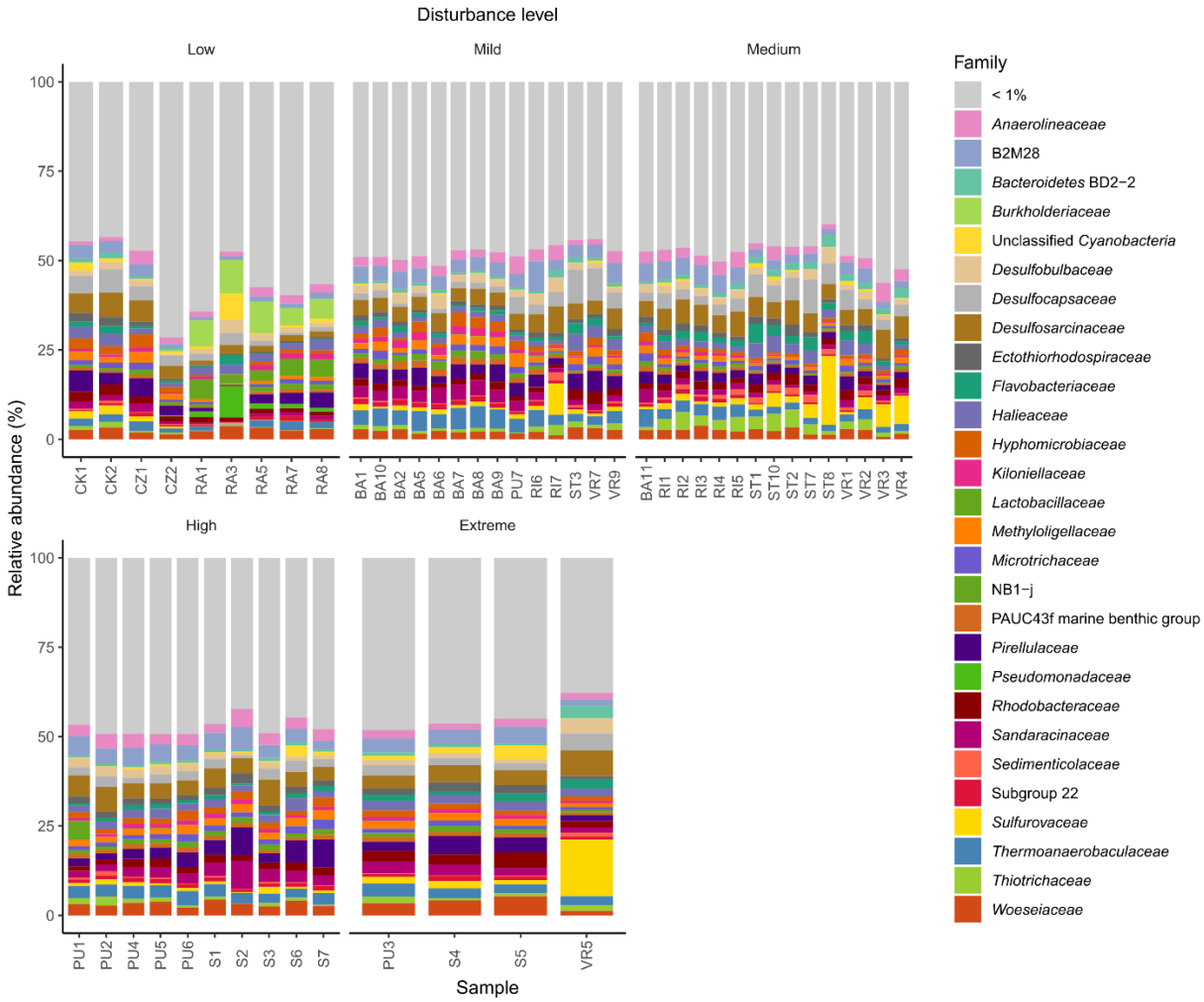

Figure 7. Prokaryotic community composition based on relative abundances (%) of 16S rRNA V4 gene region sequences, aggregated at the family level. Samples are grouped based on the defined disturbance levels. Families with <1% relative abundance are labeled as "< 1%".

4.3.1.3. Fungal community composition

Regarding fungi, a total of 16 genera and 20 different families were detected in the sediment samples, belonging to 5 different phyla (Figure S4). Overall, unclassified sequences accounted for an average of 7.3% at the phylum level, avg. 28.56% at the family level and avg. 38.4% at the genus level. The taxa with <1% relative abundances accounted for avg. 1.89 ± 1.37% at the phylum level, avg. 51.45 ± 12.86% at the family level and avg. 55.41 ± 13.76% at the genus level.

The two most abundant phyla were *Ascomycota* and *Basidiomycota*, which accounted for avg. 48.79 ± 13.12% and avg. 16.58 ± 9.09% of the identified sequences, respectively. At the family level, the highest relative abundances were detected for *Metschnikowiaceae* (17.58 ± 16.51%), *Rhyzophydiaceae* (4.50 ± 4.88%) and *Trichosporonaceae* (4.26 ± 5.19%; Figure 8). The most dominant genera were *Metschinkowia* (17.50 ± 16.48%), *Paramicrosporidium* (4.82 ± 3.65%) and LKM11 (3.70 ± 3.84%).

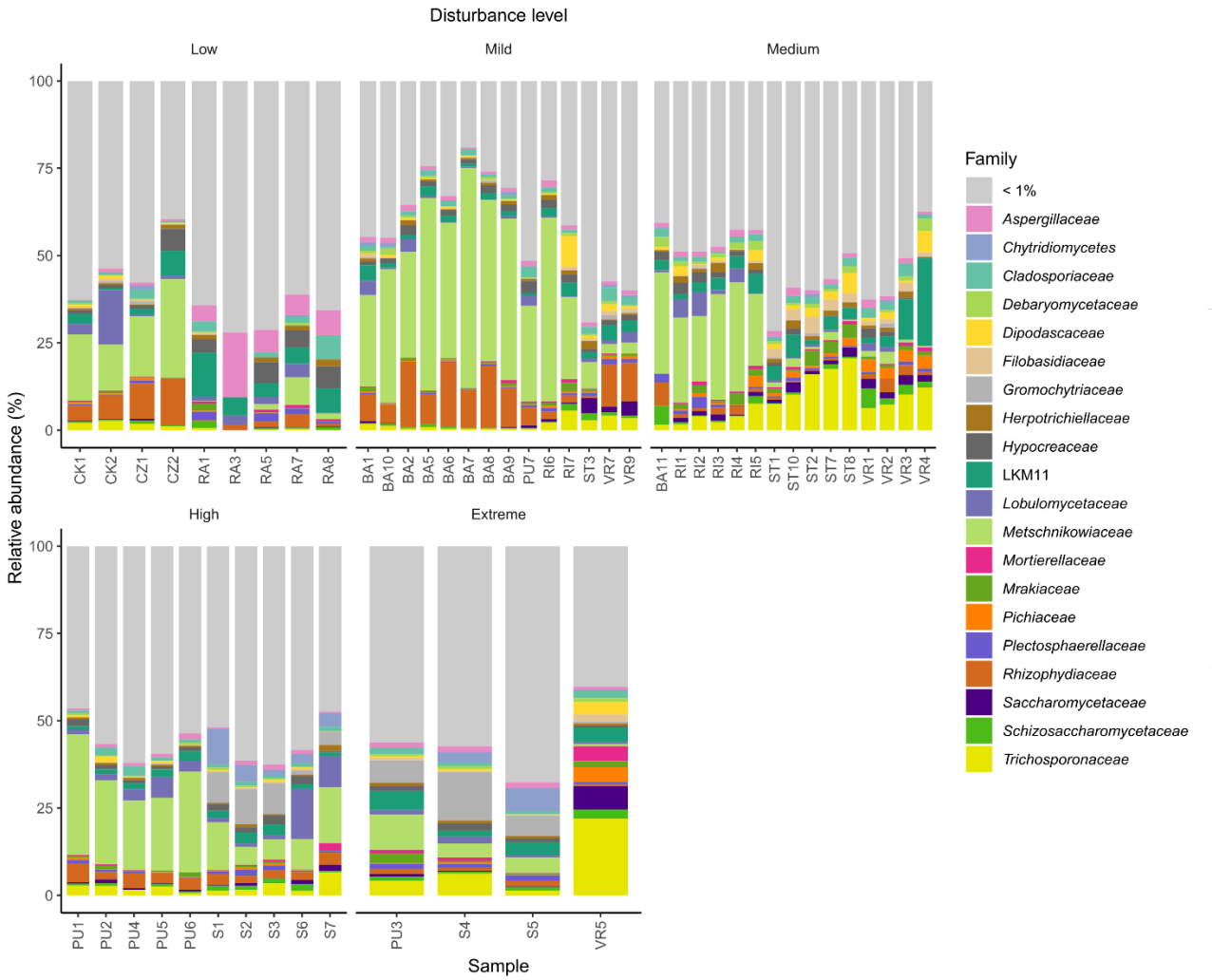

Figure 8. Fungal community composition based on relative abundances (%) of 18S rRNA V7-V8 gene region sequences, aggregated at the family level. Samples are grouped based on the defined disturbance levels. Families with <1% relative abundance are labeled as "< 1%".

4.3.1.4. Protistan community composition

Regarding protists, 24 genera along with 24 families belonging to 13 phyla were identified (Figure S5). Overall, an average of 0.96% at the phylum level of sequences were unclassified, at the family level avg. 16.98% and avg. 34.67% at the genus level. Dinoflagellata and Diatomea represented the most dominant phyla with relative abundances of avg. 31.24 ± 16.24% and 22.77 ± 14.17%, respectively.

At the family level the most abundant were *Bacillariophyceae* (avg. 15.23 ± 12.06%), followed by *Thoracosphaeraceae* (6.79 ± 3.52%), *Mediophyceae* (5.64 ± 7.18%) (Figure 9). The genera that dominated the protistan community were *Scrippsiella* (5.46 ± 2.97%), *Novel Apicomplexa Class 2* (4.38 ± 7.44%), *Gymnodinium* (3.52 ± 4.57%) and *Skeletonema* (3.49 ± 7.31%). The taxa with <1% relative abundances accounted for avg. 2.40 ± 1.02% at the phylum level, avg. 29.29 ± 6.19% at the family level and avg. 53.83 ± 8.87% at the genus level.

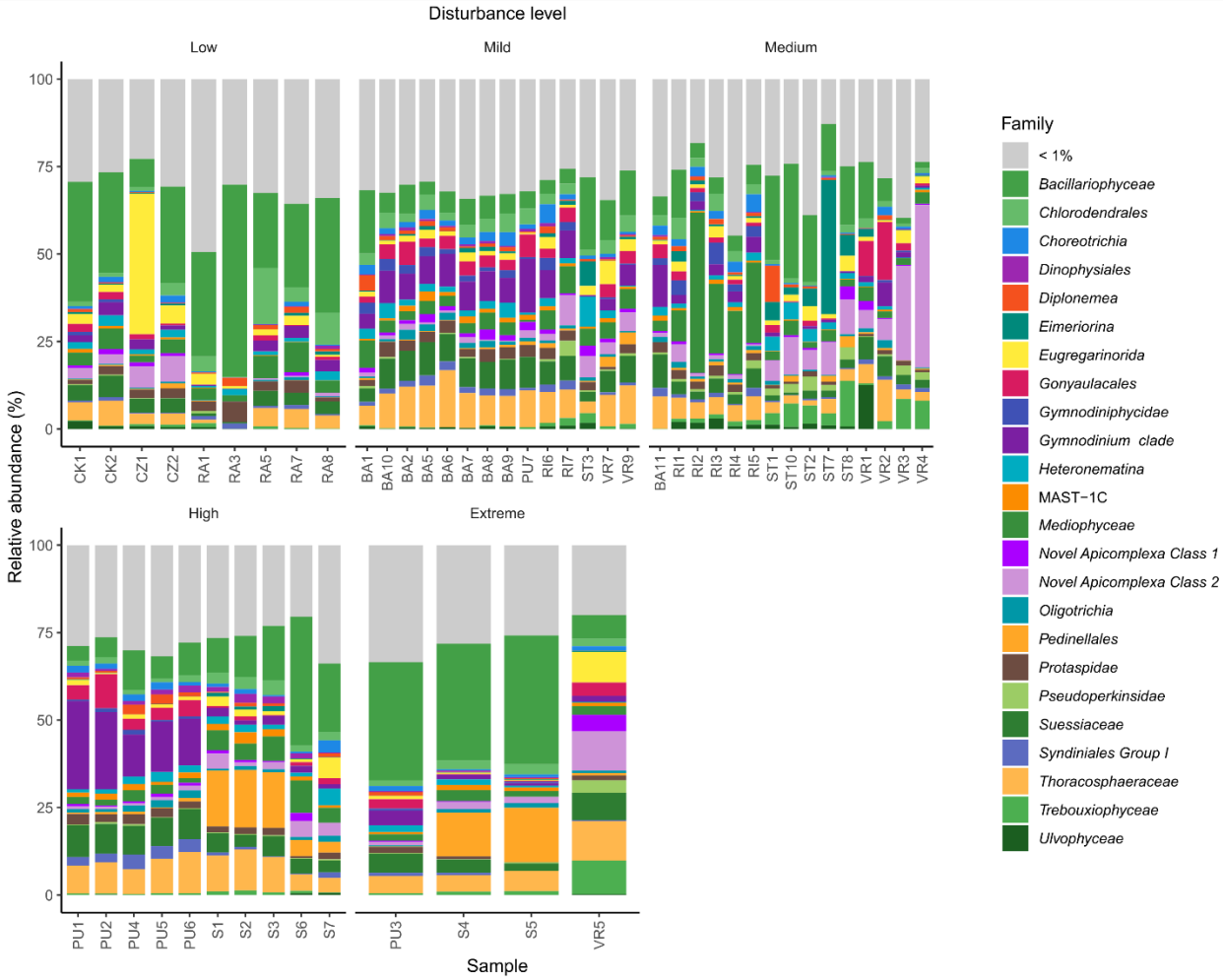

Figure 9. Protistan community composition based on relative abundances (%) of 18S rRNA V9 gene region sequences, aggregated at the family level. Samples are grouped based on the defined disturbance levels. Families with <1% relative abundance are labeled as "< 1%".

4.3.1.5. Shifts in relative abundances of microbial populations across disturbance levels

To investigate the specific microbial families that exhibited increasing or decreasing trends across the different DLs, log2 fold changes (LFC) were calculated for families with a median relative abundance >1% across the DLs (Figures 10–12, Table S20). The LFCs were calculated based on their relative abundances across all samples, comparing the Low DL with the Mild, Medium, High and Extreme DLs, separately. Statistical significance between each pair of DLs was assessed using the Wilcoxon rank-sum test.

Several prokaryotic families showed significant ($p < 0.05$) shift in relative abundances between undisturbed samples (Low DL) and disturbed samples (Mild, Medium, High and Extreme) (Figure 10). Families that showed significant negative LFCs (decreased abundance) in comparisons between Low DL and Mild, Medium and High DLs included *Burkholderiaceae*, Unclassified *Cyanobacteria*, *Lactobacillaceae*, *Pseudomonadaceae*. In contrast, families with significant positive LFCs (increased abundance) across these comparisons were B2M28, *Desulfosarcinaceae*, *Pirellulaceae*, *Thermoanaerobaculaceae*, *Woeseiaceae*. When comparing the Low and the Extreme DLs, families B2M28, *Desulfocapsaceae*, *Desulfosarcinaceae*, *Pirellulaceae*, *Thermoanaerobaculaceae* and *Woeseiaceae* showed significant negative log2 fold changes. These families showed positive log2 fold changes in all other comparisons (Low vs. Mild, Low vs. Medium, Low. vs. High), except for *Desulfocapsaceae*, which already exhibited a negative LFC in the Low vs. High DL comparison.

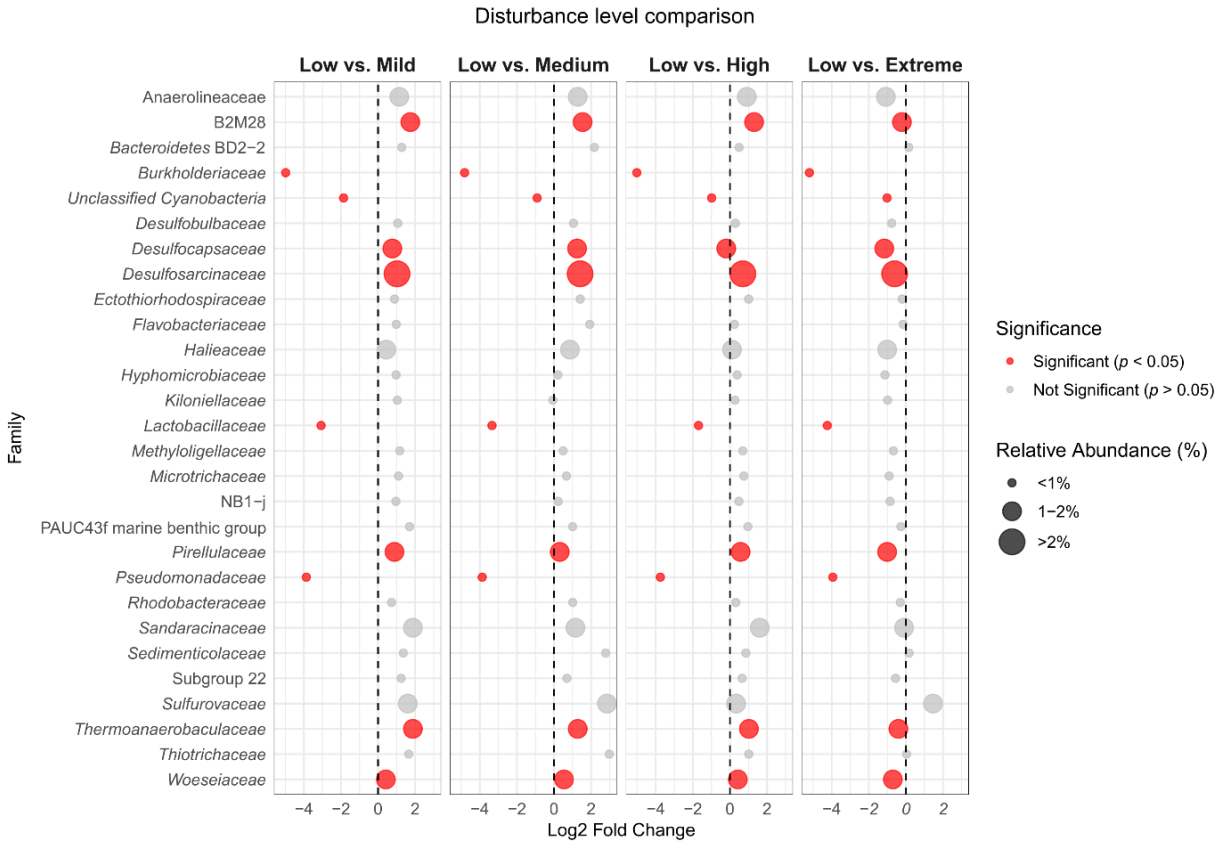

Figure 10. Log2 fold changes in relative abundances (%) of prokaryotic families between Low DL and Mild, Medium, High and Extreme DL. Only families with median relative abundance >1% are shown. Red color indicates families with significant differences between DLs ($p < 0.05$). Circle diameter is proportional to relative abundances of each family across all samples.

Using the Wilcoxon rank-sum test for fungal families and each pair of DLs, a significant difference was detected only for *Metschnikowiaceae* ($p < 0.05$) between undisturbed samples (Low DL) and disturbed samples (Mild, Medium, High and Extreme DLs) (Figure 11). Significant positive LFCs (increased abundance) were observed when comparing the Low and the Mild, Medium and High DLs. In contrast, when comparing the Low and Extreme DLs, a significant negative LFC (decreased abundance) was observed.

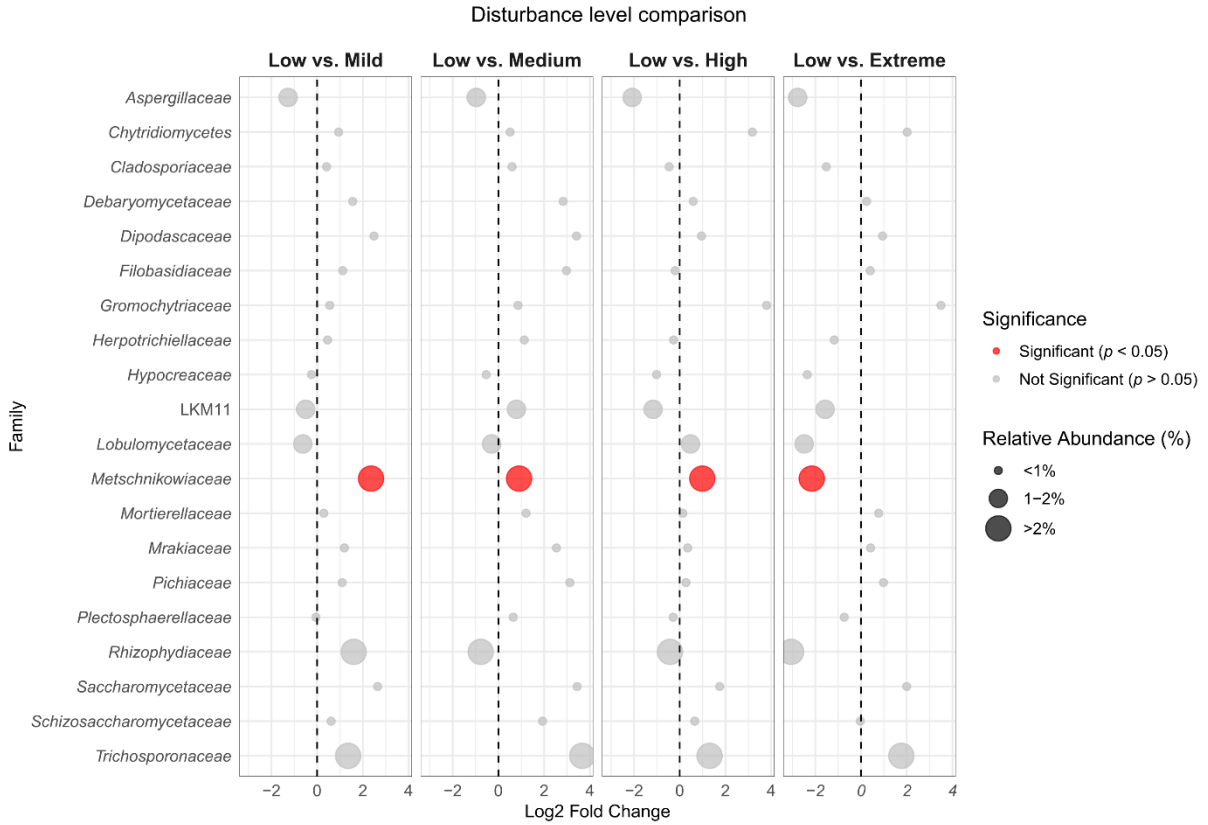

Figure 11. Log2 fold changes in relative abundances (%) of fungal families between Low DL and Mild, Medium, High and Extreme DL. Only families with median relative abundance >1% are shown. Red color indicates families with significant differences between DLs ($p < 0.05$). Circle diameter is proportional to relative abundances of each family across all samples.

Several protistan families exhibited significant ($p < 0.05$) changes between undisturbed samples (Low DL) and disturbed samples (Mild, Medium, High and Extreme). Family *Bacillariophyceae* showed a significant negative LFC between the Low and Mild, Medium, High and Extreme DLs (Figure 12). Significant positive LFCs (increased abundance) were detected in comparisons between the Low and Mild, Medium and High DLs for families *Gymnodinium clade*, *Mediophyceae*, *Suessiaceae* and *Thoracosphaeraceae*. When comparing the Low and the Extreme DLs, families *Gymnodinium clade*, *Mediophyceae*, *Suessiaceae* and *Thoracosphaeraceae* showed a significant negative LFC.

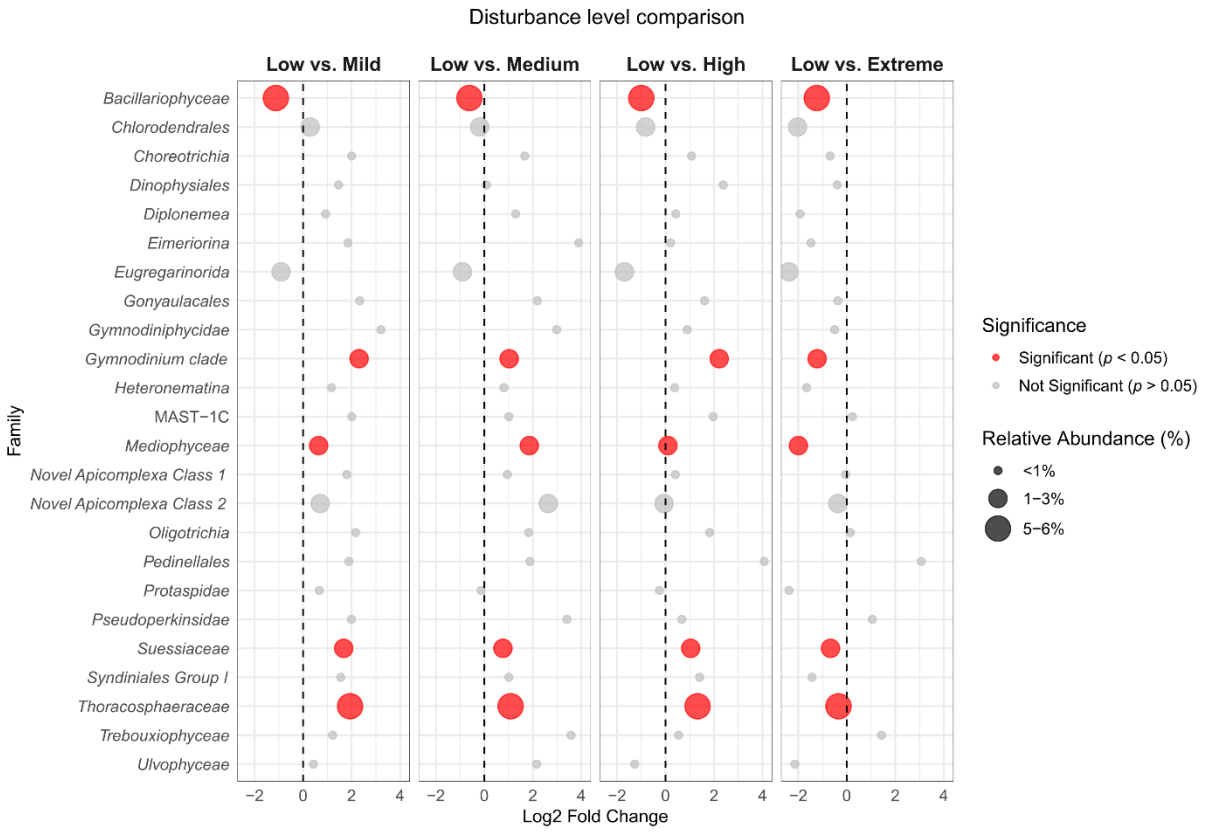

Figure 12. Log2 fold changes in relative abundances (%) of protistan families between Low DL and Mild, Medium, High and Extreme DL. Only families with median relative abundance >1% are shown. Red color indicates families with significant differences between DLs ($p < 0.05$). Circle diameter is proportional to relative abundances of each family across all samples.

4.3.2. Drivers of microbial community assembly

Further investigation examined how key dispersal and selection factors influence the abundance and incidence (presence/absence) of benthic prokaryotic, protistan and fungal communities and revealed differences in their importance for microbial community assembly and distribution.

The PERMANOVA analyses performed revealed that the abundance of all three communities was strongly influenced by dispersal factors, with location being a key driver in community assembly (p = 0.001, R^2 values > 46%; Figure 13A, Table S21). Microbial abundance was also significantly impacted by other dispersal factors (region, depth, sediment grain size; $p < 0.01$), though with lower R^2 values (Table S21). Among the selection factors (Figure 13B), disturbance level, sediment temperature and bottom water layer temperature significantly influenced the abundance of all microbial communities ($p < 0.01$). These factors explained from 6% to 12% of the variance in the community (Table S21). Additionally, salinity significantly affected prokaryotic ($p < 0.01$, R^2 = 4.797%) and fungal abundance ($p < 0.01$, R^2 = 5.239%). Fungal and protistan abundance were significantly affected by Bi, distance from shore, bioavailable fraction of As and total organic carbon ($p < 0.01$), though these factors had lower R^2 values (Figure 13B, Table S21). Despite low R^2 values, only fungal abundance was significantly impacted by contamination, sediment redox potential, Hg, Cu, Zn, Cd, total nitrogen, bioavailable fraction of Cu and Sb (Figure 13B, Table S21). Selective factors analyzed, but not found significantly influence the abundance of any community included toxicity level, Cu, As, Pb, Sb, Sn, total phosphorus and the bioavailable fractions of Pb, Zn, Cd.

When considering microbial incidence, all dispersal factors were also significantly affecting the three communities, though with the lower R^2 value in comparison to abundance (Figure 13A, Table S22). The incidence of all three microbial communities ($p < 0.01$) was significantly influenced by selection factors including disturbance level, sediment and bottom water temperature (Figure 13B, Table S22). In contrast to prokaryotic abundance, contamination, Bi and the bioavailable fraction of As were shown to significantly affect prokaryotic incidence ($p < 0.01$). Fungal incidence was significantly affected by fewer selective factors than fungal abundance which included salinity, distance from shore and Bi ($p < 0.01$). Similarly, protistan incidence was significantly impacted by Bi, total organic carbon and the bioavailable fraction of As ($p < 0.01$; Figure 13B, Table S22).

The analysis of distance-decay relationship additionally showed that community dissimilarity (Bray-Curtis) increased with geographical distance. This relationship was strongest for fungi ($p < 0.01$, R^2 = 22.368%; Figure 14B), followed by protists ($p < 0.01$, R^2 = 12.321%) and prokaryotes ($p < 0.01$, R^2 = 5.137%; Figures 14A and 14C).

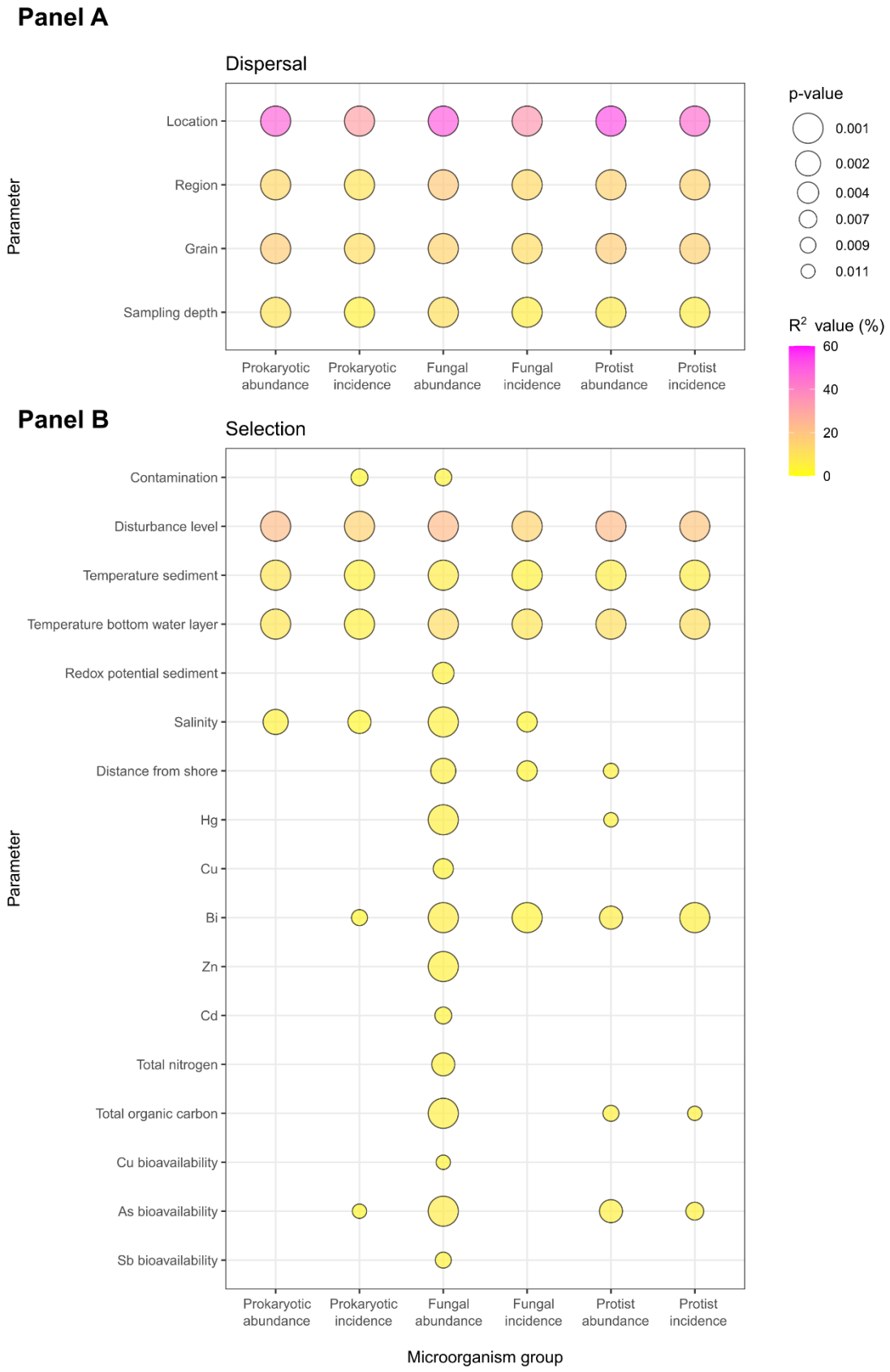

Figure 13. Bubble plot illustrating the significance of dispersal (Panel A) and selection factors (Panel B) (PERMANOVA, $p < 0.01$) on the three studied microbial communities (abundance and incidence).

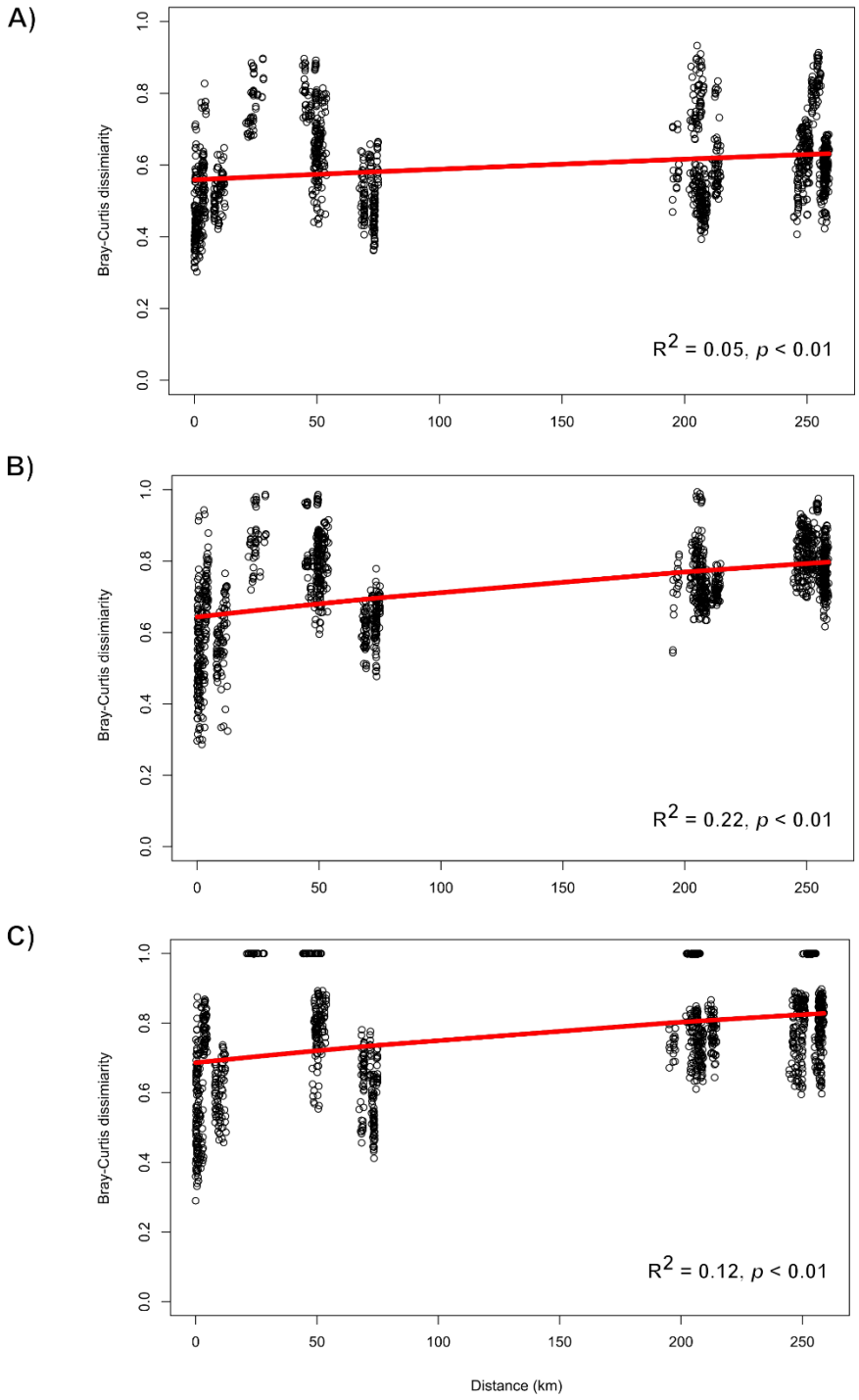

Figure 14. Distance-decay relationships showing the correlation between geographic distance (calculated using the Haversine method) and community dissimilarity (Bray-Curtis) for prokaryotic (A), fungal (B) and protistan (C) communities.

4.3.3. Benthic microbial indicators of anthropogenic disturbance

4.3.3.1. Key ASVs differentiating samples by disturbance levels and contamination

DESeq2 analysis of sequencing data from 55 samples identified the 20 most significant ASVs per microbial community that differentiated sediment samples across the five DLs and between contaminated and non-contaminated locations **(**Figure 15A, B, C). A complete list of ASVs and their taxonomic affiliations for the three microbial communities is provided in Tables S23–S25.

For the prokaryotic community (Figure 15A), a clear differentiation was observed between the low DL and all other samples and between both contaminated and non-contaminated samples. From this, seven ASVs were identified as potential key indicators of contamination that included bacteria from the genera *Thiogranum* (ASV5044), B2M28 (ASV4772 and ASV4766), Sva0485 (ASV5571), *Boseongicola* (*Rhodobacteraceae*) (ASV4491), Subgroup 23 (*Thermoanaerobaculaceae*) (ASV347) and an uncultured gammaproteobacterium (ASV5345), all of which were abundant exclusively in contaminated locations. Conversely, five ASVs were predominantly detected in non-contaminated samples, including genera *Lactobacillus* (ASV2587), *Ralstonia* (ASV4806), *Burkholderia* (ASV4796), *Pseudomonas* (ASV5274) and an unidentified member of the family *Lachnospiraceae* (ASV2830).

For fungi (Figure 15B), three ASVs were identified only in contaminated sites. They belonged to genera *Paramicrosporidium* (ASV17), an uncultured *Basidiobolus* (ASV332) and *Chytridiomycetes* (ASV270). In contrast, three ASVs were recorded almost exclusively found in non-contaminated locations, including genus *Aigialus* (ASV755), an unidentified genus from the class *Sordariomycetes* (ASV146) and genus *Aspergillus* (ASV218). In contrast, protists showed no clear separation based on the DLs or contamination status (Figure 15C).

A)

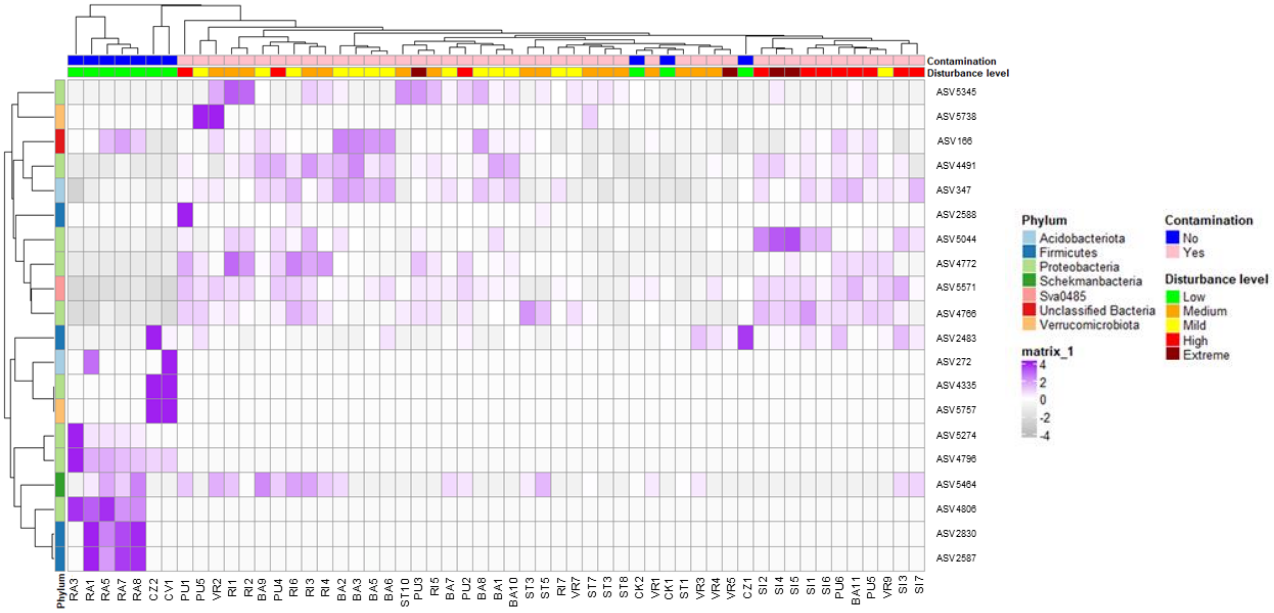
Contamination
Disturbance level
ASV5345
ASV5738
ASV166
ASV4491
ASV347
ASV2588
ASV5044
ASV4772
ASV5571
ASV4766
ASV2483
ASV272
ASV4335
ASV5757
ASV5274
ASV4796
ASV5464
ASV4806
ASV2830
ASV2587
Phylum
RA3 RA1 RA5 RA7 RA8 CZ2 CV1 PU1 PU5 VR2 RI1 RI2 BA9 PU4 RI6 RI3 RI4 BA2 BA3 BA5 BA6 ST10 PU3 RI5 BA7 PU2 BA8 BA1 BA10 ST3 ST5 RI7 VR7 ST7 ST3 ST8 CK2 VR1 CK1 ST1 VR3 VR4 VR5 CZ1 SI2 SI4 SI5 SI1 SI6 PU6 BA11 PU5 VR9 SI3 SI7
Phylum
Acidobacteriota
Firmicutes
Proteobacteria
Schekmanbacteria
Sva0485
Unclassified Bacteria
Verrucomicrobiota
matrix_1
4
2
0
-2
-4
Contamination
No
Yes
Disturbance level
Low
Medium
Mild
High
Extreme

B)

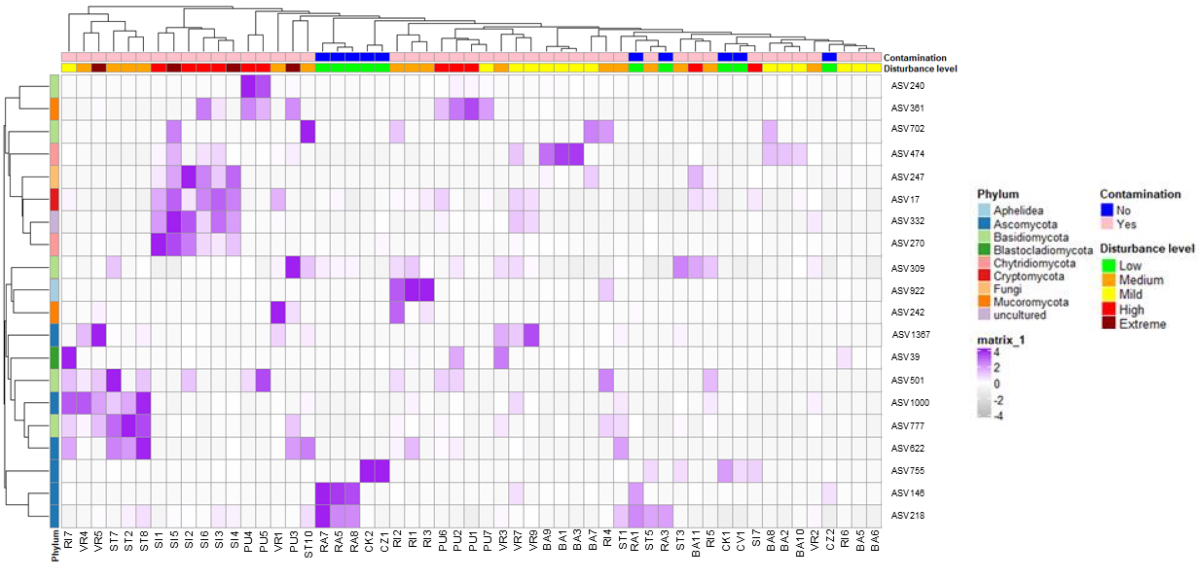
Contamination
Disturbance level
ASV240
ASV361
ASV702
ASV474
ASV247
ASV17
ASV332
ASV270
ASV309
ASV922
ASV242
ASV1367
ASV39
ASV501
ASV1000
ASV777
ASV622
ASV755
ASV146
ASV218
Phylum
RI7 VR4 VR5 ST7 ST2 ST8 SI1 SI5 SI2 SI6 SI3 SI4 PU4 PU5 VR1 PU3 ST10 RA7 RA5 RA8 CK2 CZ1 RI2 RI1 RI3 PU6 PU2 PU1 PU7 VR3 VR7 VR9 BA9 BA1 BA3 BA7 RI4 ST1 RA1 ST5 RA3 ST3 BA11 RI5 CK1 CV1 SI7 BA8 BA2 BA10 VR2 CZ2 RI6 BA5 BA6
Phylum
Aphelidea
Ascomycota
Basidiomycota
Blastocladiomycota
Chytridiomycota
Cryptomycota
Fungi
Mucoromycota
uncultured
matrix_1
4
2
0
-2
-4
Contamination
No
Yes
Disturbance level
Low
Medium
Mild
High
Extreme

C)

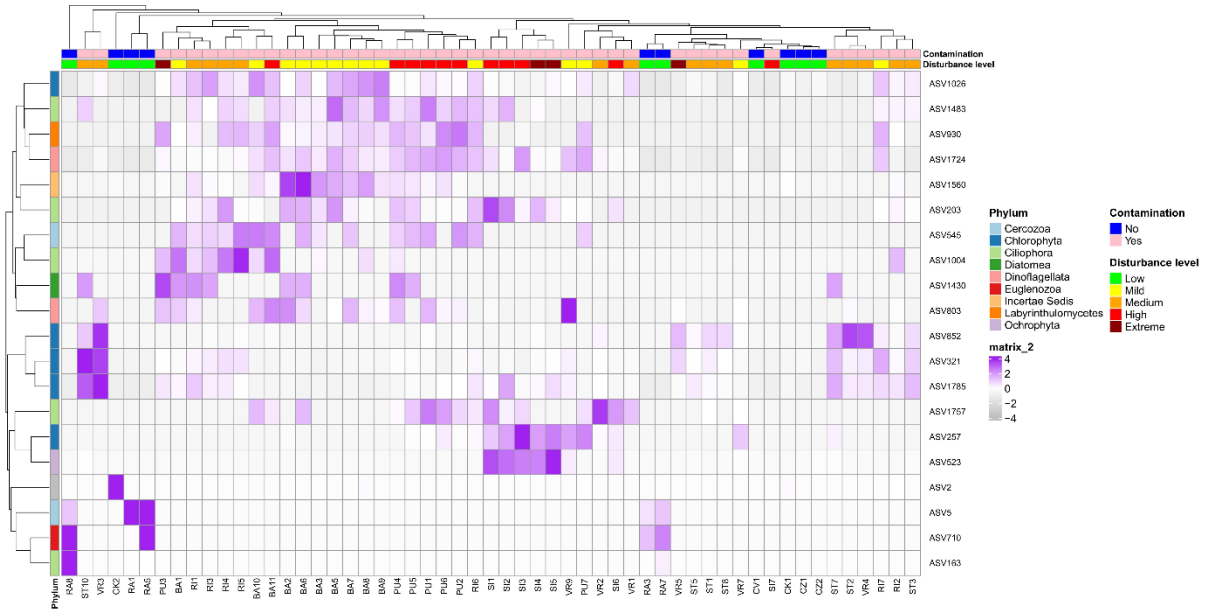

Figure 15. Heatmap of the top 20 amplicon sequence variants (ASVs) for the prokaryotic (A), fungal (B) and protistan (C) communities. Clustering was performed based on contamination status (contaminated vs. non-contaminated samples) and the five defined DLs (low, mild, medium, high and extreme). Heatmap data were generated using DESeq2 analysis (p_{adj} < 0.05). Each row represents the taxonomic assignment of an ASV, with relative abundance represented using a color gradient from gray (low abundance) to purple (high abundance).

4.3.3.2. Key microbial indicator variables from Classification and Regression Tree analysis

The CRT analysis identified key indicator variables – specific taxonomic groups whose presence and relative abundance change in a manner that directly correlates with each of the five defined DLs. Table 3 lists taxonomic groups that define each DL with 100% certainty and occur in more than 50% of the samples within that DL. Detailed results of the analysis are shown in Figures S6A, B and C.

For prokaryotes, the CRT analysis identified seven families – *Bacillaceae, Sulfurovaceae, Thiotrichaceae, Thermoanaerobaculaceae, Marine Benthic Group D and DHVEG-1, Saprospiraceae* and *Nitrosopumilaceae* – as the most significant for classifying samples into the five DLs. Each DL was characterized by a unique combination of up to four of these families, which needed to be present in sediment samples at defined relative abundances (Table 3).

Even though among protists, nine most significant families were singled out as key indicators (*Dinophysiales, Suessiaceae, Trebouxyiophyceae, Heteronematina, Prostomatea, Pseudoperkinsidae, Euglyphida,* unclassified *Cercozoa* and unclassified *Apicomplexa*) detailed examination (Table 3) revealed difficulties in data interpretations, with no logic grouping of protist families (i.e. key indicator variables) depending on the DLs. For example, the low, medium and extreme DL groups exhibited similarities in key indicator variables, sharing three familes, in contrast to the high and mild DL groups.

For fungi, CRT analysis identified key indicator variables only for low, mild and medium DL (Table 3) and therefore this was not further explored.

Table 3. Key indicator variables for prokaryotic, protistan and fungal communities identified using the Classification and Regression Tree analysis. The presence and relative abundance (RA) of these variables define levels of anthropogenic disturbance in sediment (low, mild, medium, high and extreme). NI - key indicator variables not identified in >50% of samples. Key indicator variables in bold represent those common to more than two DLs.

Disturbance level	Prokaryotes		Protists		Fungi	
	Key indicator variable	RA	Key indicator variable	RA	Key indicator variable	RA
Low	***Thiotrichaceae***	≤ 1.964	***Dinophysiales***	≤ 0.548	*Rynchogastremataceae*	≤ 0.282
	Bacillaceae	**> 0.353**	***Suessiaceae***	≤ 4.539	Unclassified *Pleosporales*	> 8.666
			Trebouxyiophyceae	≤ 0.389		
	Thermoanaerobaculaceae	≤ 2.610	*Heteronematina*	≤ 1.952		
Mild	***Thiotrichaceae***	≤ 1.964	***Dinophysiales***	≤ 0.548	*Rynchogastremataceae*	≤ 0.282
	Bacillaceae	≤ 0.353	***Suessiaceae***	≤ 4.539	Unclassified *Pleosporales*	≤ 8.666
	Sulfurovaceae	**> 0.813**				
	Marine Benthic Group D and DHVEG-1	≤ 0.096	*Prostomatea*	≤ 1.264		
Medium	***Thiotrichaceae***	**> 1.964**	***Dinophysiales***	≤ 0.548	*Rynchogastremataceae*	> 0.282
			Suessiaceae	≤ 4.539		
			Trebouxyiophyceae	> 0.389		
	Saprospiraceae	> 0.138	*Pseudoperkinsidae*	> 0.231	LKM15	≤ 3.315
			Euglyphida	≤ 0.275		
High	***Thiotrichaceae***	≤ 1.964	***Dinophysiales***	≤ 0.548	NI	
	Bacillaceae	≤ 0.353				
	Sulfurovaceae	**≤ 0.813**	Unclassified *Cercozoa*	≤ 0.514		
	Thermoanaerobaculaceae	≤ 4.453				
Extreme	***Thiotrichaceae***	≤ 1.964	***Dinophysiales***	≤ 0.548	NI	
			Suessiaceae	≤ 4.539		
	Bacillaceae	≤ 0.353	***Trebouxyiophyceae***	> 0.389		
	Sulfurovaceae	**> 1.766**	*Pseudoperkinsidae*	≤ 0.231		
	Nitrosopumilaceae	> 0.039	Unclassified *Apicomplexa*	≤ 0.099		

4.3.4. Effects of pollutants on benthic microbial community interactions

The effect of pollution on microbial community was further explored at the level of mutual interactions. Mantel tests were performed to compare Bray-Curtis dissimilarity matrices between pairs of communities, differentiating sediment samples into those with low and high pollution levels (Table S26). The pollutants tested for potential interaction effects were heavy metals Bi, Cd, Cu, Zn and Hg. These metals were selected from the set of significant selection factors based on their relevance to at least one community (abundance/incidence), as determined by PERMANOVA analysis ($p < 0.01$). The results showed that, under low pollution levels, interactions among all three pairs of communities (prokaryotes-fungi, fungi-protists, prokaryotes-protists) were similar, with Mantel r values ranging from $r = 0.792$ to $r = 0.849$ (Figure 16). The prokaryotes-protists interaction was the strongest under low pollution levels across all heavy metals, with r values ranging from 0.824 to 0.849, except in the presence of Cu, where fungi-protists interaction showed the strongest correlation ($r = 0.820$) (Table S27).

Conversely, a decline in Mantel r values was recorded under heavy metal pollution (sediments under high pollution level). This was most pronounced for the interaction between prokaryotes and protists, with the largest decline in correlation in samples under high levels of pollution with Bi, showing a reduction in correlation of $r = 0.226$, followed by Cd, Hg, Zn and Cu. The prokaryotes-fungi interaction also strongly declined, especially for Cd (reduction in correlation of $r = 0.172$) and Hg (reduction in correlation of $r = 0.116$), followed by Bi, Zn and Cu. The interaction between fungi and protists showed a smaller decrease, with the greatest decline in correlation observed under high levels of pollution with Cd (from $r = 0.838$ to $r = 0.747$), followed by Bi, Zn and Cu. In contrast, fungi-protists interaction was not impacted by high levels of pollution with Hg, as the correlation increased from $r = 0.809$ to $r = 0.813$ (Table S27). Among all the studied communities, the smallest negative effect on interactions was observed under high Cu pollution.

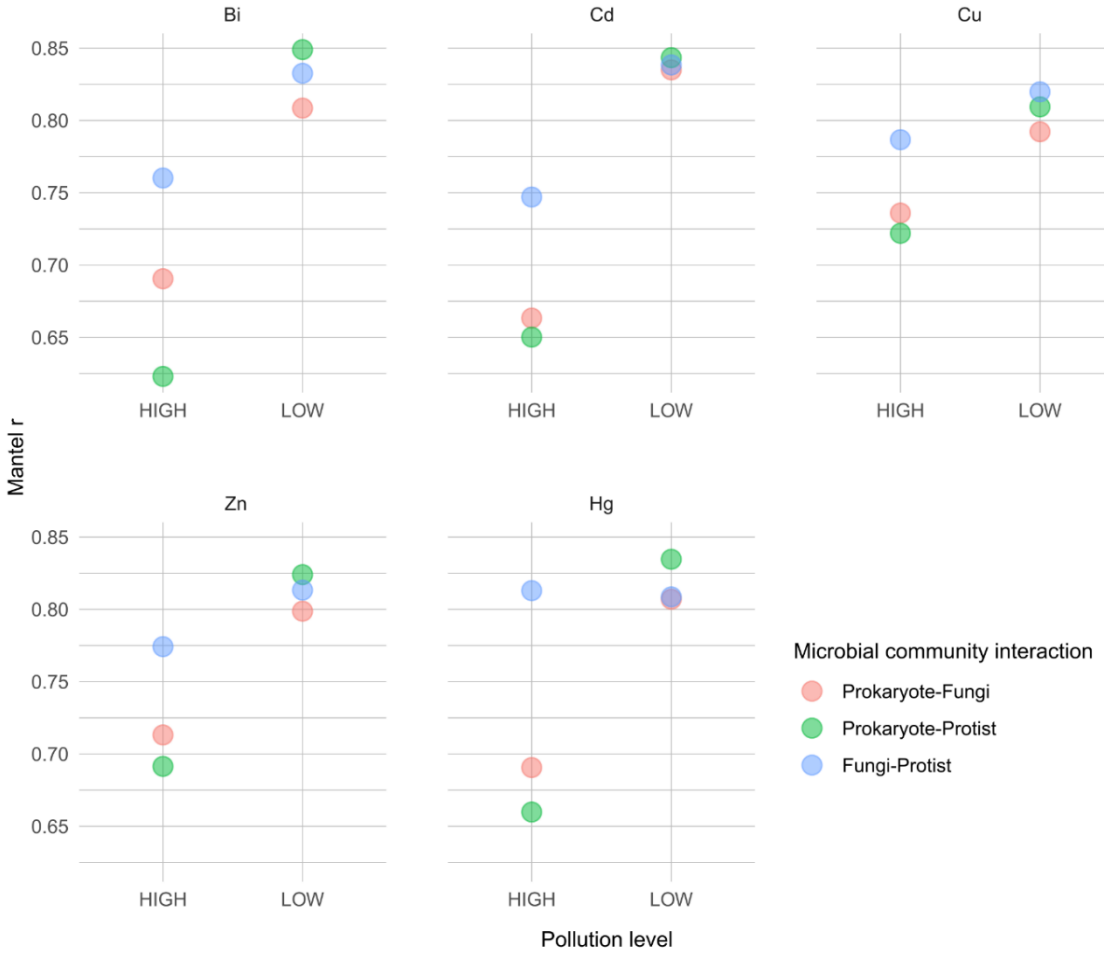

Figure 16. Interactions between each microbial community under high and low level of pollution based on Mantel's test. Pollutants tested belong to significant selection factors (PERMANOVA, $p < 0.01$). Each point represents the interaction of one pair of communities.

4.4. Results of metagenomic data analysis

4.4.1. Dataset description and achieved genomic content and biomarker coverage

A total of 1,728,306,104 read pairs were obtained using metagenomic sequencing analysis. Of these, 1,692,298,162 high-quality sequences were used for further analysis, with an average of 48,351,376 sequences per sample. The analyzed sequences were derived either from contigs of merged pairs or, when merging was not possible, from the forward read alone. This resulted in a median metagenome coverage of approximately 47% according to the Nonpareil algorithm, indicating the coverage achieved by the sequencing effort across all samples. Additionally, a median coverage exceeding 90% was recorded for the remaining marker databases (biomarkers), according to Good's coverage estimates (Figure 17).

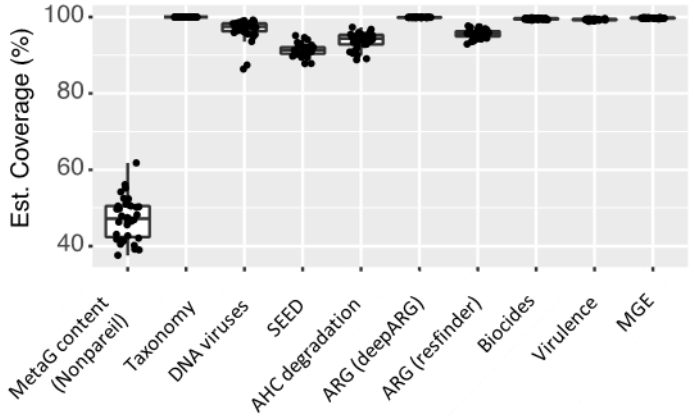

Figure 17. Nonpareil values for the metagenome coverage and Good's coverage estimates for the selected biomarkers.

4.4.2. Biomarker responses to disturbance, contamination and location-based grouping

4.4.2.1. Key biomarkers for location, disturbance levels and contamination

Among the nine tested biomarkers (*Taxonomy*, *SEED*, *ARG (deepARG)*, *ARG (resfinder)*, *MGE*, *DNA viruses*, *Biocides*, *AHC degradation* and *Virulence*), sample classification based on location consistently exhibited the highest PERMANOVA coefficient of determination values (R^2), followed by classification based on disturbance levels (Figure 18). Classification based on contamination yielded relatively low R^2 values regardless of the biomarker considered. When considering location for sample classification, two distinct groups of biomarkers emerged in terms of responsiveness: (i) *DNA viruses*, *Virulence*, *MGE*, *Biocides* and *Taxonomy*, with R^2 values ranging from 43.1 to 48.6%, and (ii) *ARGs (resfinder)*, *AHC degradation*, *ARGs (deepARG)* and functional annotations (*SEED*), with R^2 ranging from 28.2 to 34.7%.

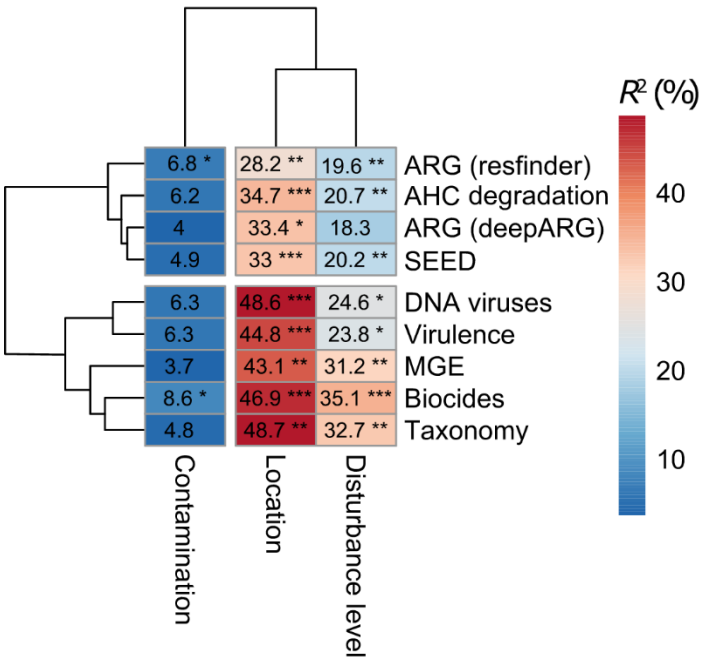

Figure 18. Key biomarker categories associated with location, disturbance level and contamination, according to PERMANOVA. The color scheme shows the range of coefficients of determination values (R^2). Asterisks indicate significance levels: $p \leq 0.05$ (*), $p \leq 0.01$ (**), $p \leq 0.001$ (***). Hierarchical clustering was performed using Euclidean distances and average linkage.

4.4.2.2. Major drivers of alpha diversity and key biomarkers

Alpha diversity indices, when analyzed by location, consistently showed the highest values in Split across most biomarker types, followed mostly by Vranjic Basin and the Port of Rijeka (Figure 19). Notable exceptions were observed for *AHC degradation* biomarker, where the highest values for the Shannon (representing richness and evenness) and inverse Simpson's indices (representing dominant taxa and overall evenness) were found in samples from the Port of Rijeka and Bakar Bay. The Shannon index represents the less dominant majority, while the inverse Simpson's index represents the more dominant microorganisms.

When *Taxonomy* biomarker was considered, control locations and the Port of Pula showed the highest values for Fisher's *α* (representing highly dominant microorganisms), observed richness (representing the total community) and ACE (representing rare taxa).

When disturbance levels (DLs) were assessed, medium and extreme DLs generally displayed the highest diversity values across most biomarkers. However, the low DL group exhibited the highest values when *Taxonomy*, particularly for Fisher's *α* and richness (observed and estimated). Additionally, the highest values for the low DL were observed for *MGE* (inverse Simpson's) and *Virulence* (Shannon and inverse Simpson's) biomarkers.

Regarding contamination (yes/no), contaminated locations exhibited higher diversity across most biomarkers. Exceptions included the *Taxonomy* biomarker, which showed higher Fisher's *α* index and the richness (observed and estimated). Again, *Virulence* and *MGE* had higher values for the inverse Simpson's index in non-contaminated locations, with *Virulence* showing higher values in the less contaminated when using the Shannon index.

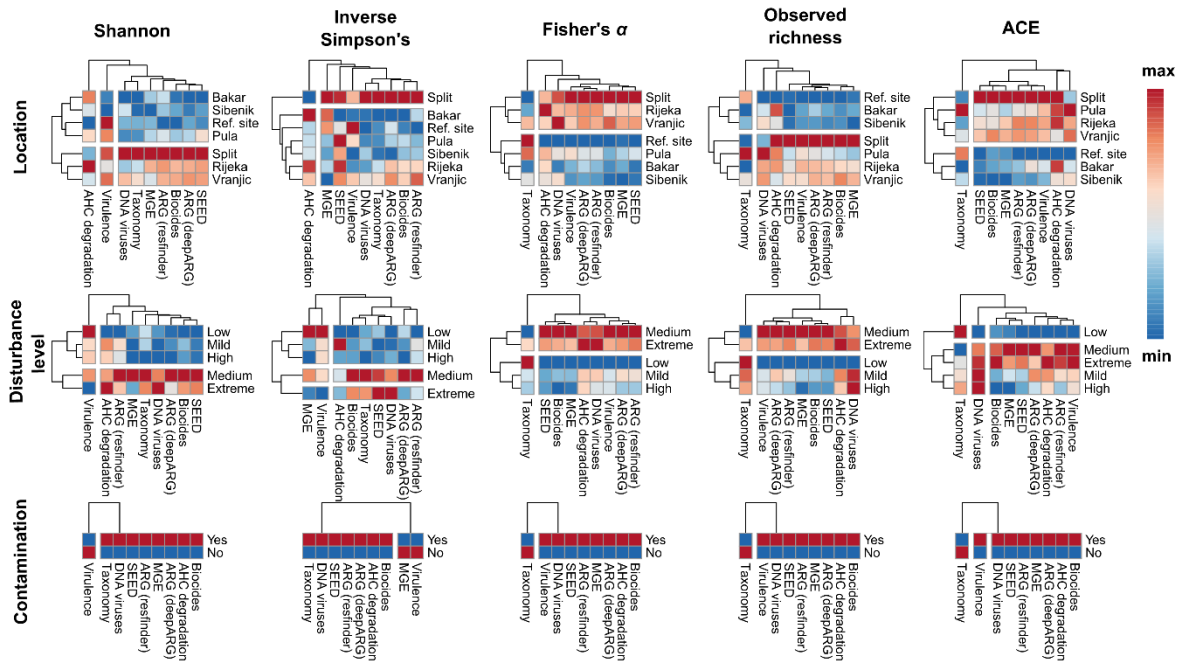

Figure 19. Heatmaps displaying alpha diversity index values for the sample means based on location, disturbance level and contamination, for each biomarker type (*Taxonomy*, *SEED*, *ARG (deepARG)*, *ARG (resfinder)*, *MGE*, *DNA viruses*, *Biocides*, *AHC degradation* and *Virulence*). Scaled values (minimum–maximum) across the three groups and each alpha diversity index are shown using a color gradient (blue–red). Hierarchical clustering was performed using Euclidean distances and average linkage.

4.4.2.3. Boruta-selected resistance gene profiles

To explore resistance genes under pollution conditions, Boruta feature selection was applied to the AHC degradation, antibiotic resistance genes (ARG, specifically deepARG), and biocides biomarkers, focusing on location-driven differences.

The AHC degradation gene profile (Figure 20A) included several dioxygenases, with different genes detected across samples from the same sampling locations. These included genes such as protocatechuate 4,5-dioxygenase, 3,4-dihydroxyphenylacetate 2,3-dioxygenase and aromatic ring-hydroxylating dioxygenases. Some of these genes were clearly enriched in samples ST2 i ST4 from the Port of Split, as well as in some samples from Šibenik Bay, the Port of Pula and Bakar Bay. In particular, sample VR7 exhibited high abundances of several dioxygenase genes, distinctly separating it from the other samples.

The biocide resistance gene profile (Figure 20B) was dominated by genes encoding resistance to As, Cu, Cd, Zn and Fe. Notably, sample SI5 from Šibenik Bay showed enrichment of several Cu resistance genes (*golT*, *copB*, *copR*, *actP*) along with Cd/Zn (*czcP*) and As resistance genes (*aioB*/*aoxA*). Additionally, in sample SI3, genes related to As (*arrA*, *arrB*), As/Sb (*arsB*) and Zn (*ziaA*) resistance were the most prevalent. High abundance of specific metal resistance genes were also found in samples PU1 and PU2 from the Port of Pula (*ziaA*), ST8 from the Port of Split (*nrsD*/*nreB*, *arsT*, *acn*, *ideR*) and in CK1 and CZ1 from control locations (*aioA*/*aoxB*, *aioB*/*aoxA*).

The antibiotic resistance gene (ARG) profile (Figure 20C) revealed a highly diverse and enriched resistome. Detected ARGs included those encoding resistance to triclosan, glycopeptide, macrolide-lincosamide-streptogramin (MLS), beta-lactam, tetracycline, sulfonamide and aminoglycoside. The resistome was also composed of several multidrug resistance genes which were particularly enriched in samples from Vranjic Basin, especially VR3 and VR4.

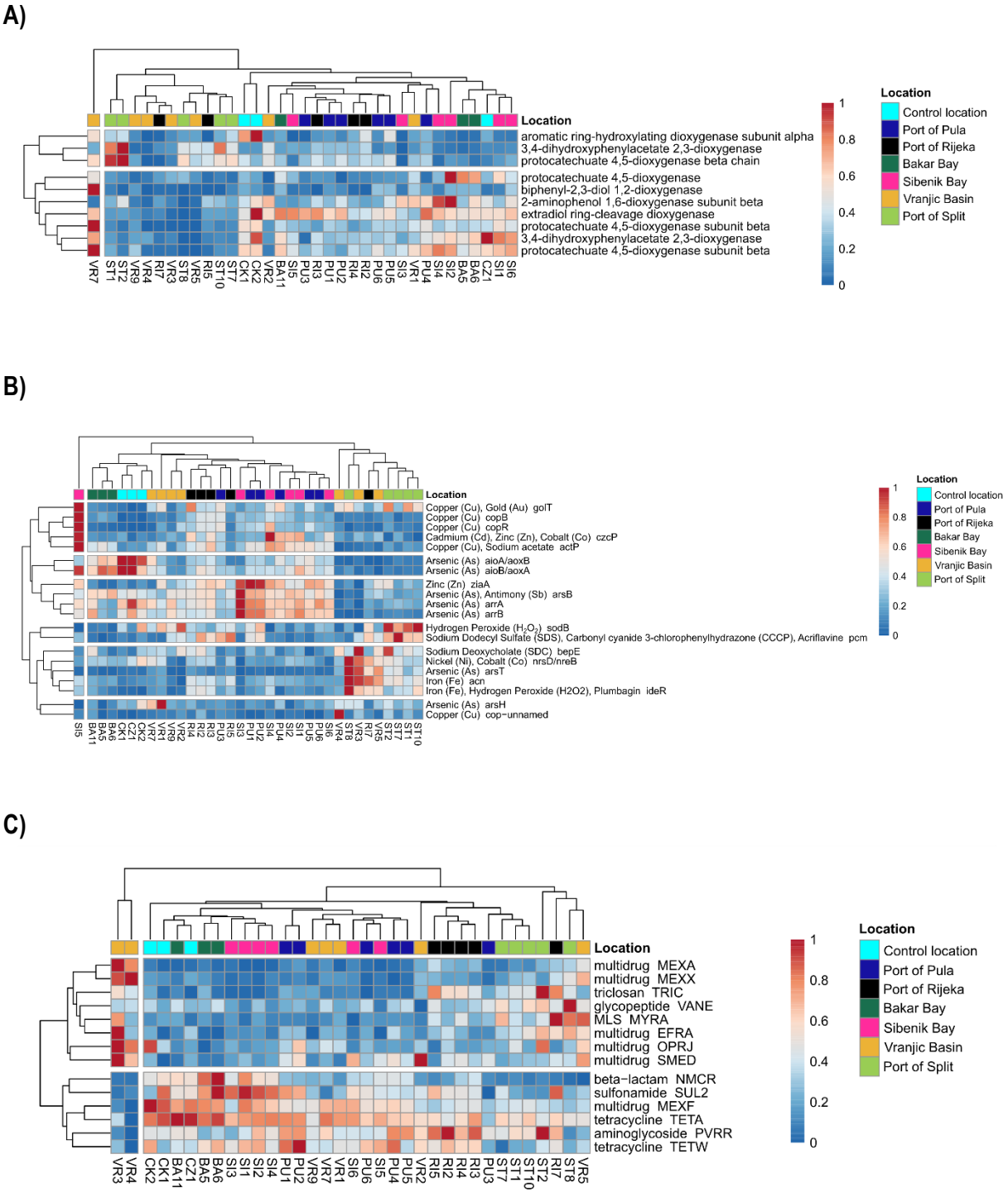

Figure 20. Boruta-selected features based on (A) AHC degradation, (B) Biocides and (C) ARG (deepARG) biomarkers across sediment samples and locations. Gene abundances are scaled between 0 (minimum) and 1 (maximum) across all samples and visualized using a color gradient from blue to red. Hierarchical clustering was performed using Euclidean distances and average linkage.

4.4.2.4. Boruta-selected features for Taxonomy and SEED as biomarkers

The Boruta algorithm identifed the most relevant features for the Taxonomy and SEED biomarkes. For the Taxonomy biomarker, the results revealed a separation of the 47 most important features between control locations (non-contaminated) and all other samples (Figure 21). These features include various members of bacterial phyla *Proteobacteria* (25 genera), *Planctomycetes* (9 genera), *Cyanobacteria* (5 genera) and the fungal phylum *Ascomycota* (3 genera). Similarly, the Boruta analysis on the SEED biomarker led to the selection of 44 most important features that distinguished control locations (non-contaminated) and all other samples (Figure 22). Additionally, these features showed clustering into two groups: one comprising samples predominantly from Šibenik Bay (most of the SI samples), Bakar Bay and one sample form Vranjic Basin, while the other contained the remaining samples. These features primarily included genes related to protein, DNA and RNA metabolism, respiration, cell division and the cell cycle, nitrogen metabolism and carbohydrates.

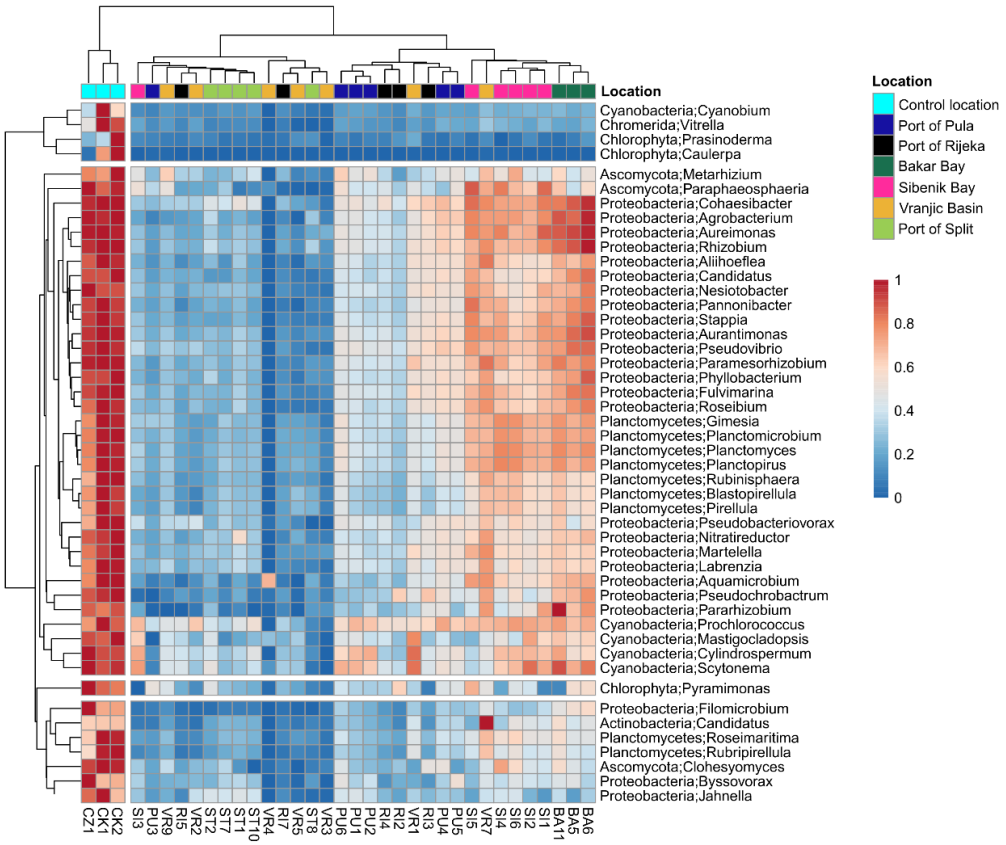

Figure 21. Heatmap of Boruta-selected features for each sample and locations, based on the *Taxonomy* biomarker. Gene abundances are scaled between 0 (minimum) and 1 (maximum) across all samples and visualized using a color gradient from blue to red. Hierarchical clustering was performed using Euclidean distance and average linkage.

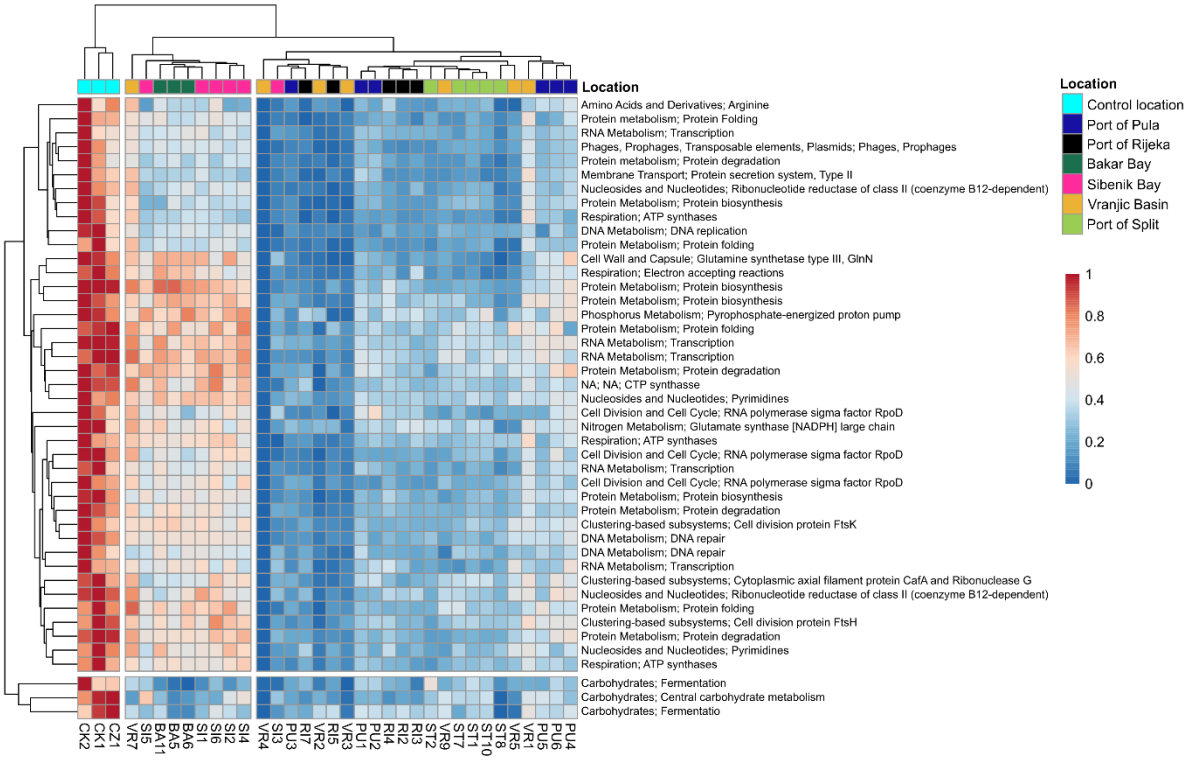

Figure 22. Heatmap of Boruta-selected features for each sample and locations, based on the *SEED* biomarker. Gene abundances are scaled between 0 (minimum) and 1 (maximum) across all samples and visualized using a color gradient from blue to red. Hierarchical clustering was performed using Euclidean distance and average linkage.

4.5. Benthic bacteria resistant to pollutants

A total of 74 pure bacterial isolates (Table S28) were obtained from the polluted sediment sample from Šibenik Bay through culturing on marine agar plates. The 16S rRNA marker gene sequences obtained from these isolates were used to construct a phylogenetic tree (Figure 23). Phylogenetic analysis revealed sequence similarities ranging from 98% to 100% with various bacterial isolates available in NCBI GenBank database, including members of the phyla *Proteobacteria* (*Alpha* and *Gamma*) and *Firmicutes*. Based on the neighbour-joining tree analysis, the isolates were divided into nine distinct taxonomic clusters: *Pseudoalteromonas* cluster 1 (2 isolates), *Ruegeria/Cribrihabitans* cluster 2 (17 isolates), *Bacillus berkeleyi/decolorationis* cluster 3 (1 isolate), *Bacillus/Fictibacillus* cluster 4 (2 isolates), *Bhargavaea* cluster 5 (1 isolate), *Lysinobacillus/Sporosarcina* cluster 6 (6 isolates), *Bacillus/Pseudoalkalibacillus/Alkalibacillus* cluster 7 (7 isolates), *Bacillus/Peribacillus/Rossellomorea* cluster 8 (14 isolates) and *Bacillus/Mesobacillus/Cytobacillus* cluster 9 (24 isolates).

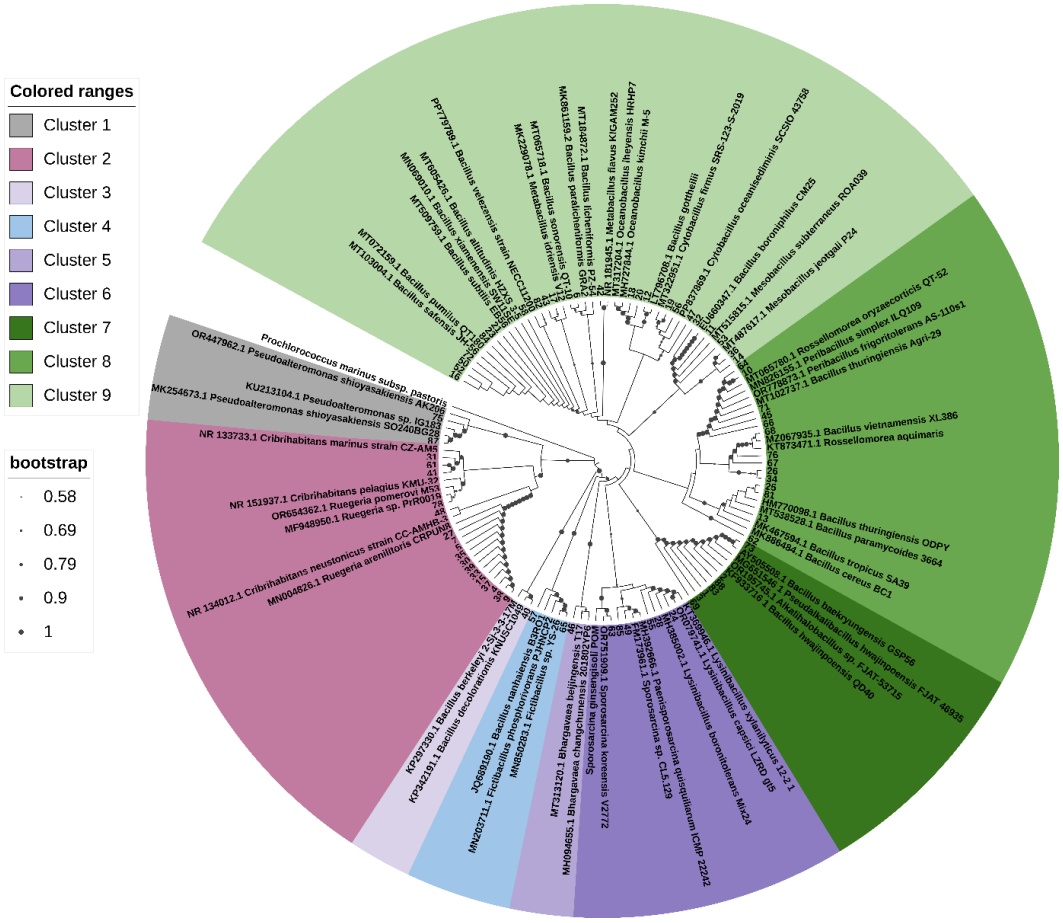

Figure 23. Neighbour-joining tree based on 16S rRNA gene sequences showing the phylogenetic positions of bacterial strains isolated from polluted sediment sample from Šibenik Bay. The tree was constructed using K2+G model (Kimura 2+ Gamma distribution). The analysis was performed based on 1,000 replications.

To investigate and determine the ranges of bacterial resistance to pollutants, the identified bacterial isolates were exposed to a range of concentrations of nine heavy metals (Cd, Co, Cr, Cu, Hg, Ni, Pb, Sn, Zn) and tributyltin (TBT), all of which are continuously monitored in marine sediment under the MSFD. The results of the disk diffusion method are shown in Tables 4 and 5. The pollutants were divided into two groups: those with tested concentrations of up to 5,000 mg/l (highly toxic) and those with tested concentrations of up to 10,000 mg/l (lower toxicity).

For the majority of the 74 bacterial isolates tested, minimal inhibitory concentration (MIC), i.e. the lowest concentration of a pollutant at which bacterial growth is completely inhibited, was at 500 mg/l. This MIC value was observed for Zn (52.7% of isolates), Cr (29.7% of isolates), Cd (70.3% of isolates), Cu (27% of isolates) and Sn (30% of isolates). For TBT, 74.3% of isolates were inhibited at a concentration of 1,000 mg/l. Notably, Hg inhibited bacterial growth at relatively low concentrations, with 90.5% of isolates affected at 50 mg/l, while only 2 out of 74 isolates showed sensitivity at 500 mg/l . Most isolates demonstrated growth inhibition at 5,000 mg/l for Co and 10,000 mg/l for Ni. In contrast, bacterial isolates displayed lower sensitivity to Pb, with 75.3% of isolates exhibiting resistance even at the highest tested concentration (>10,000 mg/l).

For the metals Cu, Co and Ni, most strains showed growth inhibition at concentrations of 5,000 mg/l. Cr displayed a unique pattern, with two major groups of isolates: one group (29.7% of isolates) was inhibited at 500 mg/l , while a second group (31.1% of isolates) demonstrated high resistance, showing no inhibition even at the highest tested concentration of 5,000 mg/l.

For Zn, Cd and TBT, up to seven isolates exhibiting high resistance were identified for each pollutant. In contrast, for Sn, Cu, Co and Ni, up to 15 highly resistant isolates were identified. An overview of MIC values for each sample, along with their phylogenetic cluster assignments, is provided in Table S29. Based on these results, specific isolates exhibiting resistance to multiple pollutants will be selected for future studies on resistance genes identification.

Overall, the isolates that exhibited resistance to the majority of pollutants across all tested concentrations included: isolate 25 (resistant to Pb, Zn, Cr, Cd, Cu, Co, Ni) and isolate 81 (resistant to Sn, Pb, Zn, Cr, Cu, Co, Ni) from cluster 8, as well as isolate 36 (resistant to Sn, Pb, Cr, Co, Ni) and isolate 47 (resistant to Sn, Pb, Cr, Cu, Co, Ni) from cluster 9.

Table 4. Minimal inhibitory concentrations of metals with concentrations up to 5,000 mg/l, based on the disk diffusion method. The total number of isolates for each MIC is given in parentheses. Bolded values indicate the concentration at which the highest percentage of resistance was observed for each pollutant. ND - not detected.

	Minimal inhibitory concentrations (mg/l)						
Pollutant	50	100	500	1,000	2,500	5,000	>5,000
Zn	ND	1.35%	**52.7%**	22.97%	17.6%	1.4%	5.4%
Cr	ND	ND	29.7%	18.9%	10.8%	9.5%	**31.1%**
Cd	5.4%	4.1%	**70.3%**	14.9%	1.4%	2.7%	1.4%
TBT	1.4%	ND	1.4%	**74.3%**	5.4%	8.1%	9.5%
Hg	**90.5%**	6.8%	2.7%	ND	ND	ND	ND

Table 5. Minimal inhibitory concentrations of metals with concentrations up to 10,000 mg/l based on the disk diffusion method. The total number of isolates for each MIC is given in parentheses. Bolded values indicate the concentration at which the highest percentage of resistance was observed for each pollutant. ND - not detected.

	Minimal inhibitory concentrations (mg/l)						
Pollutant	100	500	1,000	2,500	5,000	10,000	>10,000
Sn	25.7%	**28.4%**	12.2%	10.8%	8.1%	5.4%	9.5%
Pb*	1.4%	ND	1.4%	5.5%	8.2%	8.2%	**75.3%**
Cu	1.4%	**27%**	16.2%	24.3%	21.6%	5.4%	4.1%
Co	ND	ND	1.4%	18.9%	**37.8%**	27%	14.9%
Ni	ND	ND	1.4%	9.5%	33.8%	**35.1%**	20.3%

*A total of 73 isolates were tested for Pb resistance

5. Discussion

5.1. Anthropogenic disturbance in coastal sediments

To determine the presence and intensity of anthropogenic disturbance and establish a link to changes in microbial community dynamics, a comprehensive assessment was conducted across seven ports and bays along the eastern Adriatic coast. These locations are subjected to multiple sources of pollution and are continuously monitored as part of the national monitoring programme, established under the *Strategy for the Management of the Marine Environment and Coastal Area* of the Republic of Croatia, as part of the implementation of the MSFD (MSFD, 2008/56/EC). Chemical analyses of sediment samples confirmed that the selected locations are polluted ecosystems, with many measured pollutants identified as significantly enriched. However, pollutant concentrations varied among samples collected from the same sampling location. Notably, based on chemical analyses and subsequent *k*-means clustering, sediment samples from the estuarine Raša Bay were classified as low DL, grouping together with samples from control locations. Sediments classified as medium DL predominantly included those collected from Port of Split and Vranjic Basin, while sediments from port of Rijeka and Bakar Bay were classified as mild or medium DL. The most polluted sediment samples, classified as high and extreme DLs, predominantly originated from the Port of Pula and Šibenik Bay, with one sample from Vranjic Basin. Notably, sediment samples from Šibenik Bay and the Port of Pula demonstrated significant pollution with Hg and TBT and have been previously reported as locations subjected to multiple stressors, including active shipyards, marinas and former industrial facilities (Cukrov et al. 2008; Di Cesare et al. 2020; Erdelez et al. 2017). High TBT enrichments were found in most sediment samples from Vranjic Basin, a location known for the occurrence of imposex – a pseudo-hermaphroditic condition in gastropods – attributed to TBT pollution (Stagličić et al., 2008). A recent comprehensive assessment of TBT pollution along the Adriatic coast reported persistently high levels, particularly in ports, bays and estuaries, despite the global ban of its use more than two decades ago (Furdek Turk et al., 2024).

Pb, Cu and Zn have been characterized as primary heavy metal pollutants in the sediments of the eastern Adriatic Sea (Obhođaš and Valković, 2010; Popadić et al. 2013). In this study, high concentrations of these metals were detected in samples from the Ports of Pula and Rijeka, Šibenik Bay and Vranjic Basin. Potential sources of these metals include antifouling paints, traffic emissions, agricultural runoff and wastewater discharges (Bogner et al. 2005; Popadić et al. 2013). Additionally, the bioavailable fractions of selected metals were evaluated, revealing high levels of bioavailable Pb, Cu and Zn at several locations, particularly in Šibenik Bay, Port of Pula, Port of Rijeka and Vranjic Basin.

Nutrient inputs, such as nitrogen and phosphorus, were sporadically detected, primarily at locations with known wastewater discharges or near a former phosphate ore transshipment terminal or coking plant (Popadić et al. 2013). The cumulative effect of unidentified organic pollutants on bacterial

communities was assessed using the Microtox toxicity test. The highest toxicity levels were observed in samples from Šibenik Bay, Bakar Bay and the Ports of Pula and Rijeka, indicating significant pressure from unknown organic pollutants, presumably petroleum hydrocarbons, including PAHs, or pesticides. Some of these pollutants have consistently been recorded at elevated concentrations in the national monitoring program. High toxicity levels in Bakar Bay sediments had previously been detected using the same test, attributed mainly to toxic compounds from industrial facilities (Fafanđel et al. 2015).

These results served as the basis for grouping sediment samples, a critical step for further investigation of microbial community dynamics in relation to varying levels of anthropogenic disturbance.

5.2. Microbial community dynamics under disturbance

To better understand the effects of long-term pollution on benthic microorganisms, community dynamics of three microbial communities, prokaryotes, protists and fungi, were examined across the defined levels of anthropogenic disturbance. Additionally, using multiple methodological approaches, both taxonomic shifts (amplicon sequencing) and variations in gene profiles (metagenomics sequencing) of benthic microbial communities exposed to pollution were investigated.

Analysis of amplicon sequence data revealed that alpha diversity responses varied significantly among these microbial communities depending on disturbance intensity. While prokaryotic alpha diversity, in terms of both richness (observed ASVs) and Shannon diversity index, remained largely unchanged, fungal and protistan communities exhibited significant variations at specific disturbance levels. This finding suggests that prokaryotic communities possess a high level of adaptability to long-term pollution in coastal sediments. Notably, even in heavily contaminated sediments, microbial communities have been shown to remain comparably abundant and diverse to those in uncontaminated sediments, as previously observed by Gillan et al. (2005). However, a study by Korlević et al. (2015) reported a decrease in bacterial diversity in oil-contaminated sediments from the northern Adriatic Sea. This finding emphasizes the importance of broader studies across multiple sites with varying levels of anthropogenic disturbance to better understand diversity changes in benthic microbial communities. Interestingly, fungal alpha diversity patterns based on the Shannon index are partially consistent with the intermediate disturbance hypothesis, which suggests that moderate disturbance promotes higher diversity (Kang et al., 2024). In our study, this relationship was also observed in terms of richness (observed ASVs). Conversely, protistan diversity demonstrated significant variability across multiple disturbance levels, indicating high sensitivity to pollutants and environmental fluctuations, especially at higher DLs. This observation aligns with previous findings suggesting that protists are more sensitive to pollution than bacteria and fungi, as seen in soil ecosystems polluted with PAHs (Wu et al., 2022).

Metagenomic analysis further demonstrated that both contamination and the defined DLs influenced changes in the alpha diversity of several biomarker types. While taxonomic diversity decreased under contamination (as shown by Fisher's α index, observed richness and ACE index), specific biomarkers, including antibiotic and metal resistance genes, aromatic hydrocarbon degradation genes, mobile genetic elements, virulence factors and functional genes, exhibited an increased diversity. The highest taxonomic diversity recorded in non-contaminated sediments indicated that the structural integrity of microbial communities is maintained in pristine environments. The observed reduction of diversity under contamination likely reflects the selection of disturbance-tolerant taxa (Jurburg et al., 2024). This pattern was also largely consistent when considering the defined DLs, with both extreme and medium disturbance

exerting the strongest effects on the diversification of specific biomarkers, including metal resistance genes, aromatic hydrocarbon degradation genes, mobile genetic elements, virulence factors and functional genes. These results align with previous studies showing that increased pollution drives the diversification of specific gene pools in various environments subjected to different anthropogenic pressures (Durand et al., 2023; Sutton et al., 2013; Yang et al., 2016).

Beta diversity analysis revealed significant differences between all three communities across the five defined DLs and sampling locations, with the magnitude of explained variance (R^2) varying among communities. The analysis showed that location explained a higher proportion of community variation compared to the defined DLs. Prokaryotic beta diversity showed consistent and moderate differences between the DLs, indicating a gradual turnover along the disturbance gradient. Fungal communities also exhibited significant beta diversity differences across most DLs, although pairwise R^2 values were lower in comparisons involving high and extreme DLs. These results suggest that fungal communities tend to stabilize at high and extreme DLs, likely due to loss of sensitive taxa and dominance of tolerant ones (Nogales et al., 2011). In contrast, protistan communities exhibited the strongest overall differences across the DLs, reflecting a high sensitivity to disturbance. Moreover, clear regional clustering patterns (northern and southern Adriatic) were observed across all three microbial communities. Notably, samples from estuarine sediments in Raša Bay formed distinct clusters, suggesting the specific adaptation of these communities to unique conditions of estuarine habitats (Burgaud et al., 2013; Anas et al., 2021). Furthermore, the similarity between prokaryotic and protistan communities from the Port of Split and Vranjic Basin may be attributed to their geographical proximity.

Our study identified predominant taxa from all three communities, showing consistency with previous research findings. The most abundant bacterial phyla were *Proteobacteria*, *Actinobacteriota* and *Desulfobacterota*, while the dominant fungal taxa belonged to *Ascomycota* and *Basidiomycota* (Sarma, 2019; Hoshino et al., 2020; Dell'Anno et al., 2021a). Among protists, the diatoms *Bacillariophyceae* dominated the benthic environment (Mahmudi et al., 2025). However, a considerable portion of the community consisted of microbial populations with less than 1% relative abundance, indicating an abundant rare microbial biosphere. Additionally, many ASVs remained unclassified, highlighting the database limitations for marine microbes, especially for fungal sequences (Breyer and Baltar, 2023).

Analyzing the log2 fold changes of relative abundances between samples across the DLs provided initial insights into the responses of specific microbial families to environmental stress. Based on these patterns, families could be classified as either sensitive or tolerant to disturbance. Several families exhibited changes in relative abundances across the DLs, however, these results should be interpreted with caution due to the unequal distribution of samples across the DLs. Nevertheless, families

such as *Burkholderiaceae*, *Pseudomonadaceae* and *Cyanobacteria*, which have previously been reported as tolerant to anthropogenic stress (Morya et al., 2020; Chen et al., 2021; Mehdizadeh Allaf and Peerhossaini, 2022), showed increased abundance in extremely disturbed samples. Similarly, *Lactobacillaceae*, identified as a potential bioremediators due to heavy metal biosorption capabilities, also increased in abundance at the extreme DL (Ameen et al., 2020).

Interestingly, the *Woeseiaceae* family, known for its ability to use a range of electron donors, demonstrated increased abundance at the mild, medium and high DLs, but declined under extreme disturbance (Lian et al., 2025). The rarely studied B2M28, whose indicator potential has only recently been highlighted in marine sediments, also exhibited a significant decrease in relative abundance under extreme disturbance (Wang et al., 2024). Similarly, *Thermoanaerobaculaceae*, known for its sensitivity to environmental changes, demonstrated reduced abundance at the extreme DL (Moreira et al., 2023). Among sulphate-reducing bacteria, *Desulfocapsaceae* and *Deulfosarcinaceae*, previously identified as mercury bioindicators, displayed reduced abundance under high and extreme disturbances, respectively (Rincón-Tomás et al., 2024).

Regarding fungal taxa, only the yeast family *Metschnikowiaceae* showed significant changes across the DLs, with a decline at the extreme DL. Despite limited research on this family in marine sediments, a previous study reported high abundance along sediment depth gradients, suggesting tolerance to diverse environmental conditions (Rojas-Jimenez et al., 2020). Among protists, diatoms are frequently used as bioindicators of pollution due to their sensitivity to environmental changes (Potapova and Charles, 2007). In this study, *Bacillariophyceae* showed a gradual decline in relative abundance with increasing DLs, except at the extreme DL, where an increase was observed. This pattern may reflect the resilience of certain diatom species capable of tolerating high levels of pollutants, such as metals (Martínez et al., 2021).

5.3. Anthropogenic and environmental drivers of microbial community dynamics in coastal sediments

After establishing general patterns of microbial community dynamics under long-term disturbance, the impact of individual factors on both microbial abundance and presence/absence (i.e. microbial incidence) was investigated using amplicon sequence data. Metagenomic analysis was also performed to explore changes in gene abundances across different disturbance levels, locations and the presence or absence of contamination.

Among the various dispersal and selection factors tested, including physicochemical parameters, chemical and nutrient pollutants and geographical aspects, dispersal factors (location, region, depth and grain size) were found to be the primary drivers affecting both microbial abundance and incidence. Among these, location emerged as the most dominant factor influencing benthic prokaryotes, fungi and protists. These findings align with previous studies, emphasizing the importance of biogeography in shaping microbial communities. Geographic isolation and local habitat conditions are key determinants of species distribution and drive microbial diversity across various marine ecosystems (Martiny et al., 2006; Hanson et al., 2012; Nemergut et al., 2013). Our results suggest that distinct microbial communities develop within individual ports or bays, highlighting the more substantial role of biogeography compared to anthropogenic factors, such as chemical pollutants and nutrient inputs. This observation was further supported by the distance-decay relationship recorded for all three microbial communities, consistent with previous studies demonstrating scale-dependent biogeographic patterns in prokaryotes, fungi and protists (Trouche et al., 2021; Zhao et al., 2022; Clark et al., 2021).

Of the selection factors analyzed, only temperature (in both the sediment and bottom water layer) and the defined anthropogenic disturbance levels (DLs) significantly influenced all three microbial communities. This highlights the relevance of ongoing temperature shifts and climate change, which inevitably affect marine ecosystems, alongside continuous anthropogenic pressures present in coastal ecosystems (IPCC, 2023). Numerous studies have demonstrated that temperature changes significantly impact prokaryotic community composition, structure, metabolism and growth (Abreu et al., 2023; Ward et al., 2017; Seidel et al., 2023). Additionally, changes in the structure of marine fungi and protists due to temperature shifts have also been previously reported (Taylor and Cunliffe, 2016; Ahme et al., 2024). These impacts could have significant consequences for nutrient cycling and ecosystem services (Danovaro et al., 2017; Hicks et al., 2018). Interestingly, prokaryotic abundance showed a statistically significant, albeit weak, response to salinity, suggesting limited yet detectable sensitivity to broader environmental gradients. No other selection factors significantly affected prokaryotic abundance,

suggesting potential resistance and the ability to maintain stability despite nutrient and heavy metal stress (Zhang et al., 2025).

Protistan abundance appeared to be influenced by a few additional selection factors, including Hg, TOC, Bi and As, suggesting potential sensitivity of protistan communities to certain pressures. However, the proportion of variation explained by these factors was low, and their influence should be interpreted with caution. In contrast to our findings, previous studies reported that marine protistan communities are predominantly shaped by selection pressures rather than dispersal limitation, although the influence of dispersal limitation was found to increase with water depth (Wu et al., 2018). Their abundance may also be influenced by untested factors, such as trophic interactions, particularly bacterial grazing, which can be shaped by local environmental conditions. Furthermore, dormant protistan taxa may obscure the impact of selection factors (Wu and Huang, 2019).

Fungal abundance showed statistically significant responses to several selection factors, including sediment redox potential, Cu, Zn, Cd and total nitrogen. However, compared to disturbance level and bottom water temperature, these relationships should be interpreted with caution, as the proportion of explained variance was relatively low. This suggests that while these factors may influence fungi to some extent, their effects may be limited in ecological relevance. Marine fungi have been reported across a variety of habitats and are recognized for their adaptability to diverse environmental conditions, including their tolerance to and ability to degrade pollutants (Amend et al., 2019; Dell'Anno et al., 2021a). Additionally, previous research has shown that dispersal factors have a greater impact on benthic fungi compared to benthic bacteria (Zhao et al., 2022), while environmental conditions and geographical location significantly influence pelagic fungal communities (Tisthammer et al., 2016).

The incidence of all three microbial communities (prokaryotes, fungi and protists), reflecting the presence or absence of taxa, was influenced by fewer selection factors compared to their abundance. Presence–absence (incidence) data have previously been used to highlight changes in the occurrence of rare taxa (Dorazio et al., 2011). Although the ecological roles of rare taxa remain less well understood, they have been reported to contribute to ecological stability, functional redundancy and community turnover (Kaminsky and Morales, 2018; Qiu et al., 2024).

Metagenomic data analysis further supported these findings, revealing location as the primary factor influencing biomarker diversity, compared to general presence of contamination in sediments or the defined DLs. The highest taxonomic microbial diversity, based on richness indices (observed richness, Fisher's α and ACE), was observed in the control locations and the Port of Pula. While high diversity is expected in control locations, the similarly elevated values in the Port of Pula, despite its known pollution history, may indicate microbial resilience or reflect the effects of periodical rather than chronic pollution.

Despite exhibiting lower taxonomic richness, the microbial communities in the Port of Rijeka and Bakar Bay displayed the highest values of Shannon and inverse Simpson's indices. This suggests that microbial communities in the Port of Rijeka and Bakar Bay are more evenly distributed, potentially reflecting adaptation to long-term environmental stress. The Ports of Split and Rijeka and Vranjic Basin showed the greatest diversity of functional genes, ARGs, biocide and metal resistance genes, mobile genetic elements, DNA viruses and virulence factors, across nearly all alpha diversity indices. These findings suggest that microbial communities have adapted to persistent environmental pressures, potentially facilitated by horizontal gene transfer in response to long-term pollutant exposure (Jang et al., 2022).

Furthermore, Boruta-selected most important features across locations revealed a diverse distribution of AHC degradation genes. Notable enrichments were observed in specific samples from the Port of Split, Šibenik Bay, Port of Pula, and Bakar Bay. Sample VR7 from Vranjic Basin stood out with particularly high gene abundances and clustered separately, suggesting a strong microbial response to local pollution. These locations have previously been recognized as heavily influenced by diverse anthropogenic activities, including marinas, shipyards and tourism, potentially leading to the development of microbial adaptation mechanisms (Obhođaš and Valković, 2010; Furdek Turk et al., 2024). Given the widespread presence of toxic and carcinogenic aromatic compounds, such as PAHs, phenol, toluene and aromatic amines (Mainka et al., 2021), these locations may serve as reservoirs of novel degradation genes and enzymes with potential applications in the bioremediation of hydrocarbon-contaminated marine environments.

In addition, several ARGs associated with multidrug resistance were identified using the Boruta algorithm, highlighting the potentially diverse nature of pollution sources affecting these environments. The co-occurrence of heavy metal resistance genes, including As, Cu, Cd and Zn resistance genes, indicates that antibiotic resistance may have been co-selected due to prolonged industrial pollution, resulting in a higher diversity and abundance of ARGs (Banchi et al., 2024). Elevated abundances of specific biocide resistance genes in samples from the Port of Split, Vranjic Basin, Šibenik Bay and the Port of Pula reflect microbial adaptation to historical or ongoing pollution, as these locations are known to be heavily industrialized. Notably, sample SI5 from Šibenik Bay clearly separated from the other samples, exhibiting elevated abundances of multiple metal resistance genes, including those for As, Cd, Cu and Zn. The enrichment of these resistance genes aligns with the widespread use of antifouling agents in marine paints, metal-containing industrial runoff, phosphate ore transshipment and historical activities, such as the former ferromanganese industry in Šibenik Bay (Cukrov et al., 2024). Additionally, geological processes can contribute to the natural presence of As in the environment. Previous research has shown

that even low concentrations of As can enrich antibiotic-resistant bacteria and maintain multiresistance plasmids (Gullberg et al., 2014).

These findings suggest that these locations are subject to long-term anthropogenic pressures, highlighting their potential as hotspots for the proliferation of resistance genes. This could potentially lead to resuspension, along with horizontal gene transfer and the subsequent spread of resistance within marine environments, raising health risk concerns in coastal areas (Banchi et al., 2023; Sivalingam et al., 2024).

5.4. Identification of bacterial resistance from polluted sediments

The identification of heavy metals as selection factors influencing specific microbial communities, combined with metagenomic findings, indicated that distinct gene pools related to metal resistance have developed at the studied locations. This prompted further investigation into pollutant-resistant bacteria with potential applications in the bioremediation of polluted sediments.

Bacterial isolates obtained from the polluted Šibenik Bay exhibited varying degrees of resistance to nine tested heavy metals (Cd, Co, Cr, Cu, Hg, Ni, Pb, Sn, Zn) and tributyltin (TBT). The microbial community showed relatively low tolerance to Cd, Cr, Cu, Sn and Zn, with slightly higher resistance observed for TBT. Notably, isolates demonstrated strong adaptation to elevated concentrations of Co, Ni, Cr and particularly Pb, suggesting long-term selective pressure in this environment. As expected, Hg emerged as the most toxic metal, with bacterial isolates exhibiting the lowest tolerance, reflecting its well-documented high reactivity and cellular toxicity (Joshi et al., 2022). These results align with previous studies showing that bacterial communities in metal-polluted environments develop resistance mechanisms to specific pollutants while remaining vulnerable to others (Chen et al., 2019b; Jroundi et al., 2020). The observed resistance patterns may be driven by genetic adaptations, such as metal efflux systems, enzymatic detoxification or biofilm formation, which warrant further investigation (Nnaji et al., 2024).

Despite the generally low number of highly resistant isolates, a few demonstrated strong resistance to high pollutant concentrations. Notably, several isolates (25, 36, 47, 81) exhibited resistance to up to seven pollutants. Isolates 25 and 81 were identified as *Bacillus sp.*, isolate 36 as *Mesobacillus jeotgali* and isolate 47 as *Cytobacillus oceanisediminis*, all members of the family *Bacillaceae*. Various species within the family *Bacillaceae* have previously demonstrated high levels of metal resistance (Jroundi et al., 2020). Interestingly, the genus *Rossellomorea*, which is phylogenetically related to the genus *Bacillus*, has recently been isolated from sediment samples in China, exhibiting resistance to both the antibiotic lincomycin and copper (Zhu et al., 2023). Additionally, a similar strain, *Rossellomorea arthrocnemi* has been used in phytoremediation of heavy metal-polluted soils (Navarro-Torre et al., 2021). *Mesobacillus jeotgali* isolated from coastal sediments, has been tested as a biosorbent, confirming its efficacy for Cd and Zn removal from coastal environments (Green-Ruiz et al., 2008). Furthermore, *Cytobacillus pseudoceanisediminis*, closely related to *Cytobacillus oceanisediminis*, was isolated from a deep subsurface saline spring and exhibited tolerance to high concentrations of Cd, Cu and Pb, although not Zn (Tarasov et al., 2023).

These findings highlight the critical roles of dispersal and selective factors in structuring benthic microbial communities and underscore the potential of specific resistant isolates for use in the

bioremediation of heavy metal-polluted sediments. Furthermore, a combination of culture-dependent and culture-independent techniques remains the most effective approach for comprehensively assessing microbial community dynamics under anthropogenic disturbances and for developing targeted remediation strategies.

5.5. Proposal of microbial indicators of anthropogenic pressures

Building on observed benthic microbial responses to multiple pollution pressures, the final aim of this study was to identify potential microbial indicators of anthropogenic disturbance. Microorganisms are notably underrepresented within the 11 qualitative Descriptors of the MSFD, where they are mentioned only as criterion elements, such as the abundance of heterotrophic bacteria, biomass of autotrophic picoplankton and bacterial production (MSFD, 2008/56/EC; Commission Decision, 2017/848/EU). At the same time, the availability of state-of-the-art molecular tools, including eDNA-based amplicon and metagenomic sequencing, now enables a comprehensive understanding of anthropogenic impacts on marine ecosystems and has the potential to revolutionize environmental quality monitoring approaches.

Based on results showing that specific microbial families exhibited changes across the defined levels of anthropogenic disturbance, further analysis of entire communities was performed using specific statistical approaches to identify potential microbial indicators. To achieve this, both abundant and rare taxa within all three microbial communities studied were considered, employing a multilevel approach that integrated both amplicon and metagenomic sequence data. The aim was to identify potential microbial indicators by examining: (i) community structural features (changes in specific taxa or diversity), (ii) community functional features (changes in the abundance of specific genes) and (iii) changes in microbial interactions under disturbance.

Differential expression analysis (DESeq2) and log2 fold change analysis of all obtained amplicon sequences, pointed to prokaryotes as the most suitable candidates for microbial indicator identification. The results demonstrated that protistan and fungal communities do not serve as reliable indicators of benthic health, as no clear relationship was observed between communities in contaminated vs. non-contaminated locations. Based on this analysis, seven members of the bacterial community (seven ASVs) were identified as promising indicators of disturbed sediment environments. However, their reliability was limited to distinguishing between the presence or absence of contamination rather than indicating specific disturbance levels. These contamination-tolerant bacteria included ASVs belonging to families *Rhodobacteraceae* (*Boseongicola*), *Thermoanaerobaculaceae* (Subgroup 23), *Ectothiorhodospiraceae* (*Thiogranum*), B2M28 and Sva0485. These microbial populations are chemoautotrophic, sulfur-oxidizing or sulfate/iron-reducing bacteria, with most of them remaining uncultured to date (Pohlner et al., 2019; Dedysh and Lawson, 2020; Mori et al., 2015; Wang et al., 2024; Ghezzi et al., 2024). Additionally, the analysis distinguished disturbance sensitive bacteria enriched in non-contaminated sediments, including ASVs belonging to *Lactobacillaceae* (*Lactobacillus*), unclassified *Lachnospiraceae*, *Burkholderiaceae* (*Burkholderia*, *Ralstonia*) and *Pseudomonadaceae* (*Pseudomonas*).

These results contrast with the observed log2 fold changes for *Thermoanaerobaculaceae* and B2M28, which demonstrated tolerance at the mild, medium and high DLs, but not at the extreme DL. This inconsistency is likely attributable to the unequal distribution of samples across DLs, particularly within the extreme DL group. It further highlights the challenges associated with identifying indicators based on the defined DLs, as opposed to indicators that reflect only the presence or absence of contamination in sediments. Interestingly, *Lactobacillaceae*, *Burkholderiaceae* and *Pseudomonadaceae* consistently exhibited stress sensitivity in both log2 fold changes and differential expression analyses, confirming their potential as reliable indicators of pristine sediment conditions. These findings are somewhat unexpected since specific members of *Pseudomonadaceae* and *Burkholderiaceae* have previously been recognized for their ability to degrade pollutants, such as PAHs (Dong et al., 2015; Revathy et al., 2015).

Subsequently, CRT analysis was employed which provided a deeper understanding of the complexity involved in proposing indicators of anthropogenic pressure. Previously, machine learning has been used for analyzing microbial communities for environmental and human health (Ghannam and Techtmann, 2021). The results suggested that indicators should not be limited to individual species but rather represented by a community of microorganisms. Furthermore, it was demonstrated that, in addition to the identity of the indicator organism, its precise abundance within the sediment is a critical parameter when assessing its relevance as an indicator. Consistent with the findings from the DESeq2 analysis, protists and fungi proved to be less reliable as potential indicators, since no consistent patterns were observed across different levels of anthropogenic disturbance. It is important to acknowledge that the CRT method was employed as a *de novo* testing approach, primarily due to the limited sample size, which did not meet the threshold required for robust statistical analysis (more than 1000 inputs).

The results revealed that the same bacterial population can serve as a potential indicator for both contaminated and non-contaminated locations, with its significance determined primarily by its relative abundance. A group of bacterial populations has been identified as potential indicators, whose specific relative abundances can be used to classify sediments as being under high (*Bacillaceae*/*Sulfurovaceae*/*Thermoanaerobaculaceae*) and extreme (*Bacillaceae*/*Sulfurovaceae*/*Nitrosopumilaceae*) anthropogenic pressure. Interestingly, the same populations of *Bacillaceae* and *Thermoanaerobaculaceae* were also identified as indicators of non-contaminated locations. However, compared to the anthropogenically impacted locations, these populations needed to be either enriched (*Bacillaceae)* or reduced (*Thermoanaerobaculaceae)* in pristine environments. Moreover, sediments subjected to medium anthropogenic pressure exhibited entirely distinct and specific groups of indicator populations, highlighting the variability in community composition under intermediate disturbance conditions (Santillan et al., 2019). Additionally, rare taxa with low relative abundances were consistently

identified as key members of the community, emphasizing the importance of incorporating the rare microbial biosphere into benthic health assessments (Qiu et al., 2024).

In the search for microbial indicators, it is essential to consider not only the microbial composition and relative abundances but also their interactions and ecological functions. While earlier research has predominantly focused on the selection factors shaping individual microbial communities, more recent studies have begun to explore interactions between different microbial communities, although these efforts have mostly been limited to soil environments (Ceja-Navarro et al., 2021; Wang et al., 2023). Our results demonstrated that heavy metal pollution (Bi, Cd, Cu, Zn and Hg) strongly shapes microbial interactions in marine sediments. Heavy metal pollution led to a decoupling of microbial communities, weakening interactions in polluted sediments compared to less polluted ones. In sediments with low pollution levels, the strongest correlations were observed between prokaryotes and protists, underscoring the importance of protistan grazing on prokaryotes. This grazing process significantly influences the composition and diversity of prokaryotic communities in aquatic ecosystems (Bock et al., 2020; Hu et al., 2021). Interestingly, some studies reported that protists could facilitate pollutant degradation through grazing, both in sediment and soil environments (Tso and Taghon, 2006; Mattison et al., 2005). However, protistan grazing on bacteria has also been reported to inhibit hydrocarbon degradation (Beaudoin et al., 2016). Additionally, protists have been found to exhibit greater sensitivity to toxic compounds, such as PAHs, compared to bacteria, which may lead to cascading effects on prey control. This sensitivity, however, can vary depending on the protist species and their surface-to-volume ratios (Winding et al., 2019).

In contrast, a decline of prokaryote-fungi interactions was observed in metal-polluted sediments, indicating potential disruption of functional interactions essential for ecosystem functioning (Liu et al., 2019; Nawaz et al., 2022). Previous research has highlighted the importance of bacteria-fungi interactions in marine sediments, particularly in the transformation of complex pollutants such as PAHs (Álvarez-Barragán et al., 2023). Additionally, fungi-protist interactions were observed as the least sensitive to heavy metal pollution, with even a positive correlation observed in mercury-polluted sediments. One possible explanation is that heavy metal disturbances in benthic environments may lead to a reduction in microbial diversity, resulting in intensified interactions among pollution-tolerant taxa. Similarly, protistan diversity has been reported to decrease in soil environments polluted with mercury (L. Wang et al., 2020). Such intensification of interactions at high pollution levels could potentially enhance microbial community resistance to environmental changes (Du et al., 2022). Furthermore, protists in soil have been demonstrated to act as fungal predators, thereby influencing interactions and shaping food web dynamics (Geisen et al., 2016).

Interestingly, one of the few studies applying a multitrophic approach explored co-occurrence networks among bacteria, protists, fungi and nematodes in soil (Wang et al., 2023). This study specifically reported a shift from the typical top-down regulation (where predators control prey populations), to bottom-up regulation under heavy metal disturbances. This shift indicated that protists at higher trophic levels were influenced by changes at lower levels (bacteria and fungi) (Wang et al., 2023). In summary, these findings suggest that heavy metal pollution could destabilize trophic interactions in sediments, leading to the disruption of essential ecosystem processes.

Finally, the Boruta feature selection algorithm, based on random forest approach, was applied to both taxonomy and SEED biomarkers to identify the most important features (microbial taxa and functions) that differentiate between control and anthropogenically disturbed locations. The taxonomy biomarker analysis revealed 47 microbial taxa whose reduced abundances in sediment could serve as indicators of a disturbed marine ecosystem. These taxa predominantly included bacteria from the phyla *Proteobacteria*, *Planctomycetes* and *Cyanobacteria*, along with fungi from *Ascomycota* and protists from *Chlorophyta.*

The SEED biomarker analysis identified 44 functional features that differentiated between control and polluted locations. These functions included genes involved in essential cellular processes, including protein, DNA and RNA metabolism, respiration, cell division and cell cycle regulation, nitrogen metabolism and carbohydrate metabolism. A decrease in these functions could serve as a potential indicator of a disturbed marine ecosystem (Markussen et al., 2018). The comprehensive representation of diverse functional categories suggests that long-term anthropogenic pressures significantly impact not only microbial community composition but also their metabolic and functional potential. Although no prior studies have employed the Boruta algorithm specifically to identify microbial indicators of pollution, its robustness makes it a promising tool for environmental assessments (Lawal et al., 2023). Notably, it has previously been validated in a hydroclimatic study for soil moisture estimation (Ahmed et al., 2021).

The evident clustering based on pollution further highlights the potential of these microbial indicators as reliable bioindicators of human-induced environmental stress. However, the dynamic nature of microbial communities in response to long-term anthropogenic disturbances necessitates further research to validate these microbial indicators across diverse marine environments. Ultimately, selected microbial features could be introduced as new criteria within the MSFD, particularly under Descriptor 1 (1.7.1 – Composition and relative proportions of ecosystem components), Descriptor 4 (4.3.1 – Abundance trends of functionally important selected groups/species) and/or Descriptor 6 (6.2.1 – Presence of particularly sensitive and/or tolerant species; 6.2.2 – Multi-metric indices) (Caruso et al., 2015). Additionally, integrating the identified microbial indicators at both taxonomic and functional levels

would enhance monitoring capabilities and support the development of effective strategies to protect vulnerable coastal ecosystems from ongoing anthropogenic pressures. While current environmental monitoring remains heavily focused on *chemical quality elements*, it is essential to emphasize the importance of *biological quality elements* (Caruso et al., 2015). These elements, especially those incorporating diverse indicator organisms across multiple trophic levels, are crucial for detecting the deleterious effects of human-induced stressors on marine ecosystems. Microorganisms (prokaryotes, fungi and protists), which numerically dominate marine ecosystems and play pivotal roles in ecosystem functioning, should be given thoughtful consideration as key contributors to environmental quality assessments.

6. Conclusions

This comprehensive study investigated benthic microbial communities (prokaryotes, fungi and protists) in long-term polluted coastal zones of the eastern Adriatic. Multiple analyses were conducted to identify both the key factors shaping the microbial communities and the potential microbial indicators of anthropogenic disturbance. By integrating both culture-dependent and culture-independent approaches, the study evaluated microbial responses to chronic pollution and identified specific bacteria exhibiting pollutant resistance, highlighting their potential for sediment bioremediation applications.

The following points summarize the major outcomes and insights gained from the investigation, reflecting the set objectives:

1. Hypothesis: *Under chronic anthropogenic pressures, the structure, diversity and/or interactions of benthic microbial communities are altered compared to those at control locations.*

    - Research findings support this hypothesis by demonstrating significant shifts in microbial diversity and relative abundances in response to anthropogenic disturbances, revealing the presence of both tolerant and sensitive taxa.

    - The research emphasized the significant impact of biogeographical patterns, particularly location, in shaping each of the studied microbial communities.

    - Additionally, observed changes in microbial interactions under heavy metal stress highlight the impact of anthropogenic pressures on food web dynamics and ecosystem functioning.

    - Patterns identified through metagenomic data analysis underscore the profound effects of disturbance on microbial community dynamics.

2. Hypothesis: *Specific benthic microorganisms and/or their properties exhibit indicator potential for assessing anthropogenic pressures.*

    - This hypothesis was validated through several analyses, based on differential abundance methods and algorithmic approaches, which confirmed that prokaryotes, compared to fungi and protists, serve as the most reliable indicators for assessing anthropogenic disturbance in marine sediments. Specifically, members of the families *Lactobacillaceae*, *Burkholderiaceae* and *Pseudomonadaceae* were more prevalent in non-contaminated locations, while members of the families such as *Rhodobacteraceae*, *Thermoanaerobaculaceae* and *Ectothiorhodospiraceae* were identified as taxa tolerant to contamination.

    - While prokaryotes demonstrate potential as microbial indicators of anthropogenic pressures, our findings suggest that distinguishing indicators of contamination vs. non-contamination might be a more effective strategy compared to differentiating among the varying levels of anthropogenic disturbance (DLs).

    - It's important to note that different analytical methods yielded different results regarding microbial indicators. For example, Boruta algorithm identified a completely different set of indicators, including both fungi (*Ascomycota*) and protists (*Chlorophyta*). This discrepancy underscores the need for employing multiple approaches to identify reliable microbial indicators of anthropogenic disturbances, as well as expanding the study area to capture broader variability.

    - Metagenomic data analyses further demonstrated the need to shift the focus of future studies towards identifying functional features that differentiate between contaminated and non-contaminated locations. Additionally, location emerged as a primary driver of the biomarkers, emphasizing the importance of defining location-specific microbial indicators.

3. Hypothesis: *Members of the benthic bacterial community under chronic anthropogenic pressure develop resistance to pollutants present in the sediment.*

- Specific bacterial strains were isolated and identified, exhibiting resistance to multiple pollutants, thereby indicating their potential for future studies aimed at identifying resistance genes and elucidating genetic and adaptative mechanisms.

- Bacterial strains showing the highest resistance include the genera *Bacillus*, *Mesobacillus* and *Cytobacillus*, all belonging to the family *Bacillaceae*. The identification of these taxa underscores the adaptive mechanisms of benthic bacteria under chronic environmental stress, highlighting their potential as promising candidates for sediment bioremediation applications and environmental monitoring.

Overall, the study provides novel insights into the dynamics of benthic microbial communities, particularly for understudied benthic fungi, in long-term polluted ports and bays along the Croatian Adriatic coast. The observed influence of biogeographical patterns indicates that local conditions, combined with chronic anthropogenic pressures, drive the formation of specific ecological niches. The impact on microbial interactions highlights the ecological consequences of coastal pollution and its effects on essential ecosystem services.

These findings underscore the urgent need for the development of marine pollution management strategies, with microbial indicators of pollution serving as valuable tools for environmental monitoring and guiding policy decisions. Furthermore, understanding microbial adaptations to pollution can facilitate the implementation of nature-based solutions for the restoration of polluted coastal sediments. Finally, advancing knowledge in this area will enhance the ability to predict ecosystem destabilization under multiple stressors, including both anthropogenic pressures and the impacts of ongoing climate change.

7. Literature

1. Abreu, C.I., Dal Bello, M., Bunse, C., Pinhassi, J., Gore, J., 2023. Warmer temperatures favor slower-growing bacteria in natural marine communities. *Sci. Adv.* 9(19), eade8352. https://doi.org/10.1126/sciadv.ade8352
2. Acosta-González, A., Marqués, S., 2016: Bacterial diversity in oil-polluted marine coastal sediments. *Curr. Opin. Biotechnol.* 38, 24–32. https://doi.org/10.1016/j.copbio.2015.12.010
3. Adl, S.M., Bass, D., Lane, C.E., Lukeš, J., Schoch, C.L., Smirnov, A., Agatha, S., Berney, C., Brown, M.W., Burki, F., Cárdenas, P., Čepička, I., Chistyakova, L., Del Campo, J., Dunthorn, M., Edvardsen, B., Eglit, Y., Guillou, L., Hampl, V., Heiss, A.A., Hoppenrath, M., James, T.Y., Karnkowska, A., Karpov, S., Kim, E., Kolisko, M., Kudryavtsev, A., Lahr, D.J.G., Lara, E., Le Gall, L., Lynn, D.H., Mann, D.G., Massana, R., Mitchell, E.A.D., Morrow, C., Park, J.S., Pawlowski, J.W., Powell, M.J., Richter, D.J., Rueckert, S., Shadwick, L., Shimano, S., Spiegel, F.W., Torruella, G., Youssef, N., Zlatogursky, V., Zhang, Q., 2019. Revisions to the Classification, Nomenclature, and Diversity of Eukaryotes. *J. Eukaryot. Microbiol.* 66, 4–119. https://doi.org/10.1111/jeu.12691
4. Ahme, A., Happe, A., Striebel, M., Cabrerizo, M.J., Olsson, M., Giesler, J., Schulte-Hillen, R., Sentimenti, A., Kühne, N., John, U., 2024. Warming increases the compositional and functional variability of a temperate protist community. *Sci. Total Environ.* 926, 171971. https://doi.org/10.1016/j.scitotenv.2024.171971
5. Ahmed, A.A.M., Deo, R.C., Ghahramani, A., Raj, N., Feng, Q., Yin, Z., Yang, L., 2021. LSTM integrated with Boruta-random forest optimiser for soil moisture estimation under RCP4.5 and RCP8.5 global warming scenarios. *Stoch. Environ. Res. Risk. Assess.* 35, 1851–1881. https://doi.org/10.1007/s00477-021-01969-3
6. Alkhasawneh, M.S., Ngah, U.K., Tay, L.T., Mat Isa, N.A., Al-Batah, M.S., 2014. Modeling and testing landslide hazard using decision tree. *J. Appl. Math.* 2014, 929768. https://doi.org/10.1155/2014/929768
7. Alvarado-Campo, K.L., Quintero, M., Cuadrado-Cano, B., Montoya-Giraldo, M., Otero-Tejada, E.L., Blandón, L., Sánchez, O., Zuleta-Correa, A., Gómez-León, J., 2023. Heavy metal tolerance of microorganisms isolated from coastal marine sediments and their lead removal potential. *Microorganisms* 11, 2708. https://doi.org/10.3390/microorganisms11112708
8. Álvarez-Barragán, J., Cravo-Laureau, C., Xiong, B., Wick, L.Y., Duran, R., 2023. Marine fungi select and transport aerobic and anaerobic bacterial populations from polycyclic aromatic hydrocarbon-contaminated sediments. *mBio* 14, e02761-22. https://doi.org/10.1128/mbio.02761-22

9. Álvarez-Vázquez, M.A., Farinango, G., Prego, R., 2023. Uranium as reference element to estimate the background of “Anthropocene” sensitive trace elements in sediments of the land-ocean continuum (Ulla-Arousa, NW Iberian Atlantic Margin). *Cont. Shelf Res*. 261, 105021. https://doi.org/10.1016/j.csr.2023.105021
10. Ameen, F.A., Hamdan, A.M., El-Naggar, M.Y., 2020. Assessment of the heavy metal bioremediation efficiency of the novel marine lactic acid bacterium, *Lactobacillus plantarum* MF042018. *Sci. Rep.* 10, 314–325. https://doi.org/10.1038/s41598-019-57210-3
11. Amend, A., Burgaud, G., Cunliffe, M., Edgcomb, V.P., Ettinger, C.L., Gutiérrez, M.H., Heitman, J., Hom, E.F.Y., Ianiri, G., Jones, A.C., Kagami, M., Picard, K.T., Quandt, C.A., Raghukumar, S., Riquelme, M., Stajich, J., Vargas-Muñiz, J., Walker, A.K., Yarden, O., Gladfelter, A.S., 2019: Fungi in the marine environment: open questions and unsolved problems. *mBio* 10, e01189–18. https://doi.org/10.1128/mbio.01189-18
12. Aminian-Biquet, J., Sletten, J., Vincent, T., Pieraccini, M., Queffelec, B., Laznya, A., Vaidianu, N., Claudet, J., Young, J., Horta E Costa, B., 2025. Major data gaps and recommendations in monitoring regulations of activities in EU marine protected areas. *npj Ocean Sustain.* 4, 3. https://doi.org/10.1038/s44183-025-00104-x
13. Anas, A., Tharakan, B.E.M., Jasmin, C., Chandran, C., Vipindas, P.V., Narayanan, S., Jaleel, A.K.U., 2021. Microbial community shifts along an estuarine to open ocean continuum. *Reg. Stud. Mar. Sci.* 41, 101587. https://doi.org/10.1016/j.rsma.2020.101587
14. Arango-Argoty, G., Garner, E., Pruden, A., Heath, L.S., Vikesland, P., Zhang, L., 2018. DeepARG: a deep learning approach for predicting antibiotic resistance genes from metagenomic data. *Microbiome* 6, 23. https://doi.org/10.1186/s40168-018-0401-z
15. Arango-Argoty, G.A., Dai, D., Pruden, A., Vikesland, P., Heath, L.S., Zhang, L., 2019. NanoARG: a web service for detecting and contextualizing antimicrobial resistance genes from nanopore-derived metagenomes. *Microbiome* 7, 88. https://doi.org/10.1186/s40168-019-0703-9
16. Aspila, K.I., Agemian, H., Chau, A.S.Y., 1976. A semi-automated method for the determination of inorganic, organic and total phosphate in sediments. *Analyst* 101, 187-197. https://doi.org/10.1039/AN9760100187
17. Atwood, T.B., Witt, A., Mayorga, J., Hammill, E., Sala, E., 2020. Global patterns in marine sediment carbon stocks. *Front. Mar. Sci.* 7, 165. https://doi.org/10.3389/fmars.2020.00165
18. Aylagas, E., Borja, A., Tangherlini, M., Dell’Anno, A., Corinaldesi, C., Michell, C.T., Irigoien, X., Danovaro, R., Rodríguez-Ezpeleta, N., 2017. A bacterial community-based index to assess the

ecological status of estuarine and coastal environments. *Mar. Pollut. Bull.* 114, 679–688. https://doi.org/10.1016/j.marpolbul.2016.10.050

19. Aylagas, E., Atalah, J., Sánchez-Jerez, P., Pearman, J.K., Casado, N., Asensi, J., Toledo-Guedes, K., Carvalho, S., 2021. A step towards the validation of bacteria biotic indices using DNA metabarcoding for benthic monitoring. *Mol. Ecol. Resour.* 21, 1889–1903. https://doi.org/10.1111/1755-0998.13395
20. Bakke, T., Källqvist, T., Ruus, A., Breedveld, G.D., Hylland, K., 2010. Development of sediment quality criteria in Norway. *J. Soils Sediments* 10, 172-178. https://doi.org/10.1007/s11368-009-0173-y
21. Banchi, E., Corre, E., Del Negro, P., Celussi, M., Malfatti, F., 2023. Genome-resolved metagenomics of Venice Lagoon surface sediment bacteria reveals high biosynthetic potential and metabolic plasticity as successful strategies in an impacted environment. *Mar. Life Sci. Technol.* 6, 126–142. https://doi.org/10.1007/s42995-023-00192-z
22. Banchi, E., Manna, V., Muggia, L., Celussi, M., 2024. Marine fungal diversity and dynamics in the Gulf of Trieste (Northern Adriatic Sea). *Microb. Ecol.* 87, 78. https://doi.org/10.1007/s00248-024-02394-z
23. Banos, S., Lentendu, G., Kopf, A., Wubet, T., Glockner, F.O., Reich, M., 2018. A comprehensive fungi-specific 18S rRNA gene sequence primer toolkit suited for diverse research issues and sequencing platforms. *BMC Microbiol.* 18, 190. https://doi.org/10.1186/s12866-018-1331-4.
24. Bargiela, R., Mapelli, F., Rojo, D., Chouaia, B., Tornés, J., Borin, S., Richter, M., Del Pozo, M.V., Cappello, S., Gertler, C., Genovese, M., Denaro, R., Martínez-Martínez, M., Fodelianakis, S., Amer, R.A., Bigazzi, D., Han, X., Chen, J., Chernikova, T.N., Golyshina, O.V., Mahjoubi, M., Jaouanil, A., Benzha, F., Magagnini, M., Hussein, E., Al-Horani, F., Cherif, A., Blaghen, M., Abdel-Fattah, Y.R., Kalogerakis, N., Barbas, C., Malkawi, H.I., Golyshin, P.N., Yakimov, M.M., Daffonchio, D., Ferrer, M., 2015. Bacterial population and biodegradation potential in chronically crude oil-contaminated marine sediments are strongly linked to temperature. *Sci. Rep.* 5, 11651. https://doi.org/10.1038/srep11651
25. Barrett, T., Dowle, M., Srinivasan, A. 2023. data.table: Extension of `data.frame`. R package version 1.14.10, https://CRAN.R-project.org/package=data.table
26. Baas Becking, L.G.M., 1934. Geobiologie of Inleiding Tot De Milieukunde. W.P. Van Stockum & Zoon, The Hague.
27. Baselga, A., Orme, D., Villeger, S., De Bortoli, J., Leprieur, F., Logez, M., Martinez-Santalla, S., Martin-Devasa, R., Gomez-Rodriguez, C., Crujeiras, R., 2023. betapart: partitioning beta diversity

into turnover and nestedness components. R package version 1.6, https://CRAN.R-project.org/package=betapart

28. Beaudoin, D.J., Carmichael, C.A., Nelson, R.K., Reddy, C.M., Teske, A.P., Edgcomb, V.P., 2016. Impact of protists on a hydrocarbon-degrading bacterial community from deep-sea Gulf of Mexico sediments: A microcosm study. *Deep Sea Res. Part II* 129, 350–359. https://doi.org/10.1016/j.dsr2.2014.01.007
29. Beg Paklar, B., Vilibić, I., Grbec, B., Matić, F., Mihanović, H., Džoić, T., Šantoć, D., Šestanović, S., Šolić, M., Ivatek-Šahdan, I., Kušpilić, G., 2020: Record-breaking salinities in the middle Adriatic during summer 2017 and concurrent changes in the microbial food web. *Prog. Oceanogr.* 185, 102345. https://doi.org/10.1016/j.pocean.2020.102345
30. Bihari, N., Fafanđel, M., Piškur, V., 2007. Polycyclic aromatic hydrocarbons and ecotoxicological characterization of seawater, sediment and mussel *Mytilus galloprovincialis* from the Gulf of Rijeka, the Adriatic Sea, Croatia. *Arch. Environ. Contam. Toxicol.* 52, 379–387. https://doi.org/10.1007/s00244-005-0259-5
31. Birch, G.F., 2017. Determination of sediment metal background concentrations and enrichment in marine environments–a critical review. *Sci. Total Environ.* 580, 813–831. https://doi.org/10.1016/j.scitotenv.2016.12.028
32. Bock, C., Jensen, M., Forster, D., Marks, S., Nuy, J., Psenner, R., Beisser, D., Boenigk, J., 2020. Factors shaping community patterns of protists and bacteria on a European scale. *Environ. Microbiol.* 22, 2243–2260. https://doi.org/10.1111/1462-2920.14992
33. Bogner, D., Ujević, I. and Barić, A., 2005. Trace metal (Cd, Pb, Cu, Zn and Cr) distribution in sediments along east coast of the Adriatic Sea (Croatia). *Fresenius Environ. Bull.* 14(1), 50–58.
34. Bolyen, E., Rideout, J.R., Dillon, M.R., Bokulich, N.A., Abnet, C.C., Al-Ghalith, G.A., Alexander, H., Alm, E.J., Arumugam, M., Asnicar, F., Bai, Y., Bisanz, J.E., Bittinger, K., Brejnrod, A., Brislawn, C.J., Brown, C.T., Callahan, B.J., Caraballo-Rodríguez, A.M., Chase, J., Cope, E.K., Da Silva, R., Diener, C., Dorrestein, P.C., Douglas, G.M., Durall, D.M., Duvallet, C., Edwardson, C.F., Ernst, M., Estaki, M., Fouquier, J., Gauglitz, J.M., Gibbons, S.M., Gibson, D.L., Gonzalez, A., Gorlick, K., Guo, J., Hillmann, B., Holmes, S., Holste, H., Huttenhower, C., Huttley, G.A., Janssen, S., Jarmusch, A.K., Jiang, L., Kaehler, B.D., Kang, K.B., Keefe, C.R., Keim, P., Kelley, S.T., Knights, D., Koester, I., Kosciolek, T., Kreps, J., Langille, M.G.I., Lee, J., Ley, R., Liu, Y.-X., Loftfield, E., Lozupone, C., Maher, M., Marotz, C., Martin, B.D., McDonald, D., McIver, L.J., Melnik, A.V., Metcalf, J.L., Morgan, S.C., Morton, J.T., Naimey, A.T., Navas-Molina, J.A., Nothias, L.F., Orchanian, S.B., Pearson, T., Peoples, S.L., Petras, D., Preuss, M.L., Pruesse, E.,

Rasmussen, L.B., Rivers, A., Robeson, M.S., Rosenthal, P., Segata, N., Shaffer, M., Shiffer, A., Sinha, R., Song, S.J., Spear, J.R., Swafford, A.D., Thompson, L.R., Torres, P.J., Trinh, P., Tripathi, A., Turnbaugh, P.J., Ul-Hasan, S., Van Der Hooft, J.J.J., Vargas, F., Vázquez-Baeza, Y., Vogtmann, E., Von Hippel, M., Walters, W., Wan, Y., Wang, M., Warren, J., Weber, K.C., Williamson, C.H.D., Willis, A.D., Xu, Z.Z., Zaneveld, J.R., Zhang, Y., Zhu, Q., Knight, R., Caporaso, J.G., 2019. Reproducible, interactive, scalable and extensible microbiome data science using QIIME 2. *Nat. Biotechnol.* 37, 852–857. https://doi.org/10.1038/s41587-019-0209-9

35. Borja, A., 2018. Testing the efficiency of a bacterial community-based index (microgAMBI) to assess distinct impact sources in six locations around the world. *Ecol. Indic.* 85, 594–602. https://doi.org/10.1016/j.ecolind.2017.11.018
36. Bortolaia, V., Kaas, R.S., Ruppe, E., Roberts, M.C., Schwarz, S., Cattoir, V., Philippon, A., Allesoe, R.L., Rebelo, A.R., Florensa, A.F., Fagelhauer, L., Chakraborty, T., Neumann, B., Werner, G., Bender, J.K., Stingl, K., Nguyen, M., Coppens, J., Xavier, B.B., Malhotra-Kumar, S., Westh, H., Pinholt, M., Anjum, M.F., Duggett, N.A., Kempf, I., Nykäsenoja, S., Olkkola, S., Wieczorek, K., Amaro, A., Clemente, L., Mossong, J., Losch, S., Ragimbeau, C., Lund, O., Aarestrup, F.M., 2020. ResFinder 4.0 for predictions of phenotypes from genotypes. *J. Antimicrob. Chemother.* 75, 3491–3500. https://doi.org/10.1093/jac/dkaa345
37. Bouchez, T., Blieux, A.L., Dequiedt, S., Domaizon, I., Dufresne, A., Ferreira, S., Godon, J.J., Hellal, J., Joulian, C., Quaiser, A., Martin-Laurent, F., Mauffret, A., Monier, J.M., Peyret, P., Schmitt-Koplin, P., Sibourg, O., D'oiron, E., Bispo, A., Deportes, I., Grand, C., Cuny, P., Maron, P.A., Ranjard, L., 2016: Molecular microbiology methods for environmental diagnosis. *Environ. Chem. Lett.* 14, 423–441. https://doi.org/10.1007/s10311-016-0581-3
38. Breyer, E., Baltar, F., 2023. The largely neglected ecological role of oceanic pelagic fungi. *Trends Ecol. Evol.* 38, 870–888. https://doi.org/10.1016/j.tree.2023.05.002
39. Burki, F., Roger, A.J., Brown, M.W., Simpson, A.G.B., 2020. The New Tree of Eukaryotes. *Trends Ecol. Evol.* 35, 43–55. https://doi.org/10.1016/j.tree.2019.08.008
40. Buchfink, B., Xie, C., Huson, D.H., 2015. Fast and sensitive protein alignment using DIAMOND. *Nat. Methods* 12, 59–60. https://doi.org/10.1038/nmeth.3176
41. Burgaud, G., Woehlke, S., Rédou, V., Orsi, W., Beaudoin, D., Barbier, G., Biddle, J.F., Edgcomb, V.P., 2013. Deciphering the presence and activity of fungal communities in marine sediments using a model estuarine system. *Aquat. Microb. Ecol.* 70, 45–62. https://doi.org/10.3354/ame01638

42. Burgaud, G., Edgcomb, V., Hassett, B.T., Kumar, A., Li, W., Mara, P., Peng, X., Philippe, A., Phule, P., Prado, S., Quéméner, M., Roullier, C., 2022: Marine Fungi, in: Stal, L.J., Cretoiu, M.S. (eds.): *The Marine Microbiome, Second Edition.* Springer Nature Switzerland AG, Switzerland, 243–296. https://doi.org/10.1007/978-3-030-90383-1_5
43. Callahan, B.J., McMurdie, P.J., Rosen, M.J., Han, A.W., Johnson, A.J., Holmes, S.P., 2016. DADA2: High-resolution sample inference from Illumina amplicon data. *Nat. Methods* 13, 581–583. https://doi.org/10.1038/nmeth.3869
44. Car, A., Witkowski, A., Jasprica, N., Ljubimir, S., Čalić, M., Dobosz, S., Dupčić Radić, I., Hrustić, E., 2019. Epilithic diatom communities from areas of invasive *Caulerpa* species (*Caulerpa taxifolia* and *Caulerpa cylindracea*) in the Adriatic Sea, NE Mediterranean. *Mediterr. Mar. Sci.* 20(1), 151–173. https://doi.org/10.12681/mms.14330
45. Caruso, G., La Ferla, R., Azzaro, M., Zoppini, A., Marino, G., Petochi, T., Corinaldesi, C., Leonardi, M., Zaccone, R., Fonda Umani, S., Caroppo, C., Monticelli, L., Azzaro, F., Decembrini, F., Maimone, G., Cavallo, R.A., Stabili, L., Hristova Todorova, N., Karamfilov, V.K., Rastelli, E., Cappello, S., Acquaviva, M.I., Narracci, M., De Angelis, R., Del Negro, P., Latini, M., Danovaro, R., 2015. Microbial assemblages for environmental quality assessment: Knowledge, gaps and usefulness in the European Marine Strategy Framework Directive. *Crit. Rev. Microbiol*. 42, 883–904. http://doi.org/10.3109/1040841X.2015.1087380
46. Catania, V., Santisi, S., Signa, G., Vizzini, S., Mazzola, A., Cappello, S., Yakimov, M.M., Quatrini, P., 2015. Intrinsic bioremediation potential of a chronically polluted marine coastal area. *Mar. Pollut. Bull.* 99, 138–149. https://doi.org/10.1016/j.marpolbul.2015.07.042
47. Cecchi, G., Cutroneo, L., Di Piazza, S., Besio, G., Capello, M., Zotti, M., 2021. Port sediments: problem or resource? a review concerning the treatment and decontamination of port sediments by fungi and bacteria. *Microorganisms* 9, 1279. https://doi.org/10.3390/microorganisms9061279
48. Ceja-Navarro, J.A., Wang, Y., Ning, D., Arellano, A., Ramanculova, L., Yuan, M.M., Byer, A., Craven, K.D., Saha, M.C., Brodie, E.L., Pett-Ridge, J., Firestone, M.K., 2021. Protist diversity and community complexity in the rhizosphere of switchgrass are dynamic as plants develop. *Microbiome* 9, 96. https://doi.org/10.1186/s40168-021-01042-9
49. Chao, A., 1987. Estimating the population size for capture-recapture data with unequal catchability. *Biometrics* 43, 783-791. https://doi.org/10.2307/2531532
50. Chen, S., Zhou, Y., Chen, Y., Gu, J., 2018. fastp: an ultra-fast all-in-one FASTQ preprocessor. *Bioinformatics* 34, i884–i890. https://doi.org/10.1093/bioinformatics/bty560

51. Chen, J., Wang, P., Wang, C., Wang, X., Miao, L., Liu, S., Yuan, Q., Sun, S., 2019a. Fungal community demonstrates stronger dispersal limitation and less network connectivity than bacterial community in sediments along a large river. *Environ. Microbiol.* 22(3), 832–849. https://doi.org/10.1111/1462-2920.14795
52. Chen, J., Li, J., Zhang, H., Shi, W., Liu, Y., 2019b. Bacterial heavy-metal and antibiotic resistance genes in a copper tailing dam area in Northern China. *Front. Microbiol.* 10, 1916. https://doi.org/10.3389/fmicb.2019.01916
53. Chen, Q., Li, Y., Liu, M., Zhu, B., Mu, J., Chen, Z., 2021. Removal of Pb and Hg from marine intertidal sediment by using rhamnolipid biosurfactant produced by a *Pseudomonas aeruginosa* strain. *Environ. Technol. Innov.* 22, 101456. https://doi.org/10.1016/j.eti.2021.101456
54. Clark, D.R., Underwood, G.J.C., McGenity, T.J., Dumbrell, A.J., 2021. What drives study-dependent differences in distance–decay relationships of microbial communities? *Glob. Ecol. Biogeogr.* 30(4), 811–825. https://doi.org/10.1111/geb.13266
55. Cukrov, N., Frančišković-Bilinski, S., Mikac, N., Roje, V., 2008. Natural and anthropogenic influences recorded in sediments from the Krka river estuary (eastern Adriatic coast), evaluated by statistical methods. *Fresenius Environ. Bull.* 17(7a), 855–863.
56. Cukrov, N., Frančišković-Bilinski, S., Hlača, B., Barišić, D., 2011. A recent history of metal accumulation in the sediments of Rijeka harbor, Adriatic Sea, Croatia. *Mar. Pollut. Bull.* 62, 154–167. https://doi.org/10.1016/j.marpolbul.2010.08.020
57. Cukrov, N., Frančišković-Bilinski, S., Bogner, D., 2014. Metal contamination recorded in the sediment of the semi-closed Bakar Bay (Croatia). *Environ. Geochem. Health* 36, 195–208. https://doi.org/10.1007/s10653-013-9558-3
58. Cukrov, N., Cindrić, A.-M., Omanović, D., Cukrov, N., 2024. Spatial distribution, ecological risk assessment and source identification of metals in sediments of the Krka River Estuary (Croatia). *Sustainability* 16, 1800. Https://doi.org/10.3390/su16051800
59. Cunliffe, M., 2022. Who are the marine fungi? *Environ. Microbiol.* 25(1), 131–134. https://doi.org/10.1111/1462-2920.16240
60. D'Hondt, S.L., Jørgensen, B.B., Miller, D.J., et al., 2003. 201: College Station, TX (Ocean Drilling Program). *Proc. ODP, Init. Repts.* https://doi.org/10.2973/odp.proc.ir.201.2003
61. D'Hondt, S., Pockalny, R., Fulfer, V.M., Spivack, A.J., 2019. Subseafloor life and its biogeochemical impacts. *Nat. Commun*. 10, 3519. https://doi.org/10.1038/s41467-019-11450-z

62. Danovaro, R., Corinaldesi, C., Dell'Anno, A., Rastelli, R., 2017. Potential impact of global climate change on benthic deep-sea microbes. *FEMS Microbiol. Lett.* 364 (23), fnx214. https://doi.org/10.1093/femsle/fnx214
63. Dedysh, S.N., Lawson, P., 2020. *Thermoanaerobaculales*, in: Whitman, W.B. (ed.): *Bergey's Manual of Systematics of Archaea and Bacteria.* John Wiley & Sons, USA, 1–1. https://doi.org/10.1002/9781118960608.obm00166
64. Dell'Anno, F., Brunet, C., Van Zyl, L.J., Trindade, M., Golyshin, P.N., Dell'Anno, A., Ianora, A., Sansone, C., 2020. Degradation of hydrocarbons and heavy metal reduction by marine bacteria in highly contaminated sediments. *Microorganisms* 8, 1402. https://doi.org/10.3390/microorganisms8091402
65. Dell'Anno, F., Rastelli, E., Sansone, C., Brunet, C., Ianora, A., Dell'Anno, A., 2021a. Bacteria, fungi and microalgae for the bioremediation of marine sediments contaminated by petroleum hydrocarbons in the omics era. *Microorganisms* 9, 1695. https://doi.org/10.3390/microorganisms9081695
66. Dell'Anno, F., Rastelli, E., Tangherlini, M., Corinaldesi, C., Sansone, C., Brunet, C., Balzano, S., Ianora, A., Musco, L., Montereali, M.R., Dell'Anno, A., 2021b. Highly contaminated marine sediments can host rare bacterial taxa potentially useful for bioremediation. *Front. Microbiol.* 12, 584850. https://doi.org/10.3389/fmicb.2021.584850
67. Dell'Anno, F., Joaquim Van Zyl, L., Trindade, M., Buschi, E., Cannavacciuolo, A., Pepi, M., Sansone, C., Brunet, C., Ianora, A., De Pascale, D., Golyshin, P.N., Dell'Anno, A., Rastelli, E., 2023. Microbiome enrichment from contaminated marine sediments unveils novel bacterial strains for petroleum hydrocarbon and heavy metal bioremediation. *Environ. Pollut.* 317, 120772. https://doi.org/10.1016/j.envpol.2022.120772
68. Di Cesare, A., Pjevac, P., Eckert, E., Curkov, N., Miko Šparica, M., Corno, G., Orlić, S., 2020. The role of metal contamination in shaping microbial communities in heavily polluted marine sediments. *Environ. Pollut.* 265, Part B, 114823. https://doi.org/10.1016/j.envpol.2020.114823
69. Dorazio, R., Gotelli, N., Ellison, A., 2011. Modern methods of estimating biodiversity from presence-absence surveys, in: Grillo, O., Venora, G. (ed.): *Biodiversity loss in a changing planet.* Intech Open, Croatia, 277–302. https://doi.org/10.5772/23881.
70. Dong, C., Bai, X., Sheng, H., Jiao, L., Zhou, H., Shao, Z., 2015. Distribution of PAHs and the PAH-degrading bacteria in the deep-sea sediments of the high-latitude Arctic Ocean. *Biogeosciences* 12, 2163–2177. https://doi.org/10.5194/bg-12-2163-2015

71. Du, S., Li, X.-Q., Hao, X., Hu, H.-W., Feng, J., Huang, Q., Liu, Y.-R., 2022. Stronger responses of soil protistan communities to legacy mercury pollution than bacterial and fungal communities in agricultural systems. *ISME Commun.* 2(1), 69. https://doi.org/10.1038/s43705-022-00156-x
72. Duarte, M., Jauregui, R., Vilchez-Vargas, R., Junca, H., Pieper, D.H., 2014. AromaDeg, a novel database for phylogenomics of aerobic bacterial degradation of aromatics. *Database* 2014 bau118. https://doi.org/10.1093/database/bau118
73. Durand, M., Touchette, D., Chen, Y.-J., Magnuson, E., Wasserscheid, J., Greer, C.W., Whyte, L.G., Altshuler, I., 2023. Effects of marine diesel on microbial diversity and activity in high Arctic beach sediments. *Mar. Pollut. Bull.* 194, 115226. https://doi.org/10.1016/j.marpolbul.2023.115226
74. Dyksma, S., Bischof, K., Fuchs, B.M., Hoffmann, K., Meier, D., Meyerdierks, A., Pjevac, P., Probandt, D., Richter, M., Stepanauskas, R., Mußmann, M., 2016. Ubiquitous Gammaproteobacteria dominate dark carbon fixation in coastal sediments. *ISME J.* 10(8), 1939–1953. https://doi.org/10.1038/ismej.2015.257
75. Elleuch, J., Hmani, R., Drira, M., Michaud, P., Fendri, I., Abdelkafi, S., 2021. Potential of three local marine microalgae from Tunisian coasts for cadmium, lead and chromium removals. *Sci. Total Environ.* 799, 149464. https://doi.org/10.1016/j.scitotenv.2021.149464
76. Erdelez, A., Furdek Turk, M., Štambuk, A., Župan, I., Peharda, M., 2017. Ecological quality status of the Adriatic coastal waters evaluated by the organotin pollution biomonitoring. *Mar. Pollut. Bull.* 123, 313–323. https://doi.org/10.1016/j.marpolbul.2017.08.039
77. Euler, S., Jeffrey, L.C., Maher, D.T., Mackenzie, D., Tait, D.R., 2020. Shifts in methanogenic archaea communities and methane dynamics along a subtropical estuarine land use gradient. *PLoS One* 15 (11), e0242339. https://doi.org/10.1371/journal.pone.0242339
78. European Commission, 1992. Council Directive 92/43/EEC of 21 May 1992 on the conservation of natural habitats and of wild fauna and fora. *OJEU* L206, 7–50
79. European Commission, 2000. Directive 2000/60/EC of the European Parliament and of the Council of 23 October 2000 Establishing a Framework for Community Action in the Field of Water Policy. *OJEU* L327, 0001–0073.
80. European Commission, 2008. Directive 2008/56/EC of the European Parliament and of the Council of 17 June 2008 Establishing a Framework for Community Action in the Field of Marine Environmental Policy (Marine Strategy Framework Directive). *OJEU* L164, 19–40.
81. European Commission, 2017. COMMISSION DECISION (EU) 2017/848 of 17 May 2017 laying down criteria and methodological standards on good environmental status of marine waters and

specifications and standardised methods for monitoring and assessment and repealing Decision 2010/477/EU. *OJEU* L125, 43-74.

82. Fafanđel, M., Piljagić, J., Smodlaka Tanković, M., Travizi, A., Bihari, N., 2015. Nutrients vs toxicity in sediments: A case study of two semi-closed basins in Rijeka Bay, Croatia. *Fresenius Environ. Bull.* 24(9a), 2888-2897.
83. Falkowski, P.G., Fenchel, T., Delong, E.F., 2008. The Microbial Engines That Drive Earth's Biogeochemical Cycles. *Science* 320, 1034–1039. https://doi.org/10.1126/science.1153213
84. Felja, I., Romić, M., Romić, D., Bakić, H., Pikelj, K., Juračić, M., 2016. Application of empirical model to predict background metal concentration in mixed carbonate-alumosilicate sediment (Adriatic Sea, Croatia). *Mar. Pollut. Bull.* 106(1–2), 190–199. https://doi.org/10.1016/j.marpolbul.2016.02.070
85. Ferguson, R.L., Buckley, E.N., Palumbo, A.V., 1984. Response of marine bacterioplankton to differential filtration and confinement. *Appl. Environ. Microbiol.* 47(1), 49–55. https://doi.org/10.1128/aem.47.1.49-55.1984
86. Fiket, Ž., Mikac, N., Kniewald, G., 2017. Mass fractions of forty-six major and trace elements, including rare earth elements, in sediment and soil reference materials used in environmental studies. *Geostand. Geoanal. Res.* 41, 123–135. https://doi.org/10.1111/ggr.12129
87. Fiket, Ž., Petrović, M., Medunić, G., Ivošević, T., Fiket, T., Xu, L.Z., Wang, Y., Ding, S., 2021. Evaluation of the potential release tendency of metals and metalloids from the estuarine sediments: case study of Raša Bay. *Molecules* 26, 6656. https://doi.org/10.3390/molecules26216656
88. Fillinger, L., Hug, K., Griebler, C., 2019. Selection imposed by local environmental conditions drives differences in microbial community composition across geographically distinct groundwater aquifers. *FEMS Microbiol. Ecol.* 95, fiz160. https://doi.org/10.1093/femsec/fiz160
89. Fisher, R.A., Corbet, A.S., Williams, C.B., 1943. The relation between the number of species and the number of individuals in a random sample of an animal population. *J. Anim. Ecol.* 12, 42–58. https://doi.org/10.2307/1411
90. Forster, D., Dunthorn, M., Mahé, F., Dolan, J.R., Audic, S., Bass, D., Bittner, L., Boutte, C., Christen, R., Claverie, J.-M., Decelle, J., Edvardsen, B., Egge, E., Eikrem, W., Gobet, A., Kooistra, W.H.C.F., Logares, R., Massana, R., Montresor, M., Not, F., Ogata, H., Pawlowski, J., Pernice, M.C., Romac, S., Shalchian-Tabrizi, K., Simon, N., Richards, T.A., Santini, S., Sarno, D., Siano, R., Vaulot, D., Wincker, P., Zingone, A., De Vargas, C., Stoeck, T., 2016. Benthic

protists: the under-charted majority. *FEMS Microbiol. Ecol.* 92, fiw120. https://doi.org/10.1093/femsec/fiw120

91. Furdek Turk, M., Ivanić, M., Dautović, J., Bačić, N., Mikac, N., 2020. Simultaneous analysis of butyltins and total tin in sediments as a tool for the assessment of tributyltin behaviour, long-term persistence and historical contamination in the coastal environment. *Chemosphere* 258, 127307. https://doi.org/10.1016/j.chemosphere.2020.127307
92. Furdek Turk, M., Vrana, I., Milačič, R., Ščančar, J., Dautović, J., Ciglenečki, I., Mikac, N., 2024. Spatial and temporal distribution of tributyltin in the coastal environment of the Croatian Adriatic (2016-2023): TBT remains a cause for concern. *Front. Mar. Sci.* 11, 1422057. https://doi.org/10.3389/fmars.2024.1422057
93. Gadd, G.M., 2010. Metals, minerals and microbes: geomicrobiology and bioremediation. *Microbiology* 156, 609–643. https://doi.org/10.1099/mic.0.037143-0
94. Gao, F., Zhao, H., Zhao, P., Zhang, C., Xu, G., Liu, G., Guo, X., 2022. Benthic microbial communities and environmental parameters of estuary and hypoxic zone in the Bohai Sea, China. *J. Mar. Sci. Eng.* 10 (12), 1862. https://doi.org/10.3390/jmse10121862
95. Geisen, S., Koller, R., Hünninghaus, M., Dumack, K., Urich, T., Bonkowski, M. 2016. The soil food web revisited: Diverse and widespread mycophagous soil protists. *Soil Biol. Biochem.* 94, 10–18. https://doi.org/10.1016/j.soilbio.2015.11.010
96. Ghannam, R.B., Techtmann, S.M., 2021. Machine learning applications in microbial ecology, human microbiome studies, and environmental monitoring. *Comput. Struct. Biotechnol. J.* 19, 1092–1107. https://doi.org/10.1016/j.csbj.2021.01.028
97. Ghezzi, D., Mangiaterra, G., Scardino, A., Fehervari, M., Magnani, M., Citterio, B., Frangipani, E., 2024. Characterization of bacterial communities associated with seabed sediments in offshore and nearshore sites to improve Microbiologically Influenced Corrosion mitigation on marine infrastructures. *PLoS One* 19, e0309971. https://doi.org/10.1371/journal.pone.0309971
98. Gillan, D.C., Danis, B., Pernet, P., Joly, G., Dubois, P., 2005. Structure of sediment-associated microbial communities along a heavy-metal contamination gradient in the marine environment. *Appl. Environ. Microbiol.* 71(2), 679–690. https://doi.org/10.1128/AEM.71.2.679-690.2005
99. Gloor, G.B., Macklaim, J.M., Pawlowsky-Glahn, V., Egozcue, J.J., 2017. Microbiome datasets are compositional: and this is not optional. *Front. Microbiol,* https://doi.org/810.3389/fmicb.2017.02224
100. Good, I.J., 1953. The population frequencies of species and the estimation of population parameters. *Biometrika* 40, 237–264. https://doi.org/10.1093/biomet/40.3-4.237

101. Green-Ruiz, C., Rodriguez-Tirado, V., Gomez-Gil, B., 2008. Cadmium and zinc removal from aqueous solutions by Bacillus jeotgali: pH, salinity and temperature effects. *Bioresour. Technol.* 99, 3864–3870. https://doi.org/10.1016/j.biortech.2007.06.047

102. Gullberg, E., Albrecht, L.M., Karlsson, C., Sandegren, L. andersson, D.I., 2014. Selection of a multidrug resistance plasmid by sublethal levels of antibiotics and heavy metals. *mBio* 5, e01918-14. https://doi.org/10.1128/mBio.01918-14

103. Hanson, C.A., Fuhrman, J.A., Horner-Devine, M.C., Martiny, J.B.H., 2012. Beyond biogeographic patterns: processes shaping the microbial landscape. *Nat. Rev. Microbiol*. 10(7), 497–506. https://doi.org/10.1038/nrmicro2833

104. He, T., Jin, M., Cui, P., Sun, X., He, X., Huang, Y., Xiao, X., Zhang, T., Zhang, X., 2024. Environmental viromes reveal the global distribution signatures of deep-sea DNA viruses. *J. Adv. Res*. 57, 107–117. https://doi.org/10.1016/j.jare.2023.04.009

105. Hicks, N., Liu, X., Gregory, R., Kenny, J., Lucaci, A., Lenzi, L., Paterson, D.M., Duncan, K.R., 2018. Temperature driven changes in benthic bacterial diversity influences biogeochemical cycling in coastal sediments. *Front. Microbiol.* 9, 1730. https://doi.org/10.3389/fmicb.2018.01730

106. Hijmans, R., 2023. geosphere: Spherical Trigonometry. R package version 1.5-19. https://doi.org/10.32614/CRAN.package.geosphere.

107. Hoshino, T., Doi, H., Uramoto, G.I., Wörmer, L., Adhikari, R.R., Xiao, N., Morono, Y., D'Hondt, S., Hinrichsm K.U., Inagaki, F., 2020. Global diversity of microbial communities in marine sediment. *Proc. Natl. Acad. Sci. U.S.A.* 117(44), 27587–27597. https://doi.org/10.1073/pnas.1919139117

108. Hu, S.K., Herrera, E.L., Smith, A.R., Pachiadaki, M.G., Edgcomb, V.P., Sylva, S.P., Chan, E.W., Seewald, J.S., German, C.R., Huber, J.A., 2021. Protistan grazing impacts microbial communities and carbon cycling at deep-sea hydrothermal vents. *Proc. Natl. Acad. Sci. U.S.A.* 118(29), e2102674118. https://doi.org/10.1073/pnas.2102674118

109. Ikotun, A., Ezugwu, A., Abualigah, L., Abuhaija, B., Heming, J., 2023. K-means clustering algorithms: a comprehensive review, variants analysis and advances in the era of big data. *Inf. Sci.* 622, 178–210. https://doi.org/10.1016/j.ins.2022.11.139

110. IPCC, 2023. Climate Change 2023: Synthesis Report. Contribution of Working Groups I, II and III to the Sixth Assessment Report of the Intergovernmental Panel on Climate Change, in: Lee, H., Romero, J. (eds.): *Intergovernmental Panel on Climate Change (IPCC)*, Geneva, Switzerland, 35–115. https://doi.org/10.59327/IPCC/AR6-9789291691647

111. ISO (International Organization for Standardization), 1998. ISO 13878:1998 — Soil Quality — Determination of Total Nitrogen Content by Dry Combustion ("Elemental Analysis"). ISO, Geneva.
112. ISO (International Organization for Standardization), 2004. HRN ISO 10693:2004 – Soil quality — Determination of carbonate content (Volumetric method). Croatian Standards Institute.
113. ISO (International Organization for Standardization), 2004. HRN ISO 10694:2004 – Soil quality — Determination of organic and total carbon after dry combustion (elementary analysis). Croatian Standards Institute.
114. Jang, J., Park, J., Hwang, C.Y., Choi, J., Shin, J., Kim, Y.M., Cho, K.H., Kim, J.-H., Lee, Y.M., Lee, B.Y., 2022. Abundance and diversity of antibiotic resistance genes and bacterial communities in the western Pacific and Southern Oceans. *Sci. Total Environ.* 822, 153360. https://doi.org/10.1016/j.scitotenv.2022.153360
115. Jannasch, H. W., Jones, G. E., 1959. Bacterial populations in sea water as determined by different methods of enumeration. *Limnol. Oceanogr.* 4(2), 128–139. https://doi.org/10.4319/lo.1959.4.2.0128
116. Jian, C., Luukkonen, P., Yki-Järvinen, H., Salonen, A., Korpela, K., 2020. Quantitative PCR provides a simple and accessible method for quantitative microbiota profiling. *PLoS One* 15, e0227285. https://doi.org/10.1371/journal.pone.0227285
117. Jokanović, S., Kajan, K., Perović, S., Ivanić, M., Mačić, V., Orlić, S., 2021. Anthropogenic influence on the environmental health along Montenegro coast based on the bacterial and chemical characterization. *Environ. Pollut.* 271, 116383. https://doi.org/10.1016/j.envpol.2020.116383
118. Jones, E.B.G., Pang, K.L., Abdel-Wahab, M.A., Scholz, B., Hyde, K.D., Boekhout, T., Ebel, R., Rateb, M.E., Henderson, L., Sakayaroj, J., Suetrong, S., Dayarathne, M.C., Kumar, V., Raghukumar, S., Sridhar, K.R., Bahkali, A.H.A., Gleason, F.H., Norphanphoun, C., 2019. An online resource for marine fungi. *Fungal Divers.* 96, 347–433. https://doi.org/10.1007/s13225-019-00426-5
119. Jørgensen, B.B, Boetius, A. 2007: Feast and famine – microbial life in the deep-sea bed. *Nat. Rev. Microbiol.* 5, 770–781. https://doi.org/10.1038/nrmicro1745
120. Jørgensen, B.B., Findlay, A.J., Pellerin, A., 2019. The biogeochemical sulfur cycle of marine sediments. *Front. Microbiol.* 10, 849. https://doi.org/10.3389/fmicb.2019.00849
121. Joshi, G., Verma, P., Meena, B., Goswami, P., Peter, D.M., Jha, D.K., Vinithkumar, N.V., Dharani, G., 2022. Unraveling the potential of bacteria isolated from the equatorial region of Indian Ocean in mercury detoxification. *Front. Mar. Sci.* 9, 986493. https://doi.org/10.3389/fmars.2022.986493

122. Jroundi, F., Martinez-Ruiz, F., Merroun, M.L., Gonzalez-Muñoz, M.T., 2020. Exploring bacterial community composition in Mediterranean deep-sea sediments and their role in heavy metal accumulation. *Sci. Total Environ.* 712, 135660. https://doi.org/10.1016/j.scitotenv.2019.135660

123. Jurburg, S.D., Blowes, S.A., Shade, A., Eisenhauer, N., Chase, J.M., 2024. Synthesis of recovery patterns in microbial communities across environments. *Microbiome* 12, 79. https://doi.org/10.1186/s40168-024-01802-3

124. Kajan, K., Cukrov, N., Cukrov, N., Bishop-Pierce, R., Orlić, S., 2022. Microeukaryotic and prokaryotic diversity of anchialine caves from Eastern Adriatic Sea islands. *Microb. Ecol.* 83, 257–270. https://doi.org/10.1007/s00248-021-01760-5

125. Kaleli, A., Car, A., 2024. Marine benthic diatoms from the Adriatic Sea (NE Mediterranean): review of investigations and checklist with updated nomenclature. *Acta Botan. Croat.* 84(2), 1–48. https://doi.org/10.37427/botcro-2025-024

126. Kallmeyer, J., Pockalny, R., Adhikari, R.R., Smith, D.C., D'Hondt, S. 2012. Global distribution of microbial abundance and biomass in subseafloor sediment. *Proc. Natl. Acad. Sci. USA* 109 (40), 16213–16216. https://doi.org/10.1073/pnas.1203849109

127. Kalu, E.I., Reyes-Prieto, A., Barbeau, M.A., 2023. Community dynamics of microbial eukaryotes in intertidal mudflats in the hypertidal Bay of Fundy. *ISME Commun.* 3, 21. https://doi.org/10.1038/s43705-023-00226-8

128. Kaminsky, R., Morales, S.E. 2018. Conditionally rare taxa contribute but do not account for changes in soil prokaryotic community structure. *Front. Microbiol.* 9, 809. https://doi.org/10.3389/fmicb.2018.00809

129. Kang, H., Kim, S., Song, K., Kwon, M.-J., Lee, J., 2024. Intermediate disturbances enhance microbial enzyme activities in soil ecosystems. *Microorganisms* 12, 1401. https://doi.org/10.3390/microorganisms12071401

130. Kartal, S., Aydin, Z., Tokalıoğlu, Ş., 2006. Fractionation of metals in street sediment samples by using the BCR sequential extraction procedure and multivariate statistical elucidation of the data. *J. Hazard. Mater.* 132 (1), 80–89. https://doi.org/10.1016/j.jhazmat.2005.11.091

131. Kolda, A., Gavrilović, A., Jug-Dujaković, J., Ljubešić, Z., El-Matbouli, M., Lillehaug, A., Lončarević, S., Perić, L., Knežević, D., Vukić Lušić, D., Kapetanović, D., 2020. Profiling of bacterial assemblages in the marine cage farm environment, with implications on fish, human and ecosystem health. *Ecol. Indic.* 118, 106785. https://doi.org/10.1016/j.ecolind.2020.106785

132. Korlević, M., Zucko, J., Dragić Najdek, M., Blažina, M., Pustijanac, E., Zeljko Vojvoda, T., Gacesa, R., Baranasic, D., Starcevic, A., Diminic, J., Long, P.F., Cullum, J., Hranueli, D., Orlić,

S., 2015. Bacterial diversity of polluted surface sediments in the northern Adriatic Sea. *Syst. Appl. Microbiol.*, 38(3), 189–197. https://doi.org/10.1016/j.syapm.2015.03.001

133. Kursa, M.B., Rudnicki, W.R., 2010. Feature Selection with the Boruta Package. *J. Stat. Softw.* 36, 1–13. https://doi.org/10.18637/jss.v036.i11

134. Lai, D., Hedlund, B.P., Xie, W., Liu, J., Phelps, T.J., Zhang, C., Wang, P., 2020. Impact of terrestrial input on deep-sea benthic archaeal community structure in South China Sea Sediments. *Front. Microbiol.* 11, 572017. https://doi.org/10.3389/fmicb.2020.572017

135. Lawal, I.M., Bertram, D., White, C.J., Kutty, S.R.M., Hassan, I., Jagaba, A.H., 2023. Application of Boruta algorithms as a robust methodology for performance evaluation of CMIP6 general circulation models for hydro-climatic studies. *Theor. Appl. Climatol.* 153, 113–135. https://doi.org/10.1007/s00704-023-04466-5

136. Letunic, I., Bork, P., 2021. Interactive Tree of Life (iTOL) v5: an online tool for phylogenetic tree display and annotation. *Nucleic Acids Res.* 49(W1). https://doi.org/10.1093/nar/gkab301

137. Lian, F.-B., Zhou, B.-J., Zhou, Z.-Y., Rooney, A.P., Xu, Z.-X., Du, Z.-J., 2025. Describing five new strains in the family Woeseiaceae and emended description of the order Woeseiales with genomic features related to environmental adaptation. *Syst. Appl. Microbiol.* 48, 126563. https://doi.org/10.1016/j.syapm.2024.126563

138. Liu, J., Meng, Z., Liu, X., Z., X.-H., 2019. Microbial assembly, interaction, functioning, activity and diversification: a review derived from community compositional data. *Mar. Life Sci. Technol.* 1, 112–128. https://doi.org/10.1007/s42995-019-00004-3

139. Liu, B., Zheng, D., Zhou, S., Chen, L., Yang, J., 2022. VFDB 2022: a general classification scheme for bacterial virulence factors. *Nucleic Acids Res.* 50, D912–D917. https://doi.org/10.1093/nar/gkab1107

140. Love, M.I., Huber, W., Anders, S. 2014. Moderated estimation of fold change and dispersion for RNA-seq data with DESeq2. *Genome Biol.* 15, 550. https://doi.org/10.1186/s13059-014-0550-8

141. Lučić, M., Mikac, N., Vidović, N., Bačić, N., Dinis, P., Milačić, R., 2023. Distinguishing between natural and anthropogenic sources of potentially toxic elements in sedimentary materials along the Sava River (Slovenia, Croatia). *Appl. Geochem.* 151, 105619. https://doi.org/10.1016/j.apgeochem.2023.105619

142. Maglione, G., Zinno, P., Tropea, A., Mussagy, C.U., Dufossé, L., Giuffrida, D., Mondello, A., 2024. Microbes' role in environmental pollution and remediation: a bioeconomy focus approach. *AIMS Microbiol.* 10, 723–755. https://doi.org/10.3934/microbiol.2024033

143. Mahmudi, M., Arsad, S., Musa, M., Lusiana, E.D., Buwono, N.R., Forest, A., Hutabarat, E.P., Siregar, M.A., Elradinan, N.S., Fatimah, S., Hidayat, V.L., Putri Agessi, Y.A., 2025. Relationship between habitat characteristics and microalgae community on the coastal area of Malang Regency, Indonesia. *Ecol. Eng. Environ. Tech.* 26, 86–95. https://doi.org/10.12912/27197050/196661

144. Mainka, T., Weirathmüller, D., Herwig, C., Pflügl, S., 2021. Potential applications of halophilic microorganisms for biological treatment of industrial process brines contaminated with aromatics. *J. Ind. Microbiol. Biotechnol.* 48, kuab015. https://doi.org/10.1093/jimb/kuab015

145. Manten. A. A., 1972. C. Wyville Thomson, J. Murray and the "Challenger" expedition. *Earth Sci. Rev.* 8, 255–266. https://doi.org/10.1016/0012-8252(72)90108-0

146. Marcon, E., Hérault, B., 2015. entropart: An R package to measure and partition diversity. *J. Stat. Softw.* 67(8), 1–26. https://doi.org/10.18637/jss.v067.i08

147. Markovski, M., Najdek, M., Herndl, G.J., Korlević, M., 2022. Compositional stability of sediment microbial communities during a seagrass meadow decline. *Front. Mar. Sci.* 9, 966070. https://doi.org/10.3389/fmars.2022.966070

148. Markussen, T., Happel, E.M., Teikari, J.E., Huchaiah, V., Alneberg, J., Andersson, A.F., Sivonen, K., Riemann, L., Middelboe, M., Kisand, V., 2018. Coupling biogeochemical process rates and metagenomic blueprints of coastal bacterial assemblages in the context of environmental change. *Environ. Microbiol.* 20, 3083–3099. https://doi.org/10.1111/1462-2920.14371

149. Mars Brisbin, M., Conover, A.E., Mitarai, S., 2020. Influence of regional oceanography and hydrothermal activity on protist diversity and community structure in the Okinawa Trough. *Microb. Ecol.* 80, 746–761. https://doi.org/10.1007/s00248-020-01583-w

150. Martínez, Y.J., Siqueiros-Beltrones, D.A., Marmolejo-Rodríguez, A.J., 2021. Response of benthic diatom assemblages to contamination by metals in a marine environment. *J. Mar. Sci. Eng.* 9, 443. https://doi.org/10.3390/jmse9040443

151. Martiny, J. B. H., Bohannan, B. J. M., Brown, J. H., Colwell, R. K., Fuhrman, J. A., Green, J. L., et al., 2006. Microbial biogeography: putting microorganisms on the map. *Nat. Rev. Microbiol.* 4(2), 102–112. https://doi.org/10.1038/nrmicro1341

152. Massana, R., Gobet, A., Audic, S., Bass, D., Bittner, L., Boutte, C., Chambouvet, A., Christen, R., Claverie, J., Decelle, J., Dolan, J.R., Dunthorn, M., Edvardsen, B., Forn, I., Forster, D., Guillou, L., Jaillon, O., Kooistra, W.H.C.F., Logares, R., Mahé, F., Not, F., Ogata, H., Pawlowski, J., Pernice, M.C., Probert, I., Romac, S., Richards, T., Santini, S., Shalchian-Tabrizi, K., Siano, R., Simon, N., Stoeck, T., Vaulot, D., Zingone, A., De Vargas, C., 2015. Marine protist diversity in

European coastal waters and sediments as revealed by high-throughput sequencing. *Environ. Microbiol.* 17, 4035–4049. https://doi.org/10.1111/1462-2920.12955

153. Mattison, R., Taki, H., Harayama, S., 2005. The soil flagellate *Heteromita globosa* accelerates bacterial degradation of alkylbenzenes through grazing and acetate excretion in batch culture. *Microb. Ecol.* 49, 142–150. https://doi.org/10.1007/s00248-003-0226-5
154. Matys Grygar, T., Popelka, J., 2016. Revisiting geochemical methods of distinguishing natural concentrations and pollution by risk elements in fluvial sediments. *J. Geochem. Explor.* 170, 39–57. https://doi.org/10.1016/j.gexplo.2016.08.003
155. McMurdie, P. J., Holmes, S., 2013. Phyloseq: an R package for reproducible interactive analysis and graphics of microbiome census data. *PLoS One* 8, e61217. https://doi.org/10.1371/journal.pone.0061217
156. Mehdizadeh Allaf, M., Peerhossaini, H., 2022. Cyanobacteria: model microorganisms and beyond. *Microorganisms* 10, 696. https://doi.org/10.3390/microorganisms10040696
157. Menzel, P., Ng, K.L., Krogh, A., 2016. Fast and sensitive taxonomic classification for metagenomics with Kaiju. *Nat. Commun.* 7, 11257. https://doi.org/10.1038/ncomms11257
158. Milke, F., Wagner-Doebler, I., Wienhausen, G., Simon, M., 2022. Selection, drift and community interactions shape microbial biogeographic patterns in the Pacific Ocean. *ISME J.* 16(12), 2653–2665. https://doi.org/10.1038/s41396-022-01318-4
159. Ministry of Environmental Protection and Energetics, 2019. Update of the Marine Environment and Coastal Area Management Strategy Documents Based on Obligations under Articles 8, 9 and 10 of the Marine Strategy Framework Directive 2008/56/EC. *Republic of Croatia.*
160. Misson, B., Garnier, C., Lauga, B., Dang, D.H., Ghiglione, J.-F., Mullot, J.-U., Duran, R., Pringault, O., 2016. Chemical multi-contamination drives benthic prokaryotic diversity in the anthropized Toulon Bay. *Sci. Total Environ.* 556, 319–329. https://doi.org/10.1016/j.scitotenv.2016.02.038
161. Moreira, V.A., Cravo-Laureau, C., De Carvalho, A.C.B., Baldy, A., Bidone, E.D., Sabadini-Santos, E., Duran, R., 2023. Microbial indicators along a metallic contamination gradient in tropical coastal sediments. *J. Hazard. Mater.* 443, 130244. https://doi.org/10.1016/j.jhazmat.2022.130244
162. Mori, K., Suzuki, K., Yamaguchi, K., Urabe, T., Hanada, S., 2015. *Thiogranum longum* gen. nov., sp. nov., an obligately chemolithoautotrophic, sulfur-oxidizing bacterium of the family Ectothiorhodospiraceae isolated from a deep-sea hydrothermal field and an emended description

of the genus *Thiohalomonas*. *Int. J. Syst. Evol. Microbiol.* 65, 235–241. https://doi.org/10.1099/ijs.0.070599-0

163. Morya, R., Salvachúa, D., Thakur, I.S., 2020. Burkholderia: an untapped but promising bacterial genus for the conversion of aromatic compounds. *Trends Biotechnol.* 38, 963–975. https://doi.org/10.1016/j.tibtech.2020.02.008
164. Munn, C., 2020: *Marine Microbiology: Ecology and Applications, Third edition*, CRC Press, SAD.
165. Muntañola-Cvetković, M., Ristanović, B., 1980. A mycological survey of the South Adriatic Sea. *J. Exp. Mar. Biol. Ecol.* 43, 193–206. https://doi.org/10.1016/0022-0981(80)90047-7
166. Navarro-Torre, S., Carro, L., Igual, J.M., Montero-Calasanz, M.D.C., 2021. Rossellomorea arthrocnemi sp. nov., a novel plant growth-promoting bacterium used in heavy metal polluted soils as a phytoremediation tool. *Int. J. Syst. Evol. Microbiol.* 71. https://doi.org/10.1099/ijsem.0.005015
167. Nawaz, M.Z., Subin Sasidharan, R., Alghamdi, H.A., Dang, H., 2022. Understanding interaction patterns within deep-sea microbial communities and their potential applications. *Mar. Drugs* 20(2), 108. https://doi.org/10.3390/md20020108
168. Nekola, J.C., White, P.S., 2004. The distance decay of similarity in biogeography and ecology. *J. Biogeogr.* 26(4), 867–878. https://doi.org/10.1046/j.1365-2699.1999.00305.x
169. Nemergut, D.R., Schmidt, S.K., Fukami, T., O'Neill, S.P., Bilinski, T.M., Stanish, L.F., Knelman, J.E., Darcy, J.L., Lynch, R.C., Wickey, P., Ferrenberg, S., 2013. Patterns and processes of microbial community assembly. *Microbiol. Mol. Biol. Rev.* 77(3), 342–356. https://doi.org/10.1128/mmbr.00051-12
170. Nnaji, N.D., Anyanwu, C.U., Miri, T., Onyeaka, H., 2024. Mechanisms of heavy metal tolerance in bacteria: a review. *Sustainability* 16, 11124. https://doi.org/10.3390/su162411124
171. Nogales, B., Lanfranconi, M.P., Piña-Villalonga, J.M., Bosch, R., 2011. Anthropogenic perturbations in marine microbial communities. *FEMS Microbiol. Rev.* 35, 275–298. https://doi.org/10.1111/j.1574-6976.2010.00248.x
172. Nordstrom, D.K., Wilde, F.D., 2005. Reduction-oxidation potential (Electrode method). Chapter 6: Field measurements, in: Wilde, F.D., Radke, D.B. (eds.): *Techniques of Water-Resources Investigations,* U.S. Geological Survey, USA, 22. https://doi.org/10.3133/twri09A6.5
173. Obhođaš, J., Valković, V., 2010. Contamination of the coastal sea sediments by heavy metals. *Appl. Radiat. Isot.* 68, 807–811. https://doi.org/10.1016/j.apradiso.2009.12.026
174. Oksanen, J., Simpson, G., Blanchet, F., Kindt, R., Legendre, P., Minchin, P., O'Hara, R., Solymos, P., Stevens, M., Szoecs, E., Wagner, H., Barbour, M., Bedward, M., Bolker, B., Borcard,

D., Carvalho, G., Chirico, M., De Caceres, M., Durand, S., Evangelista, H., FitzJohn, R., Friendly, M., Furneaux, B., Hannigan, G., Hill, M., Lahti, L., McGlinn, D., Ouellette, M., Ribeiro Cunha, E., Smith, T., Stier, A., Ter Braak, C., Weedon, J., 2022. vegan: Community Ecology Package. R package version 2.6-4. https://CRAN.R-project.org/package=vegan

175. Overbeek, R., Olson, R., Pusch, G.D., Olsen, G.J., Davis, J.J., Disz, T., Edwards, R.A., Gerdes, S., Parrello, B., Shukla, M., Vonstein, V., Wattam, A.R., Xia, F., Stevens, R., 2014. The SEED and the Rapid Annotation of microbial genomes using Subsystems Technology (RAST). *Nucleic Acids Res.* 42, D206–D214. https://doi.org/10.1093/nar/gkt1226

176. Pajares, S., Ramos, R., 2019. Processes and microorganisms involved in the marine nitrogen cycle: knowledge and gaps. *Front. Mar. Sci.* 6, 739. https://doi.org/10.3389/fmars.2019.00739

177. Pal, C., Bengtsson-Palme, J., Rensing, C., Kristiansson, E., Larsson, D.G.J., 2014. BacMet: antibacterial biocide and metal resistance genes database. *Nucleic Acids Res.* 42, D737–D743. https://doi.org/10.1093/nar/gkt1252

178. Panseriya, H.Z., Gosai, H.B., Sachaniya, B.K., Vala, A.K., Dave, B.P., 2019. Marine microbial mettle for heavy metal bioremediation: a perception, in: Pei, D.-S., Junaid, M. (eds.): *Marine Ecology: Current and Future Developments.* Bentham Science Publisher, United Arab Emirates, 409–434. https://doi.org/10.2174/9789811412691119010021

179. Pedersen, T., 2024. patchwork: The Composer of Plots. R package version 1.2.0, https://CRAN.R-project.org/package=patchwork.

180. Pepper, I.L., Gerba, C.P., 2009: Cultural Methods, in: Maier, R.M., Pepper, I.L., Gerba, C.P. (eds.): *Environmental Microbiology* (Second Edition), Academic Press, SAD, 173–189. https://doi.org/10.1016/B978-0-12-370519-8.00010-9

181. Pereira-García, C., Del Amo, E.H., Vigués, N., Rey-Velasco, X., Rincón-Tomás, B., Pérez-Cruz, C., Sanz-Sáez, I., Hu, H., Bertilsson, S., Pannier, A., Soltmann, U., Sánchez, P., Acinas, S.G., Bravo, A.G., Alonso-Sáez, L., Sánchez, O., 2024. Unmasking the physiology of mercury detoxifying bacteria from polluted sediments. *J. Hazard. Mater.* 467, 133685. https://doi.org/10.1016/j.jhazmat.2024.133685

182. Pohlner, M., Dlugosch, L., Wemheuer, B., Mills, H., Engelen, B., Reese, B.K., 2019. The majority of active Rhodobacteraceae in marine sediments belong to uncultured genera: a molecular approach to link their distribution to environmental conditions. *Front. Microbiol.* 10, 659. https://doi.org/10.3389/fmicb.2019.00659

183. Pomeroy, L.R., 1974. The ocean's food web, a changing paradigm. *Bioscience* 24, 499–504.

184. Popadić, A., Vidović, J., Ćosović, V., Medaković, D., Dolenec, M., Felja, I., 2013. Impact evaluation of the industrial activities in the Bay of Bakar (Adriatic Sea, Croatia): Recent benthic foraminifera and heavy metals. *Mar. Pollut. Bull.* 76, 333–348. https://doi.org/10.1016/j.marpolbul.2013.09.039

185. Potapova, M., Charles, D.F., 2007. Diatom metrics for monitoring eutrophication in rivers of the United States. *Ecol. Indic.* 7(1), 48–70. https://doi.org/10.1016/j.ecolind.2005.10.001

186. Prüsse, E., Quast, C., Yilmaz, P., Ludwig, W., Peplies, J., Glöckner, F.O., 2011. SILVA: comprehensive databases for quality checked and aligned ribosomal RNA sequence data compatible with ARB, in: de Bruijn F.J. (ed.): *Handbook of Molecular Microbial Ecology I.* John Wiley & Sons, Inc., USA, 393-398. https://doi.org/10.1002/9781118010518.ch45

187. Qiu, Z., He, S., Lian., C.-A., Qiao, X., Zhang, Q., Yao, C., Mu, R., Wang, L., Cao, X.-A., Yan, Y., Yu, K., 2024. Large scale exploration reveals rare taxa crucially shape microbial assembly in alkaline lake sediments. *npj Biofilms Microbiomes* 10, 62. https://doi.org/10.1038/s41522-024-00537-1

188. Quast, C., Pruesse, E., Yilmaz, P., Gerken, J., Schweer, T., Yarza, P., Peplies, J., Glöckner, F.O., 2013. The SILVA ribosomal RNA gene database project: Improved data processing and web-based tools. *Nucleic Acids Res.* 41, D590–D596. https://doi.org/10.1093/nar/gks1219

189. R Core Team 2022. R: A language and environment for statistical computing, reference index version 4.2.2. R Foundation for Statistical Computing. https://www.R-project.org/

190. R Core Team 2023. R: A language and environment for statistical computing, reference index version 4.3.2. R Foundation for Statistical Computing. https://www.R-project.org/

191. Reimann, L., Vafeidis, A.T., Honsel, L.E., 2023. Population development as a driver of coastal risk: current trends and future pathways. *Cambridge Prisms: Coastal Futures* 1(e14), 1–12. https://doi.org/10.1017/cft.2023.3

192. Revathy, T., Jayasri, M.A., Suthindhiran, K., 2015. Biodegradation of PAHs by *Burkholderia sp.* VITRSB1 isolated from marine sediments. *Scientifica* 2015, 1–9. https://doi.org/10.1155/2015/867586

193. Rincón-Tomás, B., Lanzén, A., Sánchez, P., Estupiñán, M., Sanz-Sáez, I., Bilbao, M.E., Rojo, D., Mendibil, I., Pérez-Cruz, C., Ferri, M., Capo, E., Abad-Recio, I.L., Amouroux, D., Bertilsson, S., Sánchez, O., Acinas, S.G., Alonso-Sáez, L., 2024. Revisiting the mercury cycle in marine sediments: A potential multifaceted role for Desulfobacterota. *J. Hazard. Mater.* 465, 133120. https://doi.org/10.1016/j.jhazmat.2023.133120

194. Roberts, D.A., 2012. Causes and ecological effects of resuspended contaminated sediments (RCS) in marine environments. *Environ. Int.* 40, 230-243. https://doi.org/10.1016/j.envint.2011.11.013

195. Robeson, M.S. II, O'Rourke, D.R., Kaehler, B.D., Ziemski, M., Dillon, M.R., Foster, J.T., Bokulich, N.A., 2021. RESCRIPt: Reproducible sequence taxonomy reference database management. *PLoS Comput. Biol.* 17(11), e1009581. https://doi.org/10.1371/journal.pcbi.1009581

196. Rodrigues, C.J.C., de Carvalho, C.C.C.R., 2022: Cultivating marine bacteria under laboratory conditions: Overcoming the "unculturable" dogma. *Front. Bioeng. Biotechnol.* 10, 964589. https://doi.org/10.3389/fbioe.2022.964589

197. Rodriguez-R, L.M., Konstantinidis, K.T., 2014a. Estimating coverage in metagenomic data sets and why it matters. *ISME J.* 8, 2349–2351. https://doi.org/10.1038/ismej.2014.76

198. Rodriguez-R, L.M., Konstantinidis, K.T., 2014b. Nonpareil: a redundancy-based approach to assess the level of coverage in metagenomic datasets. *Bioinformatics* 30, 629–635. https://doi.org/10.1093/bioinformatics/btt584

199. Rodriguez-R, L.M., 2018. Nonpareil: metagenome coverage estimation and projections for 'Nonpareil'. R package version 3.3.1. https://CRAN.R-project.org/package=Nonpareil

200. Rojas-Jimenez, K., Grossart, H.P., Cordes, E., Cortés, J., 2020: Fungal communities in sediments along a depth gradient in the Eastern Tropical Pacific. *Front. Microbiol.* 11, 575207. https://doi.org/10.3389/fmicb.2020.575207

201. Rubin-Blum, M., Sisma-Ventura, G., Yudkovski, Y., Belkin, N., Kanari, M., Herut, B., Rahav, E., 2022: Diversity, activity and abundance of benthic microbes in the southeastern Mediterranean Sea: A baseline for monitoring. *FEMS Microbiol. Ecol.* 98, fiac009. https://doi.org/10.1093/femsec/fiac009

202. Runko Luttenberger, L., Slišković, M., 2020. Implementation challenges for marine strategy framework directive in the Republic of Croatia. *Pomorski zbornik* Special edition No. 3, 89–102. https://doi.org/10.18048/2020.00.06.

203. Santillan, E., Seshan, H., Constancias, F., Drautz-Moses, D.I., Wuertz, S., 2019. Frequency of disturbance alters diversity, function, and underlying assembly mechanisms of complex bacterial communities. *npj Biofilms Microbiomes* 5, 8. https://doi.org/ 10.1038/s41522-019-0079-4

204. Sarma, V.V., 2019. Marine Fungal Diversity: Present Status and Future Perspectives, in: Satyanarayana, T., Johri, B., Das, S. (eds.): *Microbial Diversity in Ecosystem Sustainability and Biotechnological Applications.* Springer, Singapore, 267–292. https://doi.org/10.1007/978-981-13-8315-1

205. Seidel, L., Broman, E., Nilsson, E., Ståhle, M., Ketzer, M., Pérez-Martínez, C., Turner, S., Hylander, S., Pinhassi, J., Forsman, A., Dopson, M., 2023. Climate change-related warming reduces thermal sensitivity and modifies metabolic activity of coastal benthic bacterial communities. *ISME J.* 17(6), 855-869. https://doi.org/10.1038/s41396-023-01395-z

206. Sela-Adler, M., Ronen, Z., Herut, B., Antler, G., Vigderovich, H., Eckert, W., Sivan, O., 2017. Co-existence of Methanogenesis and Sulfate Reduction with Common Substrates in Sulfate-Rich Estuarine Sediments. *Front. Microbiol.* 8, 766. https://doi.org/10.3389/fmicb.2017.00766

207. Senko, H., Kajić, S., Huđ, A., Palijan, G., Petek, M., Rajnović, I., Šamec, D., Udiković-Kolić, N., Mešić, A., Brkljačić, L., Petrić, I., 2024. Will the beneficial properties of plant-growth promoting bacteria be affected by waterlogging predicted in the wake of climate change: A model study. *Appl. Soil Ecol.* 198, 105379. https://doi.org/10.1016/j.apsoil.2024.105379

208. Shannon, C.E., 1948. A mathematical theory of communication. *Bell Syst. Tech. J.* 27, 379–423. https://doi.org/10.1002/j.1538-7305.1948.tb01338.x

209. Shepard, F.P., 1954. Nomenclature based on sand-silt-clay ratios. *J. Sediment. Petrol.* 24, 151–158.

210. Sherr, E., Sherr, B., 2008: Understanding Roles Of Microbes In Marine Pelagic Food Webs: A Brief History, in: Kirchman, D. L. (ed.): *Microbial Ecology of the Oceans, Second Edition,* John Wiley & Sons Inc., SAD, 27-44.

211. Siallagan, Z.L., Fadli, M., De Fretes, C.E., Opier, R.D.A., Susanto, R.D., Wei, Z., Suhardi, V.S.H., Nugrahapraja, H., Radjasa, O.K., Dwivany, F.M., 2024. Metagenomic analysis of deep-sea bacterial communities in the Makassar and Lombok Straits. *Sci. Rep.* 14, 25472. https://doi.org/10.1038/s41598-024-74118-9

212. Simpson, E.H., 1949. Measurement of diversity. *Nature* 163, 688–688. https://doi.org/10.1038/163688a0

213. Sivalingam, P., Sabatino, R., Sbaffi, T., Corno, G., Fontaneto, D., Borgomaneiro, G., Rogora, M., Crotti, E., Mapelli, F., Borin, S., Pilar, A.L., Eckert, E.M., Di Cesare, A., 2024. Anthropogenic pollution may enhance natural transformation in water, favouring the spread of antibiotic resistance genes. *J. Hazard. Mater.* 475, 134885. https://doi.org/10.1016/j.jhazmat.2024.134885

214. Stagličić, N., Prime, M., Zoko, M., Erak, Ž., Brajčić, D., Blažević, D., Madirazza, K., Jelić, K., Peharda, M., 2008. Imposex incidence in Hexaplex trunculus from Kaštela Bay, Adriatic Sea. *Acta Adriat.* 49(2), 159–164.

215. Stal, L.J., 2022: A Sea of Microbes: What's So Special about Marine Microbiology, in: Stal, L.J., Cretoiu, M. S. (eds.): *The Marine Microbiome*, Second Edition, Springer Nature Switzerland AG, Switzerland, 1–44. https://doi.org/10.1007/978-3-030-90383-1_1

216. Stoeck, T., Bass, D., Nebel, M., Christen, R., Jones, M.D.M., Breiner, H.-W., Richards, T.A., 2010. Multiple marker parallel tag environmental DNA sequencing reveals a highly complex eukaryotic community in marine anoxic water. *Mol. Ecol.* 19, 21–31. https://doi.org/10.1111/j.1365-294X.2009.04480.x

217. Surricchio, G., Pompilio, L., Arizzi Novelli, A., Scamosci, E., Marinangeli, L., Tonucci, L., d'Alessandro, N., Tangari, A.C., 2019. Evaluation of heavy metals background in the Adriatic Sea sediments of Abruzzo region, Italy. *Sci. Total Environ.* 684, 445–457. https://doi.org/10.1016/j.scitotenv.2019.05.350

218. Sutton, N.B., Maphosa, F., Morillo, J.A., Abu Al-Soud, W., Langenhoff, A.A.M., Grotenhuis, T., Rijnaarts, H.H.M., Smidt, H., 2013. Impact of long-term diesel contamination on soil microbial community structure. *Appl. Environ. Microbiol.* 79, 619–630. https://doi.org/10.1128/AEM.02747-12

219. Šantić, D., Piwosz, K., Matić, F., Vrdoljak Tomaš, A., Arapov, J., Dean, J.L., Šolić, M., Koblížek, M., Kušpilić, G., Šestanović, S., 2021. Artificial neural network analysis of microbial diversity in the central and southern Adriatic Sea. *Sci. Rep.* 11, 11186. https://doi.org/10.1038/s41598-021-90863-7

220. Šolić, M., Krstulović, N., Šestanović, S., Šantić, D., Bojanić, N., Ordulj, M., Jozić, S., 2016. *Microbial Community Ecology of the Adriatic Sea.* Lambert Academic Publishing, Germany.

221. Šolić, M., Grbec, B., Matić, F., Šantić, D., Šestanović, S., Ninčević Gladan, Ž., Bojanić, N., Ordulj, M., Jozić, S., Vrdoljak, A., 2018. Spatio-temporal reproducibility of the microbial food web structure associated with the change in temperature: Long-term observations in the Adriatic Sea. *Prog. Oceanogr.* 161, 87–101. https://doi.org/10.1016/j.pocean.2018.02.003

222. Tarasov, K., Yakhnenko, A., Zarubin, M., Gangapshev, A., Potekhina, N.V., Avtukh, A.N., Kravchenko, E., 2023. *Cytobacillus pseudoceanisediminis sp. nov.*, a novel facultative methylotrophic bacterium with high heavy metal resistance isolated from the deep underground saline spring. *Curr. Microbiol.* 80, 31. https://doi.org/10.1007/s00284-022-03141-8

223. Taylor, J.D., Cunliffe, M., 2016. Multi-year assessment of coastal planktonic fungi reveals environmental drivers of diversity and abundance. *ISME J.* 10(9), 2118–2128. https://doi.org/10.1038/ismej.2016.24

224. Tedesco, P., Balzano, S., Coppola, D., Esposito, F.P., De Pascale, D., Denaro, R., 2024. Bioremediation for the recovery of oil polluted marine environment, opportunities and challenges approaching the Blue Growth. *Mar. Pollut. Bull.* 200, 116157. https://doi.org/10.1016/j.marpolbul.2024.116157

225. Tisthammer, K.H., Cobian, G.M., Amend, A.S., 2016. Global biogeography of marine fungi is shaped by the environment. *Fungal Ecol.* 19, 39–46. https://doi.org/10.1016/j.funeco.2015.09.003

226. Trouche, B., Brandt, M.I., Belser, C., Orejas, C., Pesant, S., Poulain, J., Wincker, P., Auguet, J.-C., Arnaud-Haond, S., Maignien, L., 2021. Diversity and biogeography of bathyal and abyssal seafloor bacteria and archaea along a Mediterranean–Atlantic gradient. *Front. Microbiol.* 12, 702016. https://doi.org/10.3389/fmicb.2021.702016

227. Tso, S.-F., Taghon, G.L. 2006. Protozoan grazing increases mineralization of naphthalene in marine sediment. *Microb. Ecol.* 51, 460–469. https://doi.org/10.1007/s00248-006-9058-4

228. Tu, C., Dong, X., Yang, H., Chang, Y., Xu, Z., Che, F., Wang, S., Huang, W., 2024. Characterization of phosphate solubilizing bacteria in the sediments of eutrophic lakes and their potential for cyanobacterial recruitment. *Chemosphere* 352, 141276. https://doi.org/10.1016/j.chemosphere.2024.141276

229. Ujević, I., Odžak, N., Barić, A., 2000. Trace metal accumulation in different grain size fractions of the sediments from a semi-enclosed bay heavily contaminated by urban and industrial wastewaters. *Water Res.* 34(11), 3055–3061. https://doi.org/10.1016/S0043-1354(99)00376-0

230. Vellend, M., 2010. Conceptual synthesis in community ecology. *Q. Rev. Biol.* 85, 183–206. https://doi.org/10.1086/652373

231. Viličić, D., Marasović, I., Mioković, D., 2002. Checklist of phytoplankton in the eastern Adriatic Sea. *Acta Botan. Croat.* 61(1), 57–91.

232. Waksman, S.A., 1934. The distribution and conditions of existence of bacteria in the Sea. *Ecol. Monogr.* 4(4), 523–529. https://doi.org/10.2307/1961655

233. Wang, M., Kong, L., 2019. pblat: a multithread blat algorithm speeding up aligning sequences to genomes. *BMC Bioinf.* 20, 28, https://doi.org/10.1186/s12859-019-2597-8

234. Wang, L., Wang, L.A., Zhan, X.Y., Huang, Y.K., Wang, J., Wang, X. 2020. Response mechanism of microbial community to the environmental stress caused by the different mercury concentration in soils. *Ecotoxicol. Environ. Saf.* 188, 109906. https://doi.org/10.1016/j.ecoenv.2019.109906

235. Wang, Z.-B., Sun, Y.-Y., Li, Y., Chen, X.-L., Wang, P., Ding, H.-T., Chen, B., Zhang, X.-Y., Song, X.-Y., Wang, M., McMinn, A., Zhang, Y.-Z., Qin, Q.-L., 2020. Significant bacterial distance-decay

relationship in continuous, well-connected Southern Ocean surface water. *Environ. Microbiol.* 80, 73–80. https://doi.org/10.1007/s00248-019-01472-x

236. Wang, F., Li, M., Huang, L., Huang, X.-H., 2021: Cultivation of uncultured marine microorganisms. *Mar. Life Sci. Technol.* 3, 117–120. https://doi.org/10.1007/s42995-021-00093-z

237. Wang, X., Dai, Z., Lin, J., Zhao, H., Yu, H., Ma, B., Hu, L., Shi, J., Chen, X., Liu, M., Ke, X., Yu, Y., Dahlgren, R.A., Xu, J., 2023. Heavy metal contamination collapses trophic interactions in the soil microbial food web via bottom-up regulation. *Soil Biol. Biochem.* 109058. https://doi.org/10.1016/j.soilbio.2023.109058

238. Wang, Y., Hu, Y., Liu, Y., Chen, Q., Xu, J., Zhang, F., Mao, J., Shi, Q., He, C., Cai, R., Lønborg, C., Liu, L., Guo, A., Jiao, N., Zheng, Q., 2024. Heavy metal induced shifts in microbial community composition and interactions with dissolved organic matter in coastal sediments. *Sci. Total Environ.* 927, 172003. https://doi.org/10.1016/j.scitotenv.2024.172003

239. Ward, C.S., Yung C.-M., Davis, K.M., Blinebry, S.K., Williams, T.C., Johnson, Z.I., Hunt, D.E., 2017. Annual community patterns are driven by seasonal switching between closely related marine bacteria. *ISME J.* 11(6), 1412–1422. https://doi.org/10.1038/ismej.2017.4

240. Weynberg, K.D., 2018. Viruses in marine ecosystems: from open waters to coral reefs. *Adv. Virus Res.* 101, 1–38. https://doi.org/10.1016/bs.aivir.2018.02.001

241. Wickham, H., 2007. Reshaping Data with the reshape Package. *J. Stat. Softw.* 21(12), 1–20. http://www.jstatsoft.org/v21/i12/.

242. Wickham H., 2016. ggplot2: Elegant Graphics for Data Analysis. Springer-Verlag, New York. https://ggplot2.tidyverse.org

243. Wickham, H. 2023. stringr: Simple, Consistent Wrappers for Common String Operations. R package version 1.5.1, https://CRAN.R-project.org/package=stringr

244. Wickham, H., François, R., Henry, L., Müller, K., Vaughan, D. 2023. dplyr: A Grammar of Data Manipulation. R package version 1.1.4, https://CRAN.R-project.org/package=dplyr

245. Wickham, H., Vaughan, D., Girlich, M., 2023. tidyr: Tidy Messy Data. R package version 1.3.0., https://CRAN.R-project.org/package=tidyr

246. Wilke, C., 2024. cowplot: Streamlined Plot Theme and Plot Annotations for 'ggplot2'. R package version 1.1.3, https://CRAN.R-project.org/package=cowplot

247. Winding, A., Modrzyński, J.J., Christensen, J.H., Brandt, K.K., Mayer, P., 2019. Soil bacteria and protists show different sensitivity to polycyclic aromatic hydrocarbons at controlled chemical activity. *FEMS Microbiol. Lett.* 366(17), fnz214. https://doi.org/10.1093/femsle/fnz214

248. Woese, C.R., Kandler, O., Wheelis, M.L., 1990. Towards a natural system of organisms: proposal for the domains Archaea, Bacteria, and Eucarya. *Proc. Natl. Acad. Sci. U.S.A.* 87(12), 4576–4579. https://doi.org/10.1073/pnas.87.12.4576

249. Wu, S., Dong, Y., Deng, Y., Cui, L., Zhuang, X., 2022. Protistan consumers and phototrophs are more sensitive than bacteria and fungi to pyrene exposure in soil. *Sci. Total Environ.* 822, 153539. https://doi.org/10.1016/j.scitotenv.2022.153539

250. Wu, W., Lu, H. P., Sastri, A., Yeh, Y.C., Gong, G.C., Chou, W.C., Hsieh, C.H. 2018. Contrasting the relative importance of species sorting and dispersal limitation in shaping marine bacterial versus protist communities. *ISME J.* 12(2), 485–494. https://doi.org/10.1038/ismej.2017.183

251. Wu, W., Huang, B., 2019. Protist diversity and community assembly in surface sediments of the South China Sea. *Microbiol. Open* 8(10), e891. https://doi.org/10.1002/mbo3.891

252. Wu, Z., Li, M., Qu, L., Zhang, C., Xie, W., 2024. Metagenomic insights into microbial adaptation to the salinity gradient of a typical short residence-time estuary. *Microbiome* 12, 115. https://doi.org/10.1186/s40168-024-01817-w

253. Xu, H., Croot, P., Zhang, C., 2021. Discovering hidden spatial patterns and their associations with controlling factors for potentially toxic elements in topsoil using hot spot analysis and K-means clustering analysis. *Environ. Int.* 151, 106456. https://doi.org/10.1016/j.envint.2021.106456

254. Yang, S., Wen, X., Shi, Y., Liebner, S., Jin, H., Perfumo, A., 2016. Hydrocarbon degraders establish at the costs of microbial richness, abundance and keystone taxa after crude oil contamination in permafrost environments. *Sci. Rep.* 6, 37473. https://doi.org/10.1038/srep37473

255. Yurchenko, A.N., Girich, E.V., Yurchenko, E.A., 2021. Metabolites of Marine Sediment-Derived Fungi: Actual Trends of Biological Activity Studies. *Mar. Drugs* 19, 88. https://doi.org/10.3390/md19020088

256. Zhang, W., Zhang, Y., Shao, Z., Sun, Y., Li, H., 2025. Differences in biogeographic patterns and mechanisms of assembly in estuarine bacterial and protist communities. *Microorganisms* 13(1), 214. https://doi.org/10.3390/microorganisms13010214

257. Zhao, Z., Li, H., Sun, Y., Yang, Q., Fan, J., 2021. Contrasting the assembly of phytoplankton and zooplankton communities in a polluted semi-closed sea: Effects of marine compartments and environmental selection. *Environ. Pollut.* 285, 117256. https://doi.org/10.1016/j.envpol.2021.117256

258. Zhao, Z., Li, H., Sun, Y., Zhan, A., Lan, W., Woo, S.P., Shau-Hwai, A.T., Fan, J., 2022. Bacteria versus fungi for predicting anthropogenic pollution in subtropical coastal sediments: Assembly

process and environmental response. *Ecol. Indic.* 134, 108484. https://doi.org/10.1016/j.ecolind.2021.108484

259. Zhu, H.-S., Liang, X., Liu, J.-C., Zhong, H.-Y., Yang, Y.-H., Guan, W.-P., Du, Z.-J., Ye, M.-Q., 2023. Antibiotic and heavy metal co-resistant strain isolated from enrichment culture of marine sediments, with potential for environmental bioremediation applications. *Antibiotics* 12, 1379. https://doi.org/10.3390/antibiotics12091379

260. Zobell, C.E., 1946. Marine microbiology. a monogram on hydrobacteriology. *Chronica Botanica Co.,* Waltham, 240.

261. Zou, D., Qi, Y., Zhou, J., Liu, Y., Li, M., 2025. Unveiling the life of archaea in sediments: Diversity, metabolic potentials and ecological roles. *iMetaOmics* 2(1), e56. https://doi.org/10.1002/imo2.56

Curriculum vitae

Ana Ramljak was born on 1st of March 1997, in Luzern, Switzerland.
After some time, she moved to a small town Živogošće Blato, on Makarska riviera.
Ana attended high school in Makarska and, in the year 2015, began her Bachelor's degree studies in Environmental sciences at the Faculty of Science, University of Zagreb.
In 2020, she obtained her Master's degree in Environmental sciences and received the Dean's award for outstanding study success.
During her studies, Ana was active in the Biology students association (BIUS) and co-founded the Sustainable development section, which remains active today.
Ana also completed an internship in the Central waste water treatment plant in Zagreb.
She performed the experimental research for her Master's degree thesis in the Laboratory for Aquaculture and Pathology of Aquatic Organisms at the Ruđer Bošković Institute.

After graduating, Ana undertook a four-month Erasmus+ traineeship at the Helmholtz Institute for environmental research in Leipzig (Germany) in the Ecotoxicology Department. She then worked as a research assistant in the same department until May 2021.

Since October 2021, Ana has been employed as an assistant (PhD student) in the Laboratory for Environmental Microbiology and Biotechnology, at the Department for marine and environmental research at the Ruđer Bošković Institute in Zagreb.

Scientific publications:

- **Ramljak, A.**, Vardić Smrzlić, I., Kapetanović, D., Barac, F., Kolda, A., Perić, L.,Balenović, I., Klanjšček, T., Gavrilović, A., 2022. Skin culturable microbiota in farmed European seabass (*Dicentrarchus labrax*) in two aquacultures with and without antibiotic use. *J. Mar. Sci. Eng.* 10, 303. https://doi.org/10.3390/jmse10030303

- **Ramljak, A.**, Žučko, J., Lučić, M., Babić, I., Morić, Z., Fafanđel, M., Furdek Turk, M., Matijević, S., Karpouzas, D., Udiković-Kolić, N., Petrić, I., 2024. Microbial communities as indicators of marine ecosystem health: Insights from coastal sediments in the eastern Adriatic Sea. *Mar. Pollut. Bull.* 205, 116649. https://doi.org/10.1016/j.marpolbul.2024.116649

Appendix

Table S1. List of the 67 sediment samples and their corresponding sampling locations with coordinates.

Sample	Sampling location	Region	Latitude	Longitude
CK1	Cape Kamenjak	NA	44° 47' 20.2194"	13° 55' 39.2406"
CK2	Cape Kamenjak	NA	44° 47' 20.2194"	13° 55' 39.2406"
CV1	Vis island	SA	43° 2' 54.5562"	16° 3' 32.1732"
CV2	Vis island	SA	43° 2' 2.922"	16° 5' 32.7294"
CZ1	Zlarin island	SA	43° 42' 18.2622"	15° 51' 2.7426"
CZ2	Zlarin island	SA	43° 42' 10.4472"	15° 50' 59.1432"
PU1	Port of Pula	NA	44° 52' 3.432"	13° 50' 23.0094"
PU2	Port of Pula	NA	44° 52' 3.432"	13° 50' 23.0094"
PU3	Port of Pula	NA	44° 52' 12.2946"	13° 50' 16.5984"
PU4	Port of Pula	NA	44° 52' 15.0594"	13° 50' 1.6902"
PU5	Port of Pula	NA	44° 52' 15.0594"	13° 50' 1.6902"
PU6	Port of Pula	NA	44° 52' 32.9118"	13° 50' 4.239"
PU7	Port of Pula	NA	44° 52' 44.6484"	13° 50' 24.0678"
RA1	Raša Bay	NA	45° 1' 41.2962"	14° 2' 40.5558"
RA2	Raša Bay	NA	45° 1' 36.9984"	14° 3' 9.6006"
RA3	Raša Bay	NA	45° 1' 26.4072"	14° 3' 9.1218"
RA4	Raša Bay	NA	45° 1' 19.9914"	14° 2' 53.1672"
RA5	Raša Bay	NA	45° 1' 11.9454"	14° 3' 17.8668"
RA6	Raša Bay	NA	45° 1' 1.6284"	14° 3' 25.5492"
RA7	Raša Bay	NA	44° 59' 59.6466"	14° 3' 45.2334"
RA8	Raša Bay	NA	44° 59' 47.5398"	14° 2' 59.01"
RA9	Raša Bay	NA	45° 1' 1.902"	14° 3' 12.675"
RA10	Raša Bay	NA	45° 1' 28.0884"	14° 2' 59.7042"
RI1	Port of Rijeka	NA	45° 19' 28.128"	14° 26' 21.372"
RI2	Port of Rijeka	NA	45° 19' 33.8304"	14° 26' 21.1014"
RI3	Port of Rijeka	NA	45° 19' 30.8712"	14° 26' 19.7874"
RI4	Port of Rijeka	NA	45° 19' 33.4518"	14° 26' 10.8276"
RI5	Port of Rijeka	NA	45° 19' 36.8466"	14° 26' 0.2076"
RI6	Port of Rijeka	NA	45° 19' 37.7682"	14° 25' 0.9186"
RI7	Port of Rijeka	NA	45° 19' 47.8698"	14° 25' 24.132"
BA1	Bakar Bay	NA	45° 18' 13.4742"	14° 32' 16.0182"
BA2	Bakar Bay	NA	45° 18' 6.984"	14° 32' 27.9378"
BA3	Bakar Bay	NA	45° 18' 4.2372"	14° 32' 32.2686"
BA4	Bakar Bay	NA	45° 18' 9.543"	14° 32' 45.2112"
BA5	Bakar Bay	NA	45° 17' 54.5994"	14° 33' 0.54"
BA6	Bakar Bay	NA	45° 17' 14.28"	14° 33' 48.168"
BA7	Bakar Bay	NA	45° 17' 4.833"	14° 33' 53.0892"
BA8	Bakar Bay	NA	45° 17' 26.757"	14° 33' 20.0664"
BA9	Bakar Bay	NA	45° 18' 18.5256"	14° 32' 19.7442"
BA10	Bakar Bay	NA	45° 18' 20.0844"	14° 32' 20.4102"
BA11	Bakar Bay	NA	45° 18' 22.9608"	14° 32' 12.231"
SI1	Šibenik Bay	SA	43° 43' 13.0938"	15° 53' 39.2964"
SI2	Šibenik Bay	SA	43° 43' 5.7036"	15° 53' 49.8258"

Sample	Sampling location	Region	Latitude	Longitude
SI3	Šibenik Bay	SA	43° 43' 3.7308"	15° 53' 59.7114"
SI4	Šibenik Bay	SA	43° 43' 1.077"	15° 54' 7.5918"
SI5	Šibenik Bay	SA	43° 42' 58.8636"	15° 54' 11.9478"
SI6	Šibenik Bay	SA	43° 43' 32.5344"	15° 53' 56.652"
SI7	Šibenik Bay	SA	43° 44' 4.8336"	15° 53' 16.8426"
VR1	Vranjic Basin	SA	43° 31' 51.8658"	16° 27' 54.648"
VR2	Vranjic Basin	SA	43° 31' 49.0728"	16° 27' 53.8986"
VR3	Vranjic Basin	SA	43° 31' 42.348"	16° 28' 16.431"
VR4	Vranjic Basin	SA	43° 31' 41.1522"	16° 28' 22.4184"
VR5	Vranjic Basin	SA	43° 31' 41.1018"	16° 27' 38.8476"
VR6	Vranjic Basin	SA	43° 31' 44.0796"	16° 26' 58.9266"
VR7	Vranjic Basin	SA	43° 32' 14.7552"	16° 26' 46.3056"
VR8	Vranjic Basin	SA	43° 32' 13.4118"	16° 27' 35.3082"
VR9	Vranjic Basin	SA	43° 31' 59.4372"	16° 28' 12.309"
ST1	Port of Split	SA	43° 30' 25.4196"	16° 26' 16.8432"
ST2	Port of Split	SA	43° 30' 26.2038"	16° 26' 11.2734"
ST3	Port of Split	SA	43° 30' 19.3314"	16° 26' 0.7224"
ST4	Port of Split	SA	43° 30' 16.3254"	16° 25' 51.1098"
ST5	Port of Split	SA	43° 30' 12.9636"	16° 26' 1.68"
ST6	Port of Split	SA	43° 30' 16.8006"	16° 26' 11.7882"
ST7	Port of Split	SA	43° 30' 20.1234"	16° 26' 22.1424"
ST8	Port of Split	SA	43° 30' 21.366"	16° 26' 26.826"
ST9	Port of Split	SA	43° 30' 25.5492"	16° 26' 20.4102"
ST10	Port of Split	SA	43° 30' 13.5756"	16° 26' 25.6524"

NA = North Adriatic
SA = South Adriatic

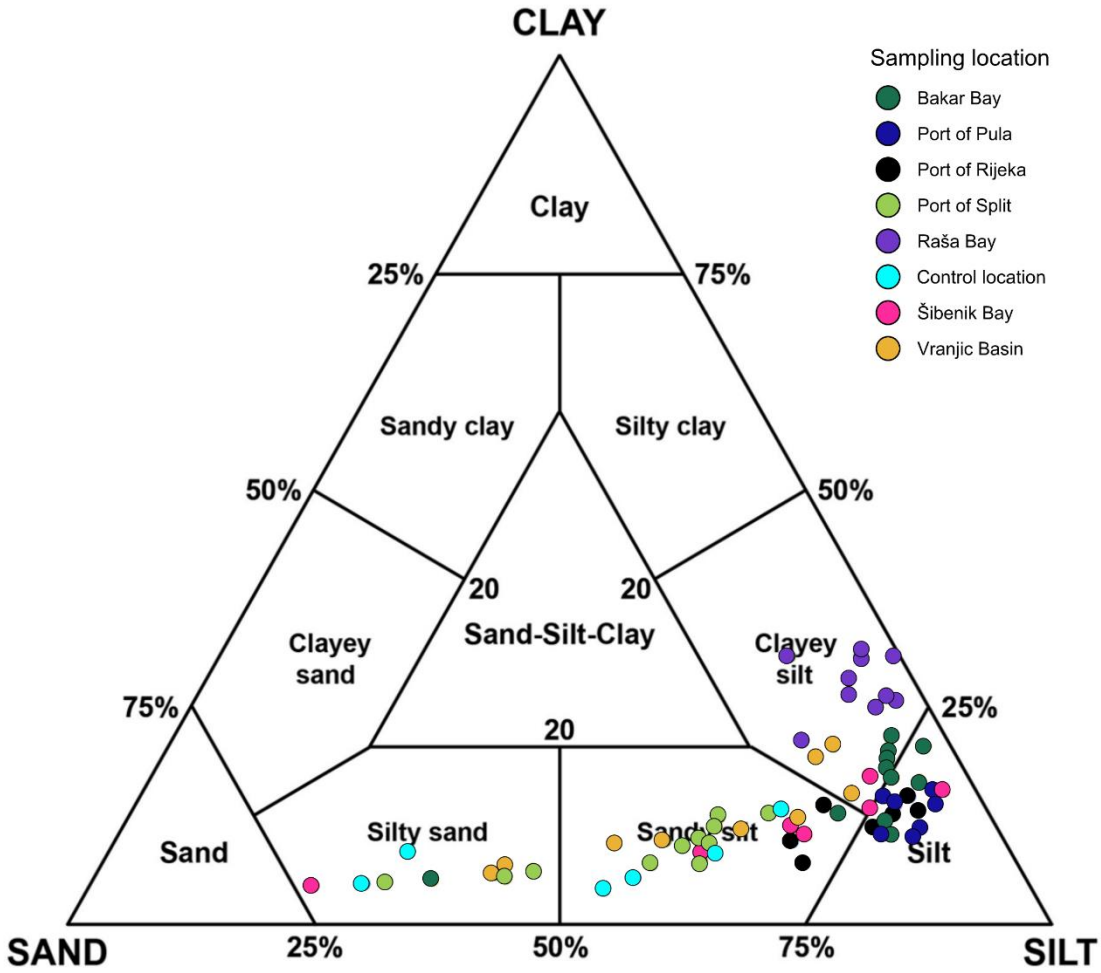

Figure S1. Ternary diagram showing the Shepard's classification of 67 sediment samples.

Table S2. Minimum, median and maximum concentrations of the measured elements in the control locations Al, Fe and Ti are given in g/kg, while the other elements are given in mg/kg.

	Al	Fe	Ti	As	Bi	Cd	Co	Cr	Cu	Li	Mo	Ni	Pb	Sb	Sn	U	Zn
Min	3.6	3.7	0.2	5.8	0.02	0.04	1.4	19.0	3.0	4.4	0.1	8.5	6.1	0.1	0.4	1.0	16.7
Med	42.7	21.4	2.7	14.1	0.1	0.2	11.1	103	17.9	41.8	0.8	51.4	22.7	0.6	2.5	1.9	78.2
Max	74.7	42.8	4.6	29.9	0.4	0.4	19.1	178	35.7	112	1.8	103	57.2	1.3	4.9	3.6	173

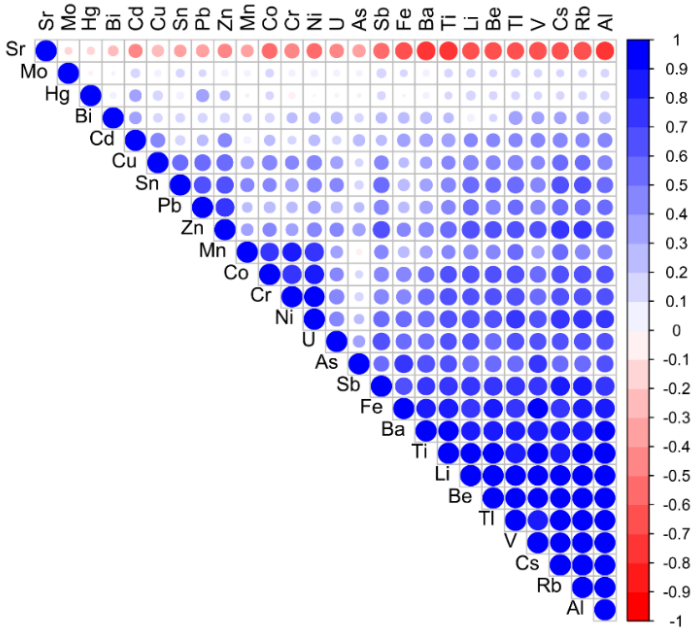

Figure S2. Correlation plot of the elements studied in geochemical background samples, showing mostly the best correlation of potentially toxic elements (PTEs) with Al.

Table S3. Primers used for amplicon sequencing targeting prokaryotes, fungi and protists.

Target gene and region	Target community	Primer	Forward/Reverse	5' -> 3'	Amplicon size (bp)	Reference
16S rRNA V4 region	**Prokaryotes**	**515F**	Forward	5'-GTGCCAGCMGCCGCGGTAA-3'	**~300 bp**	**Provided by sequencing service**
		806R	Reverse	5'-GGACTACHVGGGTWTCTAAT-3'		
18S rRNA V7-V8 region	**Fungi**	**FF390**	Forward	5'-CGATAACGAACGAGACCT-3'	**~390 bp**	**Banos et al., 2018**
		FR1	Reverse	5'-ANCCATTCAATCGGTANT-3'		
18S rRNA V9 region	**Protists**	**1391F**	Forward	5'-GTACACACCGCCCGTC-3'	**~200 bp**	**Stoeck et al., 2010**
		EukB	Reverse	5'-TGATCCTTCTGCAGGTTCACCTAC-3'		

Table S4. Samples used for metagenomic analysis, with their location, contamination status and disturbance level.

	Sample	Location	Presence of contamination	Disturbance level
Control locations	CK1	Cape Kamenjak	No	Low
	CK2		No	Low
	CZ1	Zlarin island	No	Low
Locations under disturbance	PU1	Port of Pula	Yes	High
	PU2		Yes	High
	PU3		Yes	Extreme
	PU4		Yes	High
	PU5		Yes	High
	PU6		Yes	High
	RI2	Port of Rijeka	Yes	Medium
	RI3		Yes	Medium
	RI4		Yes	Medium
	RI5		Yes	Medium
	RI7		Yes	Mild
	BA 5	Bakar Bay	Yes	Mild
	BA 6		Yes	Mild
	BA 11		Yes	Medium
	SI1	Šibenik Bay	Yes	High
	SI2		Yes	High
	SI3		Yes	High
	SI4		Yes	Extreme
	SI5		Yes	Extreme
	SI6		Yes	High
	VR1	Vranjic Basin	Yes	Medium
	VR2		Yes	Medium
	VR3		Yes	Medium
	VR4		Yes	Medium
	VR5		Yes	Extreme
	VR7		Yes	Mild
	VR9		Yes	Mild
	ST1	Port of Split	Yes	Medium
	ST2		Yes	Medium
	ST7		Yes	Medium
	ST8		Yes	Medium
	ST10		Yes	Medium

Table S5. List of compounds used for characterization of metal resistance bacteria.

Compound	Chemical formula	Pollutant tested
zinc sulfate monohydrate	$ZnSO_4 \cdot H_2O$	Zn
nickel(II) chloride	$NiCl_2$	Ni
cadmium chloride	$CdCl_2$	Cd
tin(II) chloride dihydrate	$SnCl_2 \cdot 2H_2O$	Sn
potassium dichromate	$K_2Cr_2O_7$	Cr
copper(II) sulfate	$CuSO_4$	Cu
mercury(II) chloride	$HgCl_2$	Hg
cobalt(II) chloride	$CoCl_2$	Co
lead(II) chloride	$PbCl_2$	Pb
tri-n-butyltin chloride	$C_{12}H_{27}ClSn$	TBT

Table S6. Physicochemical parameters measured in 67 sediment samples.

Sample	Grain	Sampling depth (m)	Sediment temperature (°C)	Bottom water layer temperature (°C)	Sediment pH	Sediment redox potential E_h (mV)	Salinity (‰)	Distance from shore (m)
CK1	sandy silt	12.9	17.2	14.9	7.8	-90	37.86	376.852
CK2	sandy silt	14.4	17.2	14.7	7.63	-130	36.96	376.852
CV1	silty sand	9	24.1	23.6	7.62	-387	39.38	33
CV2	silty sand	7.3	26	25.7	7.5	110	38.71	84.1690
CZ1	sandy silt	16	18.1	18.2	7.5	350	30.13	379.041
CZ2	sandy silt	7.6	18.0	17.7	7.31	-155	31.73	162.436
PU1	silt	20	12.9	13.0	7.68	-60	37.7	114.589
PU2	silt	17	13.1	13.0	7.67	-60	37.7	114.589
PU3	silt	10	14.2	13.0	7.42	-90	37.5	234.457
PU4	clay silt	20	13.3	13.0	7.41	-800	37.5	564.543
PU5	clay silt	18	13.9	13.0	7.1	-100	37.5	564.543
PU6	sandy silt	15	13.2	13.0	7.3	-80	37.6	362.715
PU7	silt	10	13	13.0	7.34	-80	37.5	465.983
RA1	sandy silt	5	12.4	14.4	7.49	-148	28	338
RA2	silt	5	11.7	13.1	7.23	-70	23.3	77
RA3	silt	10	10.2	13.1	7.43	-80	24.4	49
RA4	sandy silt	8	11.7	12.9	7.47	-50	23.5	409
RA5	silt	10	11.5	12.8	7.67	-160	29.6	90
RA6	silt	10	12.0	12.8	7.37	-90	27.0	183
RA7	silt	24	12.3	12.8	7.42	50	19.5	119
RA8	clay silt	14	12.8	12.8	7.47	-25	11.67	77
RA9	clay silt	14	12.7	12.8	7.36	-10	18.1	434
RA10	silty sand	7	14	13	7.44	-175	4.5	260
RI1	silt	12	12.1	12.4	7.69	-130	32.1	28.549
RI2	silt	6	12.3	12.4	7.62	-200	26.9	30.227
RI3	silt	10	10.9	12.4	7.70	-200	26.9	81.285
RI4	silt	14	16.2	12.4	7.44	-170	22.9	27.948
RI5	silt	22	12.3	12.1	7.67	-250	24.3	85.492
RI6	silt	40	12.1	12.8	7.48	-100	29.9	356.088
RI7	silt	22	15.4	13.2	7.77	-300	22.8	53.284
BA1	clay silt	14	13.4	13	7.46	-40	20	88.156
BA2	clay silt	25	12.7	13	7.36	-135	19.47	46.423
BA3	clay silt	25	12.6	13.5	7.50	-70.00	20.6	82.076
BA4	clay silt	28	13.0	13.7	7.44	40	18.11	52
BA5	clay silt	33	13.7	12.4	7.46	-55	16.90	174.366
BA6	clay silt	38	12	12.7	7.52	-38	20.4	386.55
BA7	clay silt	38	12.2	12.7	7.28	-85	22.1	274.739

Sample	Grain	Sampling depth (m)	Sediment temperature (°C)	Bottom water layer temperature (°C)	Sediment pH	Sediment redox potential E_h (mV)	Salinity (‰)	Distance from shore (m)
BA8	clay silt	30	13.1	14.2	7.5	-135	18.28	103.359
BA9	clay silt	23	12.1	13.5	7.52	-250	21.1	136.931
BA10	clay silt	23	11.9	13.5	7.39	-250	21.1	97.037
BA11	sandy silt	12	12.4	13.5	7.52	-200	16.80	70.123
SI1	sandy silt	28	16.6	16.2	7.71	-475	6.98	186.363
SI2	sandy silt	25.4	16.8	16.23	7.44	-300	7.65	159.031
SI3	sandy silt	22	16.7	16.2	7.53	-170	7.315	183.627
SI4	sandy silt	17.6	16.9	16.2	7.48	-250	7.315	142.312
SI5	silty sand	12	17.4	16.2	7.44	-200	7.51	89.636
SI6	sandy silt	16	17	17.6	7.5	-175	6.84	99.145
SI7	sandy silt	23.0	16.7	16.8	7.76	90	6.52	66.289
VR1	silt	2.8	18.7	17.7	7.59	-1700	20.11	33.414
VR2	clay silt	10.9	17.1	17.7	7.52	40	20.11	39.044
VR3	silt	11.2	16.7	16.6	7.32	-400	14.91	19.595
VR4	sandy silt	11.4	17.00	17.7	6.8	-1250	14.91	8.917
VR5	sandy silt	6.7	17.3	18.5	7.51	-900	20.42	45.802
VR6	sandy silt	9.4	17.4	16.5	7.52	-133	24.0	47
VR7	silty sand	4.3	17.9	18.1	7.36	-300	34.83	53.118
VR8	sandy silt	9.9	16.6	17.2	7.44	150	32.82	77
VR9	sandy silt	7.00	17.3	18.4	7.43	-250	18.75	72.119
ST1	sandy silt	2.2	17.6	17.3	7.6	-500	36.4	38.619
ST2	silty sand	2.3	17.8	18.0	7.72	-150	35.88	56.733
ST3	silty sand	6.2	16.9	17.2	7.36	-500	36.48	108.867
ST4	clay silt	5.0	17.1	17.2	7.56	-180	36.54	44
ST5	sandy silt	10.3	16.7	16.6	7.60	-125	36.89	268.494
ST6	clay silt	9.9	16.5	16.6	7.52	150	36.21	150
ST7	clay silt	7.4	16.6	16.7	7.6	50	34.34	96.708
ST8	silty sand	4.2	16.6	17.2	7.37	-400	34.27	58.173
ST9	silty sand	8.8	17.2	17.3	7.55	-350	36.20	17
ST10	sandy silt	3.4	17.4	17.3	7.45	-350	36.4	63

Table S7. Concentrations of pollutants (Hg, TBT), sediment toxicity levels, nutrient concentrations (total phosphorus, total nitrogen and nitrogen compounds) and contents of total organic carbon, total carbon and total inorganic carbon measured in 67 sediment samples.

Sample	Hg (mg/kg d.m.)	TBT (ng/g)	Sediment toxicity level	Total phosphorus TP (µmol/g)	Total nitrogen TN (%)	Total organic carbon TOC (%)	Total carbon TC (%)	Total inorganic carbon TIC (%)
CK1	0.02	0.5	27	6.89	0.166	2.89	10.22	7.33
CK2	0.02	0.5	67	5.35	0.098	1.54	8.19	6.65
CV1	0.02	0.5	8	9.92	< 0.001	1.75	11.91	10.16
CV2	0.005	0.5	22	3.75	0.004	5.11	8.05	2.94
CZ1	0.06	3.1	59	8.67	0.113	4.13	11.19	7.06
CZ2	0.05	0.5	5	4.65	0.154	5.63	11.69	6.05
PU1	9	81.1	333	28.19	0.24	4.37	7.12	2.75
PU2	11	139.6	21	30.69	0.259	4.42	7.47	3.05
PU3	9	494.3	250	37.23	0.249	9.77	14.11	4.34
PU4	12	84	9	24.86	0.224	4.04	7.03	2.99
PU5	8	71.2	29	30.03	0.208	4.52	7.39	2.87
PU6	9	17.2	91	20.16	0.178	6.83	10.59	3.76
PU7	5	2.3	50	12.97	0.086	3.46	7.42	3.96
RA1	0.07	0.5	4	20.16	0.115	1.95	6.16	4.20
RA2	0.06	0.5	14	19.05	0.105	1.72	5.88	4.16
RA3	0.06	22.7	14	18.7	0.103	1.47	5.97	4.50
RA4	0.06	102	7	18.99	0.103	1.47	5.73	4.26
RA5	0.09	0.5	14	18.14	0.112	1.65	5.58	3.93
RA6	0.08	0.5	53	18.35	0.102	1.54	5.41	3.87
RA7	0.09	0.5	143	20.5	0.124	1.55	5.02	3.46
RA8	0.08	0.5	7	18.44	0.111	1.69	5.42	3.73
RA9	0.07	0.5	11	18.62	0.098	1.50	5.53	4.02
RA10	0.06	0.5	167	17.78	0.1	1.57	5.92	4.35
RI1	3	374.6	125	21.8	0.074	1.93	3.80	1.87
RI2	5	505.9	200	42.34	0.224	4.47	6.29	1.82
RI3	6	575.3	111	53.84	0.194	3.98	6.13	2.16
RI4	5	117.1	417	144.98	0.236	4.51	7.48	2.96
RI5	2	69	18	47.23	0.281	4.57	6.46	1.89
RI6	1	27.3	0	27.19	0.132	4.81	6.98	2.17
RI7	2	22.3	143	38.82	0.192	5.50	8.23	2.73
BA1	0.5	31.7	15	32.04	0.183	5.72	7.99	2.27
BA2	0.5	25.3	63	28.58	0.193	6.00	8.43	2.43
BA3	0.5	20.6	167	28.37	0.185	5.47	8.15	2.68
BA4	0.2	54.7	71	96.26	1.116	50.17	50.73	0.56
BA5	0.4	5.4	5	30	0.195	4.37	6.72	2.35
BA6	0.5	18.3	1000	21.03	0.132	2.49	5.19	2.69
BA7	0.5	48.5	9	37.09	0.12	2.29	5.36	3.07
BA8	0.4	23.9	3	22.16	0.15	2.78	5.56	2.78
BA9	0.7	24.8	56	34.81	0.223	7.03	9.36	2.33
BA10	0.5	19.3	7	38.06	0.142	4.73	7.56	2.84
BA11	0.8	81.1	4	52.2	0.217	4.37	8.18	3.81
SI1	11	368.6	500	65.28	0.234	3.38	9.27	5.89

Sample	Hg (mg/kg d.m.)	TBT (ng/g)	Sediment toxicity level	Total phosphorus TP (µmol/g)	Total nitrogen TN (%)	Total organic carbon TOC (%)	Total carbon TC (%)	Total inorganic carbon TIC (%)
SI2	15	283.3	3	70.85	0.199	3.06	9.57	6.51
SI3	16	284.1	8	59.24	0.198	3.18	9.45	6.28
SI4	44	1679.4	333	48.55	0.142	3.48	10.92	7.44
SI5	62	5940.3	143	48.27	0.188	3.87	10.97	7.10
SI6	2	26.4	250	353.94	0.235	4.55	9.23	4.67
SI7	1	0.5	50	41.76	0.102	5.60	14.31	8.72
VR1	0.4	570.8	6	22.43	0.137	2.50	10.47	7.97
VR2	2	900.9	83	61	0.2	3.49	9.27	5.78
VR3	0.5	272.1	31	49.32	0.351	4.62	9.88	5.26
VR4	1	232.5	13	40.29	0.532	6.71	11.55	4.84
VR5	1	157.1	5	127.69	1.073	19.79	23.07	3.27
VR6	0.4	385.6	25	15.04	0.056	2.05	9.90	7.85
VR7	0.5	0.5	200	12.14	0.073	1.80	8.21	6.41
VR8	0.7	106.9	31	19.72	0.081	3.14	9.25	6.11
VR9	1	7.5	11	51.3	0.201	2.63	8.28	5.65
ST1	1	108.4	91	73.22	0.248	8.96	15.24	6.28
ST2	0.8	6.7	143	48.31	0.032	2.06	9.79	7.72
ST3	0.7	26.9	32	22.36	0.1	2.58	10.01	7.43
ST4	0.4	20.2	28	19.99	0.111	2.62	10.28	7.66
ST5	0.4	96.4	167	17.43	0.116	4.95	11.64	6.69
ST6	0.6	547.3	111	15.54	0.107	4.42	11.87	7.46
ST7	0.7	56	48	24.06	0.194	3.06	10.06	7.00
ST8	0.8	98.4	111	66.96	0.482	7.60	13.66	6.06
ST9	0.3	0.5	40	13.29	0.078	1.38	9.47	8.09
ST10	2	242.6	143	45.58	0.294	4.38	10.94	6.57

Table S8. Local enrichment factors (LEFs) normalized to Al in the analyzed sediments.

Sample	EF As	EF Ba	EF Bi	EF Cd	EF Co	EF Cr	EF Cu	EF Mn	EF Ni	EF Pb	EF Sb	EF Sn	EF U	EF Zn
CK1	1.24	0.79	0.85	1.93	1.34	0.98	1.06	1.02	1.09	1.10	1.06	1.14	1.02	1.23
CK2	1.11	0.67	0.91	1.18	1.11	1.05	1.45	0.71	1.32	1.06	0.98	1.01	1.13	0.88
CV1	0.57	1.07	1.26	1.25	1.48	1.27	1.02	1.00	0.72	0.40	0.95	1.40	1.03	0.87
CV2	0.85	1.41	1.00	1.75	0.91	1.03	0.89	1.09	0.84	0.79	1.02	1.40	0.93	0.96
CZ1	1.27	0.98	1.46	1.20	0.91	0.84	1.02	1.15	1.02	0.91	0.67	1.04	1.00	1.83
CZ2	1.19	0.95	0.65	0.92	0.82	0.89	0.70	1.11	0.94	0.81	1.24	0.76	0.88	1.10
PU1	2.07	1.82	6.70	2.76	0.96	1.03	6.70	0.96	0.98	8.60	0.99	7.37	1.54	4.30
PU2	2.06	2.11	9.68	3.92	0.98	1.18	7.98	0.97	1.05	10.97	1.04	10.13	1.78	5.67
PU3	2.42	10.93	20.70	11.33	1.15	1.12	53.80	0.95	1.18	843.2	12.21	133.2	2.95	46.63
PU4	2.75	2.02	6.45	1.75	1.19	1.22	5.90	1.06	1.07	8.89	0.98	9.10	1.81	3.77
PU5	2.25	2.71	7.28	2.03	0.99	1.12	6.03	1.03	0.95	10.82	0.85	9.71	1.60	3.88
PU6	2.38	1.99	4.89	1.31	1.13	1.15	4.99	0.94	1.02	7.52	1.15	10.68	1.90	3.52
PU7	1.61	1.78	3.38	2.14	0.69	1.01	3.55	1.04	0.78	5.17	0.92	4.28	1.82	2.65
RA1	0.48	1.18	1.47	0.99	1.22	1.24	0.98	1.33	1.28	1.11	1.11	0.95	0.98	1.00
RA2	0.58	1.07	1.11	1.16	1.14	1.22	1.06	1.37	1.27	0.87	1.04	0.89	0.96	0.93
RA3	0.62	1.12	1.11	1.16	1.14	1.19	1.08	1.22	1.30	0.91	1.00	0.85	0.98	0.98
RA4	0.64	1.03	0.99	1.10	1.13	1.18	0.97	1.37	1.28	0.82	0.97	0.97	0.88	0.88
RA5	0.91	1.14	1.34	0.81	1.10	1.24	0.98	1.19	1.26	1.15	1.10	1.01	1.05	0.98
RA6	0.87	0.98	1.04	0.97	1.03	1.13	0.96	1.14	1.25	0.97	0.95	0.96	0.94	0.92
RA7	1.21	0.91	1.24	1.01	1.02	1.12	0.97	1.10	1.22	1.06	1.13	0.92	0.97	0.97
RA8	1.04	0.94	1.11	0.95	0.98	1.09	0.89	0.99	1.13	1.08	1.05	0.92	1.02	0.84
RA9	0.80	1.20	1.87	0.90	1.16	1.25	1.01	1.60	1.30	1.06	1.12	1.57	1.06	0.93
RA10	0.57	1.09	2.18	1.02	1.10	1.16	1.01	1.22	1.26	0.98	1.02	0.92	0.96	0.95
RI1	1.18	2.24	3.20	2.65	1.22	1.90	6.91	1.08	1.37	5.49	2.87	6.41	1.14	3.50
RI2	1.58	3.36	13.82	8.50	1.19	1.88	9.09	0.94	1.47	11.20	3.78	8.22	1.52	6.51
RI3	1.79	3.38	6.31	5.96	1.14	1.62	10.36	0.89	1.43	10.81	4.14	7.69	1.53	6.59
RI4	1.88	4.58	9.21	8.52	1.17	1.94	8.79	0.94	1.50	10.02	5.27	5.81	2.67	6.34
RI5	1.67	2.06	6.52	10.59	1.11	1.48	5.68	0.76	1.28	6.79	2.87	4.46	1.75	4.93
RI6	0.88	1.41	3.31	2.46	1.09	1.33	3.26	1.54	1.24	3.67	2.04	2.59	1.80	1.95
RI7	1.27	1.74	8.35	1.57	1.11	1.29	3.38	0.82	0.95	3.07	1.31	4.80	1.29	2.08
BA1	1.12	1.45	2.66	1.81	1.09	1.38	2.71	0.90	1.20	2.13	1.41	3.70	1.34	1.63
BA2	1.18	1.03	1.58	2.27	1.02	1.13	2.31	0.89	1.17	1.95	1.00	1.95	1.37	1.41
BA3	1.29	1.17	28.19	1.94	1.06	1.25	2.29	0.88	1.16	2.00	1.21	2.22	1.55	1.42
BA4	1.45	1.46	4.39	2.54	1.93	1.32	4.08	1.00	1.57	2.39	1.20	4.57	1.36	1.55
BA5	1.34	0.96	2.23	2.28	1.00	1.08	1.91	0.79	1.11	1.81	1.07	1.64	1.42	1.31
BA6	0.98	1.08	1.88	1.55	1.05	1.20	1.68	0.87	1.10	1.61	0.88	1.80	1.42	1.14
BA7	0.84	1.01	1.61	1.65	0.95	1.07	4.48	0.80	1.02	1.45	0.78	1.91	1.30	1.23
BA8	1.03	1.17	2.10	1.51	1.00	1.18	1.81	0.81	1.12	1.65	0.88	1.82	1.45	1.17
BA9	1.14	1.38	2.29	2.05	1.04	1.27	2.71	0.85	1.15	2.40	1.00	2.94	1.37	1.46
BA10	0.66	1.82	1.89	1.84	1.09	1.37	4.97	0.93	1.19	2.30	1.02	5.34	1.17	1.41
BA11	1.71	2.33	25.24	8.63	1.25	1.42	7.82	0.75	1.19	8.28	2.27	6.25	1.84	7.03
SI1	1.99	1.65	22.55	3.92	1.03	1.14	6.86	2.07	1.14	9.57	0.82	7.26	1.64	5.56
SI2	3.21	1.73	19.15	4.98	1.00	1.08	8.65	1.89	1.05	10.07	1.41	8.15	1.71	6.45
SI3	2.59	1.82	20.27	5.52	1.07	1.15	10.17	1.67	1.00	11.39	1.24	7.65	1.80	6.45

Sample	EF As	EF Ba	EF Bi	EF Cd	EF Co	EF Cr	EF Cu	EF Mn	EF Ni	EF Pb	EF Sb	EF Sn	EF U	EF Zn
SI4	7.29	3.11	35.15	6.44	0.94	1.41	23.62	1.23	1.14	22.48	2.92	10.82	1.86	11.67
SI5	12.76	3.92	26.06	5.37	1.08	2.37	49.32	0.92	1.14	29.26	6.76	20.70	2.03	15.41
SI6	1.27	1.59	25.34	59.24	0.57	1.15	5.45	1.14	0.80	5.47	0.70	3.23	8.19	10.26
SI7	2.78	2.55	62.81	5.26	1.70	1.06	5.43	2.55	1.53	9.46	0.97	18.66	1.73	8.39
VR1	0.94	3.92	11.01	2.43	1.33	2.40	19.23	0.65	0.33	13.60	4.98	8.74	0.97	10.15
VR2	1.33	2.13	6.04	11.37	1.69	3.07	28.92	1.04	1.13	7.45	1.49	17.85	1.36	18.48
VR3	0.58	1.40	6.27	9.12	1.23	1.43	8.84	0.92	0.95	3.51	1.42	5.51	1.19	8.84
VR4	0.70	2.14	10.27	9.70	1.20	1.57	8.75	0.86	0.91	5.23	2.06	5.48	1.33	9.66
VR5	1.97	2.01	23.40	11.55	1.25	2.51	22.37	0.72	1.10	19.00	6.55	13.56	3.78	41.55
VR6	0.85	2.54	3.36	3.19	1.07	1.61	7.84	1.38	0.32	2.97	1.30	3.43	1.04	7.42
VR7	1.10	1.55	3.75	1.28	0.74	1.32	2.73	0.78	0.13	2.04	1.23	1.50	0.85	2.57
VR8	0.99	1.59	4.28	2.11	1.28	1.50	4.36	1.01	0.79	3.75	1.70	2.18	0.97	4.10
VR9	0.77	1.16	3.17	2.60	0.94	1.33	3.29	0.75	0.76	2.19	0.74	2.07	1.23	3.03
ST1	1.14	3.53	22.01	9.27	0.92	1.91	10.18	1.12	1.60	7.07	2.09	7.69	1.88	10.66
ST2	0.51	6.36	49.94	7.80	0.82	2.33	10.61	1.13	1.75	8.60	2.09	6.32	1.09	9.01
ST3	0.90	1.97	15.67	2.74	0.88	2.16	4.48	1.24	1.39	2.87	0.77	2.98	1.00	2.67
ST4	0.81	2.71	16.26	1.58	0.91	1.96	6.37	1.34	1.56	2.13	9.46	2.69	0.98	2.00
ST5	1.22	1.70	8.45	1.31	0.91	1.91	4.15	1.17	1.47	1.51	0.76	1.54	2.50	1.55
ST6	1.19	2.22	15.53	4.47	0.93	1.82	26.63	0.98	1.66	2.81	1.12	5.48	2.40	4.95
ST7	1.05	1.90	17.48	5.70	0.90	1.98	7.39	1.19	1.53	3.58	1.20	3.63	1.22	4.69
ST8	1.00	2.47	22.03	15.02	1.16	2.05	12.49	1.11	1.76	7.94	2.34	5.79	1.42	8.29
ST9	0.79	1.73	22.90	1.79	0.86	1.99	4.36	1.23	1.49	1.89	1.28	22.10	1.15	1.61
ST10	1.29	3.93	30.79	10.35	0.87	2.19	14.03	1.05	1.50	8.42	2.27	8.36	1.34	9.08

Table S9. Concentrations of major elements in 67 sediment samples (g/kg).

Sample	Al	Ca	Fe	K	Mg	P	S	Ti
CK1	11.6	282.0	6.4	4.1	15.6	0.2	3.6	0.7
CK2	11.2	350.0	6.1	3.9	24.9	0.1	4.8	0.7
CV1	33.2	192.0	14.5	10.9	55.0	0.3	3.4	2.0
CV2	1.5	359.0	1.1	0.7	14.8	0.1	1.7	0.1
CZ1	20.9	253.0	9.9	6.3	11.5	0.2	4.6	1.6
CZ2	23.2	221.0	10.8	6.2	9.5	0.2	3.7	2.0
PU1	45.8	107.0	22.4	11.3	18.3	0.7	6.7	2.9
PU2	46.1	113.0	23.9	11.4	18.9	0.8	8.1	2.9
PU3	17.5	159.0	42.1	4.9	9.9	0.8	21.9	1.0
PU4	48.9	116.0	25.2	12.3	19.1	0.7	4.6	3.2
PU5	40.3	114.0	22.1	10.9	17.4	0.7	4.4	2.8
PU6	34.1	174.0	26.7	8.6	13.9	0.5	3.7	2.5
PU7	30.0	154.0	17.0	7.2	11.6	0.3	2.9	2.7
RA1	46.7	144.0	25.3	14.0	10.7	0.4	2.3	2.9
RA2	58.9	168.0	29.4	17.0	13.6	0.5	2.5	3.4
RA3	57.8	172.0	28.8	16.7	13.5	0.5	2.4	3.3
RA4	57.1	159.0	28.9	17.6	12.7	0.5	1.9	3.3
RA5	56.5	144.0	30.3	18.8	12.9	0.5	2.3	3.3
RA6	60.9	141.0	29.7	17.9	13.3	0.5	2.1	3.2
RA7	67.2	131.0	33.4	19.9	15.1	0.5	2.5	3.5
RA8	64.3	143.0	31.3	18.5	14.0	0.5	3.5	3.5
RA9	59.1	151.0	32.3	18.1	13.5	0.5	2.1	3.4
RA10	55.3	162.0	27.4	16.0	12.9	0.5	2.1	3.2
RI1	41.6	77.9	24.1	11.1	12.1	0.6	3.1	3.0
RI2	43.1	76.9	26.4	11.4	14.4	0.9	7.3	3.0
RI3	56.5	97.2	33.9	13.6	17.0	1.2	6.0	3.5
RI4	45.1	125.0	38.4	11.0	15.4	3.6	7.4	4.6
RI5	56.8	88.4	29.6	13.5	17.4	1.1	9.0	3.4
RI6	56.0	105.0	28.6	13.6	17.7	0.7	2.8	3.2
RI7	49.3	109.0	51.5	13.9	14.2	1.1	3.4	3.5
BA1	55.9	95.7	57.5	15.9	14.4	0.8	2.4	3.7
BA2	65.1	103.0	53.1	16.2	14.9	0.7	2.3	3.6
BA3	64.7	108.0	51.2	18.1	15.0	0.7	2.5	3.8
BA4	12.7	21.0	173.0	2.6	3.4	1.3	5.0	0.9
BA5	74.0	92.8	54.5	18.5	16.7	0.8	3.1	4.0
BA6	65.5	118.0	35.4	17.9	18.7	0.5	2.4	3.9
BA7	63.3	125.0	29.7	16.5	20.0	0.5	2.1	3.5
BA8	66.7	107.0	38.2	16.6	17.3	0.6	2.3	3.9
BA9	51.8	90.0	63.1	12.1	13.1	0.8	2.4	3.3
BA10	43.5	109.0	46.0	2.6	12.5	0.9	2.2	2.9
BA11	40.6	146.0	28.7	9.6	19.2	1.4	9.4	2.9
SI1	38.8	196.0	22.8	10.8	15.0	1.5	5.2	2.0
SI2	34.0	214.0	21.5	9.2	13.4	1.6	4.8	1.7
SI3	35.3	217.0	21.8	10.0	13.3	1.5	5.0	1.9
SI4	23.2	270.0	18.7	6.0	11.7	1.2	6.3	1.3
SI5	23.5	226.0	20.6	6.0	12.3	1.1	6.0	1.4
SI6	36.3	237.0	14.6	5.8	10.8	27.4	5.2	1.3
SI7	6.7	335.0	8.2	1.9	11.5	1.4	4.4	0.4
VR1	15.3	309.0	12.2	5.4	6.9	0.5	4.9	1.9
VR2	33.0	199.0	29.4	10.2	12.9	1.0	13.2	2.1
VR3	36.1	197.0	24.6	11.9	13.3	1.4	13.4	2.2
VR4	35.0	190.0	23.9	12.0	13.4	1.5	12.6	2.2
VR5	16.5	152.0	15.1	6.6	12.2	3.2	17.5	1.5
VR6	13.0	303.0	10.6	4.6	7.7	0.4	4.2	0.9
VR7	14.7	240.0	9.6	5.8	5.9	0.3	2.8	1.1

Sample	Al	Ca	Fe	K	Mg	P	S	Ti
VR8	24.8	261.0	19.2	7.6	9.5	0.5	3.6	1.6
VR9	29.4	181.0	18.2	9.4	10.6	1.2	6.0	2.0
ST1	12.6	227.0	8.5	4.3	8.0	1.8	8.0	1.2
ST2	6.8	299.0	4.5	2.1	9.4	0.7	2.4	0.7
ST3	14.7	239.0	9.8	5.2	8.0	0.4	4.2	1.2
ST4	15.1	265.0	10.5	5.4	8.9	0.5	3.4	1.3
ST5	17.1	249.0	11.8	5.8	8.9	0.4	5.8	1.3
ST6	13.9	274.0	9.4	4.4	7.3	0.4	5.3	1.0
ST7	19.2	255.0	12.1	6.7	9.6	0.7	6.3	1.5
ST8	13.7	214.0	9.9	5.5	9.2	1.3	8.1	1.2
ST9	14.7	263.0	9.6	5.3	7.8	0.3	3.6	1.2
ST10	19.7	224.0	13.4	6.6	9.7	1.1	8.6	1.6

Table S10. Concentrations of trace elements in 67 sediment samples (mg/kg).

Sample	As	Ba	Bi	Cd	Co	Cr	Cu	Mn	Ni	Pb	Sb	Sn	U	Zn	Se	Sc
CK1	5.8	46.7	0.4	0.1	3.1	34.6	7.8	129.0	24.5	11.6	0.2	1.1	2.2	33.3	0.6	3.9
CK2	5.0	38.6	1.8	0.0	2.5	36.6	10.4	87.6	29.4	10.8	0.0	1.0	2.4	23.4	1.3	4.3
CV1	4.7	135.0	1.4	0.1	6.7	71.8	12.8	310.0	21.5	7.9	0.0	5.1	2.1	41.7	3.0	0.6
CV2	1.3	18.8	10.4	0.1	0.6	14.4	2.3	50.4	10.8	2.5	0.1	1.8	2.1	8.4	0.1	10.0
CZ1	8.1	88.4	1.1	0.1	3.0	38.6	10.1	193.0	8.2	13.5	0.1	1.6	2.1	68.2	18.6	2.5
CZ2	8.0	92.2	0.5	0.0	2.9	42.8	7.3	196.0	4.3	12.8	0.2	1.2	1.8	43.3	3.0	2.3
PU1	31.3	290.0	1.8	0.4	7.0	106.0	119.0	249.0	42.5	202.0	1.5	19.4	3.1	330.0	0.6	7.8
PU2	31.2	338.0	2.7	0.6	7.1	122.0	143.0	254.0	45.6	259.0	1.6	26.9	3.6	438.0	0.7	7.9
PU3	27.1	869.0	2.6	1.1	6.3	58.3	488.0	255.0	31.2	11250.0	6.3	175.0	4.8	1847.0	1.0	3.2
PU4	42.5	338.0	1.9	0.3	8.8	131.0	110.0	280.0	48.2	217.0	1.6	25.2	3.7	303.0	0.9	8.8
PU5	32.7	394.0	1.8	0.3	6.9	105.0	98.1	262.0	38.2	236.0	1.1	23.3	3.1	273.0	1.1	7.2
PU6	32.9	256.0	1.1	0.2	7.5	95.7	72.3	230.0	37.0	149.0	1.3	22.8	3.6	221.0	1.5	6.5
PU7	21.3	209.0	0.7	0.3	4.4	77.3	47.1	248.0	26.5	94.9	0.9	8.3	3.3	152.0	0.1	5.3
RA1	7.3	190.0	0.4	0.3	13.5	129.0	34.7	673.0	73.6	16.7	0.6	2.6	2.0	77.9	0.7	9.4
RA2	9.5	206.0	0.4	0.3	15.1	150.0	38.8	786.0	89.3	17.0	0.6	2.8	2.0	85.0	15.5	11.5
RA3	10.1	212.0	0.4	0.3	14.9	144.0	39.4	692.0	89.8	17.4	0.6	2.6	2.0	88.2	0.1	11.2
RA4	10.4	193.0	0.3	0.3	14.7	141.0	35.3	769.0	87.5	15.6	0.6	3.0	1.8	78.4	111.7	11.1
RA5	14.6	212.0	0.4	0.2	14.2	147.0	35.5	667.0	85.7	21.5	0.6	3.1	2.2	87.0	40.5	11.3
RA6	14.3	192.0	0.4	0.3	14.0	141.0	35.4	666.0	90.1	19.7	0.6	3.1	2.0	86.1	0.9	11.6
RA7	20.6	192.0	0.5	0.3	14.9	150.0	36.2	675.0	96.0	24.0	0.7	3.2	2.1	96.6	0.5	12.5
RA8	17.4	192.0	0.4	0.3	13.9	142.0	32.5	595.0	85.9	23.4	0.6	3.1	2.2	82.0	0.7	12.0
RA9	13.1	229.0	0.6	0.3	15.4	153.0	36.9	915.0	91.4	20.8	0.7	5.0	2.2	85.2	1.0	11.8
RA10	9.1	199.0	0.7	0.3	13.8	136.0	36.5	676.0	84.0	17.9	0.6	2.8	2.0	82.9	0.5	10.6
RI1	17.3	334.0	0.8	0.4	12.4	182.0	115.0	513.0	71.2	122.0	1.7	15.8	2.2	252.0	5.1	7.1
RI2	23.5	512.0	3.6	1.2	12.3	185.0	155.0	455.0	79.0	254.0	2.3	20.7	3.0	479.0	14.6	7.6
RI3	28.9	628.0	2.0	1.0	14.6	193.0	214.0	498.0	96.6	287.0	3.0	23.6	3.2	585.0	81.9	9.7
RI4	28.3	722.0	2.5	1.2	12.6	197.0	155.0	465.0	83.5	233.0	3.3	15.2	5.3	482.0	0.9	8.9
RI5	27.0	384.0	2.1	1.7	14.3	177.0	118.0	428.0	86.9	181.0	2.1	13.7	3.7	439.0	0.6	9.2
RI6	14.2	260.0	1.1	0.4	13.8	157.0	66.9	858.0	83.5	97.0	1.5	7.9	3.8	172.0	4.0	9.4
RI7	19.7	293.0	2.4	0.2	12.8	139.0	63.4	424.0	57.1	75.4	0.9	13.3	2.6	168.0	4.8	9.7
BA1	18.0	267.0	0.9	0.3	13.8	163.0	55.6	501.0	80.5	56.2	1.6	11.3	2.8	143.0	1.4	10.4
BA2	19.9	213.0	0.6	0.4	14.5	149.0	52.7	536.0	89.5	56.4	1.2	6.6	2.9	138.0	36.9	11.9
BA3	21.8	240.0	10.1	0.3	15.1	163.0	52.0	532.0	88.4	57.6	1.4	7.5	3.3	138.0	1.3	12.1
BA4	14.7	92.0	0.4	0.2	7.8	55.0	29.6	250.0	29.5	26.4	1.0	4.8	2.1	49.4	0.5	3.4
BA5	23.6	217.0	0.9	0.4	15.7	155.0	47.6	513.0	94.8	56.4	1.3	6.1	3.1	140.0	1.1	12.7
BA6	16.5	223.0	0.7	0.3	15.0	158.0	38.4	528.0	84.8	46.5	1.0	6.1	3.1	112.0	2.1	12.3
BA7	14.1	203.0	0.6	0.3	13.3	138.0	100.0	477.0	76.3	41.2	0.9	6.4	2.8	118.0	4.3	11.0
BA8	17.5	245.0	0.8	0.3	14.6	158.0	42.0	498.0	87.2	48.2	1.1	6.3	3.1	117.0	0.3	12.5
BA9	18.0	241.0	0.7	0.3	12.4	142.0	52.7	455.0	72.6	60.7	1.1	8.5	2.8	122.0	119.0	9.8
BA10	9.8	279.0	0.5	0.3	11.4	136.0	85.4	450.0	64.5	52.5	1.1	13.6	2.3	105.0	0.3	8.0
BA11	25.0	340.0	6.3	1.2	12.4	134.0	128.0	350.0	60.7	181.0	2.4	15.1	3.6	498.0	1.0	7.6
SI1	28.6	233.0	5.4	0.5	9.9	104.0	109.0	942.0	56.0	204.0	1.2	17.0	3.2	381.0	1.1	7.3
SI2	44.2	222.0	4.1	0.6	8.6	90.0	125.0	803.0	46.1	198.0	1.8	17.3	3.2	404.0	2.1	6.3
SI3	36.1	241.0	4.5	0.7	9.5	98.8	151.0	725.0	45.4	230.0	1.6	16.7	3.4	415.0	0.8	6.4

Sample	As	Ba	Bi	Cd	Co	Cr	Cu	Mn	Ni	Pb	Sb	Sn	U	Zn	Se	Sc
SI4	89.2	304.0	5.6	0.7	6.1	89.6	261.0	425.0	35.9	354.0	2.7	17.5	3.2	562.0	2.4	4.0
SI5	157.0	386.0	4.2	0.6	7.0	152.0	550.0	321.0	36.3	465.0	6.3	33.7	3.5	749.0	1.4	4.0
SI6	17.8	215.0	5.8	7.9	5.2	101.0	82.6	502.0	37.2	112.0	0.9	7.2	15.5	673.0	-0.2	5.5
SI7	23.1	102.0	3.7	0.4	4.2	28.4	25.2	450.0	16.6	72.1	0.3	12.3	2.3	173.0	1.0	1.6
VR1	10.1	283.0	1.3	0.2	6.2	114.0	159.0	178.0	7.2	168.0	1.6	10.4	1.5	367.0	6.3	2.9
VR2	18.1	268.0	1.3	1.5	14.3	251.0	409.0	435.0	48.0	144.0	1.4	37.1	2.5	1133.0	0.2	6.5
VR3	8.1	187.0	1.4	1.2	11.1	124.0	133.0	403.0	43.6	71.6	1.5	12.2	2.3	576.0	0.6	7.2
VR4	9.7	281.0	2.3	1.3	10.6	133.0	129.0	371.0	40.8	105.0	2.0	11.9	2.5	617.0	7.2	7.1
VR5	21.6	153.0	2.8	1.1	6.2	126.0	195.0	205.0	25.8	245.0	2.4	17.1	6.1	1584.0	2.4	3.1
VR6	8.7	163.0	0.3	0.3	4.4	68.5	57.8	347.0	6.1	33.3	0.4	3.7	1.6	240.0	4.7	2.6
VR7	11.6	109.0	0.4	0.1	3.4	61.0	21.9	211.0	2.7	24.6	0.4	1.8	1.3	90.6	0.2	2.6
VR8	12.4	163.0	0.7	0.2	8.7	100.0	50.4	361.0	26.3	61.4	1.1	3.7	1.7	206.0	0.2	5.1
VR9	10.1	134.0	0.6	0.3	7.3	100.0	43.0	295.0	29.3	39.7	0.6	4.0	2.2	172.0	0.7	5.7
ST1	11.5	221.0	2.2	0.8	3.7	79.2	73.3	277.0	29.9	77.7	0.7	8.0	2.9	337.0	8.6	2.6
ST2	4.3	255.0	3.0	0.5	2.0	62.9	49.6	200.0	19.1	65.9	0.6	4.2	1.5	186.0	5.0	1.3
ST3	9.6	138.0	1.7	0.3	4.0	100.0	36.0	334.0	29.7	34.7	0.3	3.5	1.6	94.0	1.6	3.2
ST4	8.7	194.0	1.8	0.2	4.2	92.6	52.3	368.0	34.0	26.1	3.5	3.2	1.5	71.8	0.6	3.4
ST5	13.6	133.0	1.1	0.1	4.6	98.8	37.1	344.0	35.7	19.9	0.3	2.0	4.1	60.8	10.5	3.7
ST6	12.4	149.0	1.6	0.4	4.0	81.1	206.0	255.0	33.6	32.7	0.4	6.1	3.7	168.0	0.8	2.9
ST7	12.1	161.0	2.4	0.6	5.0	110.0	71.5	371.0	41.0	50.4	0.5	5.1	2.0	198.0	9.4	4.0
ST8	10.4	164.0	2.3	1.3	5.0	90.4	95.5	289.0	35.3	91.9	0.8	6.4	2.2	278.0	0.9	2.7
ST9	8.3	121.0	2.5	0.2	3.9	92.5	35.1	332.0	31.7	22.8	0.5	25.7	1.8	56.6	0.6	3.2
ST10	15.0	341.0	4.3	1.1	4.9	124.0	138.0	331.0	41.1	120.0	0.9	12.0	2.2	390.0	0.8	4.1

Table S11. Bioavailable fraction of metals per gram of sediment (ng/g).

Sample	Cu	Zn	As	Cd	Sb	Pb
BA1	37.3	1862.1	212.4	4.3	5.6	98.7
BA2	39.3	1320.1	230.4	3.3	9.6	124.7
BA5	33.3	516.1	252.4	0.0	6.6	173.7
BA6	27.3	285.1	288.4	0.0	2.6	101.7
BA7	42.3	411.1	225.4	0.3	5.6	107.7
BA8	46.3	209.1	284.4	0.0	5.6	90.7
BA9	54.3	1006.1	227.4	3.3	4.6	131.7
BA10	38.3	1175.1	211.4	1.3	3.6	112.7
BA11	20.3	3165.1	189.4	4.3	19.6	239.7
CK1	25.3	380.1	150.4	3.3	7.6	11.7
CK2	62.3	345.1	209.4	6.3	14.6	18.7
CZ1	31.3	76.1	272.4	0.0	35.6	44.7
CZ2	16.3	130.1	239.4	0.0	34.6	36.7
PU1	92.3	10195.1	364.4	6.3	29.6	1034.7
PU2	71.3	13359.1	352.4	6.3	36.6	1102.7
PU3	8.3	219043.1	74.4	4.3	138.6	31532.7
PU4	73.3	6276.1	345.4	0.0	17.6	839.7
PU5	118.3	8751.1	356.4	3.3	12.6	1141.7
PU6	82.3	4622.1	269.4	2.3	32.6	725.7
PU7	74.3	3748.1	234.4	1.3	26.6	536.7
RI1	66.3	13594.1	157.4	13.3	9.6	857.7
RI2	91.3	33243.1	345.4	22.3	56.6	1785.7
RI3	72.3	21268.1	264.4	16.3	45.6	1338.7
RI4	59.3	16009.1	279.4	10.3	43.6	626.7
RI5	34.3	15391.1	432.4	9.3	46.6	920.7
RI6	30.3	3530.1	225.4	6.3	21.6	376.7
RI7	42.3	1876.1	187.4	6.3	2.6	175.7
S1	348.0	3808.3	2057.7	13.0	41.3	746.3
S2	79.3	3741.1	1025.4	10.3	35.6	817.7
S3	88.3	3940.1	856.4	8.3	62.6	918.7
S4	231.3	16496.1	1509.4	17.3	169.6	2320.7
S5	170.3	18989.1	1480.4	5.3	47.6	2051.7
S6	33.3	10785.1	506.4	2.3	4.6	278.7
S7	29.3	3681.1	408.4	0.0	6.6	153.7
ST1	41.3	3425.1	437.4	0.0	8.6	102.7
ST2	25.3	23810.1	320.4	3.3	34.6	838.7
ST3	98.3	4270.1	251.4	5.3	13.6	122.7
ST7	178.3	14881.1	359.4	26.3	46.6	297.7
ST8	33.3	6614.1	217.4	0.0	37.6	140.7
ST10	30.3	24679.1	403.4	9.3	30.6	291.7
VR1	110.3	12420.1	306.4	2.3	12.6	170.7
VR2	12.3	14697.1	192.4	0.0	32.6	47.7
VR3	104.3	14653.1	76.4	3.3	20.6	83.7
VR4	54.3	16734.1	198.4	1.3	43.6	89.7
VR5	23.3	8706.1	486.4	0.0	74.6	62.7
VR7	139.3	1762.1	308.4	2.3	6.6	114.7
R9	51.3	2711.1	208.4	0.3	19.6	90.7

Sample	Cu	Zn	As	Cd	Sb	Pb
RA1	50.3	511.1	71.4	22.3	0.0	2.7
RA2	32.3	497.1	68.4	12.3	0.0	0.0
RA3	298.3	471.1	102.4	15.3	0.0	1.7
RA4	23.3	300.1	111.4	14.3	0.0	0.0
RA5	14.3	1113.1	164.4	6.3	0.6	3.7
RA6	20.3	484.1	117.4	11.3	0.0	−0.3
RA7	24.3	299.1	160.4	2.3	0.6	10.7
RA8	22.3	165.1	125.4	4.3	0.0	1.7
RA9	43.3	632.1	98.4	11.3	0.0	6.7
RA10	28.3	375.1	92.4	14.3	0.0	0.0

Table S12. Summary of amplicon sequencing data for 55 sediment samples after QIIME2 processing, for prokaryotes (16S rRNA), protists (18S rRNA) and fungi (18S rRNA).

Total number of samples: 55	**Prokaryotes 16S**	**Protists 18S**	**Fungi 18S**
Total number of quality sequences	3,877,607	1,989,467	4,597,811
Total number of ASVs	47,337	18,629	27,948
Mean frequency	70,501.945	36,172.127	83,596.563
Minimum frequency	41,800.0	15,128.0	30,022.0
Maximum frequency	82,979.0	85,794.0	116,014.0

Table S13. Alpha diversity indices for prokaryotes.

Sample	Observed richness	ACE	Shannon	Inverse Simpson's	Fisher's α
BA1	2293	2363.253	6.935683	390.5343	528.5605
BA2	2387	2476.109	6.876545	326.5166	556.8255
BA5	2051	2124.942	6.669788	246.4813	457.7934
BA6	2003	2059.384	6.667443	241.0455	444.1037
BA7	1875	1926.348	6.582805	229.3692	408.168
BA8	1882	1940.829	6.569088	219.3525	410.1116
BA9	2058	2124.891	6.73075	298.8	459.7995
BA10	2112	2170.73	6.786113	343.5167	475.3575
BA11	1777	1817.122	6.58602	258.937	381.222
CK1	1851	1897.4	6.636597	339.8167	401.5232
CK2	1800	1847.77	6.619152	343.399	387.5015
CZ1	1846	1898.358	6.620366	296.7709	400.1426
CZ2	2784	2869.115	7.287693	740.225	680.9021
PU1	1930	1991.349	6.545319	193.525	423.507
PU2	2087	2142.889	6.814774	409.3533	468.1366
PU3	1917	1958.694	6.753501	362.0222	419.8675
PU4	2023	2082.43	6.80266	396.71	449.7937
PU5	2076	2145.529	6.810134	401.954	464.9693
PU6	1743	1782.961	6.622992	325.1059	371.9898
PU7	1652	1686.604	6.442241	232.7901	347.5786
RI1	1878	1912.6	6.715274	360.0339	409.0007
RI2	1906	1954.01	6.726857	369.978	416.7946
RI3	2191	2253.689	6.90814	458.0397	498.3797
RI4	2295	2362.785	6.921363	454.8775	529.1574
RI5	1928	1981.542	6.730191	383.9408	422.9465
RI6	2110	2187.736	6.715415	316.7958	474.7786
RI7	1962	2023.072	6.523783	171.2483	432.5024
S1	1972	2036.73	6.705646	324.1458	435.3242
S2	1908	1978.357	6.35489	130.9923	417.3528
S3	1974	2022.715	6.712696	298.3044	435.8891
S4	2219	2297.038	6.846107	363.4179	506.6137
S5	2084	2146.34	6.80895	415.5539	467.2722
S6	1928	1982.622	6.74236	359.6244	422.9465
S7	2132	2196.149	6.875939	403.4351	481.1566
ST1	2013	2085.192	6.717882	371.6727	446.9462
ST10	1811	1854.424	6.597715	299.2605	390.5144
ST2	1906	1971.683	6.627992	293.4978	416.7946
ST3	1820	1871.717	6.588868	323.7384	392.9842
ST7	1844	1910.57	6.483502	251.5724	399.5907
ST8	1801	1866.552	6.029979	53.25917	387.7751
VR1	2010	2087.393	6.654175	330.734	446.0929
VR2	2321	2406.319	6.92585	403.1274	536.9348
VR3	2186	2257.902	6.758936	229.6127	496.9134
VR4	2010	2064.258	6.625981	165.0855	446.0929
VR5	1795	1858.927	6.085044	52.46733	386.134
VR7	1997	2079.762	6.63798	308.854	442.4007
VR9	1963	2028.631	6.667901	335.2551	432.7844
RA1	2054	2093.046	6.647898	147.1959	458.6529
RA3	1553	1580.898	6.015945	78.39322	321.5213
RA5	1850	1873.569	6.534298	127.2263	401.2469
RA7	1816	1839.201	6.60695	196.9578	391.886
RA8	1652	1668.439	6.580565	200.6001	347.5786

Table S14. Alpha diversity indices for fungi.

Sample	Observed richness	ACE	Shannon	Inverse Simpson's	Fisher's *α*
BA1	196	198.01434	4.210377	18.70905	39.56627
BA2	91	91	3.458329	12.38298	15.45062
BA5	105	106.95026	2.823686	5.192061	18.36477
BA6	92	92	3.215734	9.305326	15.65529
BA7	132	133.54616	2.402102	3.408591	24.26505
BA8	108	109.28302	2.918036	5.799233	19.00256
BA9	119	119.9066	3.148693	6.008309	21.37982
BA10	122	122.70434	3.094924	6.752198	22.03848
BA11	106	107.72793	3.64925	13.63139	18.57685
CK1	156	158.67522	3.730926	14.73653	29.79619
CK2	175	177.22819	3.758686	13.41597	34.3538
CZ1	136	138.27782	3.420897	13.02225	25.16879
CZ2	62	63.57551	3.281546	17.1795	9.768013
PU1	116	116.36952	3.632966	15.32071	20.72554
PU2	152	152.84883	3.933536	23.85647	28.85648
PU3	176	176.92469	4.250171	29.90963	34.5979
PU4	155	158.13607	3.486768	11.45987	29.56061
PU5	132	133.25986	3.689451	16.33455	24.26505
PU6	140	140.42287	3.784881	19.60768	26.07989
PU7	134	135.52515	3.81365	21.98522	24.71599
RI1	154	156.73044	4.013192	19.96973	29.32546
RI2	172	172.20663	4.310528	30.25948	33.62401
RI3	210	211.56064	4.099587	14.57132	43.13992
RI4	161	161.68169	3.937345	13.63583	30.9806
RI5	244	247.54826	4.400622	25.72431	52.13586
RI6	158	159.60473	3.127541	4.982834	30.26866
RI7	238	240.59803	4.1845	18.84736	50.51632
S1	128	129.51877	3.664892	18.22288	23.36875
S2	200	206.74395	3.969525	17.6594	40.57937
S3	148	148.34172	3.990521	21.15028	27.92382
S4	193	196.32222	4.098596	21.61615	38.81066
S5	169	170.33916	3.760943	12.45078	32.89799
S6	168	170.34933	3.917724	24.6624	32.65683
S7	111	111	3.902328	24.67501	19.64493
ST1	175	175.35931	3.516308	6.596007	34.3538
ST10	258	260.04535	4.930637	84.94193	55.96711
ST2	225	227.6164	4.389436	37.07236	47.0541
ST3	195	195.91621	4.368156	33.60112	39.314
ST7	231	239.77204	4.268208	23.30694	48.64405
ST8	291	299.67579	4.631546	42.88738	65.28258
VR1	157	158.42262	4.494276	58.15771	30.0322
VR2	137	137.19525	4.351538	48.95823	25.39588
VR3	293	296.26744	4.872709	68.27748	65.85983
VR4	334	357.77206	4.292588	19.35271	78.00555
VR5	244	250.61547	4.431592	36.37682	52.13586
VR7	164	165.01132	4.18248	30.73001	31.69642
VR9	132	132.19443	4.148777	33.69992	24.26505
RA1	423	446.76484	5.178045	92.12936	106.3725
RA3	35	35.37006	2.681996	8.788439	4.986654
RA5	195	197.48241	4.460696	41.68902	39.314
RA7	227	227.68022	4.737551	63.9481	47.58255
RA8	226	227.43944	4.714358	59.65512	47.31813

Table S15. Alpha diversity indices for protists.

Sample	Observed richness	ACE	Shannon	Inverse Simpson's	Fisher's *α*
BA1	312	357.9498	5.050202	88.62526	97.18261
BA2	285	314.366	4.882125	62.9412	85.48802
BA5	232	254.7131	4.683662	59.08677	64.25969
BA6	235	249.2692	4.602964	39.4339	65.40079
BA7	303	356.2669	4.856295	58.02588	93.2176
BA8	292	328.4748	4.976803	79.16448	88.46234
BA9	297	341.9928	4.951701	78.38437	90.61147
BA10	239	263.5594	4.746269	64.59006	66.93352
BA11	318	378.1763	4.959463	70.88188	99.86332
CK1	293	326.1983	4.937532	69.81172	88.89052
CK2	211	227.5372	4.608719	47.93085	56.47424
CZ1	228	250.7208	4.071566	14.22429	62.74946
CZ2	281	306.0975	5.001941	83.56278	83.80641
PU1	255	306.2012	4.395597	23.60934	73.19312
PU2	243	296.8189	4.30074	23.56417	68.47909
PU3	243	280.5794	4.45222	34.15293	68.47909
PU4	303	365.2911	4.823257	56.81942	93.2176
PU5	298	349.1156	4.784675	46.46024	91.04377
PU6	261	319.4091	4.525693	38.21761	75.59371
PU7	252	303.8855	4.489733	36.59039	72.00373
RI1	317	372.4933	4.89437	58.32599	99.41445
RI2	244	285.9406	3.37993	4.93903	68.8675
RI3	264	303.7092	4.365932	22.79717	76.80492
RI4	227	265.4908	3.853753	11.71767	62.37391
RI5	253	286.3834	4.400933	20.7409	72.39939
RI6	271	294.3042	4.874169	64.46076	79.65944
RI7	219	236.103	4.544062	47.55813	59.39841
S1	233	247.7928	4.491342	29.45775	64.63924
S2	213	233.4696	4.328489	26.42129	57.20048
S3	224	251.4675	4.297725	26.54172	61.25208
S4	288	343.6422	4.683654	41.6804	86.75782
S5	255	298.3447	4.392733	25.65264	73.19312
S6	290	332.7726	4.759027	47.1587	87.60844
S7	145	147.4014	4.435606	56.10614	34.32071
ST1	231	255.849	4.623934	53.36166	63.88093
ST10	206	230.7338	4.50762	47.49559	54.67272
ST2	210	228.2675	4.391998	27.9776	56.11233
ST3	266	287.6589	4.83151	63.37401	77.61644
ST7	211	238.5356	3.544868	6.550378	56.47424
ST8	120	124.4816	4.082422	39.86266	26.8664
VR1	212	230.2305	4.70841	75.23779	56.83693
VR2	214	237.3556	4.576583	48.38817	57.56479
VR3	204	235.0459	3.956805	17.35051	53.95773
VR4	165	185.2677	3.514817	10.31044	40.65982
VR5	137	139.0812	4.186172	36.58639	31.87789
VR7	286	336.5319	4.87285	64.50588	85.91047
VR9	235	258.1281	4.74012	60.75912	65.40079
RA1	312	366.7926	4.689866	39.17725	97.18261
RA3	293	338.732	4.496907	25.07903	88.89052
RA5	270	325.8533	4.518058	33.84286	79.24922
RA7	308	376.0553	4.693824	38.49559	95.41209
RA8	313	430.369	4.532506	35.45739	97.62731

Table S16. Prokaryotic observed richness and Shannon diversity index statistical analysis.

Kruskal-Wallis	χ^2 (Chi squared)	df	*p*-value
Observed	4.751	4	0.3138
Shannon	3.6726	4	0.4521

Table S17. Fungal observed richness and Shannon diversity index statistical analysis. Bolded *p*-values are statistically significant ($p < 0.05$).

Kruskal - Wallis	χ^2 (Chi squared)	df	*p*-value
Observed	13.141	4	**0.01061**

Dunn's post hoc test for observed richness

Observed			
Comparison	Z	*p*-value	*p*-adjusted
Extreme-High	1.893615	0.058276	0.14569
Extreme-Low	0.944177	0.345079	0.431349
High-Low	-1.20334	0.228844	0.381406
Extreme-Medium	0.114346	0.908964	0.908964
High-Medium	-2.58649	0.009696	**0.048479**
Low-Medium	-1.19305	0.23285	0.332642
Extreme-Mild	2.093221	0.036329	0.121098
High-Mild	0.160533	0.872461	0.969401
Low-Mild	1.449666	0.147152	0.294304
Medium-Mild	3.020355	0.002525	**0.025248**

Table S17. continued

ANOVA

Shannon	Df	Sum Sq	Mean Sq	F value	Pr(>F)
Disturbance level	4	4.690501	1.172625	4.149976547	**0.005839593**
Residuals	47	13.28041	0.282562	NA	NA

Tukey's post hoc test for Shannon diversity index

Shannon	diff	lwr	upr	*p*-adjusted
High-Extreme	-0.33807	-1.23008	0.553948	0.818334
Low-Extreme	-0.13925	-1.04531	0.766815	0.992246
Medium-Extreme	0.141859	-0.70662	0.990334	0.989325
Mild-Extreme	-0.6284	-1.48323	0.226433	0.243542
Low-High	0.198819	-0.49396	0.891595	0.925015
Medium-High	0.479925	-0.13562	1.095474	0.193372
Mild-High	-0.29033	-0.91461	0.333948	0.680836
Medium-Low	0.281107	-0.35463	0.916842	0.719891
Mild-Low	-0.48915	-1.13334	0.155043	0.215277
Mild-Medium	-0.77026	-1.33057	-0.20995	**0.002703**

Table S18. Protistan observed richness and Shannon diversity index statistical analysis. Bolded *p*-values are statistically significant ($p < 0.05$).

Kruskal-Wallis	χ^2 (Chi-squared)	df	*p*-value
Observed	9.4559	4	0.05066
Shannon	16.324	4	**0.002613**

Dunn's post hoc test for Shannon diversity index

Shannon			
Comparison	Z	*p*-value	*p*-adjusted
Extreme-High	-0.50749	0.61181	0.679789
Extreme-Low	-1.33294	0.182553	0.304254
High-Low	-1.08987	0.275772	0.393959
Extreme-Medium	-0.04495	0.964147	0.964147
High-Medium	0.673466	0.500651	0.625814
Low-Medium	1.839736	0.065807	0.164518
Extreme-Mild	-2.44831	0.014353	**0.047843**
High-Mild	-2.62735	0.008605	**0.043027**
Low-Mild	-1.37407	0.169421	0.338843
Medium-Mild	-3.66718	0.000245	**0.002452**

Table S19. Pairwise PERMANOVA analysis of Bray-Curtis dissimilarity matrices for prokaryotes (A), fungi (B) and protists (C) according to disturbance level (DL).
P-values were adjusted using the Benjamini-Hochberg method.

A) prokaryotes

Comparison of DLs	*p*-value	*p*-adjusted	R^2 value (%)
Mild vs Medium	0.001	0.002	12.117
Mild vs Low	0.001	0.002	17.426
Mild vs High	0.006	0.01	8.855
Mild vs Extreme	0.021	0.026	10.916
Medium vs Low	0.001	0.002	17.545
Medium vs High	0.001	0.002	17.068
Medium vs Extreme	0.039	0.039	9.574
Low vs High	0.001	0.002	19.808
Low vs Extreme	0.03	0.033	16.126
High vs Extreme	0.019	0.02625	12.421

B) fungi

Comparison of DLs	*p*-value	*p*-adjusted	R^2 value (%)
Mild vs Medium	0.002	0.004	15.177
Mild vs Low	0.001	0.003	15.347
Mild vs High	0.014	0.02	15.140
Mild vs Extreme	0.007	0.012	18.340
Medium vs Low	0.001	0.003	13.011
Medium vs High	0.002	0.004	16.475
Medium vs Extreme	0.132	0.147	8.238
Low vs High	0.001	0.003	17.653
Low vs Extreme	0.027	0.034	15.610
High vs Extreme	0.16	0.16	11.824

C) protists

Comparison of DLs	*p*-value	*p*-adjusted	R^2 value (%)
Mild vs Medium	0.002	0.004	11.044
Mild vs Low	0.001	0.003	24.177
Mild vs High	0.010	0.017	9.026
Mild vs Extreme	0.012	0.017	13.402
Medium vs Low	0.001	0.003	15.494
Medium vs High	0.001	0.003	12.918
Medium vs Extreme	0.110	0.122	7.674
Low vs High	0.001	0.003	22.897
Low vs Extreme	0.028	0.0350	17.107
High_vs_Extreme	0.161	0.161	10.352

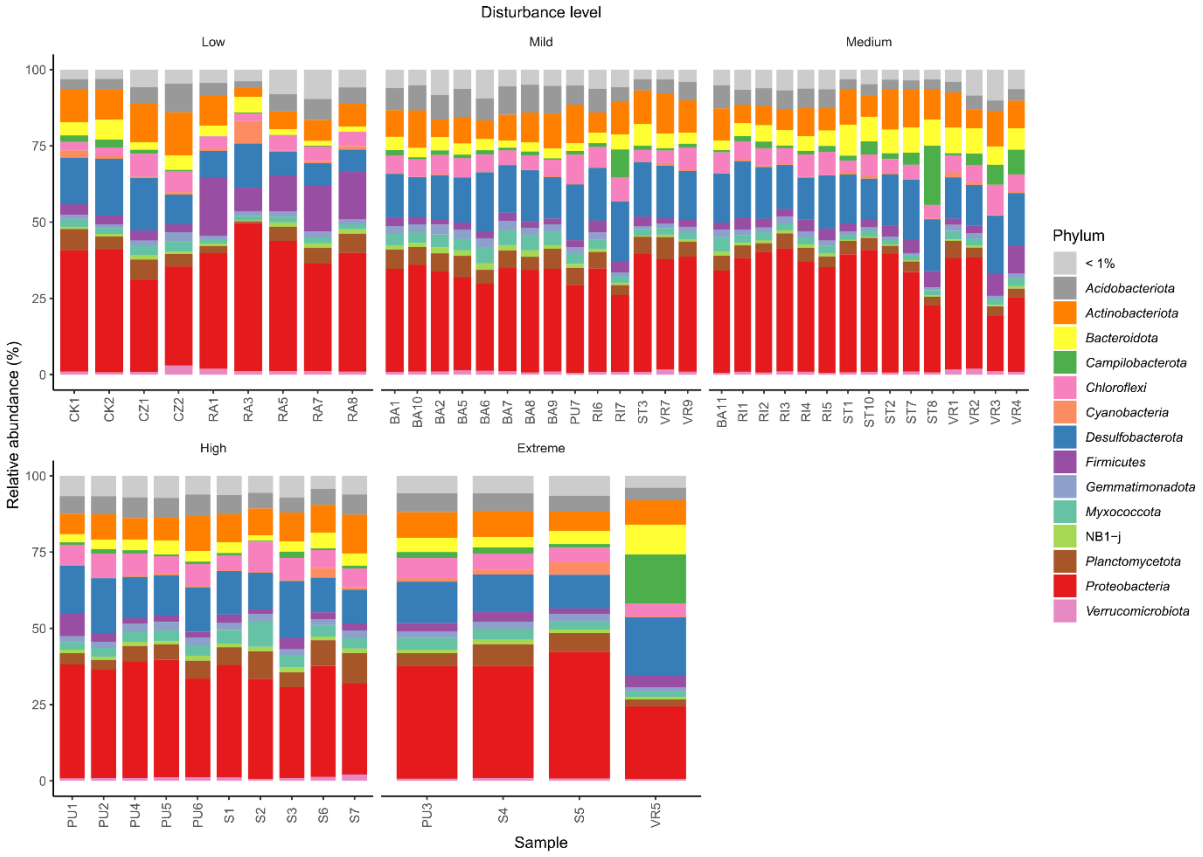

Figure S3. Composition of prokaryotic community in sediment samples across five levels of anthropogenic disturbance: low, mild, medium, high and extreme. Bar plots show the median relative abundance at the phylum level. Only ASVs represented with a median relative abundance > 1% across the DLs are shown.

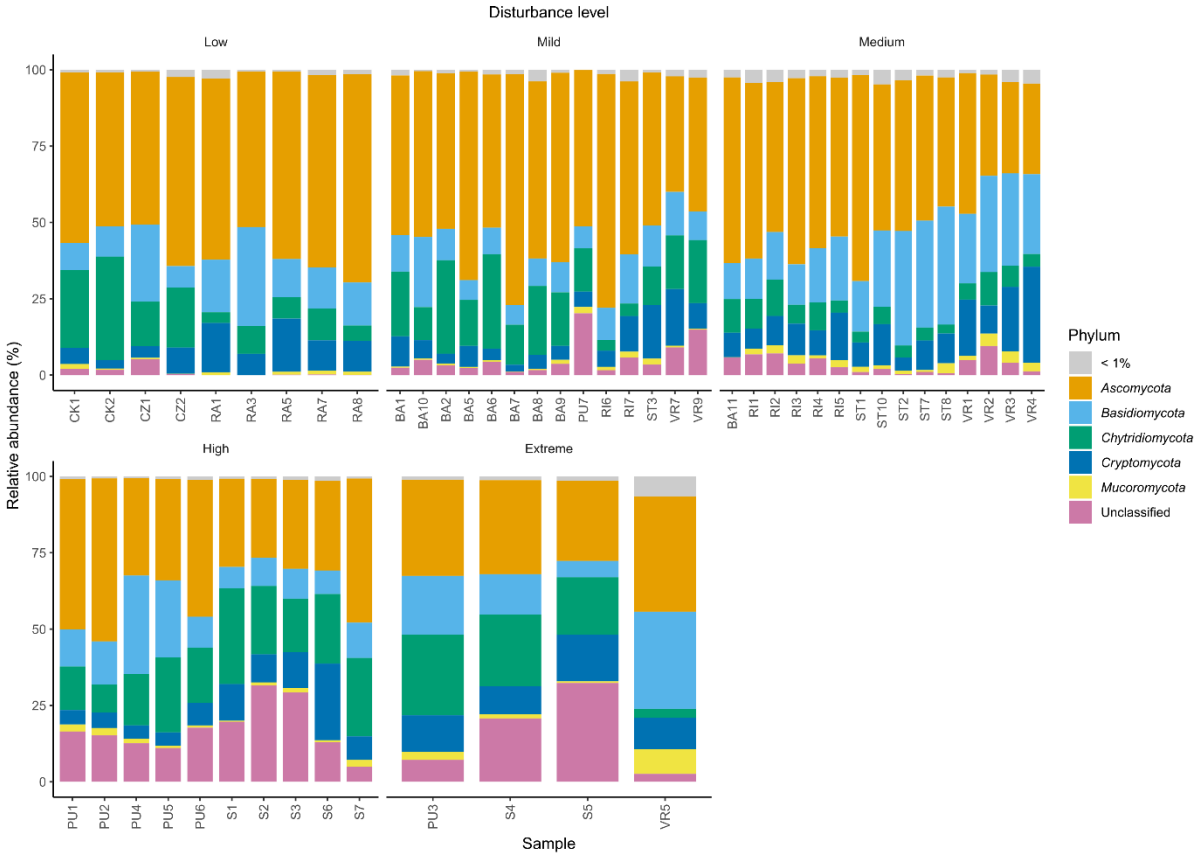

Figure S4. Composition of fungal community in sediment samples across five levels of anthropogenic disturbance: low, mild, medium, high and extreme. Bar plots show the median relative abundance at the phylum level. Only ASVs represented with a median relative abundance > 1% across the DLs are shown.

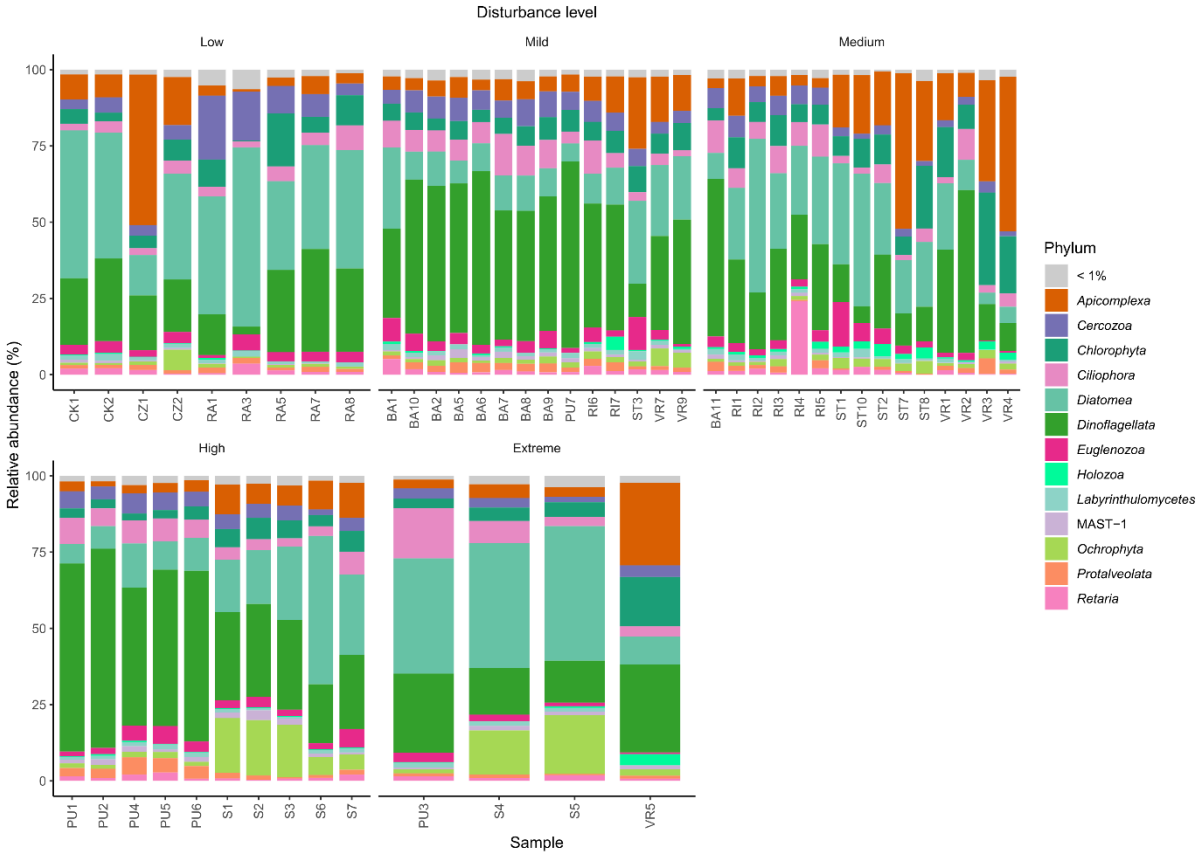

Figure S5. Composition of protistan community in sediment samples across five levels of anthropogenic disturbance: low, mild, medium, high and extreme. Bar plots show the median relative abundance at the phylum level. Only ASVs represented with a median relative abundance > 1% across the DLs are shown.

Table S20. Log2 fold changes (LFC) of microbial families (prokaryotes, fungi and protists) which showed significance ($p < 0.05$) when comparing the disturbance levels (DLs): Low vs. Mild, Low vs. Medium, Low vs. High and Low vs. Extreme.

	Family		Disturbance level comparison			
			Low vs. Mild	Low vs. Medium	Low vs. High	Low vs. Extreme
PROKARYOTES	B2M28	*p*-value		0.013		
		LFC	1.741	1.541	1.301	-0.213
	Burkholderiaceae	*p*-value		0.002		
		LFC	-4.977	-4.815	-5.018	-5.199
	Unclassified Cyanobacteria	*p*-value		0.028		
		LFC	-1.856	-0.908	-0.986	-1.017
	Desulfocapsaceae	*p*-value		0.049		
		LFC	0.770	1.244	-0.198	-1.163
	Desulfosarcinaceae	*p*-value		0.006		
		LFC	1.023	1.410	0.695	-0.605
	Lactobacillaceae	*p*-value		0.004		
		LFC	-3.070	-3.339	-1.692	-4.234
	Pirellulaceae	*p*-value		0.024		
		LFC	0.884	0.310	0.574	-1.008
	Pseudomonadaceae	*p*-value		0.002		
		LFC	-3.865	-3.865	-3.750	-3.935
	Thermoanaerobaculaceae	*p*-value		0.028		
		LFC	1.875	1.278	1.022	-0.401
	Woeseiaceae	*p*-value		0.028		
		LFC	0.420	0.540	0.426	-0.700
FUNGI	*Metschnikowiaceae*	*p*-value		0.009		
		LFC	2.358	0.904	0.988	-2.153
PROTISTS	*Bacillariophyceae*	*p*-value		0.004		
		LFC	-1.122	-0.614	-0.998	-1.232
	Gymnodinium clade	*p*-value		0.033		
		LFC	2.309	1.026	2.216	-1.218
	Mediophyceae	*p*-value		0.033		
		LFC	0.642	1.857	0.100	-1.990
	Suessiaceae	*p*-value		0.024		
		LFC	1.675	0.770	1.038	-0.667
	Thoracosphaeraceae	*p*-value		0.011		
		LFC	1.938	1.087	1.323	-0.338

Table S21. Dispersal and selection factors ($p < 0.01$ and R^2 values) based on PERMANOVA (adonis2) for microbial (prokaryotic, fungal and protistan) abundance. Factors with no significance detected for any of the three microbial communities are not shown. Asterisk (*) marks factors with a slight significance, $p = 0.011$. NS - not significant.

Theory	Factor	Prokaryotic abundance		Fungal abundance		Protistan abundance	
		R^2 value (%)	*p*-value	R^2 value (%)	*p*-value	R^2 value (%)	*p*-value
DISPERSAL	Location	46.919	0.001	49.092	0.001	51.253	0.001
	Region	13.803	0.001	18.503	0.001	15.59	0.001
	Grain	17.369	0.001	15.153	0.001	17.231	0.001
	Depth	9.55	0.001	10.859	0.001	7.34	0.001
SELECTION	Contamination	NS	0.013	4.438	0.008	NS	0.026
	Disturbance level	22.574	0.001	22.639	0.001	22.623	0.001
	Temperature sediment	9.132	0.001	6.568	0.001	6.488	0.001
	Temperature bottom water layer	8.849	0.001	12.031	0.001	10.966	0.001
	Redox sediment	NS	0.068	4.756	0.004	NS	0.043
	Salinity	4.797	0.002	5.239	0.001	NS	0.018
	Distance from shore (m)	NS	0.034	5.8	0.002	4.281	0.01
	Hg	NS	0.034	5.518	0.001	4.289	0.011*
	Cu	NS	0.097	4.176	0.005	NS	0.079
	Bi	NS	0.017	6.087	0.001	5.861	0.003
	Zn	NS	0.125	5.308	0.001	NS	0.076
	Cd	NS	0.778	4.436	0.008	NS	0.082
	Total nitrogen	NS	0.025	5.017	0.003	NS	0.039
	Total organic carbon	NS	0.06	5.811	0.001	4.587	0.009
	Cu bioavailability	NS	0.2	4.064	0.011	NS	0.103
	As bioavailability	NS	0.029	6.904	0.001	5.682	0.003
	Sb bioavailability	NS	0.037	4.274	0.009	NS	0.052

Table S22. Dispersal and selection factors ($p < 0.01$ and R^2 values) based on PERMANOVA (adonis2) for microbial (prokaryotic, fungal and protistan) incidence. Factors with no significance detected for any of the three microbial communities are not shown. Asterisk (*) marks factors with a slight significance, $p = 0.011$. NS - not significant.

Theory	Factor	Prokaryotic incidence		Fungal incidence		Protistan incidence	
		R^2 value (%)	*p*-value	R^2 value (%)	*p*-value	R^2 value (%)	*p*-value
DISPERSAL	Location	30.699	0.001	33.7	0.001	44.636	0.001
	Region	9.558	0.001	12.898	0.001	14.997	0.001
	Grain	11.477	0.001	12.351	0.001	16.148	0.001
	Depth	5.262	0.001	6.042	0.001	6.363	0.001
SELECTION	Contamination	3.374	0.008	NS	0.026	NS	0.026
	Disturbance level	15.506	0.001	15.001	0.001	19.448	0.001
	Temperature sediment	5.366	0.001	5.106	0.001	6.488	0.001
	Temperature bottom water layer	5.789	0.001	9.022	0.001	10.966	0.001
	Salinity	3.201	0.003	3.314	0.005	NS	0.028
	Distance from shore (m)	NS	0.061	3.391	0.005	NS	0.013
	Bi	3.266	0.009	4.219	0.001	5.51	0.001
	Total organic carbon	NS	0.127	NS	0.051	4.563	0.011*
	As bioavailability	3.119	0.011*	NS	0.015	4.624	0.007

Table S23. The 20 most significant prokaryotic ASVs, according to the DESeq2 analysis.

ASV	Genus	Family	Phylum
ASV5345	uncultured	*Thiotrichaceae*	*Proteobacteria*
ASV5738	*Candidatus Omnitrophus*	*Omnitrophaceae*	*Verrrucomicrobiota*
ASV166	-	-	unclassified *Bacteria*
ASV4491	*Boseongicola*	*Rhodobacteraceae*	*Proteobacteria*
ASV347	Subgroup 23	*Thermoanaerobaculaceae*	*Acidobacteriota*
ASV2588	*Lactobacillus*	*Lactobacillaceae*	*Firmicutes*
ASV5044	*Thiogranum*	*Ectothiorhodospiraceae*	*Proteobacteria*
ASV4772	B2M28	B2M28	*Proteobacteria*
ASV5571	Sva0485	Sva0485	Sva0485
ASV4766	B2M28	B2M28	*Proteobacteria*
ASV2483	*Bacillus*	*Bacillaceae*	*Firmicutes*
ASV272	RB41	*Pyrinomonadaceae*	*Acidobacteriota*
ASV4335	*Reyranella*	*Reyranellaceae*	*Proteobacteria*
ASV5757	*Candidatus Udaeobacter*	*Chthoniobacteraceae*	*Verrucomicrobiota*
ASV5274	*Pseudomonas*	*Pseudomonadaceae*	*Proteobacteria*
ASV4796	*Burkholderia*	*Burkholderiaceae*	*Proteobacteria*
ASV5464	*Schekmanbacteria*	*Schekmanbacteria*	*Schekmanbacteria*
ASV4806	*Ralstonia*	*Burkholderiaceae*	*Proteobacteria*
ASV2830	-	*Lachnospiraceae*	*Firmicutes*
ASV2587	*Lactobacillus*	*Lactobacillaceae*	*Firmicutes*

Table S24. The 20 most significant fungal ASVs, according to the DESeq2 analysis.

ASV	Genus	Family	Phylum
ASV240	-	-	*Basidiomycota*
ASV361	*Mortierellales*	*Mortierellales*	*Mucoromycota*
ASV702	*Trechispora*	*Hydnodontaceae*	*Basidiomycota*
ASV474	Rhizophydiaceae	*Rhizophydiaceae*	*Chytridiomycota*
ASV247	-	-	unclassified Fungi
ASV17	*Paramicrosporidium*	*Incertae Sedis*	*Cryptomycota*
ASV332	*Basidiobolus*	*Basidiobolaceae*	*Zoopagomycota*
ASV270	*Chytridiomycetes*	*Chytridiomycetes*	*Chytridiomycota*
ASV309	*Wallemia*	*Incertae Sedis*	*Basidiomycota*
ASV922	-	*Aphelidea*	*Aphelidea*
ASV242	*Lichtheimia*	*Lichtheimiaceae*	*Mucoromycota*
ASV1367	*Zygosaccharomyces*	*Saccharomycetaceae*	*Ascomycota*
ASV39	*Blastocladiales*	*Blastocladiales*	*Blastocladiomycota*
ASV501	*Derxomyces*	*Bulleribasidiaceae*	*Basidiomycota*
ASV1000	*Geotrichum*	*Dipodascaceae*	*Ascomycota*
ASV777	*Tausonia*	*Mrakiaceae*	*Basidiomycota*
ASV622	*Tortispora*	*Trigonopsidaceae*	*Ascomycota*
ASV755	*Aigialus*	*Aigialaceae*	*Ascomycota*
ASV146	-	Sordariomycetes *(class level)*	*Ascomycota*
ASV218	*Aspergillus*	*Aspergillaceae*	*Ascomycota*

Table S25. The 20 most significant protistan ASVs, according to the DESeq2 analysis.

ASV	Genus	Family	Phylum
ASV1026	*Tetraselmis*	*Chlorodendrales*	Chlorophyta
ASV1483	Choreotrichia	*Choreotrichia*	Ciliophora
ASV930	uncultured	uncultured	Labyrinthulomycetes
ASV1724	*Biecheleria*	*Suessiaceae*	Dinoflagellata
ASV1560	*Pirsonia*	*Incertae Sedis*	Incertae Sedis
ASV203	*Eutintinnus*	*Choreotrichia*	Ciliophora
ASV545	*Cryothecomonas*	*Protaspidae*	Cercozoa
ASV1004	*Cryptocaryon*	*Prostomatea*	Ciliophora
ASV1430	*Bacillariophyceae*	*Bacillariophyceae*	Diatomea
ASV803	*Gonyaulax*	*Gonyaulacales*	Dinoflagellata
ASV852	*Trebouxiophyceae*	*Trebouxiophyceae*	Chlorophyta
ASV321	*Trebouxiophyceae*	*Trebouxiophyceae*	Chlorophyta
ASV1785	*Trebouxiophyceae*	*Trebouxiophyceae*	Chlorophyta
ASV1757	*Spirotrichea*	*Spirotrichea*	Ciliophora
ASV257	*Tetraselmis*	*Chlorodendrales*	Chlorophyta
ASV523	*Pedinellales*	*Pedinellales*	Ochrophyta
ASV2	-	-	Unclassified Eukaryota
ASV5	*Paulinella*	*Euglyphida*	Cercozoa
ASV710	*Petalomonas*	*Heteronematina*	Euglenozoa
ASV163	-	*Oligohymenophorea*	Ciliophora

A)

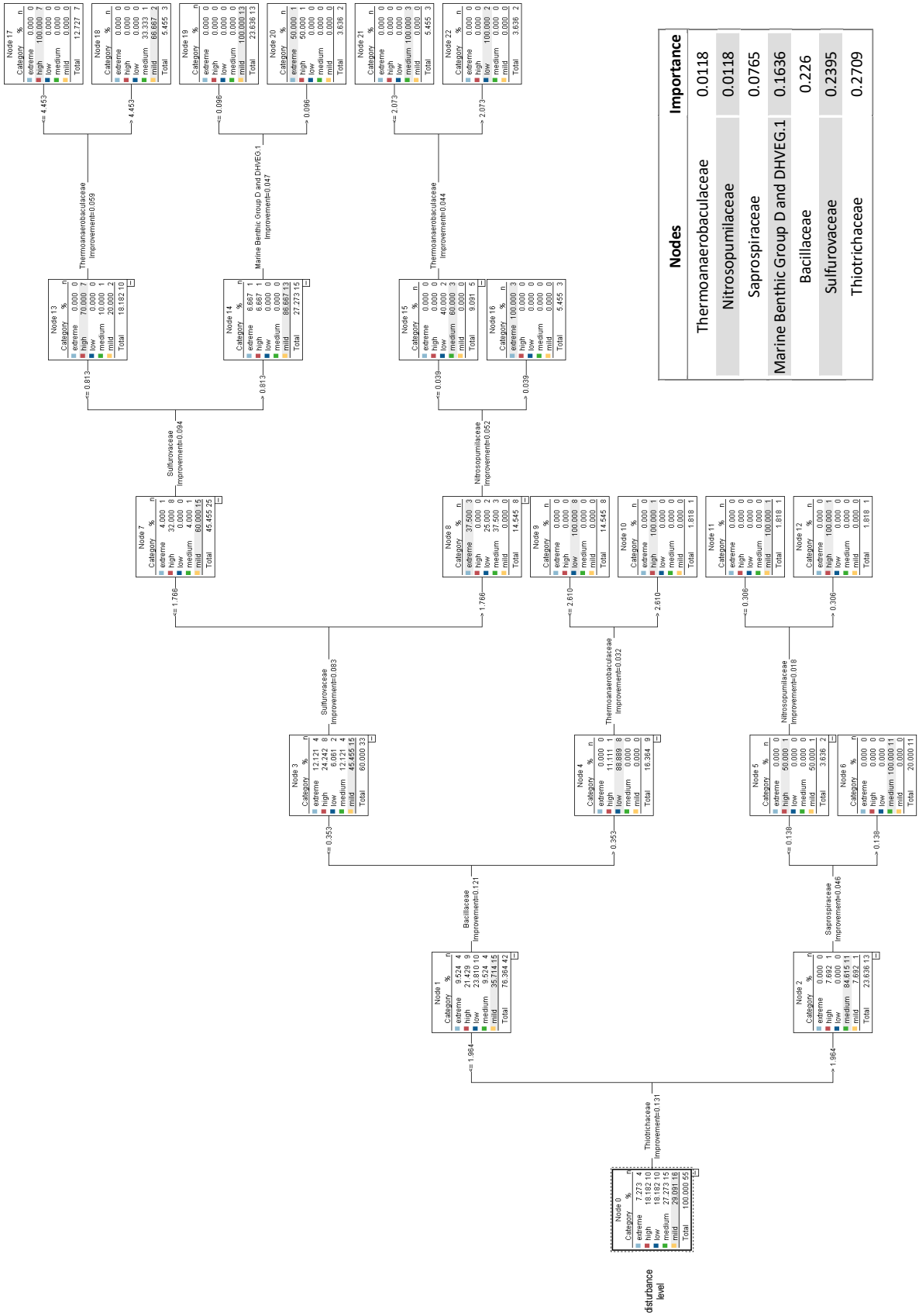
Nodes
Importance
Thermoanaerobaculaceae 0.0118
Nitrosopumilaceae 0.0118
Saprospiraceae 0.0765
Marine Benthic Group D and DHVEG.1 0.1636
Bacillaceae 0.226
Sulfurovaceae 0.2395
Thiotrichaceae 0.2709
disturbance level

B)


Nodes
Importance
Prostomatea 0.0106
Heteronematina 0.0189
Unclassified Cercozoa 0.0189
Unclassified Apicomplexa 0.0459
Euglyphida 0.0575
Trebouxiophyceae 0.0917
Pseudoperkinsidae 0.2328
Suessiaceae 0.2349
Dinophysiales 0.2888
disturbance level

C)

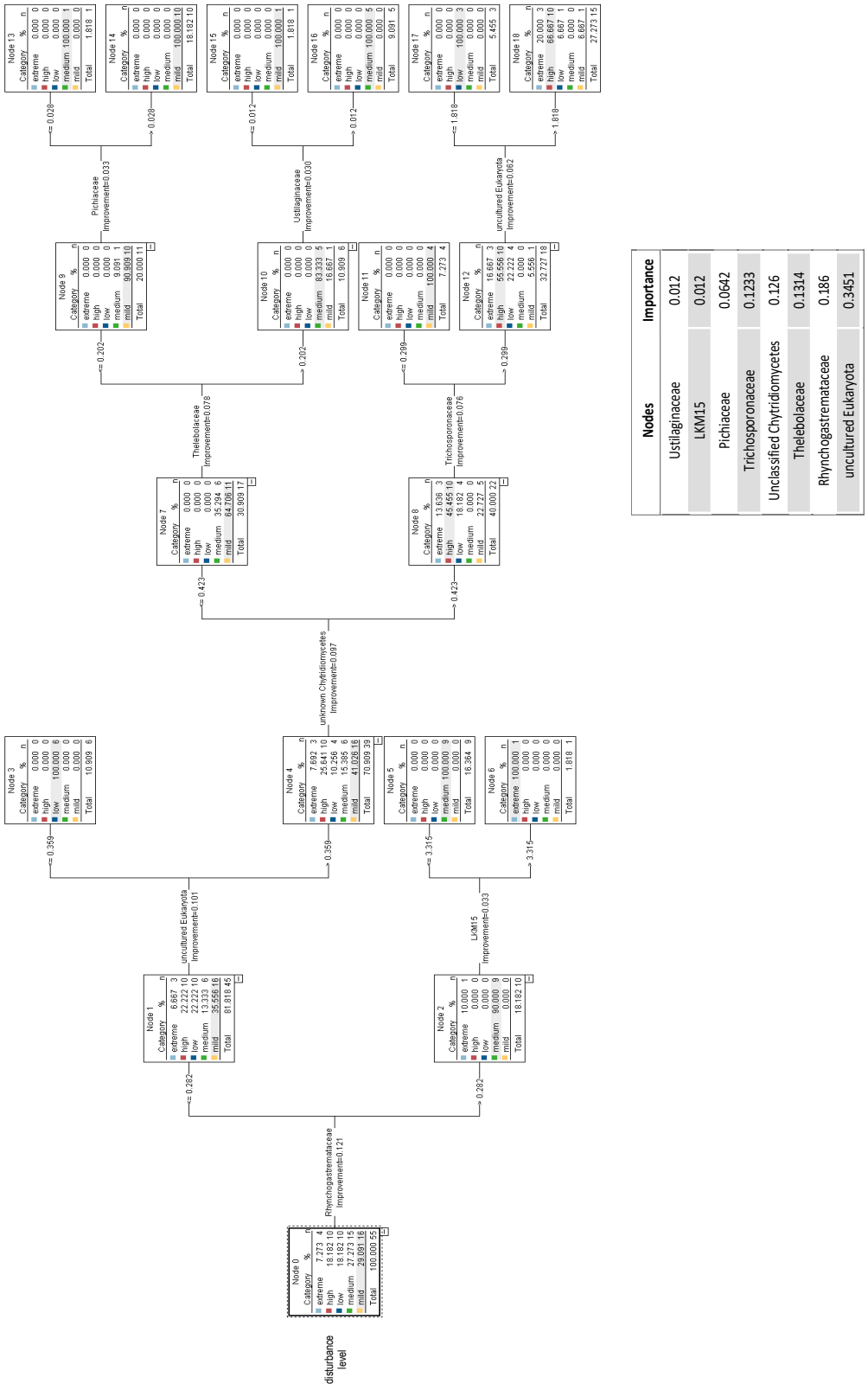

Figure S6. Prediction models on the Classification and Regression Tree analysis for each of the three microbial communities – A) prokaryotes, B) protists, C) fungi; based on the levels of anthropogenic disturbance. Presence and relative abundance of a group (node) of key indicator variables define specific level of anthropogenic disturbance within the sediment (low, mild, medium, high and extreme).% - certainty of defining a disturbance level, n – number of samples in which the specific disturbance level is determined, Importance - how much each node contributes to the model prediction.

Table S26. Significant selection factors (heavy metals) separated into two groups (low and high) based on median concentration used in Mantel's test.

Sample	Hg	Cd	Bi	Cu	Zn	Disturbance level
BA1	LOW	LOW	LOW	LOW	LOW	LOW
BA2	LOW	LOW	LOW	LOW	LOW	LOW
BA5	LOW	LOW	LOW	LOW	LOW	LOW
BA6	LOW	LOW	LOW	LOW	LOW	LOW
BA7	LOW	LOW	LOW	LOW	LOW	LOW
BA8	LOW	LOW	LOW	LOW	LOW	LOW
BA9	LOW	LOW	LOW	LOW	LOW	LOW
BA10	LOW	LOW	LOW	LOW	LOW	LOW
BA11	LOW	HIGH	HIGH	HIGH	HIGH	HIGH
CK1	LOW	LOW	LOW	LOW	LOW	LOW
CK2	LOW	LOW	LOW	LOW	LOW	LOW
CZ1	LOW	LOW	LOW	LOW	LOW	LOW
CZ2	LOW	LOW	LOW	LOW	LOW	LOW
PU1	HIGH	LOW	HIGH	HIGH	HIGH	HIGH
PU2	HIGH	HIGH	HIGH	HIGH	HIGH	HIGH
PU3	HIGH	HIGH	HIGH	HIGH	HIGH	HIGH
PU4	HIGH	LOW	HIGH	HIGH	LOW	HIGH
PU5	HIGH	LOW	HIGH	HIGH	HIGH	HIGH
PU6	HIGH	LOW	LOW	LOW	LOW	HIGH
PU7	HIGH	LOW	LOW	LOW	LOW	LOW
RI1	HIGH	LOW	LOW	HIGH	LOW	HIGH
RI2	HIGH	HIGH	HIGH	HIGH	HIGH	HIGH
RI3	HIGH	HIGH	LOW	HIGH	HIGH	HIGH
RI4	HIGH	HIGH	HIGH	HIGH	HIGH	HIGH
RI5	HIGH	HIGH	HIGH	LOW	HIGH	HIGH
RI6	HIGH	LOW	LOW	LOW	LOW	LOW
RI7	HIGH	LOW	HIGH	LOW	LOW	LOW
S1	HIGH	HIGH	HIGH	HIGH	HIGH	HIGH
S2	HIGH	HIGH	HIGH	HIGH	HIGH	HIGH
S3	HIGH	HIGH	HIGH	HIGH	HIGH	HIGH
S4	HIGH	HIGH	HIGH	HIGH	HIGH	HIGH
S5	HIGH	HIGH	HIGH	HIGH	HIGH	HIGH
S6	HIGH	HIGH	HIGH	LOW	HIGH	HIGH
S7	HIGH	HIGH	HIGH	HIGH	HIGH	HIGH
ST1	HIGH	HIGH	HIGH	HIGH	HIGH	HIGH
ST2	LOW	HIGH	HIGH	HIGH	HIGH	HIGH
ST3	LOW	HIGH	HIGH	LOW	LOW	LOW
ST7	LOW	HIGH	HIGH	HIGH	HIGH	HIGH
ST8	LOW	HIGH	HIGH	HIGH	HIGH	HIGH
ST10	HIGH	HIGH	HIGH	HIGH	HIGH	HIGH
VR1	LOW	HIGH	HIGH	HIGH	HIGH	HIGH
VR2	HIGH	HIGH	HIGH	HIGH	HIGH	HIGH
VR3	LOW	HIGH	LOW	HIGH	HIGH	HIGH
VR4	HIGH	HIGH	LOW	HIGH	HIGH	HIGH
VR5	HIGH	HIGH	HIGH	HIGH	HIGH	HIGH
VR7	LOW	LOW	LOW	LOW	LOW	LOW
VR9	HIGH	HIGH	LOW	LOW	LOW	LOW
RA1	LOW	LOW	LOW	LOW	LOW	LOW
RA3	LOW	LOW	LOW	LOW	LOW	LOW
RA5	LOW	LOW	LOW	LOW	LOW	LOW
RA7	LOW	LOW	LOW	LOW	LOW	LOW
RA8	LOW	LOW	LOW	LOW	LOW	LOW

Table S27. Mean Mantel r values (with a Pearson's correlation) for each microbial community interaction and five tested pollutants.

Interaction	Pollutant	Pollution level	Mean Mantel r	*p*-value
Prokaryote-Fungi	Hg	HIGH	0.691	0.001
Prokaryote-Protist	Hg	HIGH	0.660	0.001
Fungi-Protist	Hg	HIGH	0.813	0.001
Prokaryote-Fungi	Hg	LOW	0.807	0.001
Prokaryote-Protist	Hg	LOW	0.835	0.001
Fungi-Protist	Hg	LOW	0.809	0.001
Prokaryote-Fungi	Cd	HIGH	0.663	0.001
Prokaryote-Protist	Cd	HIGH	0.650	0.001
Fungi-Protist	Cd	HIGH	0.747	0.001
Prokaryote-Fungi	Cd	LOW	0.835	0.001
Prokaryote-Protist	Cd	LOW	0.843	0.001
Fungi-Protist	Cd	LOW	0.838	0.001
Prokaryote-Fungi	Bi	HIGH	0.691	0.001
Prokaryote-Protist	Bi	HIGH	0.623	0.001
Fungi-Protist	Bi	HIGH	0.760	0.001
Prokaryote-Fungi	Bi	LOW	0.809	0.001
Prokaryote-Protist	Bi	LOW	0.849	0.001
Fungi-Protist	Bi	LOW	0.833	0.001
Prokaryote-Fungi	Cu	HIGH	0.736	0.001
Prokaryote-Protist	Cu	HIGH	0.722	0.001
Fungi-Protist	Cu	HIGH	0.787	0.001
Prokaryote-Fungi	Cu	LOW	0.792	0.001
Prokaryote-Protist	Cu	LOW	0.809	0.001
Fungi-Protist	Cu	LOW	0.820	0.001
Prokaryote-Fungi	Zn	HIGH	0.713	0.001
Prokaryote-Protist	Zn	HIGH	0.691	0.001
Fungi-Protist	Zn	HIGH	0.774	0.001
Prokaryote-Fungi	Zn	LOW	0.799	0.001
Prokaryote-Protist	Zn	LOW	0.824	0.001
Fungi-Protist	Zn	LOW	0.813	0.001

Table S28. List of bacterial isolates used for pollutant-resistance testing, including isolate ID, taxonomic classification and corresponding cluster.

Isolate	Genus	Cluster
1	*Bacillus/Pseudoalkalibacillus/Alkalibacillus*	7
2	*Bacillus/Pseudoalkalibacillus/Alkalibacillus*	7
3	*Bacillus/Pseudoalkalibacillus/Alkalibacillus*	7
4	*Ruegeria/Cribrihabitans*	2
5	*Ruegeria/Cribrihabitans*	2
6	*Bacillus/Mesobacillus/Cytobacillus*	9
7	*Ruegeria/Cribrihabitans*	2
9	*Ruegeria/Cribrihabitans*	3
10	*Bacillus/Peribacillus/Rossellomorea*	8
11	*Bacillus/Mesobacillus/Cytobacillus*	9
12	*Bacillus/Mesobacillus/Cytobacillus*	9
13	*Bacillus/Peribacillus/Rossellomorea*	8
14	*Bacillus/Mesobacillus/Cytobacillus*	9
15	*Ruegeria/Cribrihabitans*	2
16	*Bacillus/Mesobacillus/Cytobacillus*	9
17	*Bacillus/Mesobacillus/Cytobacillus*	9
18	*Bacillus/Mesobacillus/Cytobacillus*	9
19	*Bacillus/Mesobacillus/Cytobacillus*	9
20	*Bacillus/Mesobacillus/Cytobacillus*	9
21	*Bacillus/Mesobacillus/Cytobacillus*	9
23	*Bacillus/Mesobacillus/Cytobacillus*	9
24	*Lysinobacillus/Sporosarcina*	6
25	*Bacillus/Peribacillus/Rossellomorea*	8
26	*Bacillus/Peribacillus/Rossellomorea*	8
27	*Ruegeria/Cribrihabitans*	2
28	*Lysinobacillus/Sporosarcina*	6
30	*Ruegeria/Cribrihabitans*	2
31	*Ruegeria/Cribrihabitans*	2
32	*Bacillus/Mesobacillus/Cytobacillus*	9
33	*Ruegeria/Cribrihabitans*	2
34	*Bacillus/Peribacillus/Rossellomorea*	8
35	*Ruegeria/Cribrihabitans*	2

Isolate	Genus	Cluster
36	*Bacillus/Mesobacillus/Cytobacillus*	**9**
37	*Ruegeria/Cribrihabitans*	**2**
38	*Ruegeria/Cribrihabitans*	**2**
39	*Ruegeria/Cribrihabitans*	**2**
40	*Bacillus berkeleyi/decolorationis*	**3**
41	*Ruegeria/Cribrihabitans*	**2**
42	*Bacillus/Mesobacillus/Cytobacillus*	**9**
43	*Bacillus/Mesobacillus/Cytobacillus*	**9**
45	*Bacillus/Peribacillus/Rossellomorea*	**8**
46	*Bhargavea*	**5**
47	*Bacillus/Mesobacillus/Cytobacillus*	**9**
48	*Ruegeria/Cribrihabitans*	**2**
49	*Lysinobacillus/Sporosarcina*	**6**
50	*Bacillus/Mesobacillus/Cytobacillus*	**9**
52	*Bacillus/Mesobacillus/Cytobacillus*	**9**
53	*Bacillus/Mesobacillus/Cytobacillus*	**9**
55	*Lysinobacillus/Sporosarcina*	**6**
56	*Bacillus/Mesobacillus/Cytobacillus*	**9**
57	*Bacillus/Fictibacillus*	**4**
58	*Bacillus/Mesobacillus/Cytobacillus*	**9**
61	*Ruegeria/Cribrihabitans*	**2**
62	*Bacillus/Peribacillus/Rossellomorea*	**8**
63	*Lysinobacillus/Sporosarcina*	**6**
64	*Bacillus/Peribacillus/Rossellomorea*	**8**
65	*Bacillus/Fictibacillus*	**4**
66	*Bacillus/Peribacillus/Rossellomorea*	**8**
67	*Bacillus/Peribacillus/Rossellomorea*	**8**
68	*Bacillus/Peribacillus/Rossellomorea*	**8**
69	*Bacillus/Pseudoalkalibacillus/Alkalibacillus*	**7**
71	*Bacillus/Peribacillus/Rossellomorea*	**8**
72	*Bacillus/Mesobacillus/Cytobacillus*	**9**
73	*Bacillus/Pseudoalkalibacillus/Alkalibacillus*	**7**
75	*Pseudoalteromonas*	**1**
76	*Bacillus/Peribacillus/Rossellomorea*	**8**

Isolate	Genus	Cluster
78	*Ruegeria/Cribrihabitans*	**2**
81	*Bacillus/Peribacillus/Rossellomorea*	**8**
82	*Bacillus/Mesobacillus/Cytobacillus*	**9**
83	*Bacillus/Pseudoalkalibacillus/Alkalibacillus*	**7**
84	*Bacillus/Mesobacillus/Cytobacillus*	**9**
85	*Lysinobacillus/Sporosarcina*	**6**
87	*Pseudoalteromonas*	**1**
88	*Bacillus/Pseudoalkalibacillus/Alkalibacillus*	**7**

Table S29. Minimal inhibitory concentrations (MICs) for all tested bacterial isolates (n = 74 isolates) and each pollutant. The table is separated based on the ranges of concentrations used, up to 5,000 mg/l for Zn, Cr, Cd, Hg and TBT and up to 10,000 mg/l for Sn, Pb, Cu, Co, Ni.

		Minimal inhibitory concentration (mg/l)									
Isolate	Cluster	up to 5,000					up to 10,000				
		Pollutant									
		Zn	Cr	Cd	Hg	TBT	Sn	Pb	Cu	Co	Ni
1	7	100	2,500	500	50	1,000	500	2,500	2,500	5,000	10,000
2	7	1,000	> 5,000	500	50	1,000	1,000	5,000	1,000	10,000	10,000
3	7	2,500	500	500	50	> 5,000	10,000	2,500	2,500	2,500	5,000
4	2	2,500	500	500	50	> 5,000	500	2,500	1,000	2,500	10,000
5	2	> 5,000	> 5,000	500	50	5,000	500	5,000	2,500	> 10,000	10,000
6	9	500	> 5,000	500	50	1,000	5,000	10,000	5,000	10,000	>10,000
7	2	500	> 5,000	500	50	> 5,000	1,000	5,000	1,000	10,000	10,000
9	3	1,000	> 5,000	500	50	5,000	500	2,500	2,500	10,000	> 10,000
10	8	500	2,500	500	50	1,000	100	5,000	1,000	10,000	10,000
11	9	500	5,000	100	50	1,000	500	> 10,000	2,500	1,000	>10,000
12	9	500	1,000	1,000	50	1,000	5,000	> 10,000	2,500	2,500	2,500
13	8	2,500	> 5,000	5,000	50	1,000	> 10,000	> 10,000	5,000	> 10,000	>10,000
14	9	500	5,000	1,000	50	1,000	1,000	> 10,000	2,500	5,000	2,500
15	2	1,000	1,000	500	50	5,000	500	10,000	2,500	10,000	10,000
16	9	500	> 5,000	500	100	5,000	10,000	> 10,000	2,500	5,000	10,000
17	9	500	500	500	50	1,000	500	10,000	1,000	5,000	5,000
18	9	500	1,000	500	50	1,000	100	> 10,000	2,500	5,000	5,000
19	9	2,500	> 5,000	1,000	50	1,000	10,000	> 10,000	10,000	10,000	10,000
20	9	500	> 5,000	500	50	1,000	2,500	> 10,000	5,000	5,000	>10,000
21	9	2,500	> 5,000	1,000	500	1,000	> 10,000	> 10,000	5,000	> 10,000	10,000
23	9	500	1,000	1,000	50	1,000	500	> 10,000	500	10,000	5,000
24	6	500	500	500	50	1,000	100	> 10,000	500	2,500	5,000
25	8	> 5,000	> 5,000	> 5,000	100	1,000	5,000	> 10,000	>10,000	> 10,000	>10,000
26	8	1,000	> 5,000	1,000	100	1,000	2,500	> 10,000	5,000	10,000	10,000
27	2	2,500	500	500	50	> 5,000	100	> 10,000	2,500	5,000	5,000
28	6	1,000	500	500	50	2,500	2,500	> 10,000	1,000	5,000	5,000
30	2	500	1,000	100	50	1,000	500	> 10,000	500	5,000	5,000
31	2	2,500	> 5,000	500	50	1,000	1,000	> 10,000	1,000	10,000	10,000
32	9	1,000	500	500	50	1,000	500	> 10,000	500	2,500	5,000
33	2	500	2,500	500	50	1,000	500	> 10,000	5,000	5,000	5,000

		Minimal inhibitory concentration (mg/l)									
Isolate	Cluster	up to 5,000					up to 10,000				
		Pollutant									
		Zn	Cr	Cd	Hg	TBT	Sn	Pb	Cu	Co	Ni
34	8	2,500	> 5,000	500	50	1,000	5,000	> 10,000	5,000	10,000	>10,000
35	2	1,000	500	500	50	5,000	500	> 10,000	5,000	5,000	>10,000
36	9	2,500	> 5,000	5,000	50	1,000	> 10,000	> 10,000	5,000	> 10,000	>10,000
37	2	500	2,500	500	50	> 5,000	100	> 10,000	2,500	2,500	5,000
38	2	2,500	1,000	500	50	> 5,000	100	> 10,000	5,000	5,000	10,000
39	2	1,000	1,000	500	50	5,000	500	10,000	500	10,000	10,000
40	3	2,500	5,000	500	50	1,000	2,500	> 10,000	1,000	10,000	>10,000
41	2	1,000	1,000	50	50	2,500	100	> 10,000	2,500	5,000	5,000
42	9	500	1,000	500	50	1,000	100	> 10,000	500	2,500	2,500
43	9	500	2,500	500	50	1,000	100	> 10,000	500	2,500	5,000
45	8	1,000	1,000	50	50	1,000	100	> 10,000	500	2,500	10,000
46	5	500	500	500	50	1,000	100	> 10,000	500	2,500	2,500
47	9	2,500	> 5,000	500	100	1,000	> 10,000	> 10,000	>10,000	> 10,000	>10,000
48	2	500	500	500	50	2,500	1,000	> 10,000	500	2,500	5,000
49	6	500	500	500	50	1,000	100	> 10,000	500	2,500	1,000
50	9	1,000	> 5,000	1,000	50	1,000	1,000	> 10,000	2,500	10,000	10,000
52	9	500	5,000	500	50	1,000	5,000	> 10,000	5,000	10,000	>10,000
53	9	> 5,000	500	500	50	1,000	500	> 10,000	500	5,000	5,000
55	6	500	500	100	50	1,000	500	> 10,000	500	5,000	5,000
56	9	500	2,500	500	50	1,000	500	> 10,000	500	5,000	10,000
57	4	500	2,500	1,000	50	1,000	100	> 10,000	5,000	10,000	5,000
58	9	1,000	1,000	1,000	50	1,000	100	> 10,000	500	5,000	5,000
61	2	500	500	500	50	1,000	2,500	> 10,000	1,000	> 10,000	10,000
62	8	2,500	500	500	50	1,000	500	-	500	2,500	2,500
63	6	1,000	1,000	500	50	500	500	> 10,000	5,000	5,000	2,500
64	8	500	500	100	50	1,000	100	> 10,000	500	5,000	5,000
65	4	500	> 5,000	1,000	50	1,000	2,500	> 10,000	2,500	5,000	>10,000
66	8	500	500	500	50	1,000	500	> 10,000	500	10,000	10,000
67	8	5,000	5,000	500	50	1,000	1,000	> 10,000	5,000	> 10,000	5,000
68	8	500	5,000	500	500	1,000	10,000	> 10,000	2,500	> 10,000	10,000
69	7	1,000	> 5,000	500	50	1,000	2,500	> 10,000	10,000	10,000	>10,000
71	8	500	500	50	50	2,500	100	> 10,000	2,500	5,000	10,000
72	9	500	2,500	1,000	50	1,000	1,000	5,000	1,000	5,000	5,000

		Minimal inhibitory concentration (mg/l)									
Isolate	Cluster	up to 5,000					up to 10,000				
		Pollutant									
		Zn	Cr	Cd	Hg	TBT	Sn	Pb	Cu	Co	Ni
73	7	500	500	500	50	1,000	500	5,000	500	5,000	5,000
75	1	500	1,000	500	50	> 5,000	500	1,000	1,000	5,000	10,000
76	8	500	> 5,000	500	100	1,000	> 10,000	10,000	10,000	5,000	5,000
78	2	500	1,000	500	50	1,000	100	10,000	100	> 10,000	10,000
81	8	> 5,000	> 5,000	2,500	50	1,000	> 10,000	> 10,000	>10,000	10,000	10,000
82	9	1,000	> 5,000	500	50	1,000	> 10,000	> 10,000	5,000	10,000	>10,000
83	7	500	500	500	50	1,000	100	> 10,000	500	2,500	2,500
84	9	1,000	5,000	500	50	1,000	5,000	> 10,000	10,000	5,000	10,000
85	6	1,000	> 5,000	500	50	1,000	100	> 10,000	5,000	> 10,000	10,000
87	1	500	500	500	50	50	1,000	100	1,000	5,000	5,000
88	7	500	500	500	50	1,000	2,500	> 10,000	2,500	5,000	5,000